UCSF
UC San Francisco Electronic Theses and Dissertations

**Title**
Elucidating the role of ubiquitin in controlling the endocytic trafficking of opioid receptors

**Permalink**
https://escholarship.org/uc/item/5zj8675c

**Author**
Henry, Anastasia Gail

**Publication Date**
2012

Peer reviewed|Thesis/dissertation

eScholarship.org Powered by the California Digital Library
University of California

# Elucidating the role of ubiquitin in controlling the endocytic trafficking of opioid receptors

by

Anastasia G. Henry

DISSERTATION

Submitted in partial satisfaction of the requirements for the degree of

DOCTOR OF PHILOSOPHY

in

Cell Biology

in the

GRADUATE DIVISION

of the

UNIVERSITY OF CALIFORNIA, SAN FRANCISCO

# Dedication and Acknowledgments

The text of this dissertation includes a reprint of the following articles: “Ubiquitination regulates proteolytic processing of G protein-coupled receptors after their sorting to lysosomes” as it appears in J Biol Chem. (284(29); 2009), “The role of ubiquitination in lysosomal trafficking of δ-opioid receptors” as it appears in Traffic (12(2); 2011), “Regulation of endocytic clathrin dynamics by direct ubiquitination of cargo” expanded from the version appearing in Dev. Cell (in press), and “Ubiquitination in the first cytoplasmic loop of μ-opioid receptors reveals a hierarchical mechanism of lysosomal down-regulation” as it appears in J Biol Chem. (286(46); 2011).

The coauthor Mark von Zastrow directed and supervised the research that forms the basis for the dissertation. Anastasia Henry performed the experiments and manuscript preparation of the greater majority of the following dissertation, which constitutes a substantial and comparable contribution to that of other dissertations in the greater Pharmacology and Cell Biology fields. Collaborative contributions from others are specified on the title pages of the relevant chapters.

- Mark von Zastrow, M.D., Ph.D.

I feel incredibly grateful for all of the individuals who have enhanced my experience in graduate school these past six years. First and foremost, I must thank my PI, Mark von Zastrow, who truly was the best mentor a student could ask for. Mark provides people in his lab with the perfect balance of freedom (to stumble, fail, and pick oneself back up and succeed) and of guidance to corral wayward mentees back toward the path of progress

and discovery. Mark showed me how incredibly exciting science can be, and his unwavering enthusiasm and complete lack of fear in trying new experiments is something I will take with me in all of my future scientific endeavors. He is also just a genuinely nice guy that is incredibly supportive and always willing to spare his time to listen and help his students.

My graduate career would also not have been as successful without the immeasurable contributions of the rest of the von Zastrow lab, both past and present members. I must especially thank James Hislop, who taught me how to be a scientist. He trained me to be a thorough researcher, with his relentless demand for controls, proper experimental design, and general scientific rigor. More importantly, he was a great comrade to discuss ideas and provided me with endless support, both as a mentor and as a friend. The other postdoctoral fellows in the lab each contributed in their own way to make my time at UCSF both productive and truly enjoyable. My rotation adviser, Guille Yudowski, introduced me to the exciting world of live-cell imaging and showed me how to think big and look for the most interesting questions to attack. Peter Hein showed me what a true pharmacologist was like and helped me through those early years in the lab with his knowledge, desire to always help, and just overall kindness. Roshanak Irannejad has been a great friend to bounce ideas off of and also to just laugh about life with. Additionally, the patience of Michael Tanowitz, the microscopy experience of Manoj Puthenveedu, the preciseness of Elaine Lau, the kindness of Michelle Trester-Zedlitz, the undying enthusiasm and rebelliousness of Vu Dang, the gusto of Jin Tomshine, the cell-biological

knowledge of Minjong Park, and the inquisitiveness of Aaron Marley have all helped shape me as a scientist.

My fellow graduate students in the lab have also taught me so much over the years. Sarah Kotowski is really the complete package, helping foster my interest in neuroscience and also making the lab a fun place to work. Paul Temkin was also a fantastic colleague, a creative thinker who is not restricted by the opinions and assumptions of others and is just a great person to be deep in the trenches of graduate school with. Additionally, Joy Yu's cheerful demeanor, Ben Lauffer's calming presence, Alison Leaf's perpetual enthusiasm, and Kate Varandas' strong work ethic really enriched my experience in the lab.

Others outside of our lab also provided me with exceptional mentorship and collaborative help. I would like to thank my thesis committee members Orion Weiner, Dave Morgan, and Keith Mostov for their thoughtful comments and contagious excitement for my projects and science in general. Henry Bourne served as an unofficial committee member, critiquing early manuscripts and presentations, asking the tough questions, and providing general inspiration and guidance. I also benefitted from our amazing collaborators Mark Marsh, Ian White, Joe Grove, and Kurt Thorn who not only helped us accomplish experiments we had only dreamed about previously but also offered keen insight into the work as a whole.

Throughout graduate school, my friends and colleagues offered me an endless supply of support and inspiration. My close friends Tatiana Hantig and Matthew Ginzel were invaluable over the last six years, always willing to lend a sympathetic ear and offer support and escape when life was difficult. I would also like to thank Dr. Albright for her shrewd insight, endless support, and help to appreciate that which is most important.
I feel so lucky to have developed a closely-knit group of friends during my graduate career, without whom I would not have grown as much here in San Francisco. My classmates were amazing allies, great people to chat with about the trials and tribulations that occur in graduate school and who inspired me with their intelligence, creativity, and dedication to doing good science. I would like to particularly thank my former roommate Vanessa Strings and my surrogate roommates Jeffrey Farrell and Stephen Naylor, for helping me create a home and safe haven here. The UCSF community as a whole also continually motivated me, and I feel so grateful to have been given the opportunity to learn from such incredible colleagues.

One of my greatest accomplishments during my time at UCSF was meeting and developing a relationship with a particularly influential classmate, my now-husband William Dowdle. I cannot imagine going throughout this journey without Bill, who has been a perfect partner-in-crime in graduate school. He not only has provided me with endless amounts of emotional support throughout my time here but also read early versions of manuscripts and made useful suggestions about my work in general. Graduate school certainly would not have been as much fun, successful, and enlightening without him here with me.

None of this would have been possible without the help of my family. My father, Timothy Henry, and his wife Rosemary have been my cheerleaders throughout my graduate career, encouraging me at every step of the way. My dad set a great example through his inquisitiveness and desire to always learn more. Gregory Taylor helped remind me to never give up on my dreams and also showed me why my research was so important. One of the most influential people during my graduate career has been my younger sister, Annika Henry. She has always believed in my potential and has truly been my best friend over the years. Through our nightly phone conversations, she constantly made me laugh, gave me strength to continue onward, and made me want to work harder and with more compassion through her impeccable example.

Finally, I would like to dedicate this thesis to my mother, Annett Henry. There is absolutely no way I would have made it to UCSF without her hard work, endless encouragement, and sacrifice. She passed away during my first year in graduate school, but I know she would be proud of what I have accomplished over these last six years. She instilled in me a strong work ethic, an overwhelming desire to help others, and the courage to never give up. She pushed me to always follow my dreams and to never settle for anything less. I am eternally grateful for everything she did for me and for the precious time I was able to spend with her, and I will take all of the lessons I learned from her with me through all of my future endeavors.

# Abstract

Elucidating the role of ubiquitin in controlling the endocytic trafficking of opioid receptors

by

Anastasia G. Henry

This dissertation examines the role of ubiquitination in regulating the endocytic trafficking of opioid receptors, members of the large superfamily of seven-transmembrane receptors (7TMRs). The introduction provides a basic overview of 7TMR biology and diversity, examines the role of endocytic trafficking in modulating receptor-mediated signal strength and duration, presents current models for protein sorting in the endocytic pathway, and investigates various functions of ubiquitin in regulating trafficking decisions. The second and third chapters explore the role of ubiquitin in controlling the destruction of δ-opioid receptors after their sorting to lysosomes. In chapter four, a new function of ubiquitin is identified that allows μ-opioid receptors to control the dynamics of receptor-containing clathrin-coated pits and ultimately, their own endocytosis. The fifth chapter presents findings for an additional role of μ-opioid receptor ubiquitination later in the endocytic pathway, modulating receptor destruction after lysosomal sorting, that provides further support for models developed through study of the δ-opioid receptor. The included work used a combination of live-cell imaging, flow cytometric analysis, biochemistry, and genetic manipulations to address the role of ubiquitin in opioid receptor trafficking. Two additional studies that I contributed to during my graduate career, one published (Yudowski et al., 2009) and one under preparation, were excluded as they were beyond the main focus of this dissertation.

Finally, chapter six summarizes the major new conceptual findings from the previous chapters, discusses how they fit in (or cannot be reconciled with) previously established models and dogma, and explores promising new avenues for future research.

# Table of Contents

Dedications and Acknowledgments

Abstract

List of Tables

List of Figures

**Chapter 1: Introduction** 1

1.1 Overview 2

1.2 An overview of 7TMR biology: Signaling and Diversity 3

1.3 Role of endocytic trafficking in controlling 7TMR signal strength and duration 7

1.4 Models for protein sorting in the endocytic pathway 12

1.5 Ubiquitin as a modulator of endocytic trafficking 16

1.6 References 22

**Chapter 2: "Ubiquitination regulates proteolytic processing of G protein-coupled receptors after their sorting to lysosomes"** 33

2.1 Abstract 34

2.2-4 Introduction, Results, and Discussion 35

2.5 Acknowledgements 50

2.6 Materials and Methods 51

2.7 References 57

2.8 Figures 61

**Chapter 3: "The role of ubiquitination in lysosomal trafficking of δ-opioid receptors"** 73

3.1 Abstract 74

3.2-4 Introduction, Results, and Discussion 75

3.5 Acknowledgements 91

3.6 Materials and Methods 92

3.7 References 100

3.8 Figures 106

**Chapter 4: "Regulation of endocytic clathrin dynamics by direct ubiquitination of cargo"** 120

4.1 Abstract 121

4.2-4 Introduction, Results, and Discussion 122

4.5 Acknowledgements 145

4.6 Materials and Methods 146

4.7 References 152

4.8 Figures 162

**Chapter 5: "Ubiquitination in the first cytoplasmic loop of μ-opioid receptors reveals a hierarchical mechanism of lysosomal down-regulation"** 181

5.1 Abstract 182

5.2-4 Introduction, Results, and Discussion 183

5.5 Acknowledgements 201

5.6 Materials and Methods 202

5.7 References 209

5.8 Figures 212

**Chapter 6: Discussion** 227

6.1 Ubiquitin as a regulator of endocytosis 228

6.2 Remaining questions in the regulation of receptor endocytosis 233

6.3 Sorting at the plasma membrane 246

6.4 Two step model for protein sorting in the endocytic pathway 251

6.5 Implications for signaling and physiology 256

6.6 References 261

**Appendices** 266

Appendix 1: Protocol for subcellular fractionation to separate early and late endosomes 267

Appendix 2: Protocol for FLAG opioid receptor purification 269

Appendix 3: Protocol for assessing receptor ubiquitination via Western blot analysis 270

# List of Tables

**Chapter 5**

Supplemental Table 1: Receptor expression levels of HEK293 stable cell lines 221

# List of Figures

**Chapter 2**

Figure 1: Both DOR and DOR-0cK undergo extensive proteolysis and pharmacological down-regulation after ligand-induced endocytosis 61

Figure 2: Effect of ubiquitin ligases on DOR down-regulation 63

Figure 3: DOR undergoes AIP4-dependent lysyl-ubiquitination 65

Figure 4: AIP4 is not required for lysosomal delivery of receptors detected biochemically or by immunocytochemical localization 66

Figure 5: Endosomal deubiquitinating enzymes specifically affect down-regulation of DOR but not DOR-0cK 68

Figure 6: Proposed model for the postsorting function of AIP4 in controlling DOR down-regulation 70

Supplemental Figure 1: Saturation Binding Curves to determine receptor number in cell lines used 71

Supplemental Figure 2: Downregulation of DOR measured by radioligand binding is mediated by HRS-dependent trafficking of receptors to lysosomes 72

**Chapter 3**

Figure 1: Both DOR and DOR-0cK are efficiently excluded from the recycling pathway and can undergo transfer in ILVs of endosomes 106

Figure 2: Enlargement of endosomes by Rab5 manipulation illustrates lysyl-mutant DORs differ in their extent of transfer to ILVs 107

Figure 3: Differences in the extent of DOR transfer to ILVs can be detected by live-cell imaging of non-enlarged endosomes 108

Figure 4: Intralumenal wild type and lysyl-mutant receptors visualized using a pH-sensitive GFP variant 110

Figure 5: Differential proteolysis of N and C-terminal fragments of DOR and DOR-0cK 111

Figure 6: Analysis of the proteolytic fragmentation of lysine-mutant DORs show delayed destruction specifically of the receptor endodomain 112

Figure 7: Persistence of proteolytic cleavage products is mimicked by treatment with Wortmannin 113

Figure 8: The E3 ubiquitin ligase AIP4 regulates transfer of DORs to ILVs and subsequent C-terminal proteolysis of receptors 114

Figure 9: Model for sequential ubiquitin-independent and –dependent regulation of DOR degradation 115

Supplemental Figure 1: Subcellular localization of DOR and DOR-0cK determined by both N and C terminal epitopes 117

Supplemental Figure 2: Electron Micrographs of Late Endosomes containing F-DOR-HA and F-DOR-0cK-HA 118

Supplemental Figure 3: Attachment of GFP to the C- terminus of DOR and DOR-0cK does not affect their agonist-induced proteolysis. 119

**Chapter 4**

Figure 1: Receptor ubiquitination is required for efficient endocytosis of MOR 162

Figure 2: MOR ubiquitination is not required for receptor entry into CCPs and selectively controls surface lifetime of receptors after clustering 164

Figure 3: Lysine 94 and 96 in the first intracellular loop of MOR control the surface lifetime of receptors and are the major sites of agonist-induced MOR ubiquitination 166

Figure 4: The last 17 amino acids of MOR confer ubiquitin-dependent regulation of receptor endocytosis 168

Figure 5: MOR ubiquitination decreases the surface lifetime of clathrin and affects other cargo in MOR-containing CCPs 169

Figure 6: MOR ubiquitination controls the amount of receptor loaded into individual CCPs 170

Figure 7: Mechanism of MOR ubiquitination 171

Figure 8: Smurf-2 mediated ubiquitination of MOR controls receptor surface lifetime 173

Supplemental Figure 1: Receptor clusters imaged using TIRF-M are diffraction-limited 175

Supplemental Figure 2: Compiled analysis of the time until appearance of receptor-containing CCPs under different conditions that affect receptor ubiquitination 176

Supplemental Figure 3: The role of receptor ubiquitination on MOR endocytosis measured using SpH-tagged receptors imaged in TIRF-M 177

Supplemental Figure 4: Automated analysis of overall clathrin lifetimes in receptor-expressing cells 178

Supplemental Figure 5: Smurf2 localizes both diffusely and in CCPs after agonist-induced recruitment 178

Supplemental Figure 6: Overexpression or knockdown of Epsin1 inhibits MOR endocytosis irrespective of lysyl-mutation 179

**Chapter 5**

Figure 1: Both MOR and MORΔ17 undergo ESCRT-dependent down-regulation by lysosomes 212

Figure 2: MOR down-regulation measured radioligand binding requires receptor ubiquitination 214

Figure 3: MOR trafficking to lysosomes, assessed biochemically or immunochemically, does not require receptor ubiquitination and is dictated by the C-tail 215

Figure 4: Ubiquitination promotes receptor redistribution from the limiting to intralumenal endosome membranes 217

Figure 5: Ubiquitination specifically of the first cytoplasmic loop is necessary and sufficient for agonist-induced down-regulation measured by radioligand binding 219

Figure 6: Ubiquitination in the first cytoplasmic loop is also required for pharmacological down-regulation of the MOR1B isoform 220

Supplemental Figure 1: Colocalization of receptors with early and then late endosomes 222

Supplemental Figure 2: Image stack of enlarged Rab5-Q79L endosomes 223

Supplemental Figure 3: Specific lysine residues within the first intracellular loop mediate transfer to ILVs 225

**Chapter 6**

*Section 6.1*

Figure 1: Coexpression and activation of wildtype and lysyl-mutant MORs does not alter their trafficking 232

*Section 6.2*

Figure 1: Coordination and consequences of phosporylation on ubiquitination and ubiquitin-dependent trafficking of MORs 240

Figure 2: Assessment of the importance of the C-terminus of receptors to ubiquitin-dependent regulation 241

Figure 3: Role of single lysine residues and DUBs in MOR internalization 242

Figure 4: Role of Rab5 and its GEFs in opioid receptor endocytosis 243

Figure 5: Role of HRS and STAM in MOR endocytosis 244

*Section 6.3*

Figure 1: Dual color imaging of arrestin and 7TMRs 249

*Section 6.4*

Figure 1: B2ARs retain radioligand binding capacity long after delivery to lysosomes 254

Figure 2: B2ARs do not undergo transfer from the limiting membrane of endosomes to ILVs 255

*Section 6.5*

Figure 1: Dose response curves for cAMP generation for MOR and MOR0cK 260

# Chapter 1:

# Introduction

## 1.1 Overview

This dissertation examines the role of ubiquitination in regulating the endocytic trafficking of opioid receptors, members of the large superfamily of seven-transmembrane receptors (7TMRs). The following introduction provides a basic overview of 7TMR biology and diversity, examines the role of endocytic trafficking in modulating receptor-mediated signal strength and duration, presents current models for protein sorting in the endocytic pathway, and investigates various functions of ubiquitin in regulating trafficking decisions.

## 1.2 An overview of 7TMR biology: Signaling and Diversity

Cells must respond and adapt to a constantly changing extracellular environment. This can be accomplished through a network of different signal-transducing receptors present at the cell surface, which translate a diverse array of extracellular cues into suitable intracellular responses. The seven-transmembrane receptors (7TMRs) or G-protein coupled receptors (GPCRs) comprise the largest family of such receptors in higher eukaryotes, composed of nearly 800 discrete receptors that account for approximately 2% of the human genome (Allen and Roth, 2011). These receptors play critical roles in assorted physiological processes such as the perception of smell, taste, and sight, modulation of mood and behavior, immunity, and autonomic functions. Because of the numerous essential roles of 7TMRs in the body, their misregulation can lead to a variety of disease states (Thompson et al., 2008). This tenet also explains why 7TMRs have remained a central target for therapeutics, as approximately 40-50% of drugs on the market today act by regulating their signaling pathways (Allen and Roth, 2011).

7TMRs respond to a diverse assortment of ligands including hormones, neuropeptides, biogenic amines, odorants, sites exposed by proteolytic cleavage, and even light. Although a variety of different stimuli can activate receptors, studies of rhodopsin and adrenergic receptors suggest that 7TMRs undergo a relatively similar conformational change to become active. Receptor activation involves a rearrangement in the packing of the receptor's transmembrane helices that exposes the receptor's guanine-nucleotide

exchange factor (GEF) activity, leading to the release of GDP from the inactive Gα subunit of the heterotrimeric G protein(Rasmussen et al., 2011a; Rasmussen et al., 2011b; Rosenbaum et al., 2009). This nucleotide is rapidly replaced with GTP, present in excess in the cytoplasm, which triggers the dissociation of GTP-bound Gα from the βγ subunits. The liberation of these subunits can go on to modulate the activity of many effectors, leading to the activation of downstream signaling cascades, leaving the unoccupied receptors free to activate additional heterotrimeric G proteins (Marrari et al., 2007; Oldham and Hamm, 2008).

Although 7TMRs comprise a vast and diverse superfamily of signaling receptors, they couple to relatively few G proteins to modulate intracellular signaling. For example, humans possess only 21 Gα subunits, six Gβ subunits, and 12 Gγ subunits (Oldham and Hamm, 2008). Gα subunits themselves can be broken down into four main subgroups based on sequence similariy: $G\alpha_s$, $G\alpha_i$, $G\alpha_q$, $G\alpha_{12/13}$, which differ in their effects on second messenger production. Activation of $G\alpha_s$ stimulates adenylyl cyclase, leading to an increase in intracellular concentrations of the second messenger cyclic AMP, while $G\alpha_i$ activation inhibits cyclase activity. Additionally, $G\alpha_q$ subunits activate phospholipase C, leading to the hydrolysis of phosphatidylinositol 4,5-bisphosphate and generation of the second messengers inositol 1,4,5-trisphosphate ($IP_3$) and diacylglycerol (DAG) (McCudden et al., 2005). Generation of $IP_3$ increases the concentration of intracellular calcium by stimulating release from stores in the endoplasmic reticulum , and DAG remains in the plasma membrane and activates protein kinase C. Members of the $G_{12/13}$ subgroup can regulate the activity of RhoGTPases and lead to remodeling of the actin

cytoskeleton (Kozasa et al., 2011). Further, free Gβγ dimers can also contribute to the regulation of signaling by opening G-protein-activated inwardly rectifying potassium (GIRK) channels or inhibiting the activity of voltage-gated calcium channels (Dascal, 2001). Together, the vast array of downstream second messengers of the various G protein subunits aids in contributing to the complexity and diversity of signal modulation by 7TMRs.

The termination of signaling pathways initiated by 7TMRs is also subject to multiple levels of regulation. Homologous desensitization of the 7TMRs themselves is initiated through receptor phosphorylation by G-protein coupled receptor kinases (GRKs). GRKs are stimulated by receptor activation, allowing these kinases to discriminate between the inactive and agonist-bound forms of the receptor (Gainetdinov et al., 2004). After GRK-mediated phosphorylation has occurred, activated receptors interact with members of an important family of adaptor proteins, the arrestins. The arrestin family of proteins in mammals is composed of two visual arrestins (expressed almost exclusively in the retina) and two beta-arrestins (expressed ubiquitiously). Arrestins can recognize both the activated form of the 7TMR and the GRK phosphorylated sites and sterically prevent receptors from interacting with G proteins, promoting receptor desensitization (Luttrell and Lefkowitz, 2002). Signaling is also stopped downstream at the level of Gα subunits through their intrinsic GTPase activity, which triggers the hydrolysis of GTP to GDP and allows the reassociation of GDP-bound Gα and Gβγ subunits to reform the inactive heterotrimeric G protein. Additional control can occur through the action of another group of at least 20 proteins, the Regulators of G-protein signaling (RGS), which act as

GTPase activating proteins (GAPs) to increase the rate of hydrolysis of GTP to GDP of the Gα subunit (Nunn et al., 2006). Together, these mechanisms provide multiple points of regulation using a relatively conserved set of machinery to rapidly terminate 7TMR signaling.

Additional mechanisms are also required to not only attenuate signaling in the constant presence of agonist but also to "reset" receptors for additional rounds of stimulation. These steps involve the regulated trafficking of 7TMRs to different locales within the cell and are discussed in more detail in the following section.

## 1.3 Role of endocytic trafficking in controlling 7TMR signal strength and duration

The strength and duration of 7TMR signaling is tightly modulated by where receptors travel within in the cell and how long they remain in particular locales. Trafficking decisions in the endocytic pathway provide one mechanism to control the number of receptors at the cell surface in response to varying external stimuli. After receptor activation, many 7TMRs undergo clathrin-mediated endocytosis, a process which removes receptors from the cell surface, decreasing the number available to respond to ligand, and sequesters them away from signaling effectors at the plasma membrane. The amount of receptors can be restored by the insertion of newly-synthesized receptors to the cell surface or by rapid recycling of pre-existing receptors back to the plasma membrane, contributing to sustained cellular responsiveness in the persistent presence of ligand or to effective resensitization of the cell to another round of stimulation. Alternatively, desensitization can be prolonged and cellular responsiveness to persistent stimuli can be reduced by preventing 7TMRs from returning to the cell surface, typically through the lysosomal destruction of receptors (Sorkin and von Zastrow, 2009). This effective "balancing-act" to control receptor number provides the cell with multiple ways to respond to varying physiological conditions

Receptor endocytosis involves a precisely orchestrated series of events, involving the coordination of components of conserved endocytic machinery, accessory proteins, and the receptors themselves (Perrais and Merrifield, 2005; Toret and Drubin, 2006; Traub,

2009). Approximately 40 years of electron microscopy, biochemistry, and genetic analyses have revealed the conserved mechanisms of clathrin-mediated endocytosis. The process begins with the formation of clathrin-coated pits (CCPs), which are generated by the self-assembly of a clathrin-containing lattice and the coordinated activity of curvature-inducing and/or sensing BAR and F-BAR domain proteins and ENTH domain proteins (Brodsky et al., 2001; Itoh and De Camilli, 2006; McMahon and Boucrot, 2011; Taylor et al., 2011). Nascent CCPs are stabilized by the capture of cargoes through interaction with various adaptors or CLASPs (Ehrlich et al., 2004; Maldonado-Baez and Wendland, 2006). Arrestins, in addition to uncoupling the receptor from G proteins, also serve as specific endocytic adaptors for 7TMRs by interacting with the CCP coat components clathrin and AP-2, thereby promoting receptor entry into CCPs (Goodman et al., 1997; Goodman et al., 1996; Krupnick et al., 1997). Activated 7TMRs have been shown to enter CCPs after their formation, suggesting that they do not regulate the initial stages of coat assembly (Santini et al., 2002; Scott et al., 2002; Toshima et al., 2009). Receptor-containing CCPs later undergo membrane scission, mediated in animal cells by the GTPase dynamin (Taylor et al., 2012). A large body of work suggests that dynamin polymerizes at the neck of budding vesicles and its GTPase activity triggers a structural reorganization to promote membrane fission and the generation of endocytic vesicles (Ferguson and De Camilli, 2012). The highly-coordinated process of endocytosis effectively removes receptors from the cell surface and introduces several additional points of possible regulation for this important class of signaling receptors.

After endocytosis, receptors traffic to early endosomes which can be thought of as a sorting station within the cell. From this compartment, signaling receptors can be targeted back to the cell surface for additional rounds of signal transduction or to the lysosome for their eventual destruction. Early endosomes are characterized biochemically by the presence of the small GTPase Rab5 and its effector, EEA1 (Platta and Stenmark, 2011). Morphologically, EM studies in BHK-21cells have demonstrated that the early endosome consists of a 300-500 nm vesicular structure with several tubules protruding from it, each about 60-100 nm in diameter and up to 4 μm long (Marsh et al., 1986). The tubules emanating from early endosomes are thought to be the locations by which receptors exit this compartment on their way to the plasma membrane (Puthenveedu et al., 2010; Temkin et al., 2011). Receptors can recycle through a rapid Rab4-regulated pathway directly from the early endosome or through a slower Rab11-regulated route through the recycling endosome (Stenmark, 2009). Alternatively, ligands and some receptors can remain in the early endosome as it matures to an endolysosomal compartment. The specification of the degradative organelle as a late endosome, fusion product of late endosomes and lysosomes, or bona fide lysosome is difficult as these different compartments undergo continuous maturation, fusion, and fission, and their biochemical markers associate very transiently or remain for several steps of the maturation process. Late endosomes/multivesicular bodies (MVBs) are marked biochemically by proteins such as LAMP1 and 2 in the limiting membrane and by a number of acid hydrolases that mediate protein degradation. These organelles are generally spherical with a diameter of ~ 250-1000nm and contain many intralumenal vesicles (ILVs), about 50-100nm in diameter (Huotari and Helenius, 2011). Receptors that are destined to degrade are

incorporated into ILVs that bud inward from the limiting membrane, effectively making receptors in the membrane “soluble” and accessible to lysosomal hydrolases that are activated in the acidic environment of the endosomal lumen.

Trafficking decisions made in the endocytic pathway between these divergent paths can have opposing consequences on signal strength and duration and provide the cell with many possible points at which to introduce diversity into the repertoire of 7TMR behaviors. My thesis has largely focused on how different steps in the endocytic pathway are regulated, using opioid receptors as model 7TMR cargoes. The opioid receptor family consists of three classical members: the μ, δ, and κ opioid neuropeptide receptors, catergorized based on their pharmacology and tissue distribution, and the more recently identified nociceptin/orphanin FQ peptide receptor, identified by molecular cloning and orphan receptor analysis (Satoh and Minami, 1995; Thompson et al., 2012). These receptors mediate the action of opiates and endogenous opiate peptides such as endorphins, enkephalins, and dynorphins, playing a role in the perception of pain and in analgesia. While exogenous opiate ligands remain some of the most highly effective therapeutics for pain, their prolonged use can lead to the development of tolerance and dependence. Opioid receptors are a useful tool to examine how endocytic trafficking is regulated as some of the strongest evidence for a role of endocytic trafficking in modulating signaling comes from studies of these receptors in physiological animal models. Indeed, regulation of μ-opioid receptor (MOR) endocytosis has been implicated to play a key physiological role in the development of tolerance and physical dependence to drugs of abuse, as increasing the ability of MORs to endocytose in response to

morphine leads to enhanced antinociception, reduced tolerance, and reduced withdrawal in a mouse model (Kim et al., 2008). Thus, understanding how the trafficking of opioid receptors is regulated could aid in the development of better therapeutic agents that provide effective pain relief without the potential for tolerance or abuse. Additionally, the μ- and δ- opioid receptors (DORs) vary greatly in their postendocytic trafficking itinierary, as MORs predominantly recycle back to the cell surface after their activation while DORs efficiently undergo lysosomal destruction. Together, this receptor family serves as a useful model to examine how endocytic trafficking decisions are regulated and the basic cell biological principles mediating their efficient sorting within the endocytic pathway.

## 1.4 Models for protein sorting in the endocytic pathway

Individual classes of 7TMRs differ greatly in the degree to which they traffic back to the cell surface or to lysosomes, and a fundamental question of cell biology is how different membrane proteins are segregated from one another and targeted to different cellular locales. In principle, sorting of different cargo could be achieved at the earliest stage in the endocytic pathway, by selective entry into CCPs. Supporting this idea, some cargoes have been shown to segregate into distinct CCPs and remain separated as they traffic to different populations of early endosomes that mediate trafficking back to the cell surface or to the lysosome (Lakadamyali et al., 2006). Further, several 7TMRs are known to traffic to a subset of CCPs that are distinctly marked by the adaptor beta-arrestin (Cao et al., 1998; Mundell et al., 2006; Puthenveedu and von Zastrow, 2006). Once internalized, however, receptors that were segregated into different CCPs later appear to colocalize to the same population of early endosomes, suggesting that receptor sorting at the level of CCPs could be important in the compartmentalization of specific signaling domains at the cell surface prior to receptor internalization. Particularly intriguing, two purinergic 7TMRs were shown to cluster into distinct populations of CCPs, converge into the same set of endosomes after internalization, and then take divergent trafficking routes back to the plasma membrane or to the lysosome (Mundell et al., 2006). This suggests that sorting decisions made at this early stage of the endocytic pathway could effectively determine the later trafficking fate of different 7TMRs.

A large body of work suggests sorting of receptors also occurs at the early endosome, raising the fundamental question of how the diverse fates of receptors can be determined and executed when these proteins occupy the same compartment. Early work tested two

possible hypotheses for how recycling of receptors could be decided at the early endosome: either an active process that specifically targets receptors back to the plasma membrane, or a passive mechanism by which proteins return to the cell surface with the flux of bulk membrane. The second hypothesis is supported by the geometry of the endosome, with tubules emanating from its more vesicular core. As the surface area to volume ratio is much greater for the tubule than for the rest of the endosome, the recycling tubule selectively contains more membrane, and therefore would also be enriched with membrane proteins. Classic studies using the Transferrin receptor (TfR), a non-signaling receptor that mediates rapid uptake of iron, demonstrated that TfRs return to the cell surface through an identical trafficking route and with similar kinetics and efficiency as the membrane itself, supporting the latter hypothesis (Mayor et al., 1993). While this model is sufficient to describe how many membrane proteins recycle back to the cell surface, and how receptors can separate from their ligands, it cannot be reconciled with later studies that established some receptors are instead targeted to the lysosome. To understand how integral membrane proteins are sorted from one another, additions were made to this model, suggesting that receptor sorting to the lysosome is itself an active process that selects cargoes away from this default recycling pathway and directs them to the lysosome.

Lysosomal sorting has been proposed to occur through the removal of receptors from the limiting membrane of the endosome through the process of involution. Transferring receptors to soluble ILVs isolates them away from the recycling pathway. Biochemically, particular receptors are recognized through their direct ubiquitination and targeted to

ILVs by the ESCRT machinery, a series of complexes that contain proteins with ubiquitin-interacting motifs and mediate the involution process (reviewed extensively in (Shields and Piper, 2011)). This model of ubiquitin-directed sorting by physical removal from the endosomal membrane has been supported by an extensive body of work using the EGF receptor tyrosine kinase as a model receptor (Eden et al., 2009; Raiborg and Stenmark, 2009). After ligand addition, EGFRs can be found on intralumenal vesicles and rapidly degrade in an ESCRT-dependent manner (Babst et al., 2000; Carpenter and Cohen, 1976; Felder et al., 1990). Lysyl-mutation of EGFRs, a common manipulation used to prevent receptor ubiquitination, prevents receptors from engaging the ESCRT machinery, thereby blocking transfer to ILVs and lysosomal degradation of receptors (Eden et al., 2009; Huang et al., 2006). These studies support the idea that receptors are sorted out of the recycling pathway by their direct ubiquitination and can explain how some members of the 7TMR family are targeted for lysosomal destruction (Cottrell et al., 2006; Jacob et al., 2005; Marchese and Benovic, 2001; Marchese et al., 2003).

A growing collection of data, however, has suggested that the geometric sorting and ESCRT models are not sufficient to explain how the diverse trafficking behaviors of 7TMRs are achieved. For example, several receptors have been shown to escape both the default recycling and lysosomal pathways and instead recycle back to the cell surface through an active, regulated mechanism that depends on specific sequences present in the cytoplasmic tails of 7TMRs (Cao et al., 1999; Tanowitz and von Zastrow, 2003; Vargas and Von Zastrow, 2004). This segregation can be achieved kinetically by the selective retention away from short-lived default recycling tubules and concentration into a subset

of long-lived tubules (Puthenveedu et al., 2010). This enrichment has been shown to be accomplished for one such 7TMR, the beta-2 adrenergic receptor (B2AR), through the actions of many proteins including SNX27, the retromer complex, and actin (Lauffer et al., 2010; Puthenveedu et al., 2010; Temkin et al., 2011). Further, sequence-dependent recycling of the B2AR and MOR is regulated by HRS, a component of the ESCRT machinery, although the mechanism for such control remains poorly understood (Hanyaloglu et al., 2005). Additionally, receptor ubiquitination does not appear to be a general requirement for sorting 7TMRs away from the recycling pathway to the lysosome. The DOR utilizes the same pathway and ESCRT machinery as ubiquitin-dependent receptors but does not require ubiquitination to be targeted to lysosomes, degrading in an apparently ubiquitin-independent manner. These studies suggest that additional mechanisms exist to control the endocytic trafficking fate of many 7TMRs. My thesis work examines how such complex decisions are made in the endocytic pathway and what role ubiquitin plays in this process.

## 1.5 Ubiquitin as a modulator of endocytic trafficking

Post-translational modification of receptors provides a reversible mechanism to diversify receptor behaviors and introduce added layers of regulation. While receptor phosphorylation clearly regulates the signaling and trafficking of receptors, ubiquitination of receptors has emerged as an additional modification important in controlling this process. Ubiquitin is a 76 amino acid polypeptide that predominantly forms an isopeptide bond between its carboxy-terminal group and the ε-amino group of lysine residues of its substrate or, less frequently, with its substrate's N-terminal amino group (Sorokin et al., 2009). Alternative connections through a thioester bond with cystiene residues have also been reported (Cadwell and Coscoy, 2005), but the prevalence and importance of ubiquitination at these sites remains unknown. Ubiquitin is added to target proteins through the concerted action of a cascade of three separate enzymes. Ubiquitin forms a thioester bond with the catalytic cysteine residue of an E1 or ubiquitin-activating enzyme and is then transferred to an E2, or ubiquitin-conjugating enzyme, again through a thioester linkage. The E3 enzymes, or ubiquitin ligases, recognize the final substrate and catalyze the attachment of ubiquitin to the target protein either directly, as the HECT domain family of ligases do, or indirectly by recruiting the E2 enzymes to the substrate, as is the case for RING domain-containing E3s (Staub and Rotin, 2006). Removal of ubiquitin can also occur through an assortment of different deubiquitinating enzymes (DUBs). Ubiquitin itself possesses seven lysine residues, many of which can serve as potential sites of ubiquitination, generating polyubiquitin chains. As there are approximately 10 E1s, 100 E2s, 1000 E3 ligases, 95 putative DUBs, and multiple possibilities in terms of chain length and linkage type (Clague and Urbe, 2010; Nijman et

al., 2005; Staub and Rotin, 2006), the specific combination of particular enzymes used and the final ubiquitination status of different proteins can provide an exquisite level of specificity and diversity in modes of regulation. For example, various ubiquitin ligases and DUBs localize to particular compartments within the cell, defining their individual sites of activity and number of potential substrates. Specific linkage types and chain length also affect the regulation and fate of ubiquitinated cargo. Lysine 48-linked polyubiquitin chains general mark ubiquitinated proteins for degradation via the proteasome, while monoubiquitin and Lysine 63-linked chains often are associated with endocytic trafficking (Clague and Urbe, 2010).

Ubiquitination of 7TMRs regulates many stages in the life cycle of receptors. Ubiquitination aids in the quality control of newly synthesized receptors in the endoplasmic reticulum, labeling those that are misfolded or incompletely folded for proteasomal degradation (Cook et al., 2003; Petaja-Repo et al., 2001). After mature 7TMRs reach the plasma membrane, ubiquitination can also modulate the endocytosis of some receptors, at least in the budding yeast. Studies using the yeast *Saccharomyces cerevisiae* have shown that ubiquitination of the 2 7TMRs involved in mating, Ste2p and Ste3p, can promote efficient receptor internalization. Ste2p must undergo covalent modification with ubiquitin to efficiently internalize in response to ligand, while Ste3p requires ubiquitination for its constitutive internalization (Hicke and Riezman, 1996; Roth and Davis, 2000). Elegant experiments demonstrated that translational fusion of ubiquitin to a mutant Ste2p and Ste3p lacking their cytoplasmic tail lysines was sufficient to restore receptor endocytosis (Hicke and Riezman, 1996; Terrell et al., 1998),

suggesting that monoubiquitination, and not a specific type of polyubiquitin linkage type, serves as a sufficient signal for receptor internalization. These yeast 7TMRs must first undergo phosporylation by a family of casein kinases, rather than the GRKs found in higher eukaryotes, leading to 7TMR ubiquitination (Toshima et al., 2009). Ubiquitination of yeast 7TMRs has been proposed to promote receptor accumulation in CCPs by directly linking them to ubiquitin-interacting motifs (UIMs) present in endocytic adaptors such as Epsins and Eps15 (Hicke and Riezman, 1996; Shih et al., 2002; Torrisi et al., 1999; Toshima et al., 2009).

While mammalian homologues of Epsin and Eps15 exist and many mammalian 7TMRs undergo ligand-stimulated ubiquitination on a time scale similar to that of receptor internalization, a role for receptor ubiquitination in promoting mammalian 7TMR endocytosis has not been observed (Cottrell et al., 2006; Hislop et al., 2009; Shenoy et al., 2001; Tanowitz and Von Zastrow, 2002). Indirect roles for ubiquitin have been proposed in mediating 7TMR endocytosis in higher eukaryotes. An indirect function of ubiquitin has been proposed involving the endocytic adaptor beta-arrestin. It was shown that ubiquitination of beta-arrestin, mediated by agonist activation of the beta-2 adrenergic receptor (B2AR) by the E3 ligase Mdm2, promotes B2AR endocytosis. Additionally, while beta-arrestin and receptor ubiquitination are not required for the internalization of the protease activated receptor-1 (PAR1), PAR1 internalization depends on the ubiquitin-interacting motifs of the adaptor Epsin1(Chen et al., 2011). The importance of receptor ubiquitination in PAR1 endocytosis remains unclear, as preventing PAR1 ubiquitination only manifests a defect in internalization with

concomitant knockdown of Epsin 1 and manipulations that block endocytosis decrease agonist-induced ubiquitination of PAR1, suggesting substantial ubiquitination occurs after endocytosis (Chen et al., 2011; Wolfe et al., 2007). Direct ubiquitination has been implicated to play a role in the endocytosis of many other membrane proteins in higher eukaryotes, however, such as EGFRs and ion and neurotransmitter transporters (Kazazic et al., 2009; Rotin and Staub, 2010; Sorkina et al., 2006). How ubiquitination regulates the endocytosis of different membrane proteins and whether direct ubiquitination plays a role in the endocytosis of any mammalian 7TMR is not known.

A clear role for ubiquitination has been shown in the later post-endocytic sorting of many 7TMRs in higher eukaryotes. A number of mammalian 7TMRs undergo ubiquitination in response to agonist-induced activation that is required for their efficient lysosomal destruction (Cottrell et al., 2006; Jacob et al., 2005; Marchese and Benovic, 2001; Martin et al., 2003; Shenoy et al., 2001). For example, the neurokinin-1 receptor, protease-activated receptor 2, and the chemokine receptor CXCR4 are ubiquitinated after their activation, and preventing their ubiquitination, either through lysyl-mutation or by manipulations of specific E3 ubiquitin ligases, inhibits the lysosomal destruction of receptors and promotes their recycling back to the cell surface (Cottrell et al., 2006; Jacob et al., 2005; Marchese and Benovic, 2001; Marchese et al., 2003). Degradation of many 7TMRs requires components of the ESCRT machinery, which play a multi-functional role in mediating receptor downregulation (Hasdemir et al., 2007; Hislop et al., 2009; Hislop et al., 2011; Marchese et al., 2003). Ubiquitinated receptors are thought to be selected for destruction by interactions with the ubiquitin-interacting motifs (UIMs)

within components of the ESCRT-0 complex, composed of hepatocyte growth factor-regulated tyrosine kinase substrate (HRS) and the signal-transducing adaptor molecule (STAM) (Raiborg and Stenmark, 2009). ESCRT-0 links to the additional complexes, ESCRT-I through III, some of which contain additional UIMs, and the interaction between 7TMRs and the ESCRTs is thought to lead to their transfer onto ILVs for ultimate destruction. Receptor deubiquitination has also been shown to promote receptor recycling and resensitization after prolonged agonist stimulation for the B2AR (Berthouze et al., 2009), supporting a mechanism by which selective ubiquitination and deubiquitination can dynamically regulate the trafficking fate of receptors.

A number of studies have supported a model for 7TMR destruction by which ubiquitination of 7TMRs mediates their engagement with the ESCRT machinery and later transfer onto ILVs, physically isolating receptors away from the recycling path as a means of post-endocytic sorting. However, recent work provides several lines of evidence that cannot be explained by this model. For example, the Stenmark lab examined various components of the ESCRT and demonstrated that the involution step is not required for the degradative sorting of receptor cargo; instead, all that is required is ubiquitin-mediated scaffolding of receptors into the ESCRT domain of the endosomal membrane (Raiborg et al., 2008). Further, the yeast 7TMR Ste3p recycles and undergoes turnover in an essentially ubiquitin-independent manner. Ste3p ubiquitination, instead, appears to specifically modulate the amount of receptor found on ILVs (Chen and Davis, 2002). Studies from our lab have shown that while the lysosomal trafficking of the mammalian 7TMR DOR requires the conserved ESCRT machinery, it does not require

receptor ubiquitination and can be regulated by ubiquitin-independent protein interactions (Marley and von Zastrow, 2010; Whistler et al., 2002). These observations suggest that DOR uses the same core endocytic mechanism as ubiquitination-dependent membrane cargo but question whether ubiquitination of DOR plays any role in its destruction.

My thesis examines the role of ubiquitin in controlling the trafficking of opioid receptors in the endocytic pathway, focusing on DOR and MOR. These receptors provide a useful tool to gain insight into endocytosis and post-endocytic sorting mechanisms, as their trafficking behavior and specific regulation cannot be easily explained by existing models. By investigating how these receptors utilize ubiquitin to regulate important trafficking decisions, this thesis attempts to suggest previously unanticipated points of regulation in the life cycle of the largest known family of signaling receptors in higher eukaryotes.

## 1.6 References

Allen, J. A., and Roth, B. L. (2011). Strategies to discover unexpected targets for drugs active at G protein-coupled receptors. Annu Rev Pharmacol Toxicol *51*, 117-144.

Babst, M., Odorizzi, G., Estepa, E. J., and Emr, S. D. (2000). Mammalian tumor susceptibility gene 101 (TSG101) and the yeast homologue, Vps23p, both function in late endosomal trafficking. Traffic *1*, 248-258.

Berthouze, M., Venkataramanan, V., Li, Y., and Shenoy, S. K. (2009). The deubiquitinases USP33 and USP20 coordinate beta2 adrenergic receptor recycling and resensitization. Embo J *28*, 1684-1696.

Brodsky, F. M., Chen, C. Y., Knuehl, C., Towler, M. C., and Wakeham, D. E. (2001). Biological basket weaving: formation and function of clathrin-coated vesicles. Annu Rev Cell Dev Biol *17*, 517-568.

Cadwell, K., and Coscoy, L. (2005). Ubiquitination on nonlysine residues by a viral E3 ubiquitin ligase. Science *309*, 127-130.

Cao, T. T., Deacon, H. W., Reczek, D., Bretscher, A., and von Zastrow, M. (1999). A kinase-regulated PDZ-domain interaction controls endocytic sorting of the beta2-adrenergic receptor. Nature *401*, 286-290.

Cao, T. T., Mays, R. W., and von Zastrow, M. (1998). Regulated endocytosis of G-protein-coupled receptors by a biochemically and functionally distinct subpopulation of clathrin-coated pits. J Biol Chem *273*, 24592-24602.

Carpenter, G., and Cohen, S. (1976). 125I-labeled human epidermal growth factor. Binding, internalization, and degradation in human fibroblasts. J Cell Biol *71*, 159-171.

Chen, B., Dores, M. R., Grimsey, N., Canto, I., Barker, B. L., and Trejo, J. (2011). Adaptor protein complex-2 (AP-2) and epsin-1 mediate protease-activated receptor-1 internalization via phosphorylation- and ubiquitination-dependent sorting signals. J Biol Chem *286*, 40760-40770.

Chen, L., and Davis, N. G. (2002). Ubiquitin-independent entry into the yeast recycling pathway. Traffic *3*, 110-123.

Clague, M. J., and Urbe, S. (2010). Ubiquitin: same molecule, different degradation pathways. Cell *143*, 682-685.

Cook, L. B., Zhu, C. C., and Hinkle, P. M. (2003). Thyrotropin-releasing hormone receptor processing: role of ubiquitination and proteasomal degradation. Mol Endocrinol *17*, 1777-1791.

Cottrell, G. S., Padilla, B., Pikios, S., Roosterman, D., Steinhoff, M., Gehringer, D., Grady, E. F., and Bunnett, N. W. (2006). Ubiquitin-dependent down-regulation of the neurokinin-1 receptor. J Biol Chem *281*, 27773-27783.

Dascal, N. (2001). Ion-channel regulation by G proteins. Trends Endocrinol Metab *12*, 391-398.

Eden, E. R., White, I. J., and Futter, C. E. (2009). Down-regulation of epidermal growth factor receptor signalling within multivesicular bodies. Biochem Soc Trans *37*, 173-177.

Ehrlich, M., Boll, W., Van Oijen, A., Hariharan, R., Chandran, K., Nibert, M. L., and Kirchhausen, T. (2004). Endocytosis by random initiation and stabilization of clathrin-coated pits. Cell *118*, 591-605.

Felder, S., Miller, K., Moehren, G., Ullrich, A., Schlessinger, J., and Hopkins, C. R. (1990). Kinase activity controls the sorting of the epidermal growth factor receptor within the multivesicular body. Cell *61*, 623-634.

Ferguson, S. M., and De Camilli, P. (2012). Dynamin, a membrane-remodelling GTPase. Nat Rev Mol Cell Biol *13*, 75-88.

Gainetdinov, R. R., Premont, R. T., Bohn, L. M., Lefkowitz, R. J., and Caron, M. G. (2004). Desensitization of G protein-coupled receptors and neuronal functions. Annu Rev Neurosci *27*, 107-144.

Goodman, O. B., Jr., Krupnick, J. G., Gurevich, V. V., Benovic, J. L., and Keen, J. H. (1997). Arrestin/clathrin interaction. Localization of the arrestin binding locus to the clathrin terminal domain. J Biol Chem *272*, 15017-15022.

Goodman, O. B., Jr., Krupnick, J. G., Santini, F., Gurevich, V. V., Penn, R. B., Gagnon, A. W., Keen, J. H., and Benovic, J. L. (1996). Beta-arrestin acts as a clathrin adaptor in endocytosis of the beta2-adrenergic receptor. Nature *383*, 447-450.

Hanyaloglu, A. C., McCullagh, E., and von Zastrow, M. (2005). Essential role of Hrs in a recycling mechanism mediating functional resensitization of cell signaling. Embo J *24*, 2265-2283.

Hasdemir, B., Bunnett, N. W., and Cottrell, G. S. (2007). Hepatocyte growth factor-regulated tyrosine kinase substrate (HRS) mediates post-endocytic trafficking of protease-activated receptor 2 and calcitonin receptor-like receptor. J Biol Chem *282*, 29646-29657.

Hicke, L., and Riezman, H. (1996). Ubiquitination of a yeast plasma membrane receptor signals its ligand-stimulated endocytosis. Cell *84*, 277-287.

Hislop, J. N., Henry, A. G., Marchese, A., and von Zastrow, M. (2009). Ubiquitination regulates proteolytic processing of G protein-coupled receptors after their sorting to lysosomes. J Biol Chem *284*, 19361-19370.

Hislop, J. N., Henry, A. G., and von Zastrow, M. (2011). Ubiquitination in the first cytoplasmic loop of {micro}-opioid receptors reveals a hierarchical mechanism of lysosomal downregulation. J Biol Chem.

Huang, F., Kirkpatrick, D., Jiang, X., Gygi, S., and Sorkin, A. (2006). Differential regulation of EGF receptor internalization and degradation by multiubiquitination within the kinase domain. Mol Cell *21*, 737-748.

Huotari, J., and Helenius, A. (2011). Endosome maturation. Embo J *30*, 3481-3500.

Itoh, T., and De Camilli, P. (2006). BAR, F-BAR (EFC) and ENTH/ANTH domains in the regulation of membrane-cytosol interfaces and membrane curvature. Biochim Biophys Acta *1761*, 897-912.

Jacob, C., Cottrell, G. S., Gehringer, D., Schmidlin, F., Grady, E. F., and Bunnett, N. W. (2005). c-Cbl mediates ubiquitination, degradation, and down-regulation of human protease-activated receptor 2. J Biol Chem *280*, 16076-16087.

Kazazic, M., Bertelsen, V., Pedersen, K. W., Vuong, T. T., Grandal, M. V., Rodland, M. S., Traub, L. M., Stang, E., and Madshus, I. H. (2009). Epsin 1 is involved in recruitment of ubiquitinated EGF receptors into clathrin-coated pits. Traffic *10*, 235-245.

Kim, J. A., Bartlett, S., He, L., Nielsen, C. K., Chang, A. M., Kharazia, V., Waldhoer, M., Ou, C. J., Taylor, S., Ferwerda, M., *et al.* (2008). Morphine-induced receptor endocytosis in a novel knockin mouse reduces tolerance and dependence. Curr Biol *18*, 129-135.

Kozasa, T., Hajicek, N., Chow, C. R., and Suzuki, N. (2011). Signalling mechanisms of RhoGTPase regulation by the heterotrimeric G proteins G12 and G13. J Biochem *150*, 357-369.

Krupnick, J. G., Goodman, O. B., Jr., Keen, J. H., and Benovic, J. L. (1997). Arrestin/clathrin interaction. Localization of the clathrin binding domain of nonvisual arrestins to the carboxy terminus. J Biol Chem *272*, 15011-15016.

Lakadamyali, M., Rust, M. J., and Zhuang, X. (2006). Ligands for clathrin-mediated endocytosis are differentially sorted into distinct populations of early endosomes. Cell *124*, 997-1009.

Lauffer, B. E., Melero, C., Temkin, P., Lei, C., Hong, W., Kortemme, T., and von Zastrow, M. (2010). SNX27 mediates PDZ-directed sorting from endosomes to the plasma membrane. J Cell Biol *190*, 565-574.

Luttrell, L. M., and Lefkowitz, R. J. (2002). The role of beta-arrestins in the termination and transduction of G-protein-coupled receptor signals. J Cell Sci *115*, 455-465.

Maldonado-Baez, L., and Wendland, B. (2006). Endocytic adaptors: recruiters, coordinators and regulators. Trends Cell Biol *16*, 505-513.

Marchese, A., and Benovic, J. L. (2001). Agonist-promoted ubiquitination of the G protein-coupled receptor CXCR4 mediates lysosomal sorting. J Biol Chem *276*, 45509-45512.

Marchese, A., Raiborg, C., Santini, F., Keen, J. H., Stenmark, H., and Benovic, J. L. (2003). The E3 ubiquitin ligase AIP4 mediates ubiquitination and sorting of the G protein-coupled receptor CXCR4. Dev Cell *5*, 709-722.

Marley, A., and von Zastrow, M. (2010). Dysbindin promotes the post-endocytic sorting of G protein-coupled receptors to lysosomes. PLoS One *5*, e9325.

Marrari, Y., Crouthamel, M., Irannejad, R., and Wedegaertner, P. B. (2007). Assembly and trafficking of heterotrimeric G proteins. Biochemistry *46*, 7665-7677.

Marsh, M., Griffiths, G., Dean, G. E., Mellman, I., and Helenius, A. (1986). Three-dimensional structure of endosomes in BHK-21 cells. Proc Natl Acad Sci U S A *83*, 2899-2903.

Martin, N. P., Lefkowitz, R. J., and Shenoy, S. K. (2003). Regulation of V2 vasopressin receptor degradation by agonist-promoted ubiquitination. J Biol Chem *278*, 45954-45959.

Mayor, S., Presley, J. F., and Maxfield, F. R. (1993). Sorting of membrane components from endosomes and subsequent recycling to the cell surface occurs by a bulk flow process. J Cell Biol *121*, 1257-1269.

McCudden, C. R., Hains, M. D., Kimple, R. J., Siderovski, D. P., and Willard, F. S. (2005). G-protein signaling: back to the future. Cell Mol Life Sci *62*, 551-577.

McMahon, H. T., and Boucrot, E. (2011). Molecular mechanism and physiological functions of clathrin-mediated endocytosis. Nat Rev Mol Cell Biol *12*, 517-533.

Mundell, S. J., Luo, J., Benovic, J. L., Conley, P. B., and Poole, A. W. (2006). Distinct clathrin-coated pits sort different G protein-coupled receptor cargo. Traffic *7*, 1420-1431.

Nijman, S. M., Luna-Vargas, M. P., Velds, A., Brummelkamp, T. R., Dirac, A. M., Sixma, T. K., and Bernards, R. (2005). A genomic and functional inventory of deubiquitinating enzymes. Cell *123*, 773-786.

Nunn, C., Mao, H., Chidiac, P., and Albert, P. R. (2006). RGS17/RGSZ2 and the RZ/A family of regulators of G-protein signaling. Semin Cell Dev Biol *17*, 390-399.

Oldham, W. M., and Hamm, H. E. (2008). Heterotrimeric G protein activation by G-protein-coupled receptors. Nat Rev Mol Cell Biol *9*, 60-71.

Perrais, D., and Merrifield, C. J. (2005). Dynamics of endocytic vesicle creation. Dev Cell *9*, 581-592.

Petaja-Repo, U. E., Hogue, M., Laperriere, A., Bhalla, S., Walker, P., and Bouvier, M. (2001). Newly synthesized human delta opioid receptors retained in the endoplasmic reticulum are retrotranslocated to the cytosol, deglycosylated, ubiquitinated, and degraded by the proteasome. J Biol Chem *276*, 4416-4423.

Platta, H. W., and Stenmark, H. (2011). Endocytosis and signaling. Curr Opin Cell Biol *23*, 393-403.

Puthenveedu, M. A., Lauffer, B., Temkin, P., Vistein, R., Carlton, P., Thorn, K., Taunton, J., Weiner, O. D., Parton, R. G., and von Zastrow, M. (2010). Sequence-dependent sorting of recycling proteins by actin-stabilized endosomal microdomains. Cell *143*, 761-773.

Puthenveedu, M. A., and von Zastrow, M. (2006). Cargo regulates clathrin-coated pit dynamics. Cell *127*, 113-124.

Raiborg, C., Malerod, L., Pedersen, N. M., and Stenmark, H. (2008). Differential functions of Hrs and ESCRT proteins in endocytic membrane trafficking. Exp Cell Res *314*, 801-813.

Raiborg, C., and Stenmark, H. (2009). The ESCRT machinery in endosomal sorting of ubiquitylated membrane proteins. Nature *458*, 445-452.

Rasmussen, S. G., Choi, H. J., Fung, J. J., Pardon, E., Casarosa, P., Chae, P. S., Devree, B. T., Rosenbaum, D. M., Thian, F. S., Kobilka, T. S., *et al.* (2011a). Structure of a nanobody-stabilized active state of the beta(2) adrenoceptor. Nature *469*, 175-180.

Rasmussen, S. G., DeVree, B. T., Zou, Y., Kruse, A. C., Chung, K. Y., Kobilka, T. S., Thian, F. S., Chae, P. S., Pardon, E., Calinski, D., *et al.* (2011b). Crystal structure of the beta2 adrenergic receptor-Gs protein complex. Nature *477*, 549-555.

Rosenbaum, D. M., Rasmussen, S. G., and Kobilka, B. K. (2009). The structure and function of G-protein-coupled receptors. Nature *459*, 356-363.

Roth, A. F., and Davis, N. G. (2000). Ubiquitination of the PEST-like endocytosis signal of the yeast a-factor receptor. J Biol Chem *275*, 8143-8153.

Rotin, D., and Staub, O. (2010). Role of the ubiquitin system in regulating ion transport. Pflugers Arch *461*, 1-21.

Santini, F., Gaidarov, I., and Keen, J. H. (2002). G protein-coupled receptor/arrestin3 modulation of the endocytic machinery. J Cell Biol *156*, 665-676.

Satoh, M., and Minami, M. (1995). Molecular pharmacology of the opioid receptors. Pharmacol Ther *68*, 343-364.

Scott, M. G., Benmerah, A., Muntaner, O., and Marullo, S. (2002). Recruitment of activated G protein-coupled receptors to pre-existing clathrin-coated pits in living cells. J Biol Chem *277*, 3552-3559.

Shenoy, S. K., McDonald, P. H., Kohout, T. A., and Lefkowitz, R. J. (2001). Regulation of receptor fate by ubiquitination of activated beta 2-adrenergic receptor and beta-arrestin. Science *294*, 1307-1313.

Shields, S. B., and Piper, R. C. (2011). How ubiquitin functions with ESCRTs. Traffic *12*, 1306-1317.

Shih, S. C., Katzmann, D. J., Schnell, J. D., Sutanto, M., Emr, S. D., and Hicke, L. (2002). Epsins and Vps27p/Hrs contain ubiquitin-binding domains that function in receptor endocytosis. Nat Cell Biol *4*, 389-393.

Sorkin, A., and von Zastrow, M. (2009). Endocytosis and signalling: intertwining molecular networks. Nat Rev Mol Cell Biol *10*, 609-622.

Sorkina, T., Miranda, M., Dionne, K. R., Hoover, B. R., Zahniser, N. R., and Sorkin, A. (2006). RNA interference screen reveals an essential role of Nedd4-2 in dopamine transporter ubiquitination and endocytosis. J Neurosci *26*, 8195-8205.

Sorokin, A. V., Kim, E. R., and Ovchinnikov, L. P. (2009). Proteasome system of protein degradation and processing. Biochemistry (Mosc) *74*, 1411-1442.

Staub, O., and Rotin, D. (2006). Role of ubiquitylation in cellular membrane transport. Physiol Rev *86*, 669-707.

Stenmark, H. (2009). Rab GTPases as coordinators of vesicle traffic. Nat Rev Mol Cell Biol *10*, 513-525.

Tanowitz, M., and Von Zastrow, M. (2002). Ubiquitination-independent trafficking of G protein-coupled receptors to lysosomes. J Biol Chem *277*, 50219-50222.

Tanowitz, M., and von Zastrow, M. (2003). A novel endocytic recycling signal that distinguishes the membrane trafficking of naturally occurring opioid receptors. J Biol Chem *278*, 45978-45986.

Taylor, M. J., Lampe, M., and Merrifield, C. J. (2012). A feedback loop between dynamin and actin recruitment during clathrin-mediated endocytosis. PLoS Biol *10*, e1001302.

Taylor, M. J., Perrais, D., and Merrifield, C. J. (2011). A high precision survey of the molecular dynamics of mammalian clathrin-mediated endocytosis. PLoS Biol *9*, e1000604.

Temkin, P., Lauffer, B., Jager, S., Cimermancic, P., Krogan, N. J., and von Zastrow, M. (2011). SNX27 mediates retromer tubule entry and endosome-to-plasma membrane trafficking of signalling receptors. Nat Cell Biol *13*, 715-721.

Terrell, J., Shih, S., Dunn, R., and Hicke, L. (1998). A function for monoubiquitination in the internalization of a G protein-coupled receptor. Mol Cell *1*, 193-202.

Thompson, A. A., Liu, W., Chun, E., Katritch, V., Wu, H., Vardy, E., Huang, X. P., Trapella, C., Guerrini, R., Calo, G., *et al.* (2012). Structure of the nociceptin/orphanin FQ receptor in complex with a peptide mimetic. Nature *485*, 395-399.

Thompson, M. D., Percy, M. E., McIntyre Burnham, W., and Cole, D. E. (2008). G protein-coupled receptors disrupted in human genetic disease. Methods Mol Biol *448*, 109-137.

Toret, C. P., and Drubin, D. G. (2006). The budding yeast endocytic pathway. J Cell Sci *119*, 4585-4587.

Torrisi, M. R., Lotti, L. V., Belleudi, F., Gradini, R., Salcini, A. E., Confalonieri, S., Pelicci, P. G., and Di Fiore, P. P. (1999). Eps15 is recruited to the plasma membrane upon epidermal growth factor receptor activation and localizes to components of the endocytic pathway during receptor internalization. Mol Biol Cell *10*, 417-434.

Toshima, J. Y., Nakanishi, J. I., Mizuno, K., Toshima, J., and Drubin, D. G. (2009). Requirements for Recruitment of a G Protein-coupled Receptor to Clathrin-coated Pits in Budding Yeast. Mol Biol Cell.

Traub, L. M. (2009). Tickets to ride: selecting cargo for clathrin-regulated internalization. Nat Rev Mol Cell Biol *10*, 583-596.

Vargas, G. A., and Von Zastrow, M. (2004). Identification of a novel endocytic recycling signal in the D1 dopamine receptor. J Biol Chem *279*, 37461-37469.

Whistler, J. L., Enquist, J., Marley, A., Fong, J., Gladher, F., Tsuruda, P., Murray, S. R., and Von Zastrow, M. (2002). Modulation of postendocytic sorting of G protein-coupled receptors. Science *297*, 615-620.

Wolfe, B. L., Marchese, A., and Trejo, J. (2007). Ubiquitination differentially regulates clathrin-dependent internalization of protease-activated receptor-1. J Cell Biol *177*, 905-916.

Yudowski, G. A., Puthenveedu, M. A., Henry, A. G., and von Zastrow, M. (2009). Cargo-mediated regulation of a rapid Rab4-dependent recycling pathway. Mol Biol Cell *20*, 2774-2784.

# Chapter 2: “Ubiquitination regulates proteolytic processing of G protein-coupled receptors after their sorting to lysosomes”

Anastasia Henry generated constructs, performed preliminary experiments, and contributed to the experimental design and data interpretation. The majority of the experiments were conceived and executed by James Hislop in the von Zastrow lab. The manuscript was written by James Hislop, Anastasia Henry, and Mark von Zastrow.

## 2.1 Abstract

Ubiquitination is essential for the endocytic sorting of various G protein-coupled receptors to lysosomes. Here we identify a distinct function of this covalent modification in controlling the later proteolytic processing of receptors. Mutation of all cytoplasmic lysine residues in the murine delta-opioid receptor blocked receptor ubiquitination without preventing ligand-induced endocytosis of receptors or their subsequent delivery to lysosomes, as verified by proteolysis of extramembrane epitope tags and down-regulation of radioligand binding to the transmembrane helices. Surprisingly, a functional screen revealed that the E3 ubiquitin ligase AIP4 specifically controls down-regulation of wild type receptors measured by radioligand binding without detectably affecting receptor delivery to lysosomes defined both immunochemically and biochemically. This specific AIP4-dependent regulation required direct ubiquitination of receptors and was also regulated by two deubiquitinating enzymes, AMSH and UBPY, which localized to late endosome/lysosome membranes containing internalized delta-opioid receptor. These results identify a distinct function of AIP4-dependent ubiquitination in controlling the later proteolytic processing of G protein-coupled receptors, without detectably affecting their endocytic sorting to lysosomes. We propose that ubiquitination or ubiquitination/deubiquitination cycling specifically regulates later proteolytic processing events required for destruction of the receptor's hydrophobic core.

## 2.2 Introduction

A fundamental cellular mechanism contributing to homeostatic regulation of receptor-mediated signal transduction involves ligand-induced endocytosis of receptors followed by proteolysis in lysosomes. The importance of such proteolytic down-regulation has been documented extensively for a number of seven-transmembrane or G protein-coupled receptors (GPCRs),[3] which comprise the largest known family of signaling receptors expressed in animals, as well as for other important signaling receptors, such as the epidermal growth factor receptor tyrosine kinase (1–5).

One GPCR that is well known to undergo endocytic trafficking to lysosomes is the δ-opioid peptide receptor (DOR or DOP-R) (6). Following endocytosis, DOR traffics efficiently to lysosomes in both neural and heterologous cell models (6–8), whereas many membrane proteins, including various GPCRs, recycle rapidly to the plasma membrane (9–12). Such molecular sorting of internalized receptors between divergent recycling and degradative pathways is thought to play a fundamental role in determining the functional consequences of regulated endocytosis (2, 3, 13, 14). The sorting process that directs internalized DOR to lysosomes is remarkably efficient and appears to occur rapidly (within several min) after receptor endocytosis (11). Nevertheless, biochemical mechanisms that control lysosomal trafficking and proteolysis of DOR remain poorly understood.

A conserved mechanism that promotes lysosomal trafficking of a number of membrane proteins, including various signaling receptors, is mediated by covalent modification of cytoplasmic lysine residues with ubiquitin (4, 15–17). Ubiquitination was first identified as an endocytic sorting determinant in studies of vacuolar trafficking of the yeast GPCR

Ste2p (18). Subsequent studies have established numerous examples of lysyl-ubiquitination being required for sorting endocytic cargo to lysosomes and have identified conserved machinery responsible for the targeting of ubiquitinated cargo to lysosomes (3, 17, 19–22).

The CXCR4 chemokine receptor provides a clear example of ubiquitin-dependent lysosomal sorting of a mammalian GPCR. Ubiquitination of the carboxyl-terminal cytoplasmic domain of the CXCR4 receptor, mediated by the E3 ubiquitin ligase AIP4, is specifically required for the HRS- and VPS4-dependent trafficking of internalized receptors to lysosomes. Blocking this ubiquitination event by Lys → Arg mutation of the receptor specifically inhibits trafficking of internalized receptors to lysosomes, resulting in recycling rather than lysosomal proteolysis of receptors after ligand-induced endocytosis (23–25).

Lysosomal trafficking of DOR, in contrast, is not prevented by mutation of cytoplasmic lysine residues (26) and can be regulated by ubiquitination-independent protein interaction(s) (27, 28). Nevertheless, both wild type and lysyl-mutant DORs traffic to lysosomes via a similar pathway as ubiquitin-dependent membrane cargo and require both HRS and active VPS4 to do so (29). These observations indicate that DOR engages the same core endocytic mechanism utilized by ubiquitination-directed membrane cargo but leave unresolved whether ubiquitination of DOR plays any role in this important cellular mechanism of receptor down-regulation.

There is no doubt that DOR can undergo significant ubiquitination in mammalian cells, including HEK293 cells (30–32), where lysosomal trafficking of lysyl-mutant receptors was first observed (26). Ubiquitination was shown previously to promote proteolysis of

DOR by proteasomes and to function in degrading misfolded receptors from the biosynthetic pathway (30, 31). A specific role of ubiquitination in promoting proteasome- but not lysosome-mediated proteolysis of DOR has been emphasized (32) and proposed to contribute to proteolytic down-regulation of receptors also from the plasma membrane (33).

To our knowledge, no previous studies have determined if DOR ubiquitination plays any role in controlling receptor proteolysis mediated by lysosomes, although this represents a predominant pathway by which receptors undergo rapid down-regulation following ligand-induced endocytosis in a number of cell types, including HEK293 cells (8). In the present study, we have taken two approaches to addressing this fundamental question. First, we have investigated in greater detail the effects of lysyl-mutation on DOR ubiquitination and trafficking. Second, we have independently investigated the role of ubiquitination in controlling lysosomal proteolysis of wild type DOR. Our results clearly establish the ability of DOR to traffic efficiently to lysosomes in the absence of any detectable ubiquitination. Further, they identify a distinct and unanticipated function of AIP4-dependent ubiquitination in regulating the later proteolytic processing of receptors and show that this distinct ubiquitin-dependent regulatory mechanism operates effectively downstream of the sorting decision that commits internalized receptors for delivery to lysosomes.

## 2.3 Results

*Ubiquitination-independent Down-regulation of DOR*

Previous findings indicated that mutation of all cytoplasmic lysine residues in the murine DOR does not prevent proteolytic down-regulation of receptors mediated by endosomal sorting complex required for transport (ESCRT)-dependent trafficking of internalized receptors to lysosomes (26, 29). This was unexpected, because lysyl-ubiquitination is known to be essential for lysosomal trafficking of several other GPCRs (3) and because DOR is known to undergo extensive ubiquitination in intact cells (30, 32). Because our previous analysis of receptor proteolysis relied primarily on biochemical detection of a FLAG epitope tag engineered into the $NH_2$-terminal ectodomain of the receptor (F-DOR), we considered the possibility that receptor proteolysis detected in our previous work might reflect limited proteolysis of the proximal $NH_2$-terminal ectodomain, perhaps analogous to proteolytic "shaving" reported for the Ste3p seven-transmembrane receptor in yeast (37). Such limited proteolysis might be insufficient to destroy receptor function, since mutational studies indicate that the proximal $NH_2$ terminus of opioid receptors is not essential for ligand binding (37–39).

To further evaluate the ubiquitination dependence of receptor proteolysis, we engineered a distinct (HA) epitope tag into the COOH-terminal endodomain of F-DOR and F-DOR-0cK (F-DOR-HA and F-DOR-0cK-HA), to allow monitoring of receptor proteolysis involving both ends of the receptor protein in the primary structure on both sides of the membrane. Stable cell lines generated from these constructs showed expression levels of between 1 and 2 fmol/μg for all constructs used (supplemental Fig. 1), an expression

level that is on a similar order as that reported endogenously in the brain (40) and one at which efficient endocytic sorting of receptors occurs in HEK293 cells (11). To specifically follow the fate of the mature surface receptor, HEK293 cells stably expressing F-DOR-HA were labeled by surface biotinylation, and proteolysis of receptors was evaluated by streptavidin affinity purification and immunoblotting after incubating cells for various time periods with an agonist ligand (10μM concentration of the opioid peptide analogue DADLE) that promotes receptor endocytosis. Anti-FLAG blotting confirmed that the $NH_2$-terminal ectodomains of both the wild type (F-DOR-HA) and lysyl-mutant (F- DOR-0cK-HA) receptors were fully proteolyzed within 2–3 h after ligand-induced endocytosis (Fig. 1*A*, *left*), consistent with previous studies using this approach. Significantly, a similarly rapid time course of receptor proteolysis was observed when anti-HA blotting was assessed (Fig. 1*A*, *right*). This loss of COOH-terminal immunoreactivity was not simply the result of loss of ectodomain-linked biotin used to label surface receptors, since extensive proteolysis was also evident by immunoblotting of whole cell extracts prior to streptavidin purification (Fig. 1*B*). Further, this analysis revealed a "ladder" of HA-immunoreactive fragments derived from both F-DOR-HA and F-DOR-0cK-HA, which appeared over a similar time course after DADLE application to cells. Together, these results indicate that both wild type and lysyl-mutant receptors undergo extensive proteolytic fragmentation following ligand-induced endocytosis.

As another approach to verify efficient lysosomal proteolysis of lysyl-mutant opioid receptors (DOR-0cK), we assessed proteolytic down-regulation of receptors by loss of

receptor-mediated binding of the small molecule radioligand antagonist, [$^3$H]diprenorphine. Mutational studies indicate that diprenorphine interacts primarily with residues located in the transmembrane helical structure of the receptor protein rather than with the receptor ectodomain (39). This intramembrane binding site is also essential for association of physiologically relevant opioid peptides with receptors, although high affinity binding of opioid peptides also requires residues present in extracellular loops (41). Thus, diprenorphine binding represents an independent measure of receptor proteolysis, which is sensitive to the integrity of the receptor's hydrophobic core. Time course analysis indicated that both wild type and lysyl-mutant receptors exhibited pharmacological down-regulation with similarly rapid kinetics (Fig. 1*C*), which were comparable with (albeit slightly slower than) the kinetics of proteolytic fragmentation estimated biochemically by ecto- and endodomain immunoblotting (Fig. 1*A*) (see also Refs. 26 and 29). Moreover, as expected, down-regulation of both F-DOR and F-DOR-0cK measured pharmacologically by [$^3$H]diprenorphine binding was inhibited both by the classical inhibitor of lysosomal proteolysis chloroquine and by overexpression of HRS (supplemental Fig. 2). Taken together, these data verify definitively that the DOR-0cK lysyl-mutant receptor does indeed undergo efficient proteolytic degradation following ligand-induced endocytosis, like wild type receptors, and does so via HRS-dependent trafficking to lysosomes.

Although lysyl-mutant receptors were clearly able to undergo extensive proteolysis by lysosomes, careful comparison of the pharmacological results revealed a small reduction in the extent of down-regulation of DOR-0cK (compared with wild type DOR) measured

by radioligand binding. Although relatively subtle at all time points, this effect was most noticeable at later time points (>3 h) after endocytosis of receptors. Proteolytic fragmentation of receptors assessed biochemically was already extensive by this time, suggesting that lysyl-mutation affects a relatively late stage in a progressive process of receptor destruction. This quantitative difference in pharmacological down-regulation, although small in absolute magnitude, was statistically significant when evaluated in multiple expression-matched cell clones (Fig. 1*D*).

*The E3 Ligase, AIP4, Specifically Controls Pharmacological Down-regulation of Wild Type DOR*

Such kinetic effects could represent a secondary consequence of introducing multiple lysyl-mutations into the receptor, but might also reflect the existence of some previously unappreciated ubiquitin-dependent regulation. To distinguish these possibilities, we focused on wild type receptors and devised a screen to search for ubiquitin ligase(s) that influence ligand-induced down-regulation. A number of E3 ligases have been implicated in lysosomal sorting and/or pharmacological down-regulation of signaling receptors in mammalian cells, specifically two RING finger ligases (c-Cbl and Mdm2) (42–45) and several HECT domain ligases, including Nedd4 and related enzymes (46–50). We cloned catalytically inactive mutant forms of each of these ligases into the same cytomegalovirus-driven vector backbone to facilitate comparable heterologous expression. Radioligand binding was used to test the effect of overexpressing each mutant ligase on down-regulation of DOR measured after 5 h of continuous exposure to agonist. Most of the inactive ligases had little or no effect on ligand-induced down-

regulation of DOR. Disrupting the HECT-domain E3 ligase AIP4/Itch (C830A mutation), however, produced a strong inhibition (Fig. 2*A*).

Time course analysis confirmed the pronounced inhibitory effect of inactive AIP4 on pharmacological down-regulation of wild type receptors (Fig. 2*B*). To test for biochemical specificity with respect to ubiquitination of receptors, we next tested effects of the identified ligase on pharmacological down-regulation of lysyl-mutant receptors (F-DOR-0cK). In contrast to its pronounced inhibitory effect on down-regulation of wild type receptors, overexpression of inactive AIP4 (again, with similar expression verified by immunoblotting) did not produce any detectable effect on pharmacological down-regulation of lysyl-mutant receptors (Fig. 2*C*). This remarkable specificity of AIP4-dependent regulation was verified across multiple experiments and cell clones (Fig. 2*D*). Depleting endogenous AIP4 by RNA interference also inhibited pharmacological down-regulation of wild type F-DOR (Fig. 2*E*), and significant inhibition was observed using two independent siRNA duplexes that were verified to produce efficient depletion of endogenous AIP4 protein (Fig. 2*F*). Together, these results identify an essential function of AIP4-dependent ubiquitination specifically in controlling pharmacological down-regulation of wild type DOR without detectably affecting lysyl-mutant DOR.

The observation that down-regulation of F-DOR-0cK was insensitive to AIP4 disruption indicated that the pronounced inhibition of F-DOR down-regulation did not result from a nonspecific effect of reduced ligase activity and suggested that AIP4 mediates this regulatory effect via ubiquitination of the receptor itself. To test this, we applied an established method to assay incorporation of HA-tagged ubiquitin into F-DOR

immunopurified from HEK293 cells. Comparison of control purifications prepared from matched cells not expressing F-DOR verified the specificity of this detection (Fig. 3*A*, *293 lane*). Although a basal level of specific ubiquitin incorporation was clearly observed in F-DOR isolated from cells maintained in the absence of opioid ligand, receptor activation with DADLE produced a transient increase in HA-ubiquitin incorporation. Comparison of wild type (F-DOR; *left side* of blot) relative to lysyl-mutant (F-DOR-0cK; *right side* of blot) receptors clearly established that the lysyl-mutations fully prevented detectable ubiquitination of receptors, reducing the HA-ubiquitin signal to control levels even when lanes containing lysyl-mutant receptors were overloaded with immunoisolated receptors (Fig. 3*B*). We also noted that ubiquitinated F-DOR resolved at considerably higher apparent molecular mass (100–200 kDa; *bracket* in Fig. 3*A*) compared with the major immunoreactive receptor species detected by anti-FLAG blot (50–60 kDa; *bracket* in Fig. 3*B*).

Although the major receptor species identified by anti-FLAG blot corresponds to the complex glycosylated receptor monomer, the substantially reduced electrophoretic mobility of the ubiquitinated species suggests that, at steady state, a small population of receptors is modified by extensive multiubiquitination and/or polyubiquitination (rather than monoubiquitination). Overexpression of catalytically inactive AIP4 shifted the distribution of ubiquitinated receptor species toward lower apparent molecular mass but did not fully prevent receptor ubiquitination (Fig. 3*C*). Nevertheless, we verified in the same cells that mutant AIP4 expression strongly inhibited proteolytic down-regulation of receptors measured by radioligand binding (not shown). Thus, although preventing

receptor ubiquitination entirely had little effect on proteolytic down-regulation (F-DOR-0cK; Fig. 1*C*), partial inhibition of receptor ubiquitination (AIP4 disruption; Figs. 2*B* and 3*C*) strongly inhibited this process. These observations are clearly not consistent with the hypothesis that ubiquitin acts simply as a lysosomal sorting signal and suggest, instead, that ubiquitination mediates a distinct regulatory function on the later proteolytic processing of receptors.

*AIP4 Does Not Detectably Affect Endocytic Sorting of DOR to Lysosomes*

To further investigate this hypothesis, we examined the effect of disrupting AIP4 activity on receptor proteolysis detected biochemically. Despite strongly inhibiting down-regulation of wild type receptors measured by radioligand binding (Fig. 2*B*), catalytically inactive AIP4 did not detectably affect DOR proteolysis assessed by loss of FLAG immunoreactivity (Fig. 4*A* shows a representative immunoblot, and Fig. 4*B* summarizes quantification across multiple experiments). As yet another approach to examine the specificity of the AIP4-dependent regulatory effect, we evaluated the trafficking fate of endocytosed receptors by immunocytochemical localization. Previous studies have established that both wild type F-DOR and lysyl-mutant F-DOR-0cK colocalize with the late endosome/lysosome markers LAMP1 and -2 within ∼2 h after stimulating receptor endocytosis with DADLE (26, 29), consistent with the time course of receptor proteolysis determined biochemically. Overexpression of catalytically inactive mutant AIP4 did not prevent this colocalization, as indicated by the detection in confocal optical sections of numerous endomembrane structures labeled for both DOR (*green*) and LAMP1/2 (*red*) immunoreactivity at this time point (Fig. 4*C*). Colocalized structures were readily

apparent when optical cross-sections containing many endocytic structures were examined at higher magnification (*insets*).

*The Endosome-associated Deubiquitinating Enzymes, AMSH and UBPY, Also Specifically Control Pharmacological Down-regulation*

The ability of partial inhibition of receptor ubiquitination (by disrupting AIP4 activity) to strongly inhibit late proteolytic processing of receptors, while complete blockade of receptor ubiquitination (by lysyl-mutation) produced little inhibitory effect, suggested that the observed regulation of late proteolytic processing may require both ubiquitination and deubiquitination of receptors. To test this hypothesis, we looked for a potential regulatory effect of receptor deubiquitination by two deubiquitinating enzymes (DUBs), AMSH and UBPY, which are known to associate with endocytic membranes and act on other endocytic cargo (35, 36). The functional screen used to assess ubiquitin ligases was adapted to test these candidate DUBs, again using catalytically inactive mutant versions of each enzyme (AMSH D348A or UBPY C786S). Remarkably, overexpressing inactive versions of either DUB significantly inhibited pharmacological down-regulation of wild type receptors (Fig. 5*A*). In contrast, down-regulation of lysyl-mutant receptors continued unimpeded in the presence of either mutant DUB (Fig. 5*B*). Further, neither mutant DUB detectably affected receptor proteolysis assessed biochemically by immunoblot analysis (Fig. 5*C* shows a representative blot, and Fig. 5*D* summarizes quantification across multiple experiments). Depletion of endogenous levels of either AMSH or UBPY by RNA interference also inhibited pharmacological down-regulation of wild type F-DOR (Fig. 5*E*). This was somewhat surprising, since depletion of AMSH has been shown to increase the degradation of epidermal growth factor receptors (35), further suggesting

differences in ubiquitin-dependent regulation between DOR and epidermal growth factor receptors. Significant inhibition was again observed using two independent siRNA duplexes for each DUB that were verified to produce efficient depletion of endogenous AMSH or UBPY protein (Fig. 5*F*). Simultaneous depletion of both DUBs did not have any additional effect on down-regulation as compared with either DUB independently. Finally, we investigated the effect of DUBs on trafficking of F-DOR to the lysosome as visualized by confocal microscopy. Consistent with previous reports (35, 36), both AMSH-D/A and UBPY-C/S were visualized in a largely cytosolic distribution, with increased concentration on enlarged endosomes (Fig. 5*G*, *iii* and *vii*; higher magnification is shown in the *inset*). Interestingly, these endosomes colocalized with the late endosome/lysosome marker LAMP1/2 (*ii* and *vi*). Moreover, F-DOR localized to the same structures following prolonged agonist exposure (*i* and *v*). This overlap between internalized receptors and both DUBs in late endosome/lysosome structures is emphasized in the *merged color image* (*iv* and *viii*), particularly when examined at higher magnification (*inset*).

## 2.4 Discussion

The present results identify a specific function of AIP4-dependent ubiquitination in regulating the late proteolytic processing of GPCRs, which is clearly distinct from the previously defined function of ubiquitination by this ligase as a sorting determinant required for delivery of internalized receptors to lysosomes. We identified this function by study of a particular member of the GPCR family, DOR, which does not require ubiquitination for endocytic sorting to lysosomes yet traverses a similar endocytic pathway as ubiquitin-directed membrane cargo (26, 29). This feature of DOR trafficking was verified definitively in the present study, using several independent assays of lysosomal delivery and proteolysis and provided an advantageous system for identifying AIP4-dependent regulation of later proteolytic processing.

The specific regulatory effect of AIP4-dependent ubiquitination was manifest primarily by reduced proteolytic down-regulation of receptors detected by loss of binding to the small molecule radioligand [$^3$H]diprenorphine, a ligand that binds to residues present in the transmembrane helices (39). Proteolysis monitored biochemically by epitope tagging, however, is sensitive to extramembrane cleavage and was largely unaffected by disrupting or depleting AIP4, suggesting that ubiquitination by this ligase regulates later proteolytic processing event(s) that mediate destruction of the receptor's hydrophobic core. Moreover, the present data indicate that down-regulation of the receptors indicated by radioligand binding can be almost completely dissociated from lysosomal delivery of receptors assessed by immunocytochemical localization and from extensive proteolytic

fragmentation of extramembrane receptor domains by lysosomal proteases observed biochemically.

Perhaps the most striking observation from the present study is that ubiquitination of DOR regulates specific step(s) in the proteolytic processing pathway rather than being an absolute requirement for receptor down-regulation. Preventing all detectable ubiquitination of receptors by lysyl-mutation had little or no effect on ligand-induced endocytic trafficking of receptors to lysosomes detected by any of the assays, including down-regulation of radioligand binding (Fig. 1). Remarkably, disrupting AIP4 activity strongly inhibited pharmacological down-regulation of wild type DOR, whereas receptor ubiquitination was only partially reduced. This further supports a distinct regulatory function of DOR ubiquitination and suggests that ubiquitination of receptors is not simply a means to promote proteolysis but, under some conditions, can actually inhibit this process. The similar phenotype of disrupting membrane-associated DUB activities provides even more support for this idea. Interestingly, depleting AMSH or UBPY separately produced comparable effects on receptor down-regulation, and simultaneous knockdown of both DUBs failed to reveal additional effects. These data suggest that AMSH and UBPY are not redundant, and that they probably function at distinct stages in the same pathway of DOR trafficking. Altogether, the present findings support the hypothesis that later proteolytic processing of receptors is controlled by ubiquitination/deubiquitination cycling, involving multiple DUBs and perhaps multiple ligases, a possibility currently being investigated. Fig. 6 summarizes schematically the key features of the ubiquitination-dependent regulatory mechanism identified in the

present study of DOR and contrasts this mechanism with the current model of ubiquitin-directed sorting as exemplified by the CXCR4 receptor elucidated previously.

## 2.4 Acknowledgements

We thank Laurant Coscoy and Brian Sullivan for generously allowing the use of the unpublished Nedd4-1, Nedd4-2, Smurf1, WWP1, and WWP2 and corresponding mutant constructs; Sylvie Urbé for the DUBs and the anti-AMSH antibody; and Wes Sundquist for the Smurf2, NEDL1, and NEDL2 constructs. We also thank Michael Tanowitz for valuable discussion.

## 2.5 Materials and Methods

*Cell Culture, cDNA Constructs, and Transfection*

The Myc-tagged AIP4 and the C830A inactive mutant AIP4 have been previously described (24). Nedd4-1, Nedd4-2, WWP1, WWP2, Smurf1, and their corresponding inactive mutant versions were a gift from Laurent Coscoy and Brian Sullivan (University of California, Berkeley). Smurf2, NEDL1, and NEDL2 were a gift of Wes Sundquist (University of Utah School of Medicine) (34). Point mutations of the conserved catalytic cysteine residue were introduced by oligonucleotide-directed site-directed mutagenesis (QuikChange; Stratagene). GFP-AMSH, GFP-AMSH-D348A (D/A), GFP-UBPY, and GFP-UBPY-C786S (C/S) were a gift from Sylvie Urbé (University of Liverpool) and were previously described (35, 36). The FLAG-tagged DOR and the lysine mutant version (DOR-0cK) have been previously described (26). A COOH-terminal HA epitope was added to the F-DOR and F-DOR-0cK using PCR and encoding the HA epitope sequence (YPYDVDDYA) in the reverse primer. The resulting F-DOR-HA and F-DOR-0cK-HA coding sequences were cloned into pcDNA3 (Invitrogen) for generation of stable cell lines. Stably transfected cells expressing epitope-tagged receptors were generated by selection for neomycin resistance using 500 μg/ml G418 (Geneticin; Invitrogen). Resistant colonies were clonally isolated and selected for further study based on comparable levels of receptor expression as assessed by fluorescence microscopy and saturation binding analysis (supplemental Fig. 1). HEK293 cells (ATCC, Manassas, VA) were maintained in Dulbecco's modified Eagle's medium supplemented with 10% fetal bovine serum (University of California, San Francisco, Cell Culture Facility).

For all transient expression of ligases and deubiquitinating enzymes, cells were transfected using Lipofectamine 2000 (Invitrogen) according to the manufacturer's instructions. Cells expressing FLAG-tagged receptors were harvested by washing with EDTA and plated in 60-mm dishes at 80% confluence before transfection with plasmid DNA. Cells were reseeded into polylysine-coated 6-well or 24-well plates and cultured for a further 24 h before experimentation. For knockdown of endogenous AIP4, AMSH, or UBPY levels, the following siRNA duplexes were obtained from Qiagen: AIP4-3 (Hs_ITCH_3), CAAGAGCTATGAGCAACTGAA; AIP4-6 (Hs_ITCH_6), TGCCGCCGACAAATACAAATA; AMSH-7 (Hs_STAMBP_7), ATCACGCTCTTTATTGAGAAA; AMSH-8 (Hs_STAMBP_8), CCGCTCTGGAGTTGAGATTAT; UBPY-1 (Hs_USP8_1), CAGGGTCAATTCAAATCTACA; UBPY-2 (HS_USPB_2), AAGGCTCGTATTCATGCAGAA. They were transfected using Lipofectamine RNAi-max according to the manufacturer's instructions.

*Biochemical Detection of Receptor Proteolysis and Protein Levels by Immunblotting*

Immunoblotting to assess total cellular receptor levels was carried out as previously described (29). Briefly, cell monolayers were washed three times in ice-cold phosphate-buffered saline (PBS) and lysed in extraction buffer (0.5% Triton X-100, 150 mm NaCl, 25 mm KCl, 25 mm Tris, pH 7.4, 1 mm EDTA) supplemented with a standard protease inhibitor mixture (Roche Applied Science). Extracts were clarified by centrifugation (12,000 × *g* for 10 min) and then mixed with SDS sample buffer for denaturation. Proteins present in the extracts were resolved by SDS-PAGE using 4–12% BisTris gels (NuPAGE; Invitrogen), transferred to nitrocellulose membranes, and probed for protein

by immunoblotting using horseradish peroxidase-conjugated sheep anti-mouse IgG or donkey anti-rabbit IgG (Amersham Biosciences) and SuperSignal detection reagent (Pierce). Apparent molecular mass was estimated using commercial protein standards (SeeBlue Plus2; Invitrogen). Band intensities of unsaturated immunoblots were analyzed and quantified by densitometry using FluorChem 2.0 software (AlphaInnotech Corp.). Antibodies used were anti-FLAG-M1, anti-FLAG-M2-HRP (Sigma), anti-HA-11 (Covance), anti-HA(3F10)-HRP (Roche Applied Science), anti-AIP4/ITCH (BD Biosciences), anti-UBPY (Sigma), and anti-AMSH (a gift from Sylvie Urbé, University of Liverpool).

*Biotinylation-Degradation Assay*

To specifically label and follow the fate of the surface receptor pool, a previously described cell surface biotinylation assay was used to label FLAG-tagged receptors present in the plasma membrane (26, 29). Briefly, stably transfected HEK293 cells were grown on 60-mm dishes, washed with ice-cold PBS, and incubated with 300 μg/ml sulfo-*N*-hydroxysuccinimide-biotin (Pierce) in PBS for 30 min at 4 °C to biotinylate surface proteins. Following washing with Tris-buffered saline to remove and quench unreacted biotinylation reagent, cells were returned to 37 °C for incubation in media, in the absence or presence of 10 μm d-Ala-d-Leu-enkephalin (DADLE) for the indicated time period and extracted as described above. Extracts were clarified by centrifugation (12,000 × *g* for 10 min), and biotinylated proteins were isolated by immobilization on streptavidin-conjugated Sepharose beads (Pierce). Washed beads were eluted with SDS sample buffer before resolving by SDS-PAGE, transferred to nitrocellulose membranes, and probed for FLAG-tagged receptor (M1 antibody; Sigma). Some samples, as indicated, were

deglycosylated by the addition of 500 units of peptide *N*-glycosidase F (New England Biolabs) and incubated for 1 h at 37 °C before the elution with SDS sample buffer.

*Biochemical Detection of Receptor Ubiquitination*

To ensure the removal of any proteins that might be associated with the receptor, denaturing conditions were used. Cells were transiently transfected with HA-ubiquitin and treated before being lysed in 400 μl of extraction buffer and clarified by centrifugation (12,000 × *g* for 10 min), mixed with 200 μl of 3× radioimmune precipitation buffer (450 mm NaCl, 150 mm Tris, pH 7.4, 15 mm EDTA, 3% Triton X-100, 1.5% sodium deoxycholate, 30 mm NaF, 30 mm $Na_2$-pyrophosphate, 0.3% SDS), and incubated overnight at 4 °C with 2 μg of M2 anti-FLAG antibody (Sigma). 30 μl of protein A/G-agarose (Pierce) was added for 2 h at 4 °C. Immunoprecipitates were pelleted by centrifugation (3000 rpm, 1 min, 4 °C) and washed three times with 500 μl of radioimmune precipitation buffer before the addition of 20 μl of SDS sample buffer (Invitrogen) supplemented with β-mercaptoethanol and analysis by Western blotting using anti-HA-HRP (Roche Applied Science). Blots were then stripped (Restore Western blot stripping buffer; Pierce) and reprobed with anti-FLAG M2-HRP to verify relative receptor levels.

*Analysis of Receptor Levels by Radioligand Binding*

Receptor down-regulation was determined by radioligand binding, as previously described (11). Following transfection, HEK293 cells stably expressing FLAG-tagged receptors were replated into 12-well plates. 24 h later, 10 μm DADLE was added to the cells for the indicated time period, cells were washed twice with ice-cold PBS, 300 μl of PBS was added to the cells, and the plates were frozen. Plates were thawed, and cells

were resuspended. Binding assays were performed in triplicate in 96-well plates using a 10 nm concentration of the radiolabeled opioid receptor antagonist [$^3$H]diprenorphine (DPN) (88 Ci/mmol; Amersham Biosciences) and incubated for 1 h at room temperature, a saturating concentration that is sufficient to access both surface and internal receptors (11). Incubations were terminated by vacuum filtration through glass fiber filters (Whatman), and unbound radioligand was removed by repeated washes with Tris-buffered saline. Bound radioactivity was determined by liquid scintillation counting of washed filters. Nonspecific binding was determined by carrying out parallel determinations in the presence of excess unlabeled competitive antagonist (10 μm naloxone). Data presented represent the specific binding (total minus nonspecific binding) at each time point, expressed as a percentage of specific binding in similarly transfected but agonist-naive cells.

*Fluorescence Microscopy*

Colocalization of receptors with late endosome/lysosome markers was visualized using HEK293 cells stably expressing the indicated FLAG-tagged receptor constructs plated on polylysine-coated glass coverslips (Corning Glass). Cells were incubated in the presence of 10 μm DADLE for 2 h before fixation with 4% formaldehyde and permeabilization with 0.1% Triton X-100 in PBS. Cells were labeled using rabbit anti-FLAG (Sigma) and mouse antibodies recognizing LAMP-1 and -2 (Santa Cruz Biotechnology, Inc., Santa Cruz, CA), followed by secondary detection using Alexa594-conjugated anti-mouse and Alexa647 anti-rabbit secondary antibodies (Invitrogen). Colocalization of receptors with ubiquitin hydrolases was carried out using an identical procedure but with cells transiently transfected with GFP-ASMH-D348A or GFP-UBPY-C786S. Specimens were

imaged by confocal fluorescence microscopy using a Zeiss LSM 510 microscope fitted with a Zeiss ×63, numeric aperture 1.4 objective operated in single photon mode, with standard filter sets verified for lack of detectable cross-channel bleed-through and standard (1 Airy disc) pinhole. Acquired optical sections were analyzed with LSM Image Examiner (Zeiss) and rendered with Adobe Photoshop software.

*Statistical Analysis*

Quantitative data were averaged across multiple independent experiments, with the number of experiments specified in the corresponding figure legend. Unless indicated otherwise, the *error bars* represent the S.E. value determined after compiling mean determinations across experiments. The statistical significance of the indicated differences was analyzed using the appropriate variations of one-way ANOVA and post-test and Student's *t* test, as specified in the figure legends, calculated using Prism 4.0 software (GraphPad Software, Inc.). The relative significance of each of the reported differences is specified by calculated *p* values that are also listed in the figure legends and annotated graphically in the figures.

## 2.7 References


1. Ferguson, S. S. (2001) *Pharmacol. Rev.* 53, 1–24

2. Hanyaloglu, A. C., and von Zastrow, M. (2008) *Annu. Rev. Pharmacol. Toxicol.* 48, 537–568

3. Marchese, A., Paing, M. M., Temple, B. R., and Trejo, J. (2008) *Annu. Rev. Pharmacol. Toxicol.* 48, 601–629

4. Shenoy, S. K. (2007) *Circ. Res.* 100, 1142–1154

5. Sorkin, A., and Goh, L. K. (2008) *Exp. Cell Res.* 314, 3093–3106

6. Law, P. Y., Wong, Y. H., and Loh, H. H. (2000) *Annu. Rev. Pharmacol. Toxicol.* 40, 389–430

7. Law, P. Y., Hom, D. S., and Loh, H. H. (1984) *J. Biol. Chem.* 259, 4096–4104

8. Tsao, P., and von Zastrow, M. (2000) *Curr. Opin. Neurobiol.* 10, 365–369

9. Maxfield, F. R., and McGraw, T. E. (2004) *Nat. Rev. Mol. Cell Biol.* 5, 121–132

10. Vickery, R. G., and von Zastrow, M. (1999) *J. Cell Biol.* 144, 31–43

11. Tsao, P. I., and von Zastrow, M. (2000) *J. Biol. Chem.* 275, 11130–11140

12. Tanowitz, M., and von Zastrow, M. (2003) *J. Biol. Chem.* 278, 45978–45986

13. Carman, C. V., and Benovic, J. L. (1998) *Curr. Opin. Neurobiol.* 8, 335–344

14. Tsao, P. I., and von Zastrow, M. (2001) *Pharmacol. Ther.* 89, 139–147

15. Hicke, L. (1999) *Trends Cell Biol.* 9, 107–112

16. Urbe´, S. (2005) *Essays Biochem.* 41, 81–98

17. Raiborg, C., Rusten, T. E., and Stenmark, H. (2003) *Curr. Opin. Cell Biol.* 15, 446–455

18. Hicke, L., and Riezman, H. (1996) *Cell* 84, 277–287

19. Katzmann, D. J., Babst, M., and Emr, S. D. (2001) *Cell* 106, 145–155

20. Katzmann, D. J., Odorizzi, G., and Emr, S. D. (2002) *Nat. Rev. Mol. Cell Biol.* 3, 893–905

21. Saksena, S., Sun, J., Chu, T., and Emr, S. D. (2007) *Trends Biochem. Sci.* 32, 561–573

22. Russell, M. R., Nickerson, D. P., and Odorizzi, G. (2006) *Curr. Opin. Cell Biol.* 18, 422–428

23. Marchese, A., and Benovic, J. L. (2001) *J. Biol. Chem.* 276, 45509–45512

24. Marchese, A., Raiborg, C., Santini, F., Keen, J. H., Stenmark, H., and Benovic, J. L. (2003) *Dev. Cell* 5, 709–722

25. Bhandari, D., Trejo, J., Benovic, J. L., and Marchese, A. (2007) *J. Biol. Chem.* 282, 36971–36979

26. Tanowitz, M., and Von Zastrow, M. (2002) *J. Biol. Chem.* 277, 50219–50222

27. Whistler, J. L., Enquist, J., Marley, A., Fong, J., Gladher, F., Tsuruda, P., Murray, S. R., and Von Zastrow, M. (2002) *Science* 297, 615–620

28. Simonin, F., Karcher, P., Boeuf, J. J., Matifas, A., and Kieffer, B. L. (2004) *J. Neurochem.* 89, 766–775

29. Hislop, J. N., Marley, A., and Von Zastrow, M. (2004) *J. Biol. Chem.* 279, 22522–22531

30. Petaja-Repo, U. E., Hogue, M., Laperriere, A., Bhalla, S., Walker, P., and Bouvier, M. (2001) *J. Biol. Chem.* 276, 4416–4423

31. Petaja-Repo, U. E., Hogue, M., Laperriere, A., Walker, P., and Bouvier, M. (2000) *J. Biol. Chem.* 275, 13727–13736

32. Chaturvedi, K., Bandari, P., Chinen, N., and Howells, R. D. (2001) *J. Biol. Chem.* 276, 12345–12355

33. Yadav, P. N., Chaturvedi, K., and Howells, R. D. (2007) *J. Pharmacol. Exp. Ther.* 320, 1186–1194

34. Chung, H. Y., Morita, E., von Schwedler, U., Mu¨ller, B., Kra¨usslich, H. G., and Sundquist, W. I. (2008) *J. Virol.* 82, 4884–4897

35. McCullough, J., Clague, M. J., and Urbe´, S. (2004) *J. Cell Biol.* 166, 487–492

36. Row, P. E., Prior, I. A., McCullough, J., Clague, M. J., and Urbe´, S. (2006) *J. Biol. Chem.* 281, 12618–12624

37. Chen, L., and Davis, N. G. (2002) *Traffic* 3, 110–123

38. Befort, K., Tabbara, L., Bausch, S., Chavkin, C., Evans, C., and Kieffer, B. (1996) *Mol. Pharmacol.* 49, 216–223

39. Befort, K., Tabbara, L., Kling, D., Maigret, B., and Kieffer, B. L. (1996) *J. Biol. Chem.* 271, 10161–10168

40. Scherrer, G., Tryoen-To´th, P., Filliol, D., Matifas, A., Laustriat, D., Cao, Y. Q., Basbaum, A. I., Dierich, A., Vonesh, J. L., Gave´riaux-Ruff, C., and Kieffer, B. L. (2006) *Proc. Natl. Acad. Sci. U.S.A.* 103, 9691–9696

41. Mosberg, H. I., and Fowler, C. B. (2002) *J. Pept. Res.* 60, 329–335

42. Shenoy, S. K., McDonald, P. H., Kohout, T. A., and Lefkowitz, R. J. (2001) *Science* 294, 1307–1313

43. Jacob, C., Cottrell, G. S., Gehringer, D., Schmidlin, F., Grady, E. F., and Bunnett, N. W. (2005) *J. Biol. Chem.* 280, 16076–16087

44. Duan, L., Miura, Y., Dimri, M., Majumder, B., Dodge, I. L., Reddi, A. L., Ghosh, A., Fernandes, N., Zhou, P., Mullane-Robinson, K., Rao, N., Donoghue, S., Rogers, R. A., Bowtell, D., Naramura, M., Gu, H., Band, V., and Band, H. (2003) *J. Biol. Chem.* 278, 28950–28960

45. Levkowitz, G., Waterman, H., Ettenberg, S. A., Katz, M., Tsygankov, A. Y., Alroy, I., Lavi, S., Iwai, K., Reiss, Y., Ciechanover, A., Lipkowitz, S., and Yarden, Y. (1999) *Mol. Cell* 4, 1029–1040

46. Medina, G., Pincetic, A., Ehrlich, L. S., Zhang, Y., Tang, Y., Leis, J., and Carter, C. A. (2008) *Virology* 377, 30–38

47. McNatt, M. W., McKittrick, I., West, M., and Odorizzi, G. (2007) *Mol. Biol. Cell* 18, 697–706

48. Martin-Serrano, J., Perez-Caballero, D., and Bieniasz, P. D. (2004) *J. Virol.* 78, 5554–5563

49. Shenoy, S. K., Xiao, K., Venkataramanan, V., Snyder, P. M., Freedman, N. J., and Weissman, A. M. (2008) *J. Biol. Chem.* 283, 22166–22176

50. Staub, O., and Rotin, D. (2006) *Physiol. Rev.* 86, 669–707

# 2.8 Figures

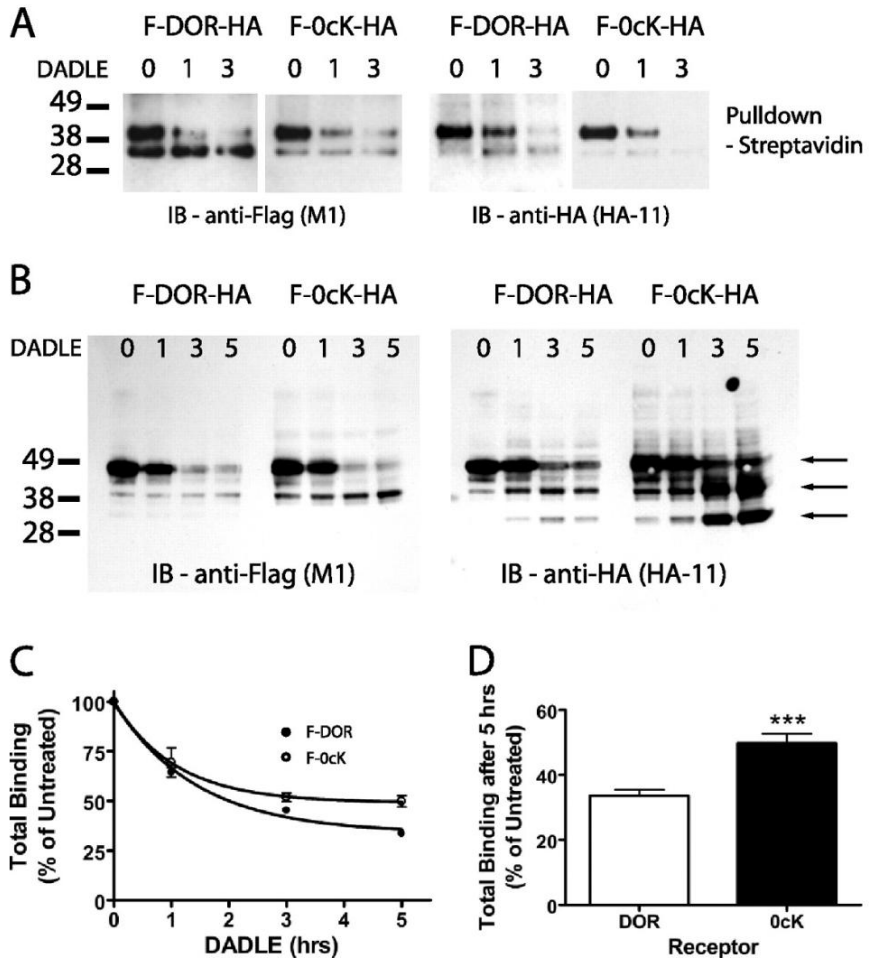


**Figure 1. Both DOR and DOR-0cK undergo extensive proteolysis and pharmacological down-regulation after ligand-induced endocytosis.** A) HEK293 cells stably expressing F-DOR-HA and F-DOR-0cK-HA were biotinylated (as described under "Experimental Procedures") before incubation in the presence of 10 μm DADLE for the indicated time period (in hours). Extracts were split in two before pull-down with streptavidin beads, deglycosylation with peptide *N*-glycosidase F, and SDS-PAGE separation. Shown are representative anti-FLAG blots (*left*) and anti-HA blots (*right*) of F-DOR-HA (*left*) and F-DOR-0cK-HA (*right*). B) Cells stably expressing F-DOR-HA or F-DOR-0cK-HA, as indicated, were incubated for the indicated periods in the presence of 10 μm DADLE before lysis and division into two identical samples. Shown is a representative anti-FLAG (*left*) and anti-HA (*right*) immunoblot. The *arrows* denote major proteolytic cleavage products, indicating that both wild type and lysyl-mutant receptors undergo

extensive ligand-induced proteolysis over a similarly rapid time course, as indicated by the generation of multiple proteolytic cleavage events. C) cells stably expressing F-DOR (*closed symbols*) or F-DOR-0cK (*open symbols*) were treated for the indicated time with 10 μm DADLE before freeze-thawing and undergoing ligand binding with [$^3$H]DPN. Results shown represent specific binding expressed as a percentage of binding in untreated cells. D) total binding after 5 h of DADLE treatment expressed as a percentage of total binding in untreated cells (***, $p < 0.001$; Student's *t* test, $n = 10$).

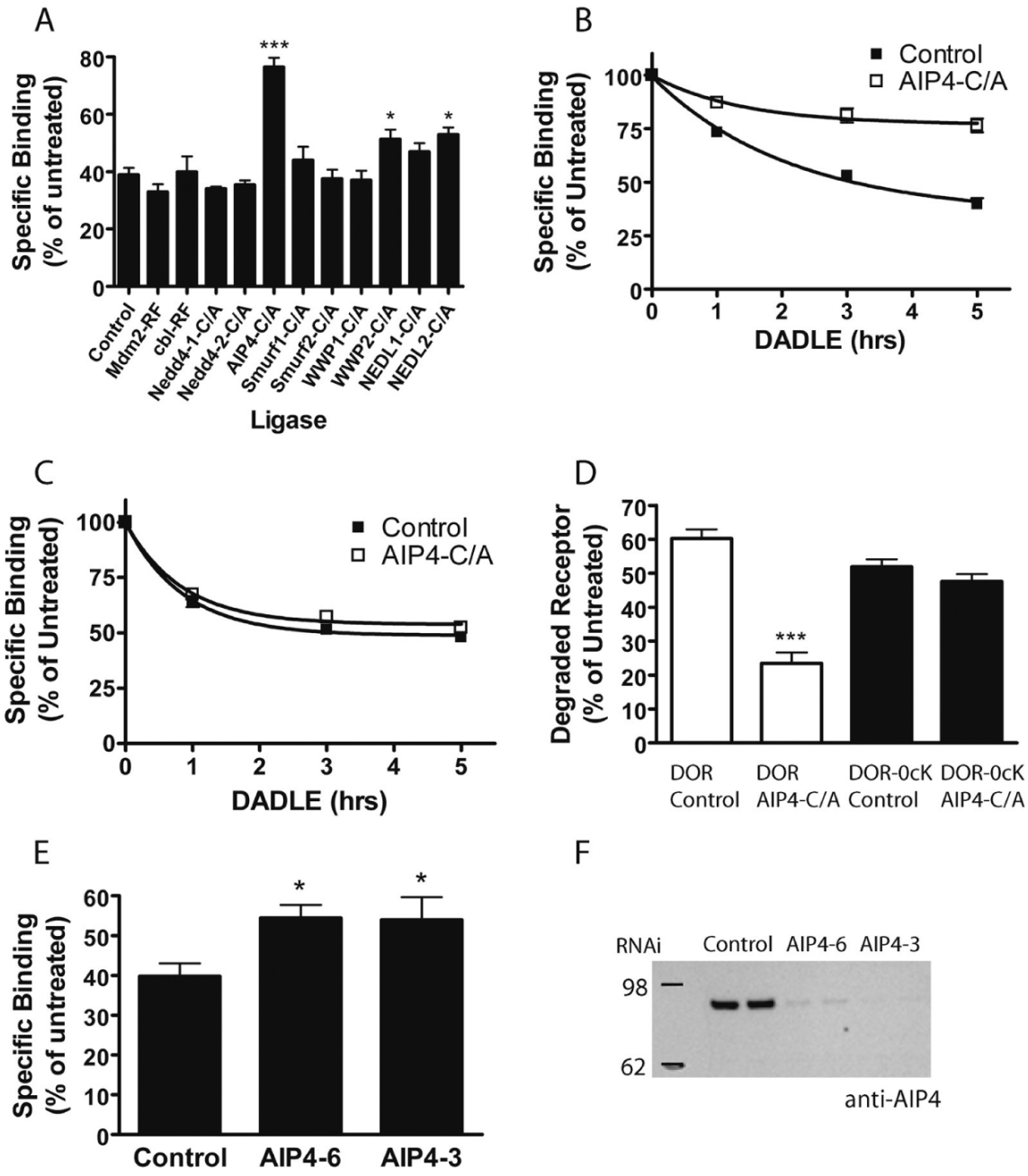


**Figure 2. Effect of ubiquitin ligases on DOR down-regulation** A) F-DOR-expressing HEK293 cells were transiently transfected with the indicated inactive ubiquitin ligase constructs and 24 h later replated in 12-well plates. After 24 h, cells were treated with 10 μm DADLE for 5 h before freeze-thaw and assay by radioligand binding with [$^3$H]DPN. Specific binding was expressed as a percentage of binding in similarly transfected, agonist-naive cells (one-way ANOVA, Bonferroni multiple comparison test; ***, $p < 0.001$; *, $p < 0.05$, $n \geq 4$). HEK293 cells stably expressing F-DOR (B) or F-DOR-0cK (C) were transiently

transfected with AIP4-C/A (*open symbols*) and 48 h later treated for the indicated time with 10 μm DADLE before freeze-thawing and determining receptor down-regulation by [$^3$H]DPN binding assay. Specific binding detected at the indicated times is expressed as a percentage of that measured in agonist-naive cells. D) The same data expressed as a percentage of receptor degraded after 5 h of DADLE treatment (one-way ANOVA, Bonferroni multiple comparison test; $p < 0.001$, $n = 14$). E) F-DOR cells were transfected with siRNA duplexes against AIP4 and, 72 h later, assayed for DADLE-induced down-regulation by [$^3$H]DPN binding. Results shown represent specific binding expressed as a percentage of binding in untreated cells (one-way ANOVA, Bonferroni multiple comparison test; *, $p < 0.05$, $n = 7$). F) Knockdown was verified by lysing the remaining cells from the down-regulation assay, resolving equal amounts of total cellular protein on NuPAGE 4–12% BisTris gel, and detecting endogenous AIP4 by immunoblotting. A representative Western blot is shown.

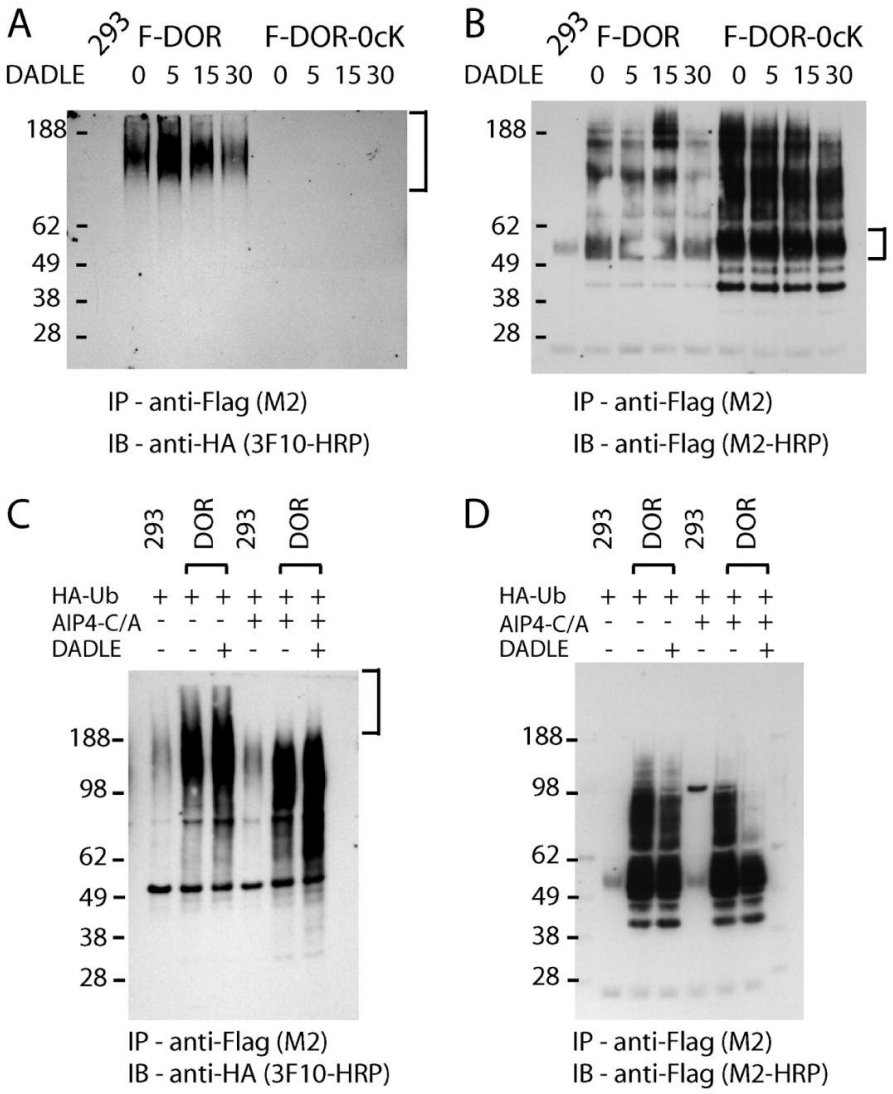


**Figure 3. DOR undergoes AIP4-dependent lysyl-ubiquitination.** A) HEK293 cells stably expressing F-DOR or F-DOR-0cK were transfected with HA-tagged ubiquitin and, 24 h later, were stimulated with 10 µm DADLE for the indicated time period before extraction and immunoprecipitation under denaturing conditions with mouse anti-FLAG antibody (M2) and SDS-PAGE separation. Shown is a representative anti-HA (3F10)-HRP blot with untransfected HEK293 cells (no receptor expressed; *293*), the F-DOR (*left*), and F-DOR-0cK (*right*). B) The same blot stripped and reprobed with anti-FLAG (M2)-HRP to show the relative size and amount of the major receptor species. C) HEK293 cells stably expressing F-DOR were transfected with HA-tagged ubiquitin and either empty pcDNA vector or mycAIP4-C/A construct and 24 h later were stimulated with 10 µm DADLE for 20 min before extraction and immunoprecipitation with mouse anti-FLAG antibody (M2) and SDS-PAGE separation. Shown is a representative anti-HA (3F10)-

HRP blot. D) The same blots were stripped and reprobed with anti-FLAG (M2)-HRP to show the relative size and amount of the major receptor species. *IP*, immunoprecipitation; *IB*, immunoblot.

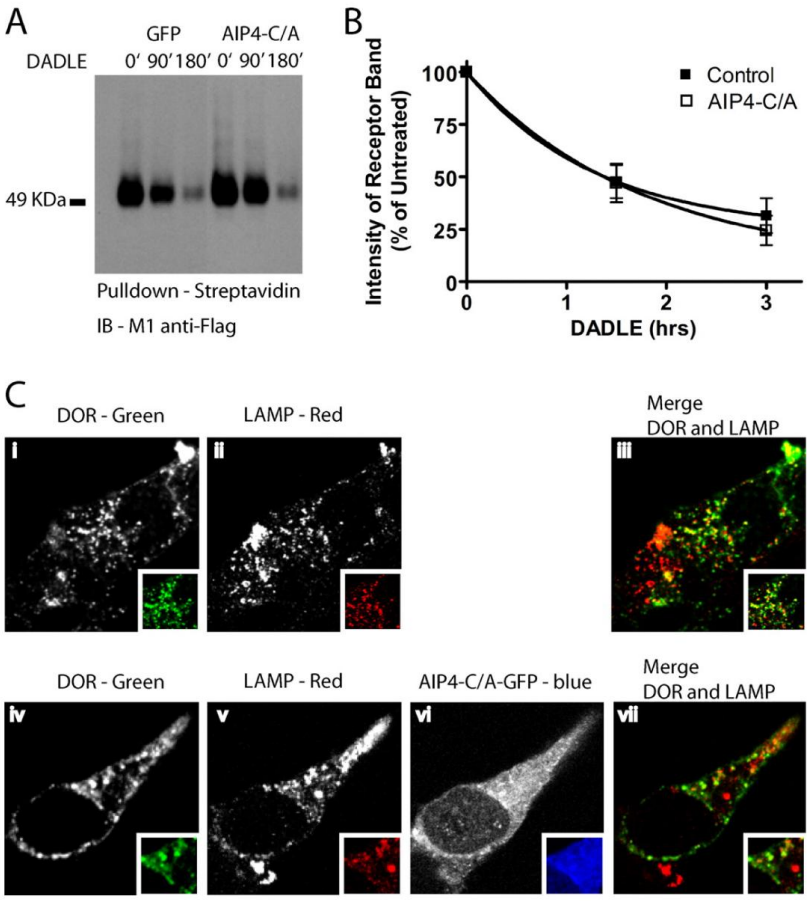


**Figure 4. AIP4 is not required for lysosomal delivery of receptors detected biochemically or by immunocytochemical localization.** A) F- DOR-expressing HEK293 cells were transfected with GFP or AIP4-C/A and, 48 h later, underwent cell surface biotinylation before incubation for the indicated time periods with 10 µm DADLE. Cells were lysed, and biotinylated protein was pulled down with streptdavidin-agarose beads and separated by SDS-PAGE. A representative anti-FLAG immunoblot is shown. B) Blots generated in multiple experiments were scanned to estimate the amount of FLAG-tagged receptor remaining at each time point after incubation in the presence of 10 µm DADLE, expressed as a percentage of that measured in identically transfected cells not exposed to opioid. Results were pooled and averaged across multiple experiments ($n$ = 5). *Closed symbols*, degradation curve measured in control cells transfected with GFP; *open symbols*, degradation curve measured in cells transfected with AIP4-C/A-GFP ($n$ = 5 for each set). C) F-DOR cells were transfected with empty pcDNA or AIP4-C/A-GFP (*vi*), replated

onto coverslips, and incubated in the presence of 10 μm DADLE for 2 h before fixation and labeling for anti-FLAG (*i* and *iv*) and anti-LAMP1/2 (*ii* and *v*). Shown are representative confocal optical sections imaged under nonsaturating conditions and rendered using simple background subtraction and a linear lookup table. *Merged images* (*iii* and *vii*) display DOR and LAMP channels *pseudocolored* in *green* and *red*, respectively. The AIP4 channel has not been included in the merged image displayed, to make receptor localization more easily compared, but this signal can be seen in the *grayscale image* and *pseudocolored inset* (*vi*). *IB*, immunoblot.

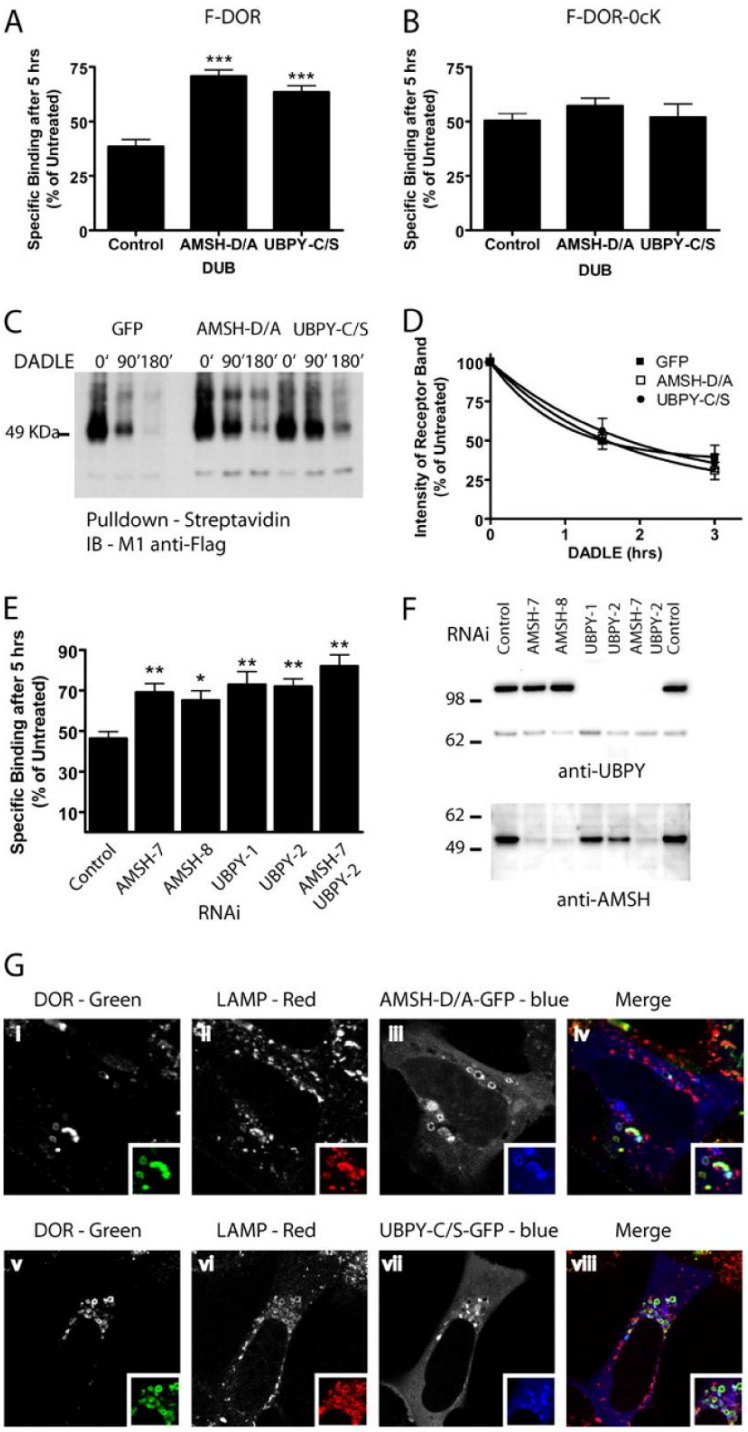


**Figure 5. Endosomal deubiquitinating enzymes specifically affect down-regulation of DOR but not DOR-0cK.** HEK293 cells stably expressing F-DOR (A) or F-DOR-0cK (B) were transiently transfected with GFP, GFP-AMSH-D/A, or GFP-UBPY-C/S and, 48 h later, treated for 5 h with 10 μm DADLE before freeze-thawing and radioligand binding assay using [$^3$H]DPN. Data shown represent specific binding

expressed as a percentage of binding in untreated cells (one-way ANOVA, Bonferroni multiple comparison test; ***, $p < 0.001$, $n = 5$). C) F-DOR expressing HEK293 cells were transfected with GFP, GFP-AMSH-D/A, or GFP-UBPY-C/S and, 48 h later, underwent cell surface biotinylation before incubation of cells for the indicated time period with 10 μM DADLE. Cells were lysed, and biotinylated protein was isolated with streptdavidin-agarose beads and resolved by SDS-PAGE. A representative anti-FLAG blot is shown. *D*, anti-FLAG blots were scanned to estimate the amount of FLAG-tagged receptor remaining at each time point after DADLE incubation relative to that detected in parallel samples of cells not exposed to opioid agonist. Results were pooled and averaged across multiple experiments ($n = 4$). *Closed squares*, results from cells expressing GFP; *open squares*, results from cells expressing GFP-AMSH-D/A; *closed circles*, results from cells expressing GFP-UBPY-C/S. E) F-DOR cells were transfected with siRNA duplexes against AMSH or UBPY and, 72 h later, assayed for DADLE-induced down-regulation by [$^3$H]DPN binding. Results shown represent specific binding expressed as a percentage of binding in untreated cells (one-way ANOVA, Dunnett multiple comparison test; *, $p < 0.05$; **, $p < 0.01$, $n = 7$). F) Knockdown was verified by lysing the remaining cells, resolving equal protein loads on NuPAGE 4–12% BisTris gel, and detecting endogenous UBPY (*top*) or AMSH (*bottom*) by immunoblotting. A representative Western blot is shown for each. G) F-DOR-expressing cells were transfected with GFP-AMSH-D/A (*iii*) or GFP-UBPY-C/S (*vii*) and replated onto coverslips and incubated for 2 h with 10 μm DADLE before being fixed and stained with rabbit-anti-FLAG (*i* and *v*) antibody and anti-LAMP1/2 (*ii* and *vi*). Shown are representative confocal optical sections imaged under nonsaturating conditions and rendered using simple background subtraction and a linear lookup table. *Merged images* and *insets* show receptor, LAMP, and the indicated DUB immunoreactivity *pseudocolored* in *green*, *red*, and *blue*, respectively (*iv* and *viii*). *IB*, immunoblot; *RNAi*, RNA interference.

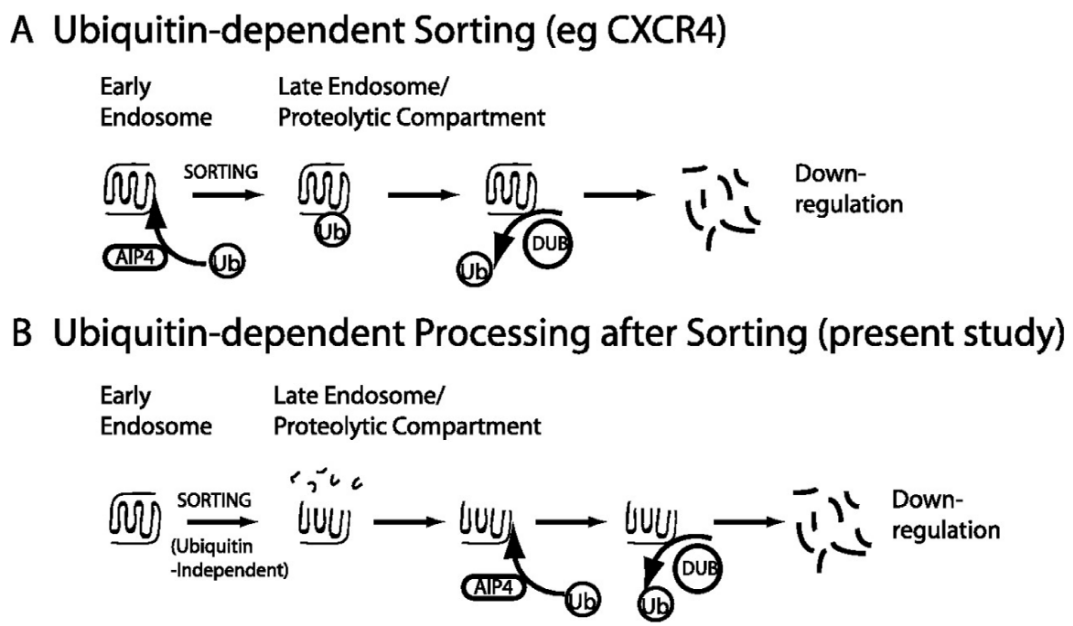


**Figure 6. Proposed model for the postsorting function of AIP4 in controlling DOR down-regulation**

A) Depiction of the current view of AIP4-dependent regulation of GPCR proteolysis, based on previous studies of the CXCR4 receptor (3, 24). Ubiquitination acts as a sorting determinant that is required for delivery of internalized receptors to the late endosome/lysosome pathway, and receptor proteolysis follows. Receptors presumably undergo deubiquitination, as indicated, which is not specifically required for lysosomal sorting of receptors but is thought to occur generally after sorting is complete to prevent depletion of free cytoplasmic ubiquitin (*Ub*) pools (36). B) The currently proposed function of AIP4-dependent ubiquitination in regulating later proteolytic processing of DOR. Endocytic sorting of the DOR into the late endosome/lysosome pathway does not require receptor ubiquitination, in contrast to that of the CXCR4 receptor, as indicated by the ability of the lysyl-mutant DORs to undergo complete proteolytic destruction at a rate similar to that of wild type receptors. Wild type receptors are also sorted into the late endosome/lysosome pathway irrespective of their ubiquitination state, as indicated by LAMP1/2 colocalization and initial proteolytic fragmentation detected biochemically. Subsequent proteolytic processing required to destroy the hydrophobic core of the receptor is specifically regulated by both ubiquitination/deubiquitination, as indicated by the pronounced inhibition produced by disrupting either ubiquitin ligase (AIP4) or hydrolase (DUB) activity on down-regulation of wild type but not lysyl-mutant receptors detected by radioligand binding. The critical distinctions from model A are 1) that ubiquitination affects proteolytic processing of the wild type DOR clearly *after* receptor sorting to a lysosomal fate and

the occurrence of initial proteolytic cleavage events, and 2) that later proteolytic processing of receptors is specifically regulated by both receptor ubiquitination and deubiquitination.

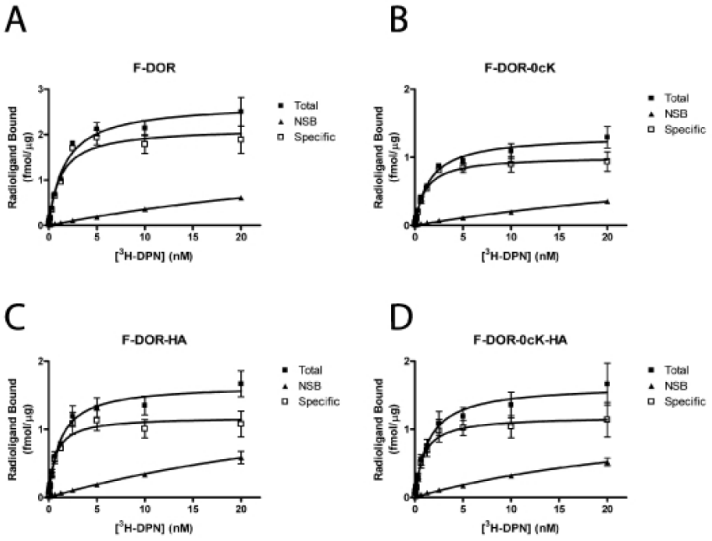


| | Bmax (fmol/µg) | | Kd (nM) | | n |
|---|---|---|---|---|---|
| Receptor | Mean | SEM | Mean | SEM | |
| F-DOR | 2.14 | 0.12 | 1.22 | 0.25 | 3 |
| F-DOR-0cK | 1.01 | 0.05 | 1.04 | 0.19 | 3 |
| F-DOR-HA | 1.18 | 0.07 | 0.68 | 0.17 | 3 |
| F-DOR-0cK-HA | 1.19 | 0.08 | 0.86 | 0.23 | 3 |

**Supplemental Figure 1. Saturation Binding Curves to determine receptor number in cell lines used**

HEK293 cells stably expressing F-DOR (A), F-DOR-0cK (B), F-DOR-HA (C) or F-DOR-0cK-HA (D) were incubated with varying concentrations of [3H]DPN and bound ligand was measured by vacuum filtration through glass fiber filters, and bound radioactivity was determined by liquid scintillation counting of washed filters. Shown are Total binding, NSB (binding in the precence of 10µM Naloxone) and Specific binding (Total – NSB), expressed as fmol bound/ µg of protein. E) Curves were fitted by non-linear regression assuming a single binding site, and Bmax and Kd calculated (Prism 4.0).

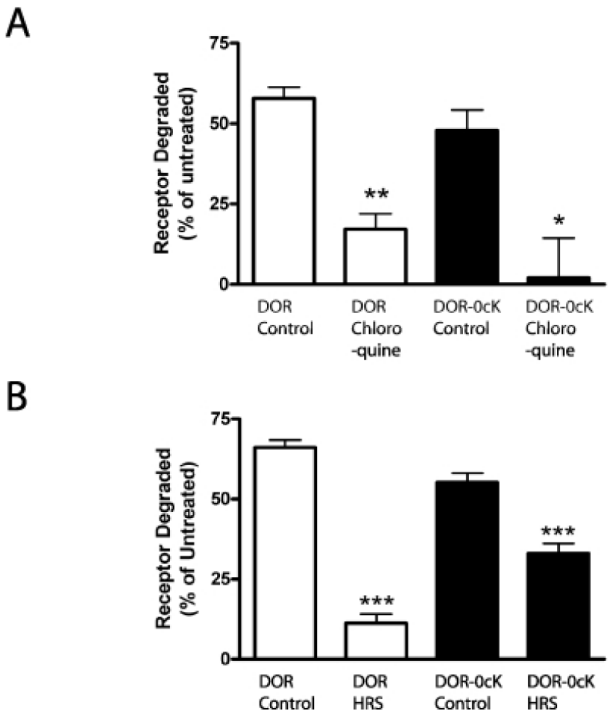


**Supplemental Figure 2. Downregulation of DOR measured by radioligand binding is mediated by HRS-dependent trafficking of receptors to lysosomes** A) HEK293 cells stably expressing F-DOR or F-DOR-0cK were pretreated for 15 minutes with 200μM chloroquine and then incubated in the presence of chloroquine and 10μM DADLE for an additional 3 hours. Ligand-induced downregulation was determined by saturation radioligand binding using [3H]-DPN. The mean extent of receptor downregulation was calculated from specific binding detected in DADLE-incubated cells compared to specific binding detected in parallel cell samples not exposed to opioid agonist. Bars represent mean extent of downregulation averaged across experiments, and error bars represent the standard error of the mean (** $p<0.01$, * $p< 0.05$, n=3). B) Cells were transfected with control plasmid or myc-HRS before being replated and incubated in the absence or presence of 10μM DADLE for an additional 5 hours and analysis of receptor downregulation by radioligand binding assay. Bars represent mean extent of downregulation averaged across experiments, and error bars represent the standard error of the mean (*** $p<0.001$, n=6).

# Chapter 3: “The role of ubiquitination in lysosomal trafficking of δ-opioid receptors”

Anastasia Henry and James Hislop conceived the project and performed the experiments and data analysis. Ian White, in the laboratory of Mark Marsh (UCL), performed the cryo-immuno electron microscopy experiments. Anastasia Henry, James Hislop, Mark Marsh, and Mark von Zastrow wrote the manuscript.

## 3.1 Abstract

The δ-opioid receptor (DOR) undergoes ligand-induced downregulation by endosomal sorting complex required for transport (ESCRT)-dependent endocytic trafficking to lysosomes. In contrast to a number of other signaling receptors, the DOR can downregulate effectively when its ubiquitination is prevented. We explored the membrane trafficking basis of this behavior. First, we show that internalized DORs traverse the canonical multivesicular body (MVB) pathway and localize to intralumenal vesicles (ILVs). Second, we show that DOR ubiquitination stimulates, but is not essential for, receptor transfer to ILVs and proteolysis of the receptor endodomain. Third, we show that receptor ubiquitination plays no detectable role in the early sorting of internalized DORs out of the recycling pathway. Finally, we show that DORs undergo extensive proteolytic fragmentation in the ectodomain, even when receptor ubiquitination is prevented or ILV formation itself is blocked. Together, these results are sufficient to explain why DORs downregulate effectively in the absence of ubiquitination, and they place a discrete molecular sorting operation in the MVB pathway effectively upstream of the ESCRT. More generally, these findings support the hypothesis that mammalian cells can control the cytoplasmic accessibility of internalized signaling receptors independently from their ultimate trafficking fate.

## 3.2 Introduction

Endocytosis represents perhaps the most highly conserved mechanism by which cells control receptor-mediated signaling processes (1, 2). The importance of endocytic regulation is clearly evident for seven-transmembrane receptors (7TMRs), the largest family of signaling receptors expressed in animals. Endocytosis of 7TMRs can mediate diverse functional effects, which depend largely on the subsequent trafficking itinerary of internalized receptors. Recycling of receptors to the plasma membrane typically promotes rapid recovery (resensitization) of cellular responsiveness in the face of repeated stimulation (3-5). Receptor trafficking to lysosomes, in contrast, results in proteolytic down-regulation of receptors and typically attenuates cellular signaling responsiveness (6). Given these effectively opposite functional consequences, a critical question is how receptor-specific differences in post-endocytic trafficking are determined.

Lysyl-ubiquitination has emerged as a fundamental biochemical determinant directing the endocytic trafficking of signaling receptors, as well as various other membrane cargo, to lysosomes (6-10). Ubiquitination of yeast 7TMRs has been shown to promote endocytosis of receptors, prevent internalized receptors from recycling to the plasma membrane, and accelerate proteolytic destruction of internalized receptors by driving their transfer from the limiting endosome membrane to intralumental vesicles (ILVs). Ubiquitination of the mammalian EGF receptor tyrosine kinase is not essential for regulated endocytosis, but functions both to prevent recycling and accelerate proteolysis via receptor transfer to ILVs (11-15). Ubiquitination is thought to function similarly in promoting lysosomal down-regulation of a number of mammalian 7TMRs (*e.g.*, (6, 16,

17)). To our knowledge, however, no previous study has defined particular step(s) in the down-regulation pathway that are regulated by ubiquitination of a 7TMR in mammalian cells.

The δ-opioid neuropeptide receptor (DOR) is a mammalian 7TMR that undergoes efficient lysosomal down-regulation in cultured cell models and native tissues (18-21). Down-regulation of the DOR is particularly interesting because this process can occur effectively when receptor ubiquitination is prevented by mutation of all cytoplasmic lysine residues, yet requires ESCRT components (22-24). Previous studies have identified additional proteins affecting down-regulation of the DOR, which are distinct from the conserved ESCRT machinery (25, 26) but may interact with the ESCRT indirectly (27). Nevertheless, it is clear the wild type DOR is subject to extensive ubiquitination in intact cells (28, 29). What significance, if any, direct ubiquitination plays in membrane trafficking event(s) mediating lysosomal down-regulation of the DOR has remained an unresolved issue.

The first evidence for any effect of DOR ubiquitination on lysosomal trafficking emerged from a functional screen identifying a role of the HECT domain ubiquitin ligase AIP4 in modulating the kinetics of DOR down-regulation assessed by radioligand binding (24). AIP4-dependent ubiquitination of a distinct 7TMR, the CXCR4 chemokine receptor, was shown previously to function as a direct sorting determinant directing internalized receptors out of the recycling pathway and promoting their delivery to lysosomes (30). However, two observations argued against this canonical sorting model in the case of

DORs. First, while inactivation or depletion of AIP4 inhibited down-regulation of wild type DORs, down-regulation of lysine-mutant DORs occurred with nearly wild type kinetics. Second, preventing DOR ubiquitination produced a relatively subtle effect on net down-regulation, which was detectable only after destruction of a substantial fraction radioligand binding sites had already occurred (24). It was therefore proposed that ubiquitination of the DOR mediates a regulatory, rather than essential, role in directing lysosomal destruction of this 7TMR. The nature of this proposed regulatory function has not been defined, nor has there been any progress in determining the membrane trafficking basis underlying the ability of ubiquitination-defective receptors to undergo effective ESCRT-dependent down-regulation.

We addressed these questions in the present study using a combination of biochemical, morphological and live imaging approaches. Our results establish that DORs traffic to lysosomes via MVBs, that AIP4-dependent ubiquitination of DORs promotes but is not essential for receptor localization to ILVs, and that the previously identified alternate sorting mechanism functions upstream of the ESCRT in a sequential pathway of molecular sorting operations driving receptor trafficking to lysosomes. These results resolve a specific function of ubiquitination in ligand-induced down-regulation of the DOR, and suggest a means by which mammalian cells can regulate the cytoplasmic accessibility of internalized signaling receptors independently from ultimate trafficking fate.

## 3.3 Results

*Ubiquitination is not required for efficient sorting of the DOR out of the rapid recycling pathway*

We investigated the post-endocytic sorting of both the wild type DOR and a previously described mutant, DOR-0cK, which is devoid of all cytoplasmic lysine residues and is not ubiquitinated in intact cells (22-24). We added distinct N-terminal (FLAG) and C-terminal (HA) epitope tags to facilitate selective immunochemical detection of the receptor ectodomain and endodomain (F-DOR-HA and F-DOR-0cK-HA, Fig 1A), and expressed the tagged constructs in stably transfected HEK293 cells at moderate levels (~1 pmol / mg, see *Materials and Methods*) that do not saturate the endocytic pathway (24).

We first asked if the lysine mutation caused increased recycling of DORs after agonist-induced endocytosis. We did so because a hallmark of ubiquitin-directed sorting of other signaling receptors in both yeast (31) and mammalian cells (14, 17) is that lysyl mutation effectively redirects internalized receptors into the rapid recycling pathway. We measured DOR recycling using a previously described flow cytometric assay that monitors surface return of antibody-labeled receptors from the internalized pool (18, 32). Both F-DOR-HA and F-DOR-0cK-HA internalized robustly in response to activation by the opioid peptide agonist 2-D-Ala, 5-D-Leu-enkephalin (DADLE), consistent with previous evidence that ubiquitination is not required for DOR endocytosis (22). Further, and also as shown previously (18), the vast majority of F-DOR-HA was retained in the endocytic pathway at all time points tested after removal of agonist from the culture medium (Fig 1B, filled squares). Importantly, and not previously established, the lysine-

mutant F-DOR-0cK-HA receptor construct was retained in the endocytic pathway with indistinguishable efficiency relative to the 'wild type' F-DOR-HA (Fig 1B, open squares). Other mammalian 7TMRs, such as the $\beta_2$-adrenergic receptor, largely return to the plasma membrane in this assay within ≤30 min after agonist washout (18). We also verified, in parallel samples, nearly complete return of internalized transferrin receptors (TfRs; Fig 1B, filled circles) that mark the rapid recycling pathway (33). Moreover we verified visually obvious retention in the endocytic pathway of both F-DOR-HA and F-DOR-0cK-HA after agonist washout by fluorescence microscopy using either epitope tag (Supplemental Fig.1).

*Both wild type and lysine-mutant DORs localize to MVBs*

Having established that lysine mutation of DORs is not required to prevent receptors from recycling to the plasma membrane, we next asked if internalized receptors traverse MVBs. While a number of 7TMRs have been shown to localize to MVBs, and to be capable of accessing intralumenal membranes (34-37), this has not been investigated previously for opioid receptors. Moreover, to our knowledge, no previous study has specifically determined whether ubiquitination is essential for intralumenal localization of any 7TMR in mammalian cells. We initially addressed these questions using immunogold labeling of cryosections followed by electron microscopy, an established method allowing unambiguous resolution of intralumenal membranes. We examined receptor localization in cells fixed 90 min after DADLE application, a time point chosen because it is clearly after receptor sorting out of the recycling pathway (Fig 1B) and the onset of DOR proteolysis (see below). We localized anti-HA immunoreactivity because, irrespective of the degree of proteolytic fragmentation of receptors occurring at this time

point, intralumenal localization of the C-terminal epitope is topologically impossible unless physical transfer to ILVs has occurred.

In cells expressing 'wild type' F-DOR-HA, anti-HA immunoreactivity localized robustly to MVBs, and could be clearly resolved in association with both the limiting and intralumenal membranes (Fig 1C). Anti-HA immunoreactivity in cells expressing the lysine-mutant DOR-0cK also localized to MVBs at this time point and, remarkably, was observed in association with both limiting and intralumenal membranes (Fig 1D). Examination across numerous sections verified these findings, establishing definitively the ability of both wild type and lysine-mutant receptors to localize to MVBs and gain intralumenal access. We noted, however, considerable variability across individual MVBs in the apparent degree of intralumenal localization (randomly selected examples for each receptor construct are shown in Supplemental Fig 2). This motivated us to verify, and further investigate, intralumenal localization of receptors using methods that are more amenable to global analysis across a larger representation of the cell population.

As a first step to do so, we replaced the C-terminal HA tag with GFP (F-DOR-GFP and F-DOR-0cK-GFP). We verified biochemically that the GFP tag did not compromise agonist-induced down-regulation (Supplemental Fig 3), and then expressed a mutationally activated form of Rab5 (CFP-Rab5Q79L) to enlarge endosomes and facilitate optical resolution of limiting and intralumenal membranes (35, 38). As observed with electron microscopy, confocal fluorescence microscopy verified that both GFP-tagged wild type and lysine-mutant receptor variants localized both peripherally and

intralumenally in endosomes. Also consistent with the electron microscopic observations, we observed considerable variability in localization across individual endosomes, including among those imaged within the same cell (Fig. 2A and B, see *).

Having established that both the DOR and DOR-0cK are able to access ILVs, we next asked if lysine mutation affects the degree to which tagged receptors localize to the endosome lumen. To quantify the extent of intralumenal distribution, we used line scan analysis of confocal cross-sections (Fig 2C) and carried out this analysis over a large number of examples selected at random from multiple cells and experiments. This analysis revealed a partial but significant reduction in the relative amount of lysine-mutant receptors present in the endosome lumen compared to that observed for wild type receptors (Fig 2D).

Co-expression of activated Rab5 was essential to achieve optical resolution of the intralumenal space of endosomes in fixed specimens. Receptor-containing endosomes were significantly larger in living cells (typically 1 - 2μm diameter), however, making it was possible to resolve the lumen by spinning disc confocal microscopy in the absence of mutant Rab5. A similar line scan analysis verified a partial but significant reduction of intralumenal receptor fluorescence produced by lysyl mutation under these conditions (Fig 3 A – C, Supplemental Movie 1 and 2). We also observed that intralumenal localization of both receptor variants was inhibited in cells exposed to the PI3 kinase inhibitor wortmannin, and in cells over-expressing the ESCRT-0 component HRS (Fig 3 D - I). Both of these manipulations have been used previously to define the ESCRT-

dependent mechanism of ILV formation relative to alternate ESCRT-independent mechanism(s) (39, 40). Thus both wild type and lysine-mutant DORs can access the intralumenal space of MVBs, apparently do so via the canonical (ESCRT and PI3K -dependent) mechanism, and ubiquitination of the DOR stimulates but is not required for this topological sorting operation.

While our localization data clearly established intralumenal localization of both wild type and lysine-mutant DORs, they did not provide information about whether this topological sorting is sufficient to expose the receptor endodomain to the biochemical environment of the endosome lumen. As a first step to address this question, we replaced the C-terminal (endodomain) tag with a GFP variant, ecliptic pHluorin (41), whose fluorescence is efficiently and reversibly quenched when exposed to the acidic environment of the endosome lumen (Fig 4A). Using this approach, we were able to selectively visualize tagged receptors localized in the limiting membrane and then, in a time-dependent manner after addition to cells of the membrane-permeant weak base chloroquine, neutralize the endosome interior and reveal the presence of any tagged receptors present in the endosome lumen (which were previously undetectable due to fluorescence quenching). This approach definitively confirmed the presence of intralumenal receptors (Fig 4 B and C, Supplemental Movie 3 and 4), and at the same time point as used for the other analyses. Quantification of the chloroquine-induced increase in fluorescence intensity confirmed partial inhibition of intralumenal localization produced by lysyl mutation (Fig 4D). These results, in addition to definitively verifying intralumenal localization of receptors at the light microscopic level, indicated that intralumenal

receptors indeed gain biochemical access to the acidic environment of the endocytic pathway.

*Lysine mutation of DORs delays proteolytic destruction specifically of the receptor endodomain*

We next asked how this regulatory, but non-essential, function of DOR ubiquitination affects the process of receptor degradation in the endocytic pathway. To do so we used the dual epitope tagging strategy (Fig 5A) to monitor proteolysis in the receptor ectodomain (N-terminal FLAG tag) separately from the endodomain (C-terminal HA tag).

Consistent with previous studies examining proteolysis of the DOR N-terminus (22, 23), immunoblotting using anti-FLAG antibody verified proteolysis of the FLAG tag from F-DOR-HA that began ~60 min after agonist addition was essentially complete within 2 hours thereafter (Fig 5B). The rate and extent of this proteolysis were completely unaffected by lysine mutation (Fig 5C), as verified by densitometric quantification across multiple experiments (Fig 5D). Immunoblotting of the same extracts using anti-HA verified extensive proteolytic fragmentation of both F-DOR-HA and F-DOR-0cK-HA in DADLE-exposed cells (Fig 5E and F). The onset of this fragmentation corresponded precisely with loss of the ectodomain FLAG epitope. Interestingly, while essentially no full-length forms of either receptor construct (indicated by bracket) remained after ~3 hours of DADLE exposure, we noticed a relative accumulation of HA-linked proteolytic fragments at later time points in cells expressing lysine-mutant receptors (arrows at right of the blot). Quantification across multiple experiments verified a significant difference

in the persistence of HA-linked fragments between wild type and ubiquitination-defective mutant receptors (Fig 5G).

To further investigate the biochemical consequence of preventing DOR ubiquitination, we immunoprecipitated HA-linked fragments, removed Asn-linked glycans with PNGaseF, and estimated the molecular mass of each fragment by calibrated SDS-PAGE. Full-length DORs resolved at ~45 kDa after deglycosylation, as expected for the doubly tagged protein. In the presence of DADLE, we observed time-dependent formation of proteolytic fragments resolving at 38, 31 and 22 kDa (Fig 6A). All of these products mapped to cleavages occurring in the ectodomain (Fig 6B). These results support the hypothesis that DOR ubiquitination selectively promotes proteolysis of the receptor endodomain and indicate that, when DOR ubiquitination is prevented by lysine mutation, receptors can still undergo extensive proteolytic fragmentation at multiple sites distributed throughout the ectodomain.

Blockade of net MVB formation using the PI3K inhibitor wortmannin (42) had little effect on DADLE-induced destruction of the luminal FLAG epitope (Fig 7A and B), but resulted in accumulation of HA-linked proteolytic fragments similar to those accumulated by preventing receptor ubiquitination (Fig 7 C and D). This result further indicates that intra-MVB sorting selectively promotes destruction of the DOR endodomain, without affecting the ability of receptors to undergo extensive fragmentation by proteolysis in the ectodomain.

*Disrupting AIP4 activity phenocopies the lysine-dependent trafficking effect on wild type DORs*

We next asked if this selective effect on endodomain proteolysis and intra-MVB sorting of the DOR is a consequence of ubiquitination mediated by AIP4. To do so, we applied a previously established dominant negative strategy using mutationally inactivated (Cys->Ala or C/A mutant) AIP4 (24), and asked if disrupting AIP4 activity can mimic the effects of lysine mutation.

Using the dual epitope strategy, we observed that disrupting AIP4 activity did not affect DADLE-induced proteolysis of the wild type DOR ectodomain (Fig 8A) but significantly inhibited the subsequent destruction of endodomain-linked proteolytic fragments (Fig 8B). Using the GFP imaging strategy, we then established that co-expression of a (Cherry-tagged) inactive AIP4 inhibited intralumenal localization of the wild type DOR. In contrast, co-expression at similar levels (assessed by Cherry fluorescence) of an inactivated mutant form of the related HECT domain ligase, Nedd4-2, had no effect (Fig 8C). In contrast, and verifying that the DOR is a direct target of AIP4-dependent ubiquitination, inactivated AIP4 did not produce any detectable effect on intralumenal localization of the lysine mutant DOR (Fig 8D).

## 3.4 Discussion

The present results provide a systematic analysis of membrane trafficking events underlying lysosomal down-regulation of the DOR. We focused on this particular mammalian 7TMR because its lysosomal destruction is a physiologically important regulatory process (20, 21), and because DORs have the remarkable ability to down-regulate effectively via an ESCRT-dependent mechanism when their ubiquitination is prevented. Previous work identifying alternate protein connectivity modulating DOR down-regulation (25, 27) leaves unresolved whether DORs traverse MVBs and, if so, what role ubiquitination plays in mediating or controlling the down-regulation of this mammalian 7TMR.

Our data clearly establish that internalized DORs traffic via morphologically characteristic MVBs, and localize to the endosome lumen in an ESCRT and PI3K -dependent manner, supporting the hypothesis that DORs traverse the canonical MVB pathway (43). Accordingly, we took several independent approaches to discern the specific functional significance of DOR ubiquitination to receptor trafficking within this pathway. First, we assessed the sorting of receptors away from bulk membrane recycling using an established flow cytometric method. Second, we investigated whether receptors traverse MVBs using immunoelectron microscopy and optical imaging approaches. Third, we examined the effect of intra-MVB sorting on biochemical accessibility of receptors to the endosome lumen using both pH-sensitive GFP (pHluorin) imaging and biochemical analysis of domain-specific proteolytic fragmentation.

Exclusion of DORs from the rapid recycling pathway marked by TfRs was highly efficient, was not detectably inhibited by lysine mutation of receptors, and clearly preceded the onset of proteolytic digestion of receptors measured by any of the biochemical assays. These findings define receptor sorting away from the bulk recycling route as a discrete, and early, sorting operation. Quantitative imaging revealed that ubiquitination of DORs specifically promoted their localization to the intralumenal compartment of endosomes. This is consistent with the ability of ubiquitination of various integral membrane proteins to promote intra-MVB sorting, with two notable exceptions: First, ubiquitination of DORs was not essential for intralumenal localization, as lysine-mutant receptors were clearly observed to access the endosome lumen both by immuno-electron microscopy and fluorescence imaging of living cells. Second, neither DOR ubiquitination nor intra-MVB sorting was required to prevent internalized receptors from recycling to the plasma membrane.

Together, these observations support a model in which endocytic trafficking of the DOR to lysosomes involves two discrete molecular sorting operations that are arranged in series in the MVB pathway, and which differ in dependence on receptor ubiquitination (Fig 9). Importantly, the finding that lysyl mutation of DORs reduces intralumenal sorting of DORs without causing any enhancement of receptor recycling rules out the alternative hypothesis that ubiquitin -independent and -dependent mechanisms function in parallel.

The first operation is the exclusion of internalized receptors from the rapid recycling pathway ('Sorting Step I' in Fig 9); this sorting step does not require ubiquitination of the DOR and, for this particular 7TMR, represents the major determinant of subsequent endocytic trafficking fate. In contrast, lysyl mutation has been shown to markedly increase recycling of other signaling receptors in yeast and mammalian cells (14, 31), including some other mammalian 7TMRs (17, 44). This suggests that the upstream sorting step represents an elaboration of the down-regulation pathway that is engaged specifically by a subset of signaling receptors.

The second sorting operation in the sequential model is receptor transfer from the endosome limiting membrane to ILVs ('Sorting Step II' in Fig 9). This topological sorting operation is stimulated by DOR ubiquitination, and corresponds to the primary sorting operation distinguishing recycling from degradative trafficking of various other signaling receptors. A distinction is that, for the DOR, ubiquitination promotes but is not essential for topological sorting to ILVs. This verifies the dominant role of Sorting Step I in directing DOR trafficking to the MVB pathway, and suggests that this upstream sorting operation is sufficient to drive effective delivery of receptors to sites of ESCRT-mediated ILV formation even in the absence of receptor ubiquitination.

Live imaging of pHluorin-tagged receptors established that intra-MVB sorting of DORs affords access of the receptor endodomain to the acidic environment of the endosome lumen. The proteolytic cleavage analysis showed, further, that intra-MVB sorting selectively accelerates destruction of the receptor endodomain. Thus the present results

can simply explain why previous studies of DOR ubiquitination have detected only a relatively subtle effect on net proteolytic destruction of DORs.

An important question for future study is how receptors devoid of any ubiquitination retain the ability to undergo topological sorting to ILVs. While we note that there is evidence for the existence of alternate mechanisms of ILV formation and cargo traffic (39, 40), our results suggest that both wild type and lysine-mutant DORs access the endosome lumen by the canonical (ESCRT-dependent) mechanism. The simplest hypothesis capable of explaining the present findings is that non-ubiquitinated receptors, because they are unable to efficiently enter the rapid recycling pathway originating from early / sorting endosomes, are effectively 'trapped' in maturing endosomes and subsequently access the intralumenal compartment during the process of MVB biogenesis by passive diffusion into ESCRT domains formed at the limiting membrane. An additional, and not mutually exclusive, possibility is that alternate DOR connectivity to the ESCRT (25, 27), as proposed here to function in Sorting Step I, persists during MVB biogenesis to further promote ESCRT-mediated entry into the intralumenal compartment (Fig. 9, inset). Both of these mechanisms are plausible based on present information, and could simply account for the ability of non-ubiquitinated DORs to undergo sorting to ILVs. We cannot exclude the possibility that topological sorting of DORs to ILVs is promoted by interaction with a distinct (and likely ubiquitinated) endocytic cargo protein, or that DORs access ILVs by lateral partitioning into biophysically distinct microdomains of the limiting membrane from which ESCRT-dependent ILV formation occurs. We note that DORs have the ability to homo-oligomerize when present at high surface

concentration, and may also form hetero-oligomers with other 7TMRs (45). Any of these possibilities could explain the ability of DORs to undergo topological sorting in the absence of ubiquitination, and none would invalidate the present conclusion that DORs are sorted sequentially in the MVB pathway.

Another important question for future investigation is to determine the functional significance of sequential molecular sorting operations in the pathway of DOR down-regulation. An attractive possibility is that sequential sorting could afford an additional degree of freedom in the endocytic regulation of particular signaling receptors, by effectively allowing the cytoplasmic accessibility of internalized signaling receptors to be controlled specifically and independently from their ultimate trafficking fate. There is accumulating evidence that various signaling receptors, including some 7TMRs, can signal from endosomes as well as from the plasma membrane (1, 2). There is also evidence that intra-MVB sorting is a significant mechanism for terminating receptor-mediated signaling by the EGF receptor tyrosine kinase (2, 42). Thus we anticipate that the ESCRT / MVB system, besides its established function in driving ubiquitin-directed destruction of various integral membrane proteins, serves additional role(s) in controlling the duration or subcellular localization of specific receptor-mediated signaling activities.

## 3.5 Acknowledgments

This work was supported by grants from the NIH (DA010711 and DA012864 to MvZ) and the UK Medical Research Council to MM and IW. AGH is a recipient of a predoctoral fellowship from the US National Science Foundation. The authors gratefully acknowledge Kurt Thorn and the Nikon Imaging Center at UCSF for useful advice, and for providing access to fluorescence imaging instrumentation. We thank Adriano Marchese and Harald Stenmark for valuable discussion and sharing essential reagents, Scott Emr, Manoj Pathenveedu, Michael Tanowitz and Paul Temkin for critical comments and suggestions, and Aaron Marley, Laurant Coscoy, Roger Tsien and Marino Zerial for generously providing constructs used in this study.

## 3.6 Materials and Methods

*Cell culture, cDNA constructs and transfection*

The Myc tagged inactive mutant AIP4 has been previously described (30) and was a gift from Adriano Marchese (Loyola University, Chicago IL). GFP-tagged Rab5 cDNA was a gift from Marino Zerial (Max Planck Institute of Molecular Cell Biology and Genetics, Germany), and the Q79L mutation was made by site-directed mutagenesis (Stratagene), HRS cDNA was a gift from Harold Stenmark (Norwegian Radium Hospital), Nedd-4-1-C/A mutant was a gift from Laurant Coscoy (University of California, Berkeley), and the mCherry cDNA was a gift from Roger Tsien (University of California, San Diego). PCR was used to remove the stop codon from mCherry, and the resulting fragment was cloned into pcDNA3.0 (Invitrogen). This vector was then used to construct N-terminal fusions of HRS, Nedd4-1-C/A and AIP4-C/A. N-terminal FLAG-tagged, and C-terminal HA-tagged versions of wild type and lysine-mutant δ-opioid receptor have been previously described as F-DOR-HA and F-DOR-0cK-HA (24). C-terminal GFP-tagged fusion constructs were generated from these constructs by PCR, introducing an AgeI restriction site into the reverse primer at the appropriate location, and ligating in-frame into pEGFP-N1 (Clontech). We constructed pHluorin-tagged receptors using PCR to replace the EGFP coding sequence with superecliptic pHluorin (41, 46). All cDNA constructs were verified by sequencing (ElimBio, CA). Human embryonal kidney 293 (HEK293) cells (ATCC) were maintained in Dulbecco's modified Eagles medium supplemented with 10% fetal bovine serum (University of California, San Francisco, Cell Culture Facility). For transient expression, cells were transfected using Lipofectamine 2000 (Invitrogen) according to manufacturers' instructions. Cells expressing FLAG-tagged receptors were

harvested by washing with EDTA and plated in 60-mm dishes at 80% confluency, before transfection with plasmid DNA. Cells were reseeded into poly-lysine coated 6-well or 24 well plates and cultured for a further 24 hours before experiments. For stable expression, clonal selection was carried out using 500 µg/ml G418 (Geneticin, Gibco), and clones were selected for study based on comparable levels of receptor expression as determined by saturation binding analysis using $^{3}$H-diprenorphine as described previously (24). Expression levels used in this study were between 0.5 and 2 pmol / mg; this is within the range of endogenous opioid receptor expression in brain tissue (20), and does not saturate the endocytic machinery in HEK293 cells (23, 24).

*Biochemical detection of receptor proteolysis and protein levels by immunoblotting*

Immunoblotting to assess total cellular receptor levels was carried out as previously described (24). Briefly, cell monolayers were washed three times in ice-cold phosphate buffered saline (PBS) and lysed in extraction buffer (0.5% Triton X-100, 150 mM NaCl, 25 mM KCl, 25 mM Tris pH 7.4, 1 mM EDTA) supplemented with a standard protease inhibitor cocktail (Roche). Extracts were clarified by centrifugation (12,000 x g for 10 minutes), and then mixed with SDS sample buffer for denaturation. Proteins present in the extracts were resolved by SDS-PAGE using 4-12% Bis-Tris gels (Nu-PAGE, Invitrogen), transferred to nitrocellulose membranes, and probed for protein by immunoblotting using horseradish peroxidase-conjugated sheep anti-mouse IgG or donkey anti-rabbit IgG (Amersham Biosciences), and SuperSignal detection reagent (Pierce). Apparent molecular mass was estimated using commercial protein standards (SeeBlue Plus2, Invitrogen). Band intensities of unsaturated immunoblots were analyzed

and quantified by densitometry using FluorChem 2.0 software (AlphaInnotech Corp.). Antibodies used were anti-FLAG-M1 (Sigma) and anti-HA-11 (Covance).

*Biochemical detection of receptor proteolytic fragments by immunoblotting*

Following lysis as above, samples were immunoprecipitated with anti-HA-11 and protein A/G agarose beads. Washed beads were deglycosylated by the addition of 500 units of PNGase F (NEB) and incubated for 1 hour at 37˚C before the elution with SDS sample buffer, resolving by SDS-PAGE and then transferred to nitrocellulose membranes, and probed for HA-tagged receptor (anti-HA-HRP antibody, clone 3F10, Roche).

*Spinning-disc confocal microscopy of living cells*. For live imaging, HEK 293 transiently-transfected with the indicated N-terminally FLAG-tagged, C-terminally GFP-tagged receptor constructs were plated onto polylysine-coated glass coverslips (Corning Glass). Cells were incubated in the presence of 10 µM DADLE for 90 min prior to imaging. Cells were imaged in Dulbecco's Modified Eagle Medium without Phenol Red (UCSF Cell Culture Facility) supplemented with 1% fetal bovine serum (UCSF Cell Culture Facility) and 30mM Hepes adjusted to pH 7.4. Live cell imaging was performed using a Yokogawa CSU22 Spinning Disk Confocal (Solamere Technology Group) on a Nikon TE2000U inverted microscope. Cells were visualized using a 100 X 1.49 NA TIRF objective and illuminated with a 488nm Ar Laser (Melles Griot). Time-lapse sequences were acquired at a continuous rate of 5 frames per second and acquired images were analyzed with Image J software (Wayne Rasband, National Institutes of Health, Bethesda, MD). Quantification was conducted on raw data representing confocal cross-

sections of individual endosomes. For each endosome, straight-line selections were drawn across the diameter and pixel intensities across the line were measured. Endosomal diameter was normalized to account for endosomes varying in size. The pixel numbers with the first and second maximum pixel intensities, corresponding to pixels on the limiting membrane of the endosome, were normalized to 0 and 100, respectively. The location across the line of pixel 0 was then subtracted from each pixel situated on the line and this value was divided by the total diameter (in pixels) of the endosome. This generated normalized pixel distances corresponding to distance across the line occupied by each pixel, expressed as a percentage. Average background fluorescence was subtracted from raw pixel intensity values. The pixel intensities for the pixel numbers normalized to 0 and 100 were also normalized to 0 and 100, respectively, generating normalized fluorescence values. The background-corrected pixel intensity values corresponding to pixels that lay 40-60% across the endosomal diameter were averaged, generating a middle fluorescence value for each endosome. Middle fluorescence values were compiled across multiple cells and the mean values quantified for each condition are shown. Representative live images shown were rendered using Adobe Photoshop software.

*Live Cell Imaging using the pH-sensitive GFP variant*

HEK 293 cells transiently-transfected with the indicated N-terminally FLAG-tagged, C-terminally ecliptic GFP variant-tagged receptor constructs were plated onto polylysine-coated glass coverslips (Corning Glass). Cells were incubated in the presence of 10 µM DADLE for 90 min prior to imaging. Cells were imaged for 10s and then 1mM

chloroquine was added to cells while image acquisition continued. Quantification was conducted on raw data representing confocal cross-sections of individual endosomes. For each endosome, selections were drawn around each individual endosome and the mean fluorescence values were background corrected. To measure the chloroquine-induced increase in fluorescence inside the endosomal lumen, the minimum average fluorescence value in the first half of the image sequence was identified and fluorescence values for the three frames before and after this frame were averaged. This mean was the average minimum fluorescence. The maximum average fluorescence value in the second half of the image sequence was determined and fluorescence values for the three frames before and after this frame were averaged. This mean was the average maximum fluorescence. To calculate the fold increase for each individual endosome, the average maximum fluorescence value was divided by the average minimum fluorescence value. Fold increase in fluorescence measurements were compiled across multiple cells and the mean values quantified for each condition are shown.

*Laser-scanning confocal microscopy of fixed specimens*

HEK293 cells were transiently transfected with either F-DOR-HA or F-DOR-0cK-HA and then plated on polylysine-coated glass coverslips (Corning). Cells were 'fed' with Rabbit anti-FLAG antibody (1µg/ml, Sigma) for 30 minutes to label the surface pool of receptors, before being left untreated, incubated in the presence of 10 µM DADLE for 30 minutes, or incubated with agonist followed by incubation with antagonist (10µM Naloxone) for 60 minutes, before fixation with 4% formaldehyde and permeablization with 0.1% Triton-X100 in PBS. Cells were labeled using mouse anti-HA-11 (Covance),

followed by secondary detection using Alexa488-conjugated anti-mouse and Alexa555 anti-rabbit secondary antibodies (Invitrogen). Specimens were imaged by confocal fluorescence microscopy using a Zeiss LSM 510 microscope fitted with a Zeiss 63 x NA1.4 objective operated in single photon mode, with standard filter sets verified for lack of detectable cross-channel bleedthrough and standard (1 Airy disc) pinhole. Acquired optical sections were analyzed with LSM Image Examiner (Zeiss) and rendered with Adobe Photoshop software.

*Quantification of receptor recycling by fluorescence flow cytometry*

A previously described flow cytometric method for accurately measuring opioid receptor recycling (18) was used with minor variation (32). Briefly, surface N-terminally FLAG-tagged and C-terminally HA-tagged DOR and DOR0cK receptors stably expressed in HEK 293 cells were labeled with M1 anti–FLAG antibody (1 mg/mL, Sigma) conjugated to Alexa647 isothiocyanate (Invitrogen/ Molecular Probes) according to manufacturer's instructions. Cells were incubated with 10 μM DADLE for 30 min at 37 °C to drive receptor internalization to steady state, and cells were rinsed three times with calcium and magnesium-free PBS supplemented with 0.4% EDTA to dissociate antibody from receptors remaining at the plasma membrane and therefore specifically label internalized receptors. To determine whether the presence of intracellular lysine residues affects recycling of receptors, cells were incubated at 37 °C in EDTA-supplemented PBS with 10μM naloxone (to prevent residual agonist effects) for the indicated time periods. Monolayers were chilled to 4 °C, lifted, and analyzed by flow cytometry to detect antibody bound to internalized receptors remaining within the cell. Transferrin receptor

recycling was measured over the same time scale using a previously described 'pulse-chase' method (47) based on efflux of labeled transferrin bound to the internalized receptor pool, and adapted to flow cytometry using Alexa488-conjugated diferric transferrin (Invitrogen, 1 µg/mL) as described previously (32).

*Cryosectioning and immunoelectron microscopy.* Cells were fixed with 4% paraformaldehyde in 0.1 M phosphate buffer pH 7.4, infused with 2.3 M sucrose and supported in 12% gelatin. Sections (70 nm) were cut at -120°C and picked up in 1:1 sucrose:methylcellulose. For labeling, primary antibody was followed by rabbit anti-mouse intermediate antibody (DAKO) and sections were then labeled using protein A gold as described (48). Images were obtained using a Tecnai T12 transmission electron microscope (FEI, Netherlands) and captured using a Morada CCD camera (Olympus-SIS).

*Statistical analysis*

Quantitative data were averaged across multiple independent experiments, with the number of experiments specified in the corresponding figure legend. Unless indicated otherwise, error bars represent the standard error of the mean determined after compiling mean determinations across experiments. The statistical significance of the indicated differences was analyzed using the appropriate variations of two-way ANOVA and post-test, or Student's t test, as specified in the figure legends and calculated using Prism 4.0 software (GraphPad Software, Inc). The relative significance of each of the reported

differences is specified by calculated p values that are also listed in the figure legends, and annotated graphically in the figures.

## 3.7 References


1. Sorkin A, von Zastrow M. Endocytosis and signalling: intertwining molecular networks. Nat Rev Mol Cell Biol 2009;10(9):609-622.

2. Miaczynska M, Pelkmans L, Zerial M. Not just a sink: endosomes in control of signal transduction. Curr Opin Cell Biol 2004;16(4):400-406.

3. Ferguson SS, Zhang J, Barak LS, Caron MG. Molecular mechanisms of G protein-coupled receptor desensitization and resensitization. Life Sci 1998;62(17-18):1561-1565.

4. Carman CV, Benovic JL. G-protein-coupled receptors: turn-ons and turn-offs. Current Opinion in Neurobiology 1998;8(3):335-344.

5. Hanyaloglu AC, von Zastrow M. Regulation of GPCRs by endocytic membrane trafficking and its potential implications. Annu Rev Pharmacol Toxicol 2008;48:537-568.

6. Marchese A, Paing MM, Temple BR, Trejo J. G protein-coupled receptor sorting to endosomes and lysosomes. Annu Rev Pharmacol Toxicol 2008;48:601-629.

7. Hicke L. A new ticket for entry into budding vesicles-ubiquitin. Cell 2001;106(5):527-530.

8. Shenoy SK. Seven-transmembrane receptors and ubiquitination. Circ Res 2007;100(8):1142-1154.

9. Kirkin V, Dikic I. Role of ubiquitin- and Ubl-binding proteins in cell signaling. Curr Opin Cell Biol 2007;19(2):199-205.

10. Hislop JN, Von Zastrow M. Role of Ubiquitination in Endocytic Trafficking of G-Protein-Coupled Receptors. Traffic 2010.

11. Katzmann DJ, Babst M, Emr SD. Ubiquitin-dependent sorting into the multivesicular body pathway requires the function of a conserved endosomal protein sorting complex, ESCRT-I. Cell 2001;106(2):145-155.

12. Hurley JH, Wendland B. Endocytosis: driving membranes around the bend. Cell 2002;111(2):143-146.

13. Hicke L, Dunn R. Regulation of membrane protein transport by ubiquitin and ubiquitin-binding proteins. Annu Rev Cell Dev Biol 2003;19:141-172.

14. Huang F, Kirkpatrick D, Jiang X, Gygi S, Sorkin A. Differential regulation of EGF receptor internalization and degradation by multiubiquitination within the kinase domain. Mol Cell 2006;21(6):737-748.

15. Saksena S, Sun J, Chu T, Emr SD. ESCRTing proteins in the endocytic pathway. Trends Biochem Sci 2007;32(12):561-573.

16. Marchese A, Benovic JL. Agonist-promoted ubiquitination of the G protein-coupled receptor CXCR4 mediates lysosomal sorting. J Biol Chem 2001;276(49):45509-45512.

17. Jacob C, Cottrell GS, Gehringer D, Schmidlin F, Grady EF, Bunnett NW. c-Cbl mediates ubiquitination, degradation, and down-regulation of human protease-activated receptor 2. J Biol Chem 2005;280(16):16076-16087.

18. Tsao PI, von Zastrow M. Type-specific sorting of G protein-coupled receptors after endocytosis. J Biol Chem 2000;275(15):11130-11140.

19. Law PY, Wong YH, Loh HH. Molecular mechanisms and regulation of opioid receptor signaling. Annu Rev Pharmacol Toxicol 2000;40:389-430.

20. Scherrer G, Tryoen-Toth P, Filliol D, Matifas A, Laustriat D, Cao YQ, Basbaum AI, Dierich A, Vonesh JL, Gaveriaux-Ruff C, Kieffer BL. Knockin mice expressing fluorescent delta-opioid receptors uncover G protein-coupled receptor dynamics in vivo. Proc Natl Acad Sci U S A 2006;103(25):9691-9696.

21. Pradhan AA, Becker JA, Scherrer G, Tryoen-Toth P, Filliol D, Matifas A, Massotte D, Gaveriaux-Ruff C, Kieffer BL. In vivo delta opioid receptor internalization controls behavioral effects of agonists. PLoS One 2009;4(5):e5425.

22. Tanowitz M, Von Zastrow M. Ubiquitination-independent trafficking of G protein-coupled receptors to lysosomes. J Biol Chem 2002;277(52):50219-50222.

23. Hislop JN, Marley A, Von Zastrow M. Role of mammalian vacuolar protein-sorting proteins in endocytic trafficking of a non-ubiquitinated G protein-coupled receptor to lysosomes. J Biol Chem 2004;279(21):22522-22531.

24. Hislop JN, Henry AG, Marchese A, von Zastrow M. Ubiquitination regulates proteolytic processing of G protein-coupled receptors after their sorting to lysosomes. J Biol Chem 2009;284(29):19361-19370.

25. Whistler JL, Enquist J, Marley A, Fong J, Gladher F, Tsuruda P, Murray SR, Von Zastrow M. Modulation of postendocytic sorting of G protein-coupled receptors. Science 2002;297(5581):615-620.

26. Simonin F, Karcher P, Boeuf JJ, Matifas A, Kieffer BL. Identification of a novel family of G protein-coupled receptor associated sorting proteins. J Neurochem 2004;89(3):766-775.

27. Marley A, von Zastrow M. Dysbindin promotes the post-endocytic sorting of G protein-coupled receptors to lysosomes. PLoS One 2010;5(2):e9325.

28. Petaja-Repo UE, Hogue M, Laperriere A, Bhalla S, Walker P, Bouvier M. Newly synthesized human delta opioid receptors retained in the endoplasmic reticulum are retrotranslocated to the cytosol, deglycosylated, ubiquitinated, and degraded by the proteasome. J Biol Chem 2001;276(6):4416-4423.

29. Chaturvedi K, Bandari P, Chinen N, Howells RD. Proteasome involvement in agonist-induced down-regulation of mu and delta opioid receptors. J Biol Chem 2001;276(15):12345-12355.

30. Marchese A, Raiborg C, Santini F, Keen JH, Stenmark H, Benovic JL. The E3 ubiquitin ligase AIP4 mediates ubiquitination and sorting of the G protein-coupled receptor CXCR4. Dev Cell 2003;5(5):709-722.

31. Chen L, Davis NG. Ubiquitin-independent entry into the yeast recycling pathway. Traffic 2002;3(2):110-123.

32. Yudowski GA, Puthenveedu MA, Henry AG, von Zastrow M. Cargo-mediated regulation of a rapid Rab4-dependent recycling pathway. Mol Biol Cell 2009;20(11):2774-2784.

33. Maxfield FR, McGraw TE. Endocytic recycling. Nat Rev Mol Cell Biol 2004;5(2):121-132.

34. Krisch B, Feindt J, Mentlein R. Immunoelectronmicroscopic analysis of the ligand-induced internalization of the somatostatin receptor subtype 2 in cultured human glioma cells. J Histochem Cytochem 1998;46(11):1233-1242.

35. Volpicelli LA, Lah JJ, Levey AI. Rab5-dependent trafficking of the m4 muscarinic acetylcholine receptor to the plasma membrane, early endosomes, and multivesicular bodies. J Biol Chem 2001;276(50):47590-47598.

36. Fraile-Ramos A, Pelchen-Matthews A, Kledal TN, Browne H, Schwartz TW, Marsh M. Localization of HCMV UL33 and US27 in endocytic compartments and viral membranes. Traffic 2002;3(3):218-232.

37. Slagsvold T, Marchese A, Brech A, Stenmark H. CISK attenuates degradation of the chemokine receptor CXCR4 via the ubiquitin ligase AIP4. Embo J 2006;25(16):3738-3749.

38. Wegener CS, Malerod L, Pedersen NM, Prodiga C, Bakke O, Stenmark H, Brech A. Ultrastructural characterization of giant endosomes induced by GTPase-deficient Rab5. Histochem Cell Biol 2009.

39. Trajkovic K, Hsu C, Chiantia S, Rajendran L, Wenzel D, Wieland F, Schwille P, Brugger B, Simons M. Ceramide triggers budding of exosome vesicles into multivesicular endosomes. Science 2008;319(5867):1244-1247.

40. van der Goot FG, Gruenberg J. Intra-endosomal membrane traffic. Trends Cell Biol 2006;16(10):514-521.

41. Miesenbock G, De Angelis DA, Rothman JE. Visualizing secretion and synaptic transmission with pH-sensitive green fluorescent proteins. Nature 1998;394(6689):192-195.

42. Futter CE, Collinson LM, Backer JM, Hopkins CR. Human VPS34 is required for internal vesicle formation within multivesicular endosomes. J Cell Biol 2001;155(7):1251-1264.

43. Raiborg C, Stenmark H. The ESCRT machinery in endosomal sorting of ubiquitylated membrane proteins. Nature 2009;458(7237):445-452.

44. Cottrell GS, Padilla B, Pikios S, Roosterman D, Steinhoff M, Gehringer D, Grady EF, Bunnett NW. Ubiquitin-dependent down-regulation of the neurokinin-1 receptor. J Biol Chem 2006;281(38):27773-27783.

45. Rios CD, Jordan BA, Gomes I, Devi LA. G-protein-coupled receptor dimerization: modulation of receptor function. Pharmacol Ther 2001;92(2-3):71-87.

46. Sankaranarayanan S, De Angelis D, Rothman JE, Ryan TA. The use of pHluorins for optical measurements of presynaptic activity. Biophys J 2000;79(4):2199-2208.

47. Dunn KW, McGraw TE, Maxfield FR. Iterative fractionation of recycling receptors from lysosomally destined ligands in an early sorting endosome. Journal of Cell Biology 1989;109(6 Pt 2):3303-3314.

48. Slot JW, Geuze HJ, Gigengack S, Lienhard GE, James DE. Immuno-localization of the insulin regulatable glucose transporter in brown adipose tissue of the rat. J Cell Biol 1991;113(1):123-135.

# 3.8 Figures

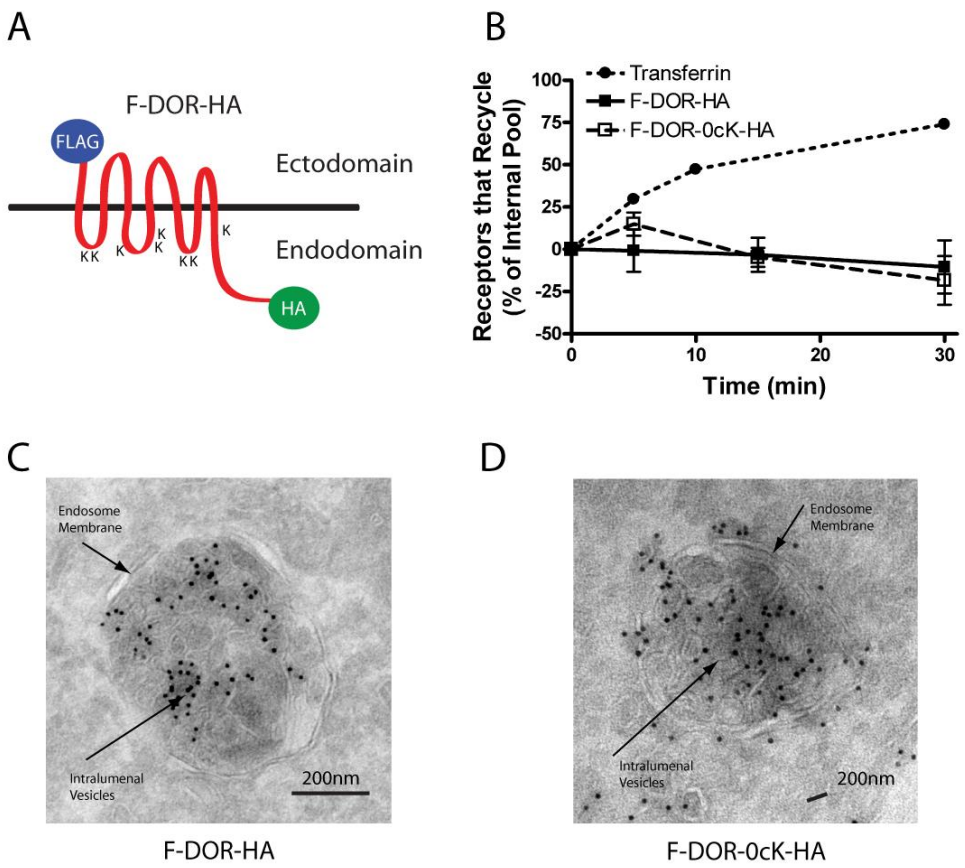


**Figure 1. Both DOR and DOR-0cK are efficiently excluded from the recycling pathway and can undergo transfer in ILVs of endosomes.** A) Schematic representation of the N and C terminally tagged DOR, indicating the positions of the respective tags and lysine residues (K) B) Recycling time course of FLAG-DOR-HA and FLAG-DOR-0cK-HA receptors relative to transferrin receptors. For the opioid receptors, internalization of antibody-labeled receptors was carried out by 30-min pre-incubation with 10µM DADLE. Cells were washed, incubated in the presence of 10µM naloxone, and antibody efflux was assayed at the indicated time points. Recycling of transferrin receptors was estimated by efflux of Alexa488-conjugated transferrin. Points represent mean determinations calculated from three independent experiments. Error bars represent the SEM calculated across experiments (n = 3). HEK293 cells stably expressing F-DOR-HA (A) or F-DOR-0cK-HA (C and D) were treated with 10µM DADLE for 90 minutes before fixation and preparation for cryosectioning, immunolabeling and electron microscopy as described

in *Materials and Methods*. Shown are representative micrographs using anti-HA labeled with 10nm gold particles. Both F-DOR-HA and F-DOR-0cK-HA were resolved in association with intralumenal vesicle membranes of multivesicular bodies. Scale bars indicate 200 nm.

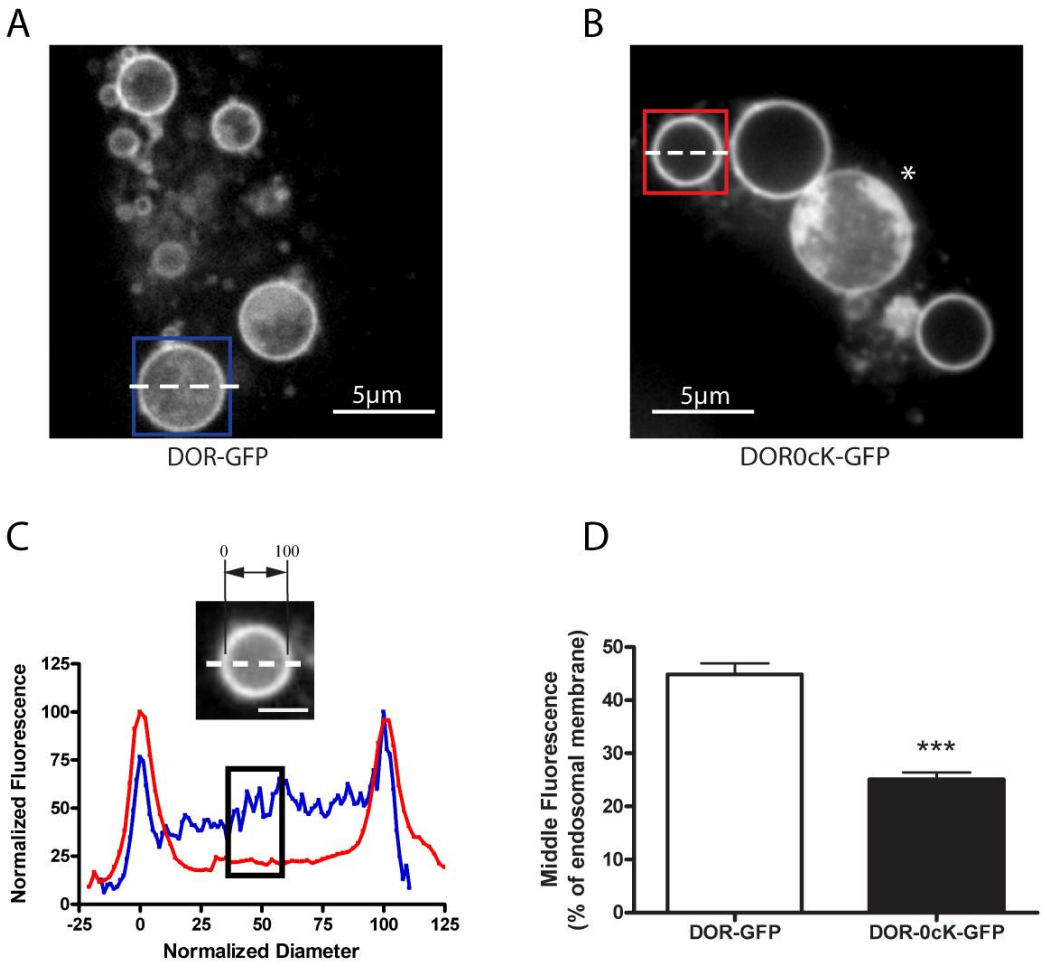


**Figure 2. Enlargement of endosomes by Rab5 manipulation illustrates lysyl-mutant DORs differ in their extent of transfer to ILVs**. A and B) HEK293 cells were transiently transfected with CFP-Rab5Q79L and either F-DOR-GFP (A) or F-DOR-0cK-GFP (B), and replated onto to coverslips before treatment for 90 minutes with 10µM DADLE. Cells were then imaged by spinning disc confocal microscopy as described in *Materials and Methods*. Shown are representative still images of the representative acquired image series, scale bars indicate 5µm. C) Line scan analysis to quantify receptor localization to the intralumenal compartment. Normalized diameter represents the diameter of the endosome shown, where 0 and 100 correspond to the pixel distances with the first and second maximum

pixel intensities measured across the dashed line, respectively (see inset image). Blue and red traces represent the normalized pixel intensity measured across the dashed line in the blue and red boxes in A and B respectively, where the maximum pixel intensity across the line is normalized to 100. The black box highlights the normalized fluorescence values of pixels from 40 to 60% of the normalized diameter. D) Compiled results of line scan analysis (mean and SEM, *** $p<0.001$, Student's t-test, n= 88 endosomes, ≥ 12 cells).

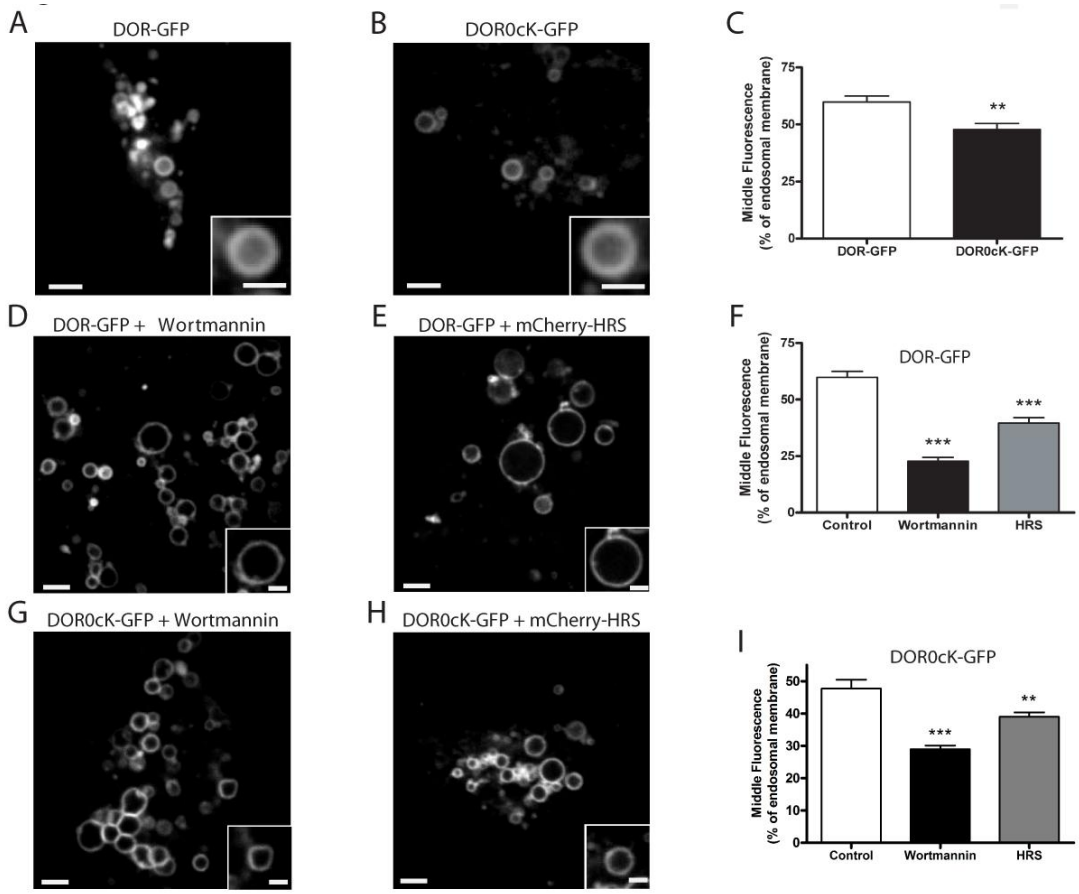


**Figure 3. Differences in the extent of DOR transfer to ILVs can be detected by live-cell imaging of non-enlarged endosomes.** A and B) Live cell imaging of non-enlarged endosomes in HEK293 cells expressing either F-DOR-GFP (A) or F-DOR-0cK-GFP (B) imaged live by spinning disc confocal microscopy after exposure for 90 minutes to 10µM DADLE. Shown are representative still images of the representative acquired image series (see Supplemental Movie 1 and 2. Scale bars are 2µm and 1µm for the insets. C) Quantification of the middle fluorescence, or percentage of endosomal membrane, measured

from individual endosomes. Mean and SEM of middle fluorescence values are shown for F-DOR-GFP transfected cells (DOR-GFP, n= 12 cells, 50 endosomes) and F-DOR0cK-GFP transfected cells (** $p<0.01$, Student's t-test, n=59 endosomes, 13 cells). D-F) The same experiment in cells transfected with F-DOR-GFP and pretreated with 500nM wortmannin (D) or transfected 48 hours before DADLE addition with mCherry-HRS (E). Scale bar on overall image = 2µm and on inset = 1 µm. F) Fluorescence intensity was measured through the center of the endosome as in (A-C) and the mean internal fluorescence is expressed as a percentage of that of the membrane of wortmannin pre-treated F-DOR-GFP transfected cells (Wortmannin, unpaired t-test; ***, $p<0.0001$, n= 11 cells, 50 endosomes), and F-DOR-GFP and mCherry-HRS transfected cells (HRS, unpaired t-test; ***, $p<0.0001$, n= 10 cells, 64 endosomes). D) The same experiment in cells transfected with F-DOR0cK-GFP and pretreated with 500nM wortmannin (G) or transfected 48 hours before DADLE addition with mCherry-HRS (H). Scale bar on overall image = 2µm and on inset = 1 µm. I) Quantification of the middle fluorescence. Mean and SEM of middle fluorescence values are shown for wortmannin pre-treated F-DOR0cK-GFP transfected cells (Wortmannin, unpaired t-test; ***, $p<0.001$, n= 11 cells, 92 endosomes), and F-DOR0cK-GFP and mCherry-HRS transfected cells (HRS, unpaired t-test; **, $p<0.01$, n= 10 cells, 116 endosomes).

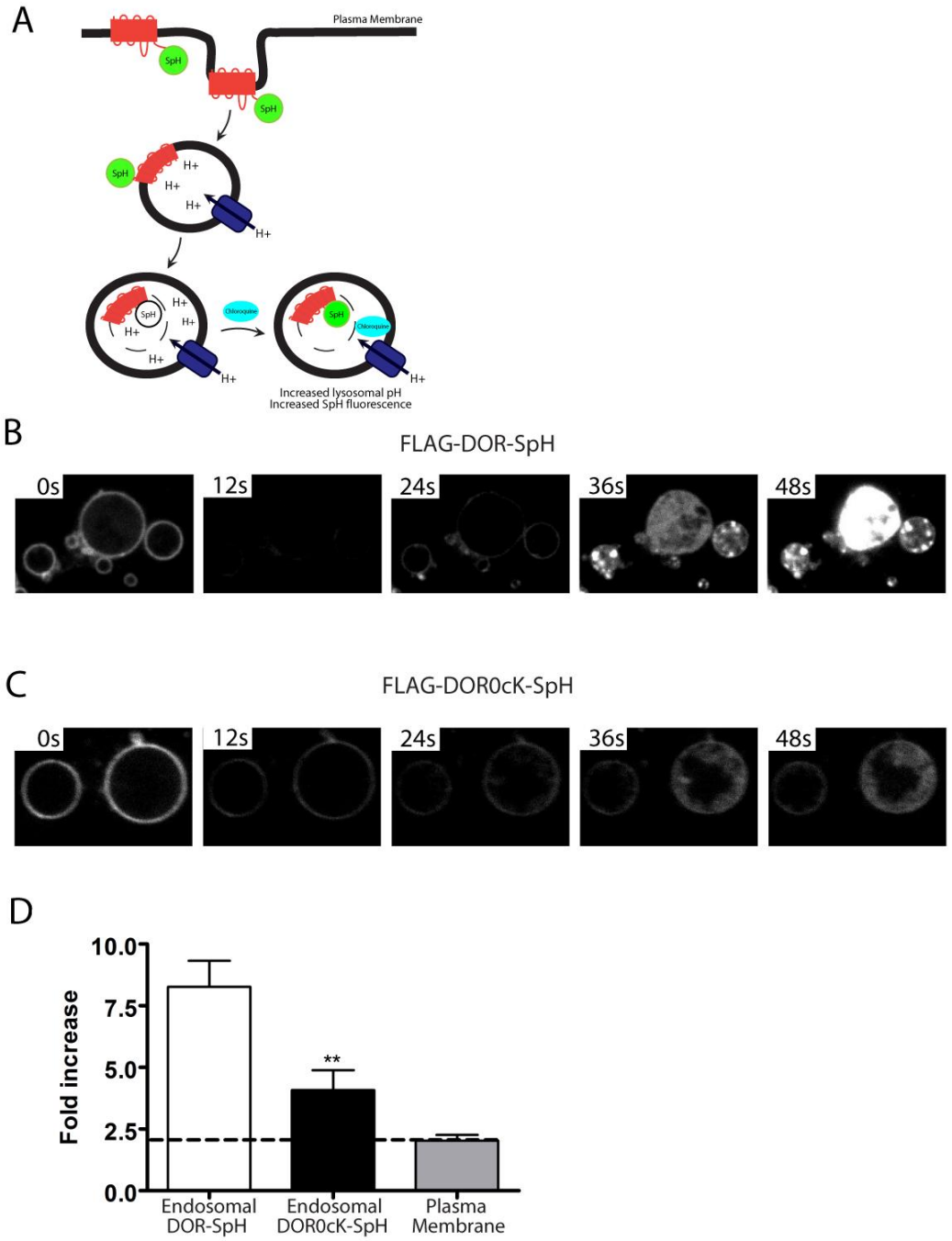


**Figure 4. Intralumenal wild type and lysyl-mutant receptors visualized using a pH-sensitive GFP variant.** A) Schematic of experimental setup following receptors fused to the GFP variant (ecliptic pHluorin) which fluoresce when located in the cytoplasm but whose fluorescence is efficiently quenched when exposed to the acidic environment of the endosome lumen. Addition of the weak base chloroquine neutralizes endosomal pH and reveals any tagged receptors present in the endosome lumen. B and C)

HEK293 cells were transiently transfected with CFP-Rab5Q79L and either F-DOR-SpH (B) or F-DOR-0cK-SpH (C), and replated onto to coverslips before treatment for 90 minutes with 10µM DADLE. Cells were then imaged at a rate of 5 frames per second by spinning disc confocal microscopy and treated with 1mM chloroquine after 50 frames. Image sequences are shown for cells expressing F-DOR-SpH (B) or F-DOR-0cK-SpH (C), see Supplemental Movies 3 and 4 for full sequence. D) Quantification of the chloroquine-induced increase in fluorescence intensity. Mean and SEM are shown for F-DOR-SpH (Endosomal DOR-SpH, n= 8 cells, 24 endosomes) and F-DOR0cK-SpH containing endosomes (Endosomal DOR0cK-SpH, unpaired t-test; ***, $p<0.01$, n= 7 cells, 22 endosomes), and F-DOR-SpH expressed on the plasma membrane (Plasma Membrane, n= 11 cells). Scale bar = 2 µm.

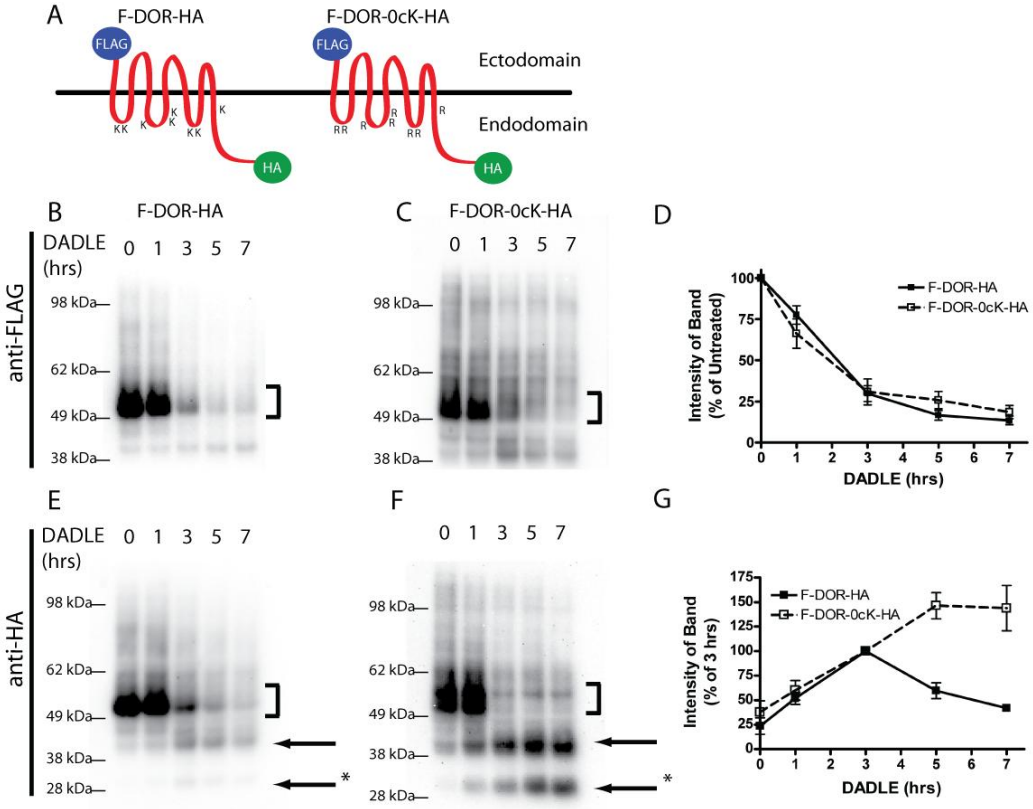


**Figure 5. Differential proteolysis of N and C-terminal fragments of DOR and DOR-0cK.** A) Schematic representation of doubly-tagged receptor constructs of F-DOR-HA and F-DOR-0cK-HA indicating the N-terminal and C-terminal locations of the FLAG and HA epitope tags, respectively. HEK293 cells stably expressing F-DOR-HA (C and F) or F-DOR-0cK-HA (D and G) were incubated with 10µM DADLE for the indicated time period before lysis and division into two identical samples. Shown

are representative anti-FLAG blots (C and D) and anti-HA blots (F and G) as indicated. Bracket indicates position of the full-length receptor species. Arrows denote major proteolytic cleavage products. E) Blots generated in multiple experiments were scanned to estimate the amount of FLAG-tagged receptor remaining at each time point after incubation in the presence of 10µM DADLE, expressed as a percentage of that in cells not exposed to agonist, results were pooled and averaged across multiple experiments (shown are mean and SEM, n=5). H) Anti-HA blots were scanned and the relative immunoreactivity of one proteolytic product (denoted *) was measured and expressed as a percentage of density at 3 hrs, where the band for DOR was most intense. Closed symbols indicate the degradation curve measured for F-DOR-HA, open symbols indicate the degradation curve measured in cells transfected with F-DOR-0cK-HA (mean and SEM, n=5)

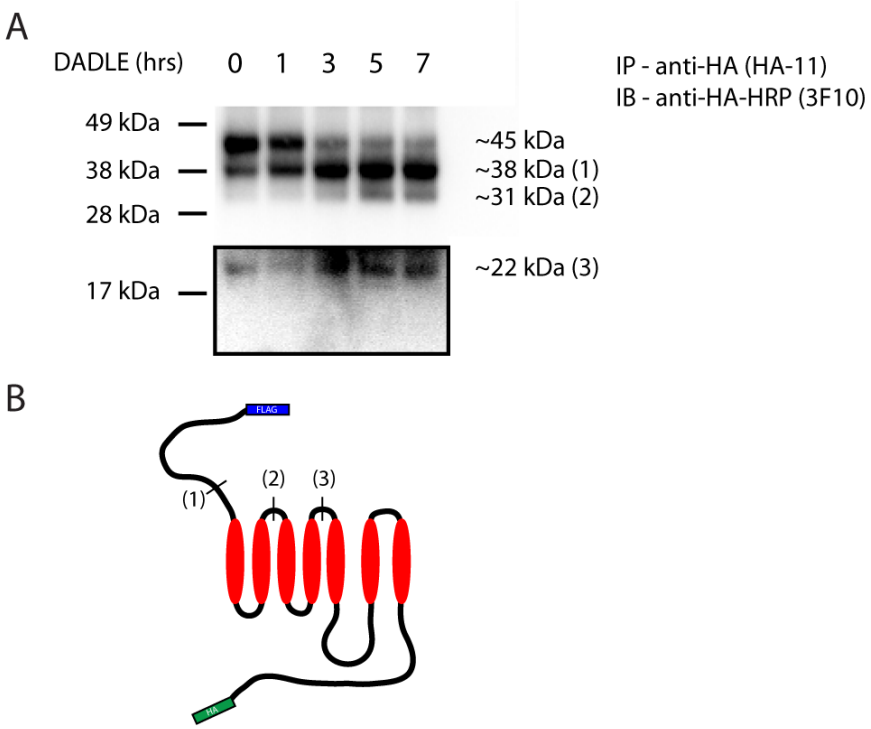


**Figure 6. Analysis of the proteolytic fragmentation of lysine-mutant DORs show delayed destruction specifically of the receptor endodomain.** HEK293 cells stably expressing F-DOR-0cK-HA were incubated with 10µM DADLE for the indicated time period before lysis. HA-linked fragments were immunoprecipitated, treated with PNGaseF, and separated via SDS-PAGE. Shown is a representative anti-

HA blot (A). Proteolytic fragments resolved to the indicated sizes, corresponding topologically as diagrammed in (B).

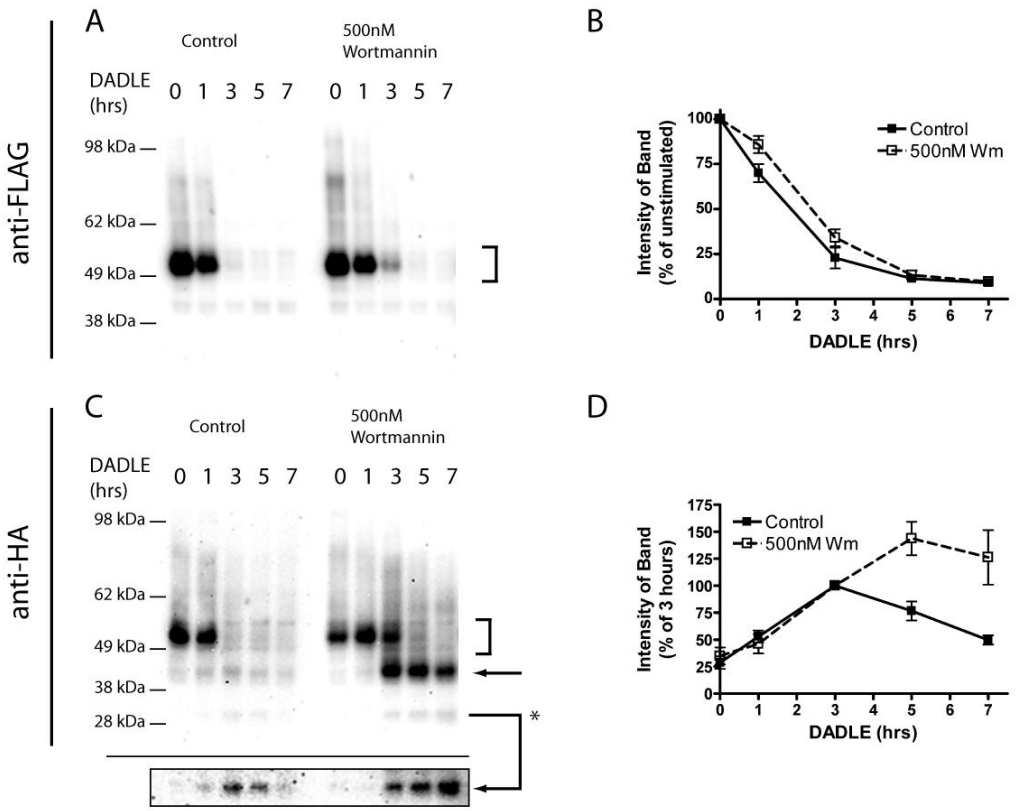


**Figure 7. Persistence of proteolytic cleavage products is mimicked by treatment with Wortmannin.** HEK293 cells stably expressing F-DOR-HA were pretreated with vehicle control (DMSO) or 500nM Wortmannin before incubation with 10µM DADLE for the indicated time period before lysis and division into two identical samples. Shown are representative anti-FLAG (A) or anti-HA (C) Western blots. Arrows denote major proteolytic cleavage products, and the highlighted box shows a darker exposure of the proteolytic product at ~30kDa. Blots generated across multiple experiments were scanned and densitometry performed to estimate the amount of FLAG-tagged receptors remaining at each time point relative to agonist naïve cells (C), and the relative abundance of one anti-HA immunoreactive proteolytic product (denoted *) expressed as a percentage of density at 3 hrs agonist treatment (D). Shown are the mean and SEM of multiple experiments (n=6); closed symbols indicate densitometry in control, DMSO treated cells, and open symbols indicate cells treated with 500nM Wortmannin.

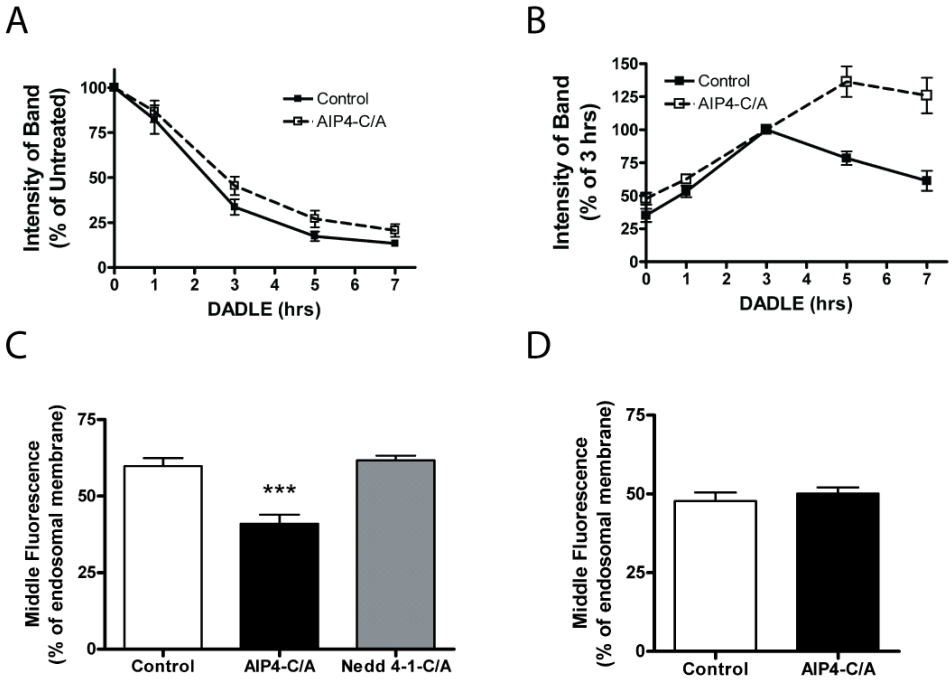


**Figure 8. The E3 ubiquitin ligase AIP4 regulates transfer of DORs to ILVs and subsequent C-terminal proteolysis of receptors.** A and B) HEK293 cells stably expressing F-DOR-HA were transfected with either control plasmid (pcDNA) or one expressing mycAIP4-C/A. Cells were then incubated with 10µM DADLE for the indicated time period before lysis and division into two identical samples. Blots generated across multiple experiments were scanned and densitometry performed to estimate the amount of FLAG-tagged receptors remaining at each time point relative to agonist naïve cells (A), and the relative abundance of one anti-HA immunoreactive proteolytic product expressed as a percentage of density at 3 hrs agonist treatment (B). Shown are the mean and SEM of multiple experiments (n=6); closed symbols indicate results from control-transfected cells, and open symbols from cells expressing mycAIP4-C/A. C) HEK 293 cells were transfected with F-DOR-GFP and mCherry-AIP4-C/A or mCherry-Nedd4-1-C/A, replated onto coverslips, and incubated for 90 min with 10µM DADLE before imaging. Quantification of the middle fluorescence measured from individual endosomes is shown. Mean and SEM of middle fluorescence values are shown for F-DOR-GFP transfected cells (Control, n= 12 cells, 50 endosomes), F-DOR-GFP and mCherry AIP4-C/A transfected cells (AIP4-C/A, unpaired t-test; ***, $p<0.0001$, n= 16 cells, 51 endosomes), and F-DOR-GFP and mCherry-Nedd 4-1-C/A transfected cells (Nedd4-1-C/A, n= 10 cells, 82 endosomes). D) HEK 293 cells were transfected with F-DOR0cK-GFP and mCherry-AIP4-C/A,

replated onto coverslips, and incubated for 90 min with 10µM DADLE before imaging. the quantification of the mean middle fluorescence, measured from individual endosomes of Control (n= 14 cells, 59 endosomes) and AIP4-C/A (n= 11 cells, 53 endosomes) is shown.

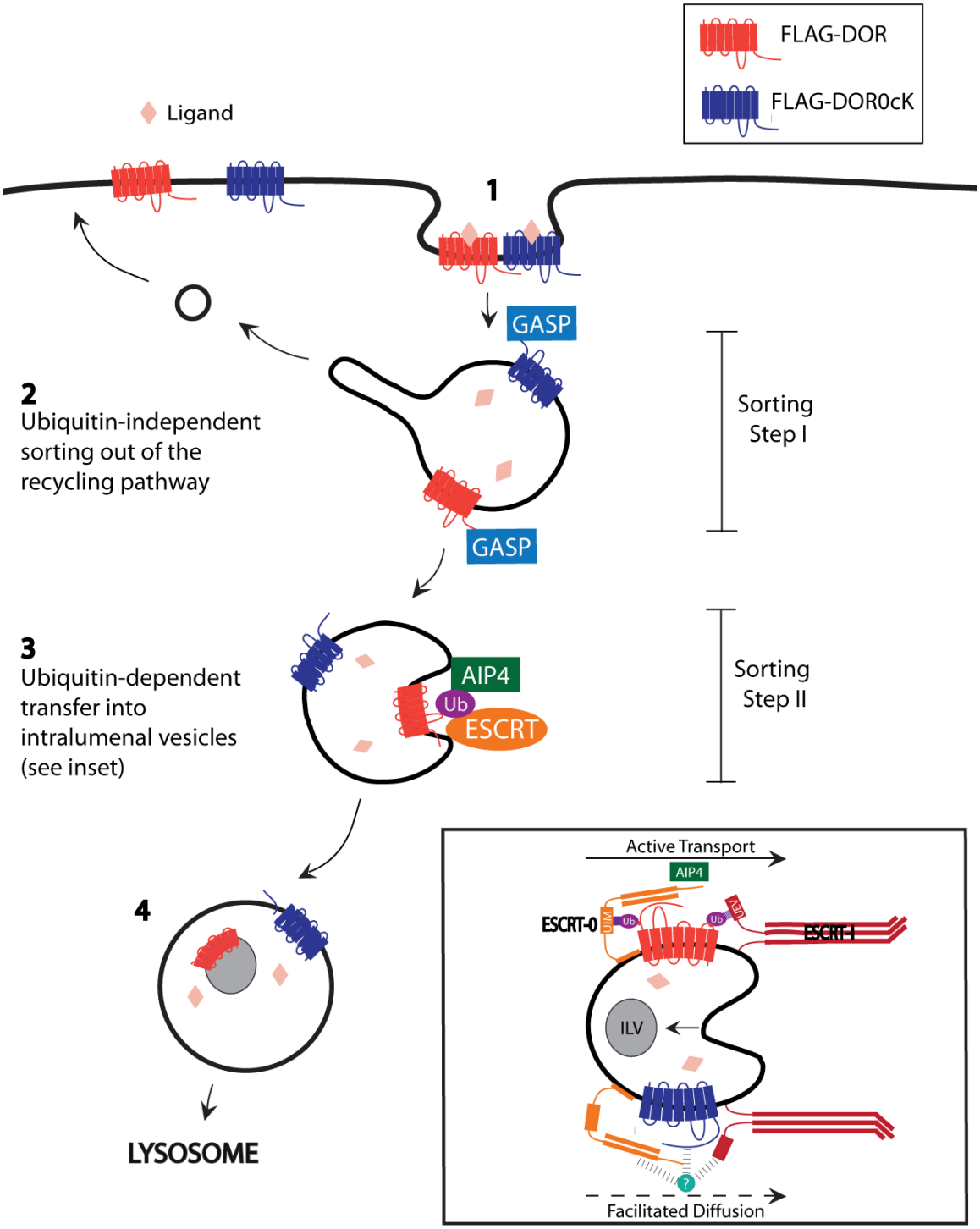

**Figure 9. Model for sequential ubiquitin-independent and –dependent regulation of DOR degradation.** The wild type DOR, as well as the lysine mutant DOR0cK that cannot be ubiquitinated, undergo regulated endocytosis following ligand-induced activation (1). Receptors are prevented from traversing the default recycling pathway by 'Sorting step I', which does not require receptor ubiquitination and is sensitive to ubiquitination-independent interaction of receptors with GASPs (2). Receptors undergo topological sorting from the limiting membrane to ILVs; this represents a discrete operation that we call 'Sorting step II'. Sorting step II resembles canonical ubiquitin-dependent sorting of other cargo and requires the ESCRT. The difference is that DORs can still undergo transfer to ILVs, albeit with moderately reduced rate or efficiency, when receptor ubiquitination is prevented (3). This sequential organization of discrete sorting operations, together with (partial) ubiquitination-dependence specifically of the downstream step, explains the ability of lysine-mutant DORs to down-regulate effectively via the canonical pathway. Accordingly, lysine mutation causes a selective and partial inhibition of later proteolytic events that require protease access to the receptor's cytoplasmic surface (4).

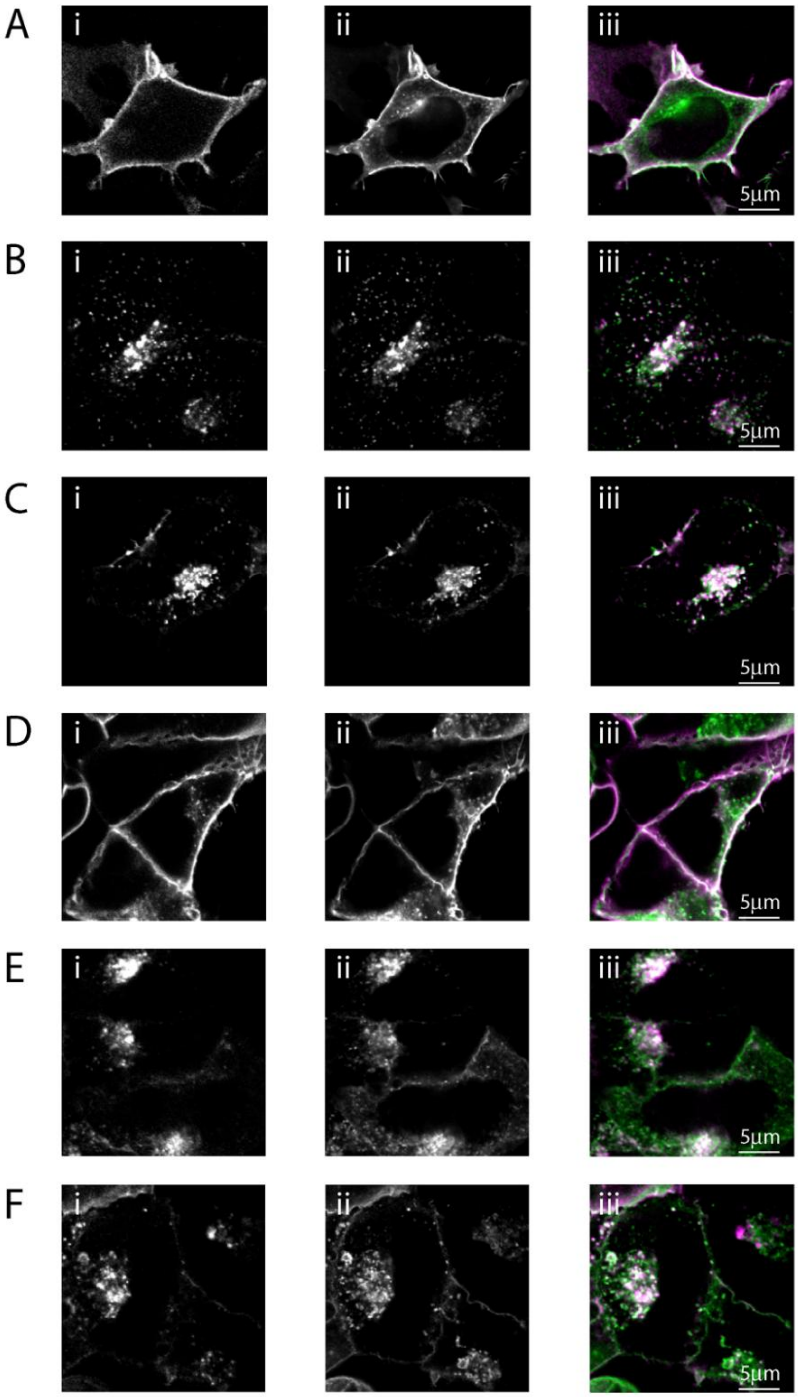


**Supplemental Figure 1. Subcellular localization of DOR and DOR-0cK determined by both N and C terminal epitopes.** HEK293 cells expressing F-DOR-HA 'fed' with rabbit anti-FLAG antibody and then left untreated (A), treated for 30 minutes with 10µM DADLE (B), or treated with 10µM DADLE for 30 minutes followed by 10µM Naloxone for 60 minutes (C) to show resting, internalized and recycled conditions respectively, before being fixed and stained as described in *Materials and Methods*. Cells were

stained with rabbit anti-FLAG (Ai, Bi, Ci, pseudocolored magenta in merged image iii) or mouse anti-HA (Aii, Bii, Ciii, pseudocolored green in merged image iii). Areas of colocalization are seen pseudocolored white (Aiii, Biii, Ciii). Similar experiments were conducted in HEK293 cells expressing F-DOR-0cK-HA (D-F)

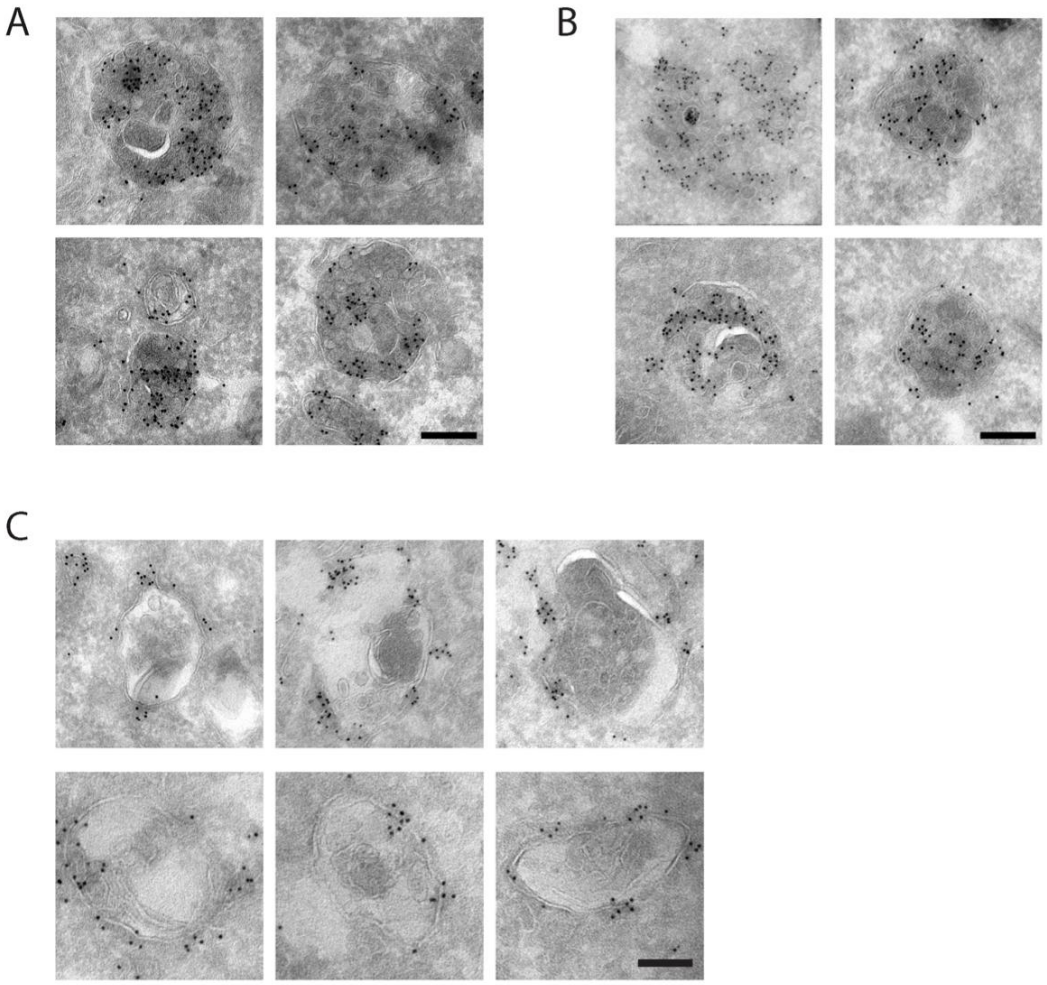


**Supplemental Figure 2. Electron Micrographs of Late Endosomes containing F-DOR-HA and F-DOR-0cK-HA.** HEK293 cells stably expressing F-DOR-HA (A) or F-DOR-0cK-HA (B and C) were treated with 10µM DADLE for 90 minutes before fixation and preparation for frozen thin section electron microscopy as described in *Materials and Methods*. Shown are representative micrographs using anti-HA labeled with 10nm gold particles. These montages demonstrate that both F-DOR-HA (A) and F-DOR-0cK-HA (B) are both localized to intralumenal vesicles of typical MVBs. They also show examples of MVBs in which F-DOR-0cK-HA is localized primarily to the limiting membrane (C). Scale bars represent 200 nm.

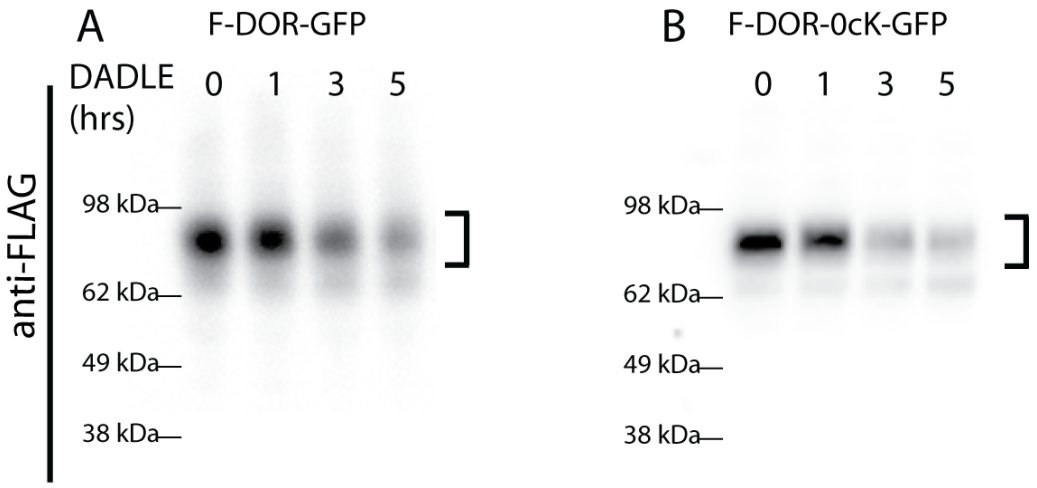


**Supplemental Figure 3. Attachment of GFP to the C- terminus of DOR and DOR-0cK does not affect their agonist-induced proteolysis.** HEK293 cells stably expressing F-DOR-GFP (A) or F-DOR-0cK-GFP (B) were incubated with 10μM DADLE for the indicated time periods before lysis. Shown are representative anti-FLAG blots of each receptor. Bracket indicates position of the full-length receptor species.

# Chapter 4: “Regulation of endocytic clathrin dynamics by direct ubiquitination of cargo”

Anastasia Henry conceived the project and performed most of the experiments and data analysis, with additional contributions from James Hislop. Joe Grove, in the laboratory of Mark Marsh (UCL), performed the cryo-immuno electron microscopy experiments. Kurt Thorn aided in the automated MATLAB analysis. Anastasia Henry, James Hislop, Mark Marsh, and Mark von Zastrow wrote the manuscript.

## 4.1 Abstract

Some endocytic cargoes control clathrin-coated pit (CCP) maturation, but it is not known how such regulation is communicated. We found that μ-opioid neuropeptide receptors signal to their enclosing CCPs by ubiquitination. Non-ubiquitinated receptors delay CCPs at an intermediate stage of maturation, after clathrin lattice assembly is complete but before membrane scission. Receptor ubiquitination relieves this inhibition, effectively triggering CCP scission and producing a receptor-containing endocytic vesicle. The ubiquitin modification that conveys this endocytosis-promoting signal is located in the receptor's first cytoplasmic loop, catalyzed by the Smurf2 ubiquitin ligase, and coordinated with activation-dependent receptor phosphorylation and clustering through Smurf2 association with the endocytic adaptor beta-arrestin. Epsin1 detects the signal at the CCP and is required for ubiquitin-promoted scission. This cargo-to-coat communication system mediates a biochemical checkpoint that ensures appropriate receptor ubiquitination for later trafficking and controls loading of specific receptors into CCPs by sensing when a sufficient "quorum" is reached.

## 4.2 Introduction

Clathrin-coated pits (CCPs) mediate endocytosis of diverse membrane cargoes and are essential for numerous cellular processes, from the uptake of nutrients to the regulation of receptor-mediated signaling. Clathrin-dependent endocytosis involves a precisely organized series of steps, subject to regulation at the level of the conserved endocytic machinery and accessory proteins (Perrais and Merrifield, 2005; Toret and Drubin, 2006; Traub, 2009). The clathrin-containing lattice promotes membrane deformation, generating CCPs into which cargoes concentrate through interaction with various adaptors or CLASPs (Brodsky et al., 2001; Farsad and De Camilli, 2003; Itoh and De Camilli, 2006; Maldonado-Baez and Wendland, 2006; McMahon and Gallop, 2005). CCPs then undergo dynamin-dependent membrane scission, producing clathrin-coated vesicles (Hinshaw, 2000; Mettlen et al., 2010). While CCP formation and function are exquisitely regulated (Kirchhausen, 2009; Taylor et al., 2011; Weinberg and Drubin, 2011), the membrane cargo has been generally viewed as an inert passenger. However, it has become increasingly clear that some cargo can influence the initial formation of CCPs or their subsequent maturation (Ehrlich et al., 2004; Liu et al., 2010; Loerke et al., 2009; Mettlen et al., 2010; Puthenveedu and von Zastrow, 2006; Rust et al., 2004). It is not known whether a particular cargo engages in active cargo-to-coat communication and, if so, whether this allows cargo-specific specialization of the endocytic pathway.

These questions are particularly interesting when one considers signal-transducing receptors, whose ability to modulate downstream signaling networks is typically regulated by clathrin-mediated endocytosis following ligand-induced activation. There is

already evidence that classical downstream signaling effectors can regulate the endocytic pathway at a global level (Le Roy and Wrana, 2005; Sorkin and von Zastrow, 2009). What is not known is whether activated receptors can also signal locally to the endocytic machinery, effectively exerting active and local control over their enclosing CCPs. Two properties of seven-transmembrane receptors (7TMRs), the largest known family of signaling receptors, suggest that these cargoes are prime candidates for mediating such local biochemical signaling. First, many 7TMRs tend to exist in oligomeric complexes and cluster non-uniformly in CCPs in response to ligand-induced activation, resulting in the formation of a subset of 7TMR-enriched CCPs under conditions of low receptor expression approximating endogenous levels (Cao et al., 1998; Kasai et al., 2011; Khelashvili et al., 2010; Mundell et al., 2006; Puthenveedu and von Zastrow, 2006). Second, some 7TMRs are already known to engage in passive cytoplasmic tethering after clustering in CCPs, thereby locally prolonging the surface residence time of 7TMR-containing CCPs (Puthenveedu and von Zastrow, 2006). In addition to this passive "brake" function of 7TMRs in prolonging CCP surface lifetime, might some receptors convey an active and local endocytosis-promoting signal?

Here, we show that this is indeed the case. Our results establish the existence of an endocytosis-promoting signal that is communicated locally to CCPs by active ubiquitination of the μ-type opioid neuropeptide receptor (MOR), a member of the largest group (family A) of 7TMRs. Ubiquitination of this receptor's first cytoplasmic loop, but not elsewhere on the cytoplasmic surface, acts effectively as an active "brake release" signal to limit the surface residence time of CCPs already delayed by the presence of

MORs within them. This kinetic control mechanism functions effectively as a conventional biochemical checkpoint, to assure proper 7TMR ubiquitination for later endocytic trafficking. It also mediates a discrete role in exerting local and active control of specific receptor loading in CCPs, by triggering endocytic vesicle formation selectively when a sufficient concentration of properly ubiquitinated receptors is reached. We propose that this latter role of 7TMR ubiquitination is operationally analogous to quorum sensing because it provides a means to tailor the conserved endocytic machinery to the physiological needs of a particular cargo locally, without requiring pre-existing specialization of the endocytic machinery and irrespective of the presence or absence of other cargoes**.**

# 4.3 Results

*Ubiquitination promotes clathrin-dependent endocytosis of MORs*

A Flag-tagged version of the wild type MOR (F-MOR), expressed in stably transfected cells at low levels within the range of opioid receptor expression observed in native tissues (Arttamangkul et al., 2008; Hislop et al., 2011; Scherrer et al., 2006) was ubiquitinated in the absence of receptor activation and its ubiquitination increased over a period of minutes in response to receptor activation by the opioid receptor peptide agonist DADLE (Fig 1A, left set of lanes). Mutating all cytoplasmic lysine residues (F-MOR0cK) prevented both basal and agonist-induced receptor ubiquitination in expression-matched cell clones (Fig 1A, right set of lanes; panels B and C verify comparable loading of total cellular ubiquitinated proteins and receptors). Agonist-induced ubiquitination of F-MORs was not blocked by expressing a dominant-negative form of dynamin (K44E mutation) or treating cells with the dynamin inhibitor Dyngo (data not shown), indicating that significant MOR ubiquitination occurs prior to endocytic scission.

Interestingly, flow cytometric analysis of surface receptor immunoreactivity revealed that cytoplasmic lysine mutation inhibited agonist-induced internalization of receptors and had no effect on the ability of receptors to recycle back to the cell surface (Fig 1D and E). MORs internalize via the conserved CCP pathway (Arttamangkul et al., 2008; Keith et al., 1996; Whistler and von Zastrow, 1998; Yu et al., 2009; Zhang et al., 1998), and we assessed whether blocking MOR ubiquitination prevented receptors from using the clathrin-mediated endocytic pathway. Consistent with previous studies, DADLE-induced

internalization of the wild type F-MOR construct was strongly reduced by siRNA-mediated depletion of endogenous clathrin-heavy chain. DADLE-induced internalization of the lysine-mutant F-MOR0cK receptor, although reduced in magnitude when compared to that of the wild type F-MOR, was still clathrin-dependent (Fig 1F and G; verification of knockdown is shown in the H). Additionally, similar inhibitory effects on endocytosis were seen for both wildtype and lysyl-mutant MORs after treatment with the dynamin inhibitor Dyngo (Fig 1I). Thus preventing MOR ubiquitination did not change the overall mechanism of regulated endocytosis but, instead, reduced the rate at which agonist-activated MORs internalize through the dynamin- and clathrin-mediated endocytic pathway.

*Ubiquitination controls how long receptor-containing CCPs reside in the plasma membrane before undergoing endocytic scission*

Regulated endocytosis of conventional 7TMRs in animal cells occurs by arrestin-promoted clustering of activated, phosphorylated receptors into pre-existing CCPs, and receptor-loaded CCPs subsequently endocytose by dynamin-dependent membrane scission (Santini et al., 2002). Based on the known ability of ubiquitin to promote endocytosis though cargo interaction with various endocytic adaptors (Hicke and Dunn, 2003; Shih et al., 2002; Torrisi et al., 1999; Toshima et al., 2009), we anticipated that lysine mutations might block the initial step of agonist-induced clustering. Interestingly, this was not the case. TIR-FM imaging indicated that both F-MORs and F-MOR0cKs were diffusely distributed in the plasma membrane in the absence of agonist, and both constructs clustered into diffraction-limited spots after agonist application (Fig 2A and Supp Fig 1). Robust surface clustering was observed using an ectodomain-directed

monoclonal antibody, or using a covalent-labeling strategy based on fusion of a pH-sensitive GFP variant (superecliptic pHluorin, or SpH) whose fluorescence is quenched in endosomes (Miesenbock et al., 1998). The receptor clustering time, defined as the interval between agonist application and the first appearance of receptor clusters as recognizable spots over the surrounding plasma membrane, was similar for F-MORs and F-MOR0cKs (Supp Fig 2A and C).

The vast majority of diffraction-limited receptor spots observed in agonist-exposed cells co-localized with clathrin light chain, defining them as receptor-containing CCPs (Fig 2B, arrows). While TIR-FM analysis was restricted to the ventral plasma membrane, examination of fixed specimens by immunoelectron microscopy revealed clustering of F-MORs and F-MOR0cKs in CCPs also on the dorsal plasma membrane (Fig 2C). Further, in TIR-FM imaging of both F-MOR and F-MOR0cK, endocytic uptake of receptors occurred concomitantly with loss of the clathrin coat from the plasma membrane (Fig 2D, right panels show simultaneous disappearance of receptor and clathrin from the evanescent illumination field; Supplemental Movie 1 shows the corresponding full image series). Moreover, the disappearance of discrete agonist-induced receptor clusters from the plasma membrane, when summed over the imaged surface and time, was sufficient to account for net receptor endocytosis as determined by integrated receptor fluorescence (Supplemental Fig 3A and B). We verified that the disappearance of both F-MOR and F-MOR0cK clusters was preceded by a characteristic burst of GFP-tagged dynamin-2 accumulation (not shown). Together these results indicate that both the wild type MOR and ubiquitination-defective MOR0cK undergo regulated endocytosis via the canonical

CCP pathway, involving agonist-induced clustering of receptors into pre-existing CCPs, followed by characteristic dynamin-dependent endocytic scission.

The only feature of MOR endocytosis that obviously deviated from the typical behavior of CCPs was the timing of endocytic scission after the onset of receptor clustering. Previous TIR-FM analyses have generally found that CCPs undergo scission into primary clathrin-coated vesicles within seconds of achieving full surface brightness (Ehrlich et al., 2004; Kaksonen et al., 2005; Merrifield et al., 2002; Taylor et al., 2011). In contrast, CCPs containing MORs, visualized by surface labeling of this endocytic cargo specifically, were consistently found to linger in the plasma membrane for a variable and sometimes prolonged time interval. We estimated for each CCP a receptor "surface residence time," defined in continuous TIR-FM image series as the interval between the initial appearance of a diffraction-limited fluorescent receptor spot (the frame in which its surface intensity visibly exceeded the plasma membrane surround) and the subsequent abrupt disappearance of this receptor spot from the evanescent illumination field. Remarkably, lysine mutation of MORs markedly extended the receptor surface residence time. This was evident simply by comparison of the mean surface residence time calculated across numerous examples and experiments (Fig 2E), as well as by a pronounced right shift in the respective frequency (Fig 2F) and cumulative probability (Fig 2G) distributions. We further verified this effect using receptors labeled covalently with SpH, to visualize surface receptors without the potential complications of bound antibody (Supp Fig 3C - E). Together, these results reveal a previously unanticipated role

of 7TMR ubiquitination in limiting the surface residence time of the CCPs that mediate their endocytosis.

*The surface residence time of receptor-containing CCPs is determined by agonist-induced ubiquitination of the receptor's first cytoplasmic loop*

To investigate if specific lysine residues determine the observed endocytic regulation, we examined the effects of systematically restoring lysine residues in each cytoplasmic domain in the context of the MOR0cK background (Fig 3A). Restoring only the lysine residues present in the first intracellular loop of MOR (MOR0cK R94,96K) was sufficient to fully rescue agonist-induced internalization to the wild type level, while replacing lysines in any other cytoplasmic domain had no effect (Fig 3B). Conversely, preventing ubiquitination specifically at lysine residues present in the first cytoplasmic loop (MOR K94,96R) inhibited agonist-induced internalization of receptors (Fig 3C), and this effect was evident at the earliest time points after agonist application (Supplemental Fig 3F). Mutating either of the two first loop lysine residues individually produced an intermediate phenotype (not shown), prompting us to focus on dual lysine mutation for the subsequent analysis.

To determine if lysine residues present in the first cytoplasmic loop correspondingly affect the dynamics of individual receptor-containing CCPs, we focused on mutant MORs containing or lacking (MOR0cK R94,96K or MOR K94,96R, respectively) only these residues. Both receptor constructs clustered robustly into diffraction-limited spots in response to DADLE addition to the imaging medium, and their clustering time (*i.e.* the interval between initial agonist application and visible appearance of receptor spots above

the plasma membrane surround) was indistinguishable (Supp Fig 2B). CCPs containing the MOR0cK R94,96K construct internalized on average within 1 min after their initial appearance as diffraction-limited receptor spots, whereas CCPs containing the F-MOR K94,96R construct exhibited markedly longer surface residence times, often persisting in the plasma membrane for several minutes before endocytic scission (Fig 3D shows a representative example of each, and quantification of measured surface residence time is shown in Fig 3E - G). Nevertheless, irrespective of systematic differences between receptor constructs in surface residence time after clustering in CCPs, careful examination of TIR-FM image series indicated that they ultimately disappeared from the evanescent illumination field with the characteristics of rapidly mobile receptor-containing endocytic vesicles. These results suggest that lysine residues present in the first cytoplasmic loop determine the surface residence time of receptors, after the onset of agonist-induced clustering in CCPs and before endocytic membrane scission.

Interestingly, these same cytoplasmic lysine residues were previously shown to be essential ubiquitination sites promoting topological sorting of receptors from the limiting membrane to intralumenal vesicles of late endosomes / multivesicular bodies, a process that occurs after receptor endocytosis (Hislop et al., 2011). Consistent with this, mutating these residues inhibited proteolytic down-regulation of receptors measured by radioligand binding assay after prolonged DADLE exposure to cells, and this effect was clearly distinguishable in kinetics from regulated endocytosis of receptors (Fig 3H). Further, immunoblot analysis verified that the first cytoplasmic loop is indeed the major site of agonist-induced receptor ubiquitination. Mutating only these cytoplasmic lysine residues (F-MOR K94,96R) abrogated the agonist-induced component of receptor ubiquitination

(Fig 3 I and J). Conversely, replacing lysine residues only into the first cytoplasmic loop (F-MOR0cK R94,96K) was sufficient to restore agonist-induced ubiquitination characteristic of wild type MORs (Fig 3 K and L). Together, these results indicate that the first cytoplasmic loop is the major site of agonist-induced MOR ubiquitination, and they suggest that the same ubiquitination that limits MOR-containing CCP surface residence time also promotes the subsequent sorting of internalized receptors in MVBs.

*The cytoplasmic-tail of MOR confers ubiquitin-dependent regulation of receptor endocytosis*

As ubiquitin-dependent endocytosis does not appear to be a characteristic of all 7TMRs, we next examined whether specific residues of the MOR were required for this regulation. We began with a previously established truncation mutant of MOR (MORΔ17), missing the last 17 amino acids of its cytoplasmic tail including a regulatory sequence important for receptor recycling back to the cell surface (Fig. 4A) {Tanowitz, 2003 #116;Hislop, 2011 #63}. Lysyl-mutation of MORΔ17 did not detectably alter agonist-induced receptor internalization compared to its lysine-containing counterpart (Fig. 4B), suggesting that the C-terminal region of MOR is necessary to engage the ubiquitin-dependent mechanism. Further, the cytoplasmic tail of MOR was sufficient to confer a requirement for ubiquitination when added to the related delta-opioid receptor, a paralogue of MOR that normally does not require ubiquitin for its efficient endocytosis (Fig. 4C). Together, these results suggest that the cytoplasmic tail of MOR plays an integral role in bestowing ubiquitin-dependence to receptor endocytosis.

*Ubiquitination of the MOR first cytoplasmic loop controls individual receptor-containing CCP dynamics*

To examine the kinetics of the CCPs themselves (rather than that of the agonist-activated 7TMR cargo after its visible concentration in CCPs), we imaged the formation and disappearance of diffraction-limited spots labeled by DsRed-tagged clathrin light chain. In cells not expressing opioid receptors, or in receptor-expressing cells not exposed to opioid agonist, most CCPs labeled in this manner increased in fluorescence intensity over a period of 10 - 20 sec after their initial appearance and then abruptly disappeared from the evanescent illumination field several seconds thereafter (Fig 5A, black line shows a representative intensity trace). This behavior is consistent with the characteristic dynamics of CCPs at 37˚C and under conditions of low clathrin expression as described previously (Doyon et al., 2011; Ehrlich et al., 2004; Kaksonen et al., 2005; Merrifield et al., 2002; Taylor et al., 2011). For subsequent analysis, we defined the clathrin surface residence time as the interval between initial visible appearance of the diffraction-limited clathrin spot over background and its subsequent disappearance from the evanescent illumination field. In cells expressing wild type MORs, and exposed to opioid agonist, we saw many CCPs with short surface residence time. However, we also saw the emergence of a subset of diffraction-limited clathrin spots with longer surface residence time. Remarkably, mutating lysine residues present in the first cytoplasmic loop dramatically prolonged the surface residence time of this CCP subpopulation. We also noted that the observed extension of surface residence time typically occurred after clathrin intensity reached its maximum value (Fig 5A, blue line shows a representative intensity trace), suggesting that the delay imposed by opioid receptor activation occurred after initial clathrin lattice assembly. Representative TIR-FM imaging series of the range of behaviors observed, from cells expressing each of the mutant receptor constructs

examined, are shown in Fig 5B. Quantification of multiple specimens and experiments verified these effects at the level of mean surface residence time. Further, the frequency distribution and cumulative probability plots revealed a pronounced rightward shift in the distribution of CCP lifetimes that, like the difference in overall mean values, was dependent both on the receptor construct expressed and previous activation by opioid agonist (Fig 5D and E). These surface residence time measurements were carried out visually to allow verification of endocytic events and exclusion of structures such as larger clathrin plaques. As an independent approach, we repeated the analysis of clathrin surface residence times using a previously described computerized algorithm (Jaqaman et al., 2008), obtaining similar results (Supp. Fig 4A and B).

Because various 7TMRs cluster non-uniformly within the CCP population when expressed at physiological levels (Cao et al., 1998; Mundell et al., 2006; Puthenveedu and von Zastrow, 2006), we next asked if the subset of CCPs exhibiting prolonged surface residence time corresponded to those containing activated MORs. To do so, we used dual label TIR-FM imaging to visualize, in the same specimens, fluorescence representing both clathrin light chain and lysine-mutant MOR. We analyzed the CCP surface residence time of diffraction-limited clathrin spots as described above, and separated the individual determinations according to the presence or absence of colocalized MOR K94,96R fluorescence. Remarkably, prolonged surface residence time appeared to be entirely specific to those CCPs enriched for agonist-activated opioid receptors (Fig 5F), and the rightward shift in the distribution of surface residence times fully segregated with this receptor-containing subset (Fig 5G and H). Together, these

results indicate that activated opioid receptors locally control CCPs based on the presence of a specific receptor cargo within them and do so in a manner determined by the receptor's specific ubiquitination status. In essence, non-ubiquitinated MORs act as a "brake" to stall receptor-containing CCPs, while ubiquitination of the receptor's first cytoplasmic loop functions as a "brake release" to trigger subsequent endocytic scission.

A prediction of this proposed cargo-control mechanism is that the surface lifetime of another endocytic cargo that is co-packaged with ubiquitin-defective opioid receptors would also be affected. To investigate this, we carried out dual-label TIR-FM imaging of mutant opioid receptors together with SpH-tagged transferrin receptors (SpH-TfRs), which cluster constitutively in CCPs. While many diffraction-limited SpH-TfR spots exhibited relatively short surface lifetimes, a subset persisted in the plasma membrane for an extended time period before abruptly disappearing from the evanescent field; precisely these spots co-localized with the activated F-MOR K94,96R (Fig 5I-K). The present results further verify that MORs locally control the dynamics of receptor-containing CCPs and indicate that ubiquitin-dependent control of CCP surface residence time affects the dynamics of a co-packaged endocytic cargo.

*Ubiquitination controls both the amount and variability of CCP cargo loading*

To begin to investigate how ubiquitin-dependent control of CCP surface residence time controls net MOR endocytosis, we next asked if this kinetic control mechanism affects either clathrin coat assembly or receptor loading within them. Mutations manipulating MOR first-loop ubiquitination did not detectably affect the overall degree of clathrin assembly at individual CCPs, as estimated by the peak value of clathrin light chain

fluorescence measured before disappearance of the diffraction-limited spot from the evanescent field (Fig 6A-C). In marked contrast, a pronounced difference was evident when the same approach was used to quantify receptor, rather than clathrin, fluorescence at individual diffraction-limited spots. Even though we were unable to discern any difference in the time of initial appearance of F-MOR K94,96R or F-MOR0cK R94,96K in CCPs after DADLE-induced activation (Supp Fig 2B), the maximum value of receptor fluorescence intensity that accumulated in CCPs prior to endocytic scission was significantly higher for receptors lacking ubiquitination sites in the first cytoplasmic loop. Preventing MOR first loop ubiquitination increased estimated receptor loading of CCPs by ~2-fold on average (Fig 6D), when compared either to the wild type F-MOR or F-MOR0cK R94,96K constructs, and this corresponded to an obvious right shift in the receptor intensity distribution of individual CCPs (Fig 6E and F). We also noted a detectable but smaller (30 - 50%) increase in the variability of receptor loading in individual CCPs, as estimated by calculating the coefficient of variation for the respective receptor intensity distributions (legend to Fig 6E). Accordingly, ubiquitin-dependent control of CCP surface residence time does not detectably affect coat assembly at individual CCPs but markedly affects the amount of receptor cargo loaded within them.

We next examined in more detail the relationship between ubiquitin-dependent kinetic control of CCP surface residence time and cargo loading measured prior to endocytic scission. When ubiquitination of the first cytoplasmic loop was allowed to occur (i.e., the wild type F-MOR or MOR0cK R94,96K), CCP lifetimes were uniformly short and cargo loading (receptor fluorescence intensity measured at individual CCPs) was relatively

tightly clustered (Fig 6G and H). However, when agonist-induced ubiquitination was prevented (MOR K94,96R), there was a much more extended distribution of CCP lifetime and receptor fluorescence intensity, and a pronounced positive correlation was evident between CCP surface residence time and corresponding receptor load (Fig 6I and J, correlation coefficient = 0.69). This suggests that ubiquitination of the MOR first cytoplasmic loop, by controlling the surface residence time of MOR-containing CCPs, effectively limits time-dependent receptor accumulation within them.

*Mechanism of agonist-induced encoding of MOR ubiquitination*

Having established ubiquitination as the critical biochemical signal conferring local control of CCP surface residence time, we next investigated the biochemical mechanism responsible for encoding this novel cargo-mediated control. We started by identifying the relevant ubiquitin ligase. To do so, we screened for E3 ubiquitin ligases that inhibit agonist-induced internalization of F-MORs when inactivated, focusing on HECT domain ligases related to Rsp5/Nedd4 because of their widespread endocytic functions and on RING domain ligases shown previously to function in the endocytic pathway (Hislop and von Zastrow, 2011; Staub and Rotin, 2006). The HECT domain E3 ligase Smurf2 emerged as a strong candidate (Fig 7A), and we pursued it further because its effects were highly cargo-specific: Expression of inactivated (C716A) Smurf2 did not affect regulated endocytosis of either the delta-opioid receptor (a close MOR paralogue that also internalizes via CCPs) or of the lysine-mutated MOR (Fig 7B). siRNA-mediated knockdown of endogenous Smurf2 independently verified that this ligase is essential for efficient internalization of MORs (Fig 7C and F). Further, Smurf2 was required for internalization of MORs containing only the lysine residues in the first loop (MOR0cK

R94,96K) but had no additional inhibitory effect on MORs whose first loop lysines residues were mutated (MOR K94,96R), providing independent genetic evidence that Smurf2 regulates MOR endocytosis specifically through ubiquitination of the first cytoplasmic loop (Fig 7D and E). Finally, we verified biochemically that disrupting Smurf2 activity inhibits agonist-induced ubiquitination of MORs in intact cells (Fig 7G and H).

We next asked how Smurf2-mediated ubiquitination of MORs is coordinated with agonist-induced receptor activation and clustering. Smurf2 associated with Arrestin3 (beta-arrestin2) when immunopurified from cell lysates (Figure 7I), and Arrestin3 is already known to undergo agonist-induced recruitment to MORs (Cen et al., 2001; Johnson et al., 2006; Zhang et al., 1998). This suggested that Arrestin3, in addition to functioning as an endocytic adaptor for MORs, might also function as a scaffold for recruiting Smurf2 to agonist-activated MORs. Supporting this hypothesis, both Arrestin3-GFP and Smurf2-GFP fluorescence rapidly increased at the plasma membrane after receptor activation, with Smurf2 recruitment following that of Arrestin3 (Figure 7J, green and purple lines, respectively). Further, Smurf2 accumulated both diffusely and in spots in the plasma membrane (Supplemental Figure 5) reminiscent of Arrestin3 localization shown previously by TIR-FM (Puthenveedu and von Zastrow, 2006), and recruitment of both proteins began before detectable receptor clustering in CCPs (compare Figure 7J with Figure S2A and C). Beta-arrestins are recruited to MORs following agonist-induced phosphorylation of the receptor's cytoplasmic tail (Groer et al., 2011; Johnson et al., 2006; Zhang et al., 1998), and the specific phosphorylation sites required for this

recruitment were recently defined (Lau et al., 2011). Mutating these residues (F-MOR 375AAANA379) blocked agonist-induced ubiquitination of MORs (Fig 7K and L), providing further support for a role of arrestin recruitment in promoting receptor ubiquitination. Further, knockdown of endogenous Smurf2 effectively phenocopied the effect seen with lysyl-mutation of MORs, as reflected by a significant increase in mean receptor surface residence time (Fig 8A) and a pronounced right shift in the frequency distribution (Fig 8B and C). Additionally, expression of GFP-tagged, catalytically-inactive mutant Smurf2 resulted in ~2-fold increase in MOR surface lifetime compared to expression of GFP alone (data not shown), similar to the effect of Smurf2 knockdown. Together, these results delineate a complete sequence of biochemical events that explain how ubiquitination of the MOR first cytoplasmic loop is mediated and how it is regulated through agonist-induced activation and clustering of receptors in CCPs (Fig 8J).

*Mechanism of MOR ubiquitination decoding*

We next sought to identify a protein that detects the ubiquitin-encoded signal and transduces it into regulation of CCP surface lifetime. To do so, we screened proteins that localize to the CCP and possess domains that are known to bind ubiquitin. Obvious candidates are epsins, a conserved family of ubiquitin-interacting motif (UIM)-containing proteins that associate with CCPs (Chen et al., 1998; Kazazic et al., 2009; Shih et al., 2002; Wendland, 2002), and whose knockdown or over-expression can alter CCP dynamics (Mettlen et al., 2009) or endocytic function (Chen et al., 2011; Rosenthal et al., 1999; Sorkina et al., 2006; Sugiyama et al., 2005). siRNA duplexes targeting Epsin2 caused no detectable effect on MOR internalization (not shown) but epsin1 depletion caused a significant inhibition (Supplemental Figure 6A). We initially rejected this

candidate because its knockdown (Supplemental Figure 6B and C) and over-expression (Supplemental Figure 6D and E) also produced effects on lysyl-mutant MORs, consistent with previous evidence that these manipulations produce global endocytic effects. We later reconsidered this candidate because deleting only the tandem UIMs in epsin1 (Epsin1ΔUIM), specifically disrupting its binding to ubiquitinated proteins (Sugiyama et al., 2005), produced a remarkably specific effect: GFP-tagged Epsin1ΔUIM localized in a punctate pattern indistinguishable from that of the wild type protein (Supplemental Figure 6F and G) and significantly inhibited internalization of wild type MOR (Figure 8D), without affecting internalization of lysyl-mutant MOR0cK or DOR (Figure 8E and F, respectively). Further, Epsin1ΔUIM phenocopied the effect of lysyl-mutation of MOR or Smurf2 knockdown, significantly increasing the mean receptor surface lifetime (Figure 8G-I), without producing any detectable effect on time to cluster (Supplemental Figure 2E). These results experimentally isolate a specific function of epsin1, through its UIMs, in recognizing appropriately ubiquitinated MORs and triggering endocytic scission of the CCPs containing them.

## 4.4 Discussion

The present results show that a signaling receptor subject to regulated endocytosis can actively and locally communicate to its enclosing CCP, thereby exerting converse, cargo-dependent control over the conserved endocytic process. We observed that MORs prolong the surface residence time of receptor-containing CCPs after their formation and initial cargo accumulation, but before the occurrence of dynamin-dependent scission, verifying and extending the observation that some 7TMRs can exert a "brake" function on the maturation of their enclosing CCPs (Puthenveedu and von Zastrow, 2006). A major new finding of the present study is that ubiquitination of MORs, specifically by agonist-induced ubiquitination of the first cytoplasmic loop, conveys an active signal that effectively counteracts this inhibitory effect, thereby allowing specific receptor ubiquitination to act as an endocytic "brake release." We further show that, by limiting the surface residence time of individual 7TMR-containing CCPs, ubiquitin-conveyed signaling locally controls endocytic receptor load. The present results add to the accumulating evidence supporting cargo-mediated regulation at various stages in the conserved CCP pathway(Ehrlich et al., 2004; Liu et al., 2010; Loerke et al., 2009; Mettlen et al., 2010; Puthenveedu and von Zastrow, 2006; Santini et al., 2002). Our findings also reveal an entirely new level of active regulation based on the specific ubiquitination of a particular endocytic cargo.

Ubiquitination is well known to promote the initial accumulation of various membrane cargoes in CCPs, through ubiquitin-binding endocytic adaptors (Hicke and Dunn, 2003; Maldonado-Baez and Wendland, 2006; Shih et al., 2002; Torrisi et al., 1999; Toshima et

al., 2009) and to promote later MVB / lysosome sorting of endocytic cargo through interactions with the ESCRT machinery (Raiborg and Stenmark, 2009; Saksena et al., 2007; Shields and Piper, 2011). The present results identify a distinct function of ubiquitin as a biochemical signal that actively controls the surface residence time of CCPs, after clathrin assembly is complete and after initial cargo accumulation in CCPs has occurred. There is accumulating evidence that ubiquitin can affect later stages of CCP maturation, after the cargo recruitment step (Jiang and Sorkin, 2003; Reider and Wendland). The present results support this idea and significantly extend it, by establishing a role of cargo ubiquitination in controlling CCP maturation. We also note that ubiquitin has recently been implicated in cargo-dependent regulation of secretion through the biosynthetic pathway (Jin et al., 2012). Together, our data add to an emergent role of ubiquitin as a cargo-specific regulator of coat protein dynamics.

Our results also explain how the ubiquitin-transmitted endocytic signal is actively encoded and coordinated with agonist-induced concentration of receptors in CCPs (Fig 8D). Central to this mechanism is arrestin-dependent recruitment of a particular ubiquitin ligase, Smurf2. While this is the first report of a role for Smurf2 in the endocytic trafficking of seven transmembrane receptors, arrestin-dependent recruitment of ubiquitin ligases to particular membrane cargo is emerging as a repeated theme in cell biology (Bhandari et al., 2007; Shenoy et al., 2001; Shenoy et al., 2008). Because preventing the specific agonist-dependent phosphorylation event responsible for arrestin recruitment and CCP association of receptors also blocked ubiquitination (Fig 7I and J), our results suggest that ubiquitin-dependent control of CCP lifetime is closely integrated with the

conserved arrestin-dependent mechanism that initiates recruitment of activated, phosphorylated receptors to CCPs (Fig 8D). Our results also identify epsin1 as a CCP protein that senses the critical MOR ubiquitination, providing initial insight to the decoding mechanism.

Ubiquitination of the same cytoplasmic domain was shown previously to be required for efficient topological sorting of a truncated mutant MOR construct in MVBs (Hislop et al., 2011), and we verified a significant effect of mutating these residues on later proteolytic downregulation of full-length MORs in the present study (Fig 3H). These events occur after endocytosis and are important to the physiological modulation of signal transduction under conditions of prolonged or repeated receptor activation. This suggests that one cellular function of ubiquitin-dependent control of CCP surface residence is to optimize the later endocytic trafficking of this particular membrane cargo, and to act effectively as a biochemical checkpoint (Fig 8F, red bar) that delays endocytic scission of receptor-containing CCPs until appropriate ubiquitination has been achieved.

Remarkably, while disrupting MOR ubiquitination did not detectably affect CCP assembly, it caused previously formed CCPs to subsequently overfill with agonist-activated receptors (Fig 6D - F). Further, there was a positive correlation between the extension of surface residence time of discrete CCPs and the amount of receptor loading within them (Fig 6G - J). Accordingly, these findings identify a unique cellular function of ubiquitin, and of ubiquitin-dependent control of CCP surface residence time, in limiting and enhancing the uniformity of cargo loading.

Clearly much remains to be learned about this new mechanism of kinetic control and its physiological ramifications. However, when viewed simply from the systems-level, we believe that the presently identified cargo communication process has properties reminiscent of quorum sensing, as described initially in bacterial ecology (Fuqua et al., 1994; Nealson et al., 1970). Here, physical properties of the environment cause local accumulation of bacteria, and a species-specific secreted factor acts as an active biochemical signal. The signal conveys information about the local population density of particular bacterial species, driving a relevant gene expression program after a threshold is reached (Fuqua and Greenberg, 1998; Hastings and Greenberg, 1999; Jayaraman and Wood, 2008). This density-dependent signaling principle is widely deployed in bacterial populations and represents a remarkably robust evolutionary strategy for generating group-like and species-specific behavior in a complex ecological niche (Miller and Bassler, 2001). We propose that ubiquitin-dependent control of local CCP dynamics facilitates a fundamentally analogous process (Fig 8F, blue bar). Here, the relevant niche is the CCP, into which cargo is trapped by adaptor interactions compounded by stalling of CCP maturation (highlighted in pink). The biochemical signal communicating local population density is a specific ubiquitin modification of the receptor cargo itself; this effectively triggers endocytic vesicle formation when a threshold of receptor density is reached (highlighted in green). This elaboration of the quorum sensing principle thereby allows receptor-specific ensemble behavior to emerge in the conserved endocytic pathway, largely irrespective of the presence of other cargoes.

By facilitating uniform loading of a particular membrane cargo, we anticipate that the quorum-sensing function of cargo ubiquitination enhances the efficiency of later endocytic trafficking. This is supported by the present observation linking the same ubiquitinated residues to the checkpoint controlling later endocytic trafficking (Fig 8F, red bar). Further, when one considers the critical importance of local concentration and proximity in most receptor-linked signaling systems, we also think it likely that the presently identified cargo control mechanism confers additional fitness at the level of cellular signaling.

In sum, the present results identify a new role of ubiquitination in the signaling-trafficking nexus, in bidirectionally connecting mechanistically distinct but functionally interdependent processes of signaling and endocytosis. We propose that this allows the conserved endocytic pathway to become selectively populated and flexibly tailored "on demand" by particular cargo and thereby produce emergent, cargo-specific behavior in the mixed and dynamic environment of the endocytic pathway.

## 4.5 Acknowledgments

We thank Laurant Coscoy, Brian Sullivan, Adriano Marchese, Christien J. Merrifield, Wolfhard Almers, Wes Sunquist, Phil Robinson, and Michael Tanowitz for providing important constructs and reagents. We would also like to thank Guillermo Yudowski, Manojkumar Puthenveedu, Paul Temkin, Allen Liu, Frances Brodsky, William Dowdle, David Morgan, Keith Mostov, Orion Weiner, and Henry Bourne for useful comments and valuable discussion. This work was supported by grants from the NIH (DA010711 and DA012864 to MvZ), and AGH is a recipient of a predoctoral fellowship from the US National Science Foundation. JG and MM are supported by UK MRC funding to the Cell Biology Unit.

# 4.6 Materials and Methods

*Expression Constructs, Cell Culture, and Reagents*

The FLAG-tagged MOR construct, DsRed-tagged clathrin light chain, and inactive mutant versions of the E3 ligases Cbl, Mdm2, AIP4, Nedd 4.1 and 4.2, Nedd L1 and 2, WWP1 and 2, and Smurf1 and 2 were previously described (Hislop et al., 2009; Merrifield et al., 2002; Tanowitz and von Zastrow, 2003). FLAG-tagged MOR0cK, MOR0cK R94,96K, MOR0cK R170,181K, MOR0cK R256,265,267K, MOR0cK R340K, and MOR K94,96R were made by site-directed mutagenesis (QuikChange, Stratagene). Myc-tagged Smurf2 and GFP-tagged inactive mutant version of Smurf2 were made using PCR and ligation into pcDNA3 and pEGFP-C1, respectively. Epsin1 cDNA was obtained from Open Biosystems and subloned into pEGFP-C1. GFP-Epsin1ΔUIM was generated using site-directed mutagenesis (QuikChange, Stratagene). Transfections were done using Lipofectamine 2000 or RNAi-max (Invitrogen) for transient expression or knockdown of endogenous proteins, respectively, according to manufacturer's instructions. Stably-transfected cell lines expressing FLAG-tagged receptors were generated by selection for neomycin resistance with G418 (Geneticin; Invitrogen). Alexa 555-labelled siRNA duplexes against Smurf2 were obtained from Qiagen and siRNA duplexes against clathrin (CHC 17) were ordered from Qiagen based on an established siRNA sequence (Vassilopoulos et al., 2009). Antibodies used were anti-Smurf2 (Santa Cruz Biotechnology), anti-ubiquitin (P4D1, Santa Cruz Biotechnology), anti-clathrin heavy chain (Santa Cruz Biotechnology), rabbit anti-FLAG (Sigma), anti-FLAG-M1 (Sigma), and anti-HA-11 (Covance). Dyngo-4a was obtained from abcam and used at a final concentration of 30μM.

*Flow cytometric analysis of endocytosis*

A previously described flow cytometric assay was used to quantify internalization of transiently-expressing FLAG-tagged receptor constructs labeled with Alexa Fluor 647-conjugated M1 anti-FLAG antibody (Invitrogen/ Molecular Probes) (Hislop et al., 2011; Tsao and von Zastrow, 2000). Receptor internalization was quantified as a reduction of surface receptor immunoreactivity after incubation of cells with the opioid agonist DADLE (10μM) for the indicated time points.

*TIRF Microscopy*

Cells were imaged in Opti-MEM I reduced serum media (UCSF Cell Culture Facility) at 37˚C, maintained with a temperature-controlled stage (Bioscience Tools) and objective warmer (Bioptechs). Live-cell imaging was performed using a Nikon TE-2000E inverted microscope with a 60X1.45 NA TIRF objective, using through-the-objective illumination. We used a 488 nm Argon-ion laser (Melles Griot) and a 543 nm HeNe laser (Spectra Physics) as light sources. A C9100-12 camera (Hamamatsu Photonics) was used to acquire image sequences with a pixel size of 176 x 176 nm, controlled by Andor IQ software, and cells were imaged with an exposure time of 100ms and an EM gain of 300. Surface FLAG-tagged receptors were labeled with Alexa Fluor 488- or 647-conjugated M1 anti-FLAG antibody for visualization. For dual imaging experiments, minimal bleed-through between channels was verified by imaging samples labeled only with single fluorophores. Representative live images shown were rendered using Adobe Photoshop software.

*Immunoelectron microscopy of plasma membrane sheets*

HEK 293 cells stably-expressing F-MOR or F-MOR0cK were grown on coverslips and incubated with 10µM DADLE for 2 minutes. Cells were then washed with cold PBS and placed on ice to prevent further receptor internalization. Cell surface receptor was detected by sequential incubation with 10µg/ml rabbit anti-FLAG IgG (Sigma-Aldrich, MO, USA) and protein A conjugated to 10nm gold particles, after which the cells were washed in HEPES buffer (25 mM HEPES, 25 mM KCl, and 2.5 mM Mg acetate, pH 7.0). Plasma membrane sheets were prepared using a previously described "rip-off" technique (Sanan and Anderson, 1991; Signoret et al., 2005). Briefly, cover slips were inverted on to formvar/carbon/poly-L-lysine coated electron microscopy grids and light pressure applied for 10 sec using a rubber cork. The cover slips were lifted away to rip open adhered cells and leave portions of the dorsal plasma membrane attached to the grids. The material was briefly washed in HEPES buffer and fixed in 4% glutaraldehyde. Samples were post-fixed by sequential incubation in 1% osmium, 1% tannic acid and 1% uranyl acetate, and then air-dried. Images were taken using a Tecnai G2 Spirit transmission EM (FEI, Eindhoven, the Netherlands) fitted with a Morada 11 MegaPixel TEM camera (Olympus Soft Imaging Solutions, Münster, Germany).

*Image Analysis*

Image analysis was performed using ImageJ software (Wayne Rasband, National Institutes of Health, Bethesda, MD). For surface lifetime measurements, the time between the appearance and disappearance of clusters was measured as previously described (Puthenveedu and von Zastrow, 2006). Cluster appearance was identified as the frame where the cluster fluorescence increased above the background fluorescence of an adjacent point of the cell being analyzed. Disappearance of a cluster was determined as

the frame where cluster fluorescence decreased to the background fluorescence of a neighboring area of the imaged cell, or when the cluster split off and the subsequent cluster decreased to background levels of fluorescence. Only clusters that clearly appeared and disappeared during image acquisition were included. For cluster intensity measurements, cells were chosen with similar fluorescence values, to ensure equal expression of receptor and clathrin. The mean intensity value of clusters immediately prior to endocytic scission and of an identically-sized background region of the cell at that same frame was quantified. Fluorescence values of clusters were divided by those of background regions and expressed as "Fold over background" values. For change in intensity over time measurements, ROIs were drawn around individual cells and the change in integrated intensity was measured and background-corrected. These values were normalized to the intensity of the cell immediately prior to agonist treatment and are represented as "% of initial fluorescence" values.

*Analysis of Receptor Degradation by Radioligand Binding*

The amount of receptor remaining after prolonged agonist treatment was measured by radioligand binding, as previously described (Hislop et al., 2009; Tsao and von Zastrow, 2000). Briefly, cells stably-expressing FLAG-tagged receptors were treated with 10 µM DADLE for the indicated time frames, washed with cold PBS, treated with PBS, and frozen. After thawing, binding assays were performed using 10nM of the radiolabeled antagonist [$^{3}$H] diprenorphine (88Ci/mmol; Amersham Biosciences). Incubations were stopped, and unbound radioligand was removed by multiple washes with Tris-buffered saline. The amount of bound radioactivity was measured by liquid scintillation counting. Nonspecific binding was quantified using parallel samples treated with an excess of the

unlabeled competitive antagonist, 10μM naloxone. Specific binding values are shown, measured as total binding minus the nonspecific binding at each time point and expressed as the percentage of the binding in untreated cells.

*Detection of ubiquitination by Western blot analysis*

Cells stably-expressing FLAG-tagged receptors were treated with agonist for the indicated time points, lysed in 10mM Tris pH 7.4, 1% SDS, and 10mM iodoacetamide supplemented with a standard protease inhibitor mixture (Roche Applied Science), sonicated, and clarified by centrifugation as previously described (Hislop et al., 2011). Samples were incubated overnight with rabbit anti-FLAG antibody (Sigma) and later with protein A/G-agarose beads (Piece), then washed and incubated with SDS sample buffer (Invitrogen) supplemented with DTT. Western immunoblot analysis was performed using anti-HA-11 (Covance) or anti-ubiquitin (Santa Cruz Biotechnology). Blots were probed with anti-ubiquitin or anti-FLAG antibody to verify equal loading and receptor levels. Densitometric analysis of band intensities from unsaturated immunoblots were analyzed and quantified by densitometry using FluorChem 2.0 software (Alpha Innotech Corp.).

*Coimmunoprecipitation*

For immunoprecipitation studies, cells were transiently transfected, lysed in IP buffer (0.2% Triton-X, 150mM NaCl, 25mM KCl, 10mM Tris pH 7.4, 1mM EDTA) supplemented with standard protease inhibitor cocktail (Roche Applied Science), and clarified by centrifugation. Samples were incubated with anti-myc, clone 9E10 antibody (Millipore) overnight and later with protein A/G beads (Piece), washed, and analyzed by Western blotting. Immunoblots were probed with anti-HA antibody (Covance).

*Automated CCP lifetime analysis*

Cells were transiently-transfected with DsRed-tagged clathrin light chain and pCDNA 3.0, F-MOR K94,96R, or F-MOR0cK R94,96K and were treated with agonist while imaging using TIRF-M. Fluorescent particle detection and CCP lifetime tracking was performed on raw image sequences using a previously established Matlab package that is publicly available (Jaqaman, 2008;Loerke, 2009).

*Statistical analysis*

Quantitative measurements were averaged across multiple independent experiments, with the number of experiments indicated in the corresponding figure legends. Error bars represent the standard error of the mean quantified after compiling mean determinations across multiple experiments. The statistical significance of the measured differences between conditions were analyzed using the appropriate variations of two-way ANOVA and post-test, specified in figure legends, and calculated using Prism 4.0 software (GraphPad Software, Inc). The relative significance of each of the reported differences is indicated by the calculated p values listed in the figure legends and shown graphically in the figures themselves.

## 4.7 References

Arttamangkul, S., Quillinan, N., Low, M. J., von Zastrow, M., Pintar, J., and Williams, J. T. (2008). Differential activation and trafficking of micro-opioid receptors in brain slices. Mol Pharmacol *74*, 972-979.

Bhandari, D., Trejo, J., Benovic, J. L., and Marchese, A. (2007). Arrestin-2 interacts with the ubiquitin-protein isopeptide ligase atrophin-interacting protein 4 and mediates endosomal sorting of the chemokine receptor CXCR4. J Biol Chem *282*, 36971-36979.

Brodsky, F. M., Chen, C. Y., Knuehl, C., Towler, M. C., and Wakeham, D. E. (2001). Biological basket weaving: formation and function of clathrin-coated vesicles. Annu Rev Cell Dev Biol *17*, 517-568.

Cao, T. T., Mays, R. W., and von Zastrow, M. (1998). Regulated endocytosis of G-protein-coupled receptors by a biochemically and functionally distinct subpopulation of clathrin-coated pits. J Biol Chem *273*, 24592-24602.

Celver, J. P., Lowe, J., Kovoor, A., Gurevich, V. V., and Chavkin, C. (2001). Threonine 180 is required for G-protein-coupled receptor kinase 3- and beta-arrestin 2-mediated desensitization of the mu-opioid receptor in Xenopus oocytes. J Biol Chem *276*, 4894-4900.

Cen, B., Xiong, Y., Ma, L., and Pei, G. (2001). Direct and differential interaction of beta-arrestins with the intracellular domains of different opioid receptors. Mol Pharmacol *59*, 758-764.

Chen, B., Dores, M. R., Grimsey, N., Canto, I., Barker, B. L., and Trejo, J. (2011). Adaptor protein complex-2 (AP-2) and epsin-1 mediate protease-activated

receptor-1 internalization via phosphorylation- and ubiquitination-dependent sorting signals. J Biol Chem *286*, 40760-40770.

Chen, H., Fre, S., Slepnev, V. I., Capua, M. R., Takei, K., Butler, M. H., Di Fiore, P. P., and De Camilli, P. (1998). Epsin is an EH-domain-binding protein implicated in clathrin-mediated endocytosis. Nature *394*, 793-797.

Doyon, J. B., Zeitler, B., Cheng, J., Cheng, A. T., Cherone, J. M., Santiago, Y., Lee, A. H., Vo, T. D., Doyon, Y., Miller, J. C., *et al.* (2011). Rapid and efficient clathrin-mediated endocytosis revealed in genome-edited mammalian cells. Nat Cell Biol *13*, 331-337.

Ehrlich, M., Boll, W., Van Oijen, A., Hariharan, R., Chandran, K., Nibert, M. L., and Kirchhausen, T. (2004). Endocytosis by random initiation and stabilization of clathrin-coated pits. Cell *118*, 591-605.

Farsad, K., and De Camilli, P. (2003). Mechanisms of membrane deformation. Curr Opin Cell Biol *15*, 372-381.

Fuqua, C., and Greenberg, E. P. (1998). Self perception in bacteria: quorum sensing with acylated homoserine lactones. Curr Opin Microbiol *1*, 183-189.

Fuqua, W. C., Winans, S. C., and Greenberg, E. P. (1994). Quorum sensing in bacteria: the LuxR-LuxI family of cell density-responsive transcriptional regulators. J Bacteriol *176*, 269-275.

Groer, C. E., Schmid, C. L., Jaeger, A. M., and Bohn, L. M. (2011). Agonist-directed interactions with specific beta-arrestins determine mu-opioid receptor trafficking, ubiquitination, and dephosphorylation. J Biol Chem *286*, 31731-31741.

Hastings, J. W., and Greenberg, E. P. (1999). Quorum sensing: the explanation of a curious phenomenon reveals a common characteristic of bacteria. J Bacteriol *181*, 2667-2668.

Hicke, L., and Dunn, R. (2003). Regulation of membrane protein transport by ubiquitin and ubiquitin-binding proteins. Annu Rev Cell Dev Biol *19*, 141-172.

Hinshaw, J. E. (2000). Dynamin and its role in membrane fission. Annu Rev Cell Dev Biol *16*, 483-519.

Hislop, J. N., Henry, A. G., Marchese, A., and von Zastrow, M. (2009). Ubiquitination regulates proteolytic processing of G protein-coupled receptors after their sorting to lysosomes. J Biol Chem *284*, 19361-19370.

Hislop, J. N., Henry, A. G., and von Zastrow, M. (2011). Ubiquitination in the first cytoplasmic loop of {micro}-opioid receptors reveals a hierarchical mechanism of lysosomal downregulation. J Biol Chem.

Hislop, J. N., and von Zastrow, M. (2011). Role of ubiquitination in endocytic trafficking of g-protein-coupled receptors. Traffic *12*, 137-148.

Itoh, T., and De Camilli, P. (2006). BAR, F-BAR (EFC) and ENTH/ANTH domains in the regulation of membrane-cytosol interfaces and membrane curvature. Biochim Biophys Acta *1761*, 897-912.

Jaqaman, K., Loerke, D., Mettlen, M., Kuwata, H., Grinstein, S., Schmid, S. L., and Danuser, G. (2008). Robust single-particle tracking in live-cell time-lapse sequences. Nat Methods *5*, 695-702.

Jayaraman, A., and Wood, T. K. (2008). Bacterial quorum sensing: signals, circuits, and implications for biofilms and disease. Annu Rev Biomed Eng *10*, 145-167.

Jiang, X., and Sorkin, A. (2003). Epidermal growth factor receptor internalization through clathrin-coated pits requires Cbl RING finger and proline-rich domains but not receptor polyubiquitylation. Traffic *4*, 529-543.

Jin, L., Pahuja, K. B., Wickliffe, K. E., Gorur, A., Baumgartel, C., Schekman, R., and Rape, M. (2012). Ubiquitin-dependent regulation of COPII coat size and function. Nature *482*, 495-500.

Johnson, E. A., Oldfield, S., Braksator, E., Gonzalez-Cuello, A., Couch, D., Hall, K. J., Mundell, S. J., Bailey, C. P., Kelly, E., and Henderson, G. (2006). Agonist-selective mechanisms of mu-opioid receptor desensitization in human embryonic kidney 293 cells. Mol Pharmacol *70*, 676-685.

Kaksonen, M., Toret, C. P., and Drubin, D. G. (2005). A modular design for the clathrin- and actin-mediated endocytosis machinery. Cell *123*, 305-320.

Kasai, R. S., Suzuki, K. G., Prossnitz, E. R., Koyama-Honda, I., Nakada, C., Fujiwara, T. K., and Kusumi, A. (2011). Full characterization of GPCR monomer-dimer dynamic equilibrium by single molecule imaging. J Cell Biol *192*, 463-480.

Kazazic, M., Bertelsen, V., Pedersen, K. W., Vuong, T. T., Grandal, M. V., Rodland, M. S., Traub, L. M., Stang, E., and Madshus, I. H. (2009). Epsin 1 is involved in recruitment of ubiquitinated EGF receptors into clathrin-coated pits. Traffic *10*, 235-245.

Keith, D. E., Murray, S. R., Zaki, P. A., Chu, P. C., Lissin, D. V., Kang, L., Evans, C. J., and von Zastrow, M. (1996). Morphine activates opioid receptors without causing their rapid internalization. J Biol Chem *271*, 19021-19024.

Khelashvili, G., Dorff, K., Shan, J., Camacho-Artacho, M., Skrabanek, L., Vroling, B., Bouvier, M., Devi, L. A., George, S. R., Javitch, J. A., *et al.* (2010). GPCR-OKB: the G Protein Coupled Receptor Oligomer Knowledge Base. Bioinformatics *26*, 1804-1805.

Kirchhausen, T. (2009). Imaging endocytic clathrin structures in living cells. Trends Cell Biol *19*, 596-605.

Lau, E. K., Trester-Zedlitz, M., Trinidad, J. C., Kotowski, S. J., Krutchinsky, A. N., Burlingame, A. L., and von Zastrow, M. (2011). Quantitative encoding of the effect of a partial agonist on individual opioid receptors by multisite phosphorylation and threshold detection. Sci Signal *4*, ra52.

Le Roy, C., and Wrana, J. L. (2005). Clathrin- and non-clathrin-mediated endocytic regulation of cell signalling. Nat Rev Mol Cell Biol *6*, 112-126.

Liu, A. P., Aguet, F., Danuser, G., and Schmid, S. L. (2010). Local clustering of transferrin receptors promotes clathrin-coated pit initiation. J Cell Biol *191*, 1381-1393.

Loerke, D., Mettlen, M., Yarar, D., Jaqaman, K., Jaqaman, H., Danuser, G., and Schmid, S. L. (2009). Cargo and dynamin regulate clathrin-coated pit maturation. PLoS Biol *7*, e57.

Maldonado-Baez, L., and Wendland, B. (2006). Endocytic adaptors: recruiters, coordinators and regulators. Trends Cell Biol *16*, 505-513.

McMahon, H. T., and Gallop, J. L. (2005). Membrane curvature and mechanisms of dynamic cell membrane remodelling. Nature *438*, 590-596.

Merrifield, C. J., Feldman, M. E., Wan, L., and Almers, W. (2002). Imaging actin and dynamin recruitment during invagination of single clathrin-coated pits. Nat Cell Biol *4*, 691-698.

Mettlen, M., Loerke, D., Yarar, D., Danuser, G., and Schmid, S. L. (2010). Cargo- and adaptor-specific mechanisms regulate clathrin-mediated endocytosis. J Cell Biol *188*, 919-933.

Mettlen, M., Stoeber, M., Loerke, D., Antonescu, C. N., Danuser, G., and Schmid, S. L. (2009). Endocytic accessory proteins are functionally distinguished by their differential effects on the maturation of clathrin-coated pits. Mol Biol Cell *20*, 3251-3260.

Miesenbock, G., De Angelis, D. A., and Rothman, J. E. (1998). Visualizing secretion and synaptic transmission with pH-sensitive green fluorescent proteins. Nature *394*, 192-195.

Miller, M. B., and Bassler, B. L. (2001). Quorum sensing in bacteria. Annu Rev Microbiol *55*, 165-199.

Mundell, S. J., Luo, J., Benovic, J. L., Conley, P. B., and Poole, A. W. (2006). Distinct clathrin-coated pits sort different G protein-coupled receptor cargo. Traffic *7*, 1420-1431.

Nealson, K. H., Platt, T., and Hastings, J. W. (1970). Cellular control of the synthesis and activity of the bacterial luminescent system. J Bacteriol *104*, 313-322.

Perrais, D., and Merrifield, C. J. (2005). Dynamics of endocytic vesicle creation. Dev Cell *9*, 581-592.

Puthenveedu, M. A., and von Zastrow, M. (2006). Cargo regulates clathrin-coated pit dynamics. Cell *127*, 113-124.

Raiborg, C., and Stenmark, H. (2009). The ESCRT machinery in endosomal sorting of ubiquitylated membrane proteins. Nature *458*, 445-452.

Reider, A., and Wendland, B. Endocytic adaptors--social networking at the plasma membrane. J Cell Sci *124*, 1613-1622.

Rust, M. J., Lakadamyali, M., Zhang, F., and Zhuang, X. (2004). Assembly of endocytic machinery around individual influenza viruses during viral entry. Nat Struct Mol Biol *11*, 567-573.

Saksena, S., Sun, J., Chu, T., and Emr, S. D. (2007). ESCRTing proteins in the endocytic pathway. Trends Biochem Sci *32*, 561-573.

Sanan, D. A., and Anderson, R. G. (1991). Simultaneous visualization of LDL receptor distribution and clathrin lattices on membranes torn from the upper surface of cultured cells. J Histochem Cytochem *39*, 1017-1024.

Santini, F., Gaidarov, I., and Keen, J. H. (2002). G protein-coupled receptor/arrestin3 modulation of the endocytic machinery. J Cell Biol *156*, 665-676.

Scherrer, G., Tryoen-Toth, P., Filliol, D., Matifas, A., Laustriat, D., Cao, Y. Q., Basbaum, A. I., Dierich, A., Vonesh, J. L., Gaveriaux-Ruff, C., and Kieffer, B. L. (2006). Knockin mice expressing fluorescent delta-opioid receptors uncover G protein-coupled receptor dynamics in vivo. Proc Natl Acad Sci U S A *103*, 9691-9696.

Shenoy, S. K., McDonald, P. H., Kohout, T. A., and Lefkowitz, R. J. (2001). Regulation of receptor fate by ubiquitination of activated beta 2-adrenergic receptor and beta-arrestin. Science *294*, 1307-1313.

Shenoy, S. K., Xiao, K., Venkataramanan, V., Snyder, P. M., Freedman, N. J., and Weissman, A. M. (2008). Nedd4 mediates agonist-dependent ubiquitination, lysosomal targeting, and degradation of the beta2-adrenergic receptor. J Biol Chem *283*, 22166-22176.

Shields, S. B., and Piper, R. C. (2011). How ubiquitin functions with ESCRTs. Traffic *12*, 1306-1317.

Shih, S. C., Katzmann, D. J., Schnell, J. D., Sutanto, M., Emr, S. D., and Hicke, L. (2002). Epsins and Vps27p/Hrs contain ubiquitin-binding domains that function in receptor endocytosis. Nat Cell Biol *4*, 389-393.

Signoret, N., Hewlett, L., Wavre, S., Pelchen-Matthews, A., Oppermann, M., and Marsh, M. (2005). Agonist-induced endocytosis of CC chemokine receptor 5 is clathrin dependent. Mol Biol Cell *16*, 902-917.

Sorkin, A., and von Zastrow, M. (2009). Endocytosis and signalling: intertwining molecular networks. Nat Rev Mol Cell Biol *10*, 609-622.

Sorkina, T., Miranda, M., Dionne, K. R., Hoover, B. R., Zahniser, N. R., and Sorkin, A. (2006). RNA interference screen reveals an essential role of Nedd4-2 in dopamine transporter ubiquitination and endocytosis. J Neurosci *26*, 8195-8205.

Staub, O., and Rotin, D. (2006). Role of ubiquitylation in cellular membrane transport. Physiol Rev *86*, 669-707.

Sugiyama, S., Kishida, S., Chayama, K., Koyama, S., and Kikuchi, A. (2005). Ubiquitin-interacting motifs of Epsin are involved in the regulation of insulin-dependent endocytosis. J Biochem *137*, 355-364.

Tanowitz, M., and von Zastrow, M. (2003). A novel endocytic recycling signal that distinguishes the membrane trafficking of naturally occurring opioid receptors. J Biol Chem *278*, 45978-45986.

Taylor, M. J., Perrais, D., and Merrifield, C. J. (2011). A high precision survey of the molecular dynamics of mammalian clathrin-mediated endocytosis. PLoS Biol *9*, e1000604.

Toret, C. P., and Drubin, D. G. (2006). The budding yeast endocytic pathway. J Cell Sci *119*, 4585-4587.

Torrisi, M. R., Lotti, L. V., Belleudi, F., Gradini, R., Salcini, A. E., Confalonieri, S., Pelicci, P. G., and Di Fiore, P. P. (1999). Eps15 is recruited to the plasma membrane upon epidermal growth factor receptor activation and localizes to components of the endocytic pathway during receptor internalization. Mol Biol Cell *10*, 417-434.

Toshima, J. Y., Nakanishi, J. I., Mizuno, K., Toshima, J., and Drubin, D. G. (2009). Requirements for Recruitment of a G Protein-coupled Receptor to Clathrin-coated Pits in Budding Yeast. Mol Biol Cell.

Traub, L. M. (2009). Tickets to ride: selecting cargo for clathrin-regulated internalization. Nat Rev Mol Cell Biol *10*, 583-596.

Tsao, P. I., and von Zastrow, M. (2000). Type-specific sorting of G protein-coupled receptors after endocytosis. J Biol Chem *275*, 11130-11140.

Vassilopoulos, S., Esk, C., Hoshino, S., Funke, B. H., Chen, C. Y., Plocik, A. M., Wright, W. E., Kucherlapati, R., and Brodsky, F. M. (2009). A role for the CHC22 clathrin heavy-chain isoform in human glucose metabolism. Science *324*, 1192-1196.

Weinberg, J., and Drubin, D. G. (2011). Clathrin-mediated endocytosis in budding yeast. Trends Cell Biol.

Wendland, B. (2002). Epsins: adaptors in endocytosis? Nat Rev Mol Cell Biol *3*, 971-977.

Whistler, J. L., and von Zastrow, M. (1998). Morphine-activated opioid receptors elude desensitization by beta-arrestin. Proc Natl Acad Sci U S A *95*, 9914-9919.

Yu, Y. J., Arttamangkul, S., Evans, C. J., Williams, J. T., and von Zastrow, M. (2009). Neurokinin 1 receptors regulate morphine-induced endocytosis and desensitization of mu-opioid receptors in CNS neurons. J Neurosci *29*, 222-233.

Zhang, J., Ferguson, S. S., Barak, L. S., Bodduluri, S. R., Laporte, S. A., Law, P. Y., and Caron, M. G. (1998). Role for G protein-coupled receptor kinase in agonist-specific regulation of mu-opioid receptor responsiveness. Proc Natl Acad Sci U S A *95*, 7157-7162.

# 4.8 Figures

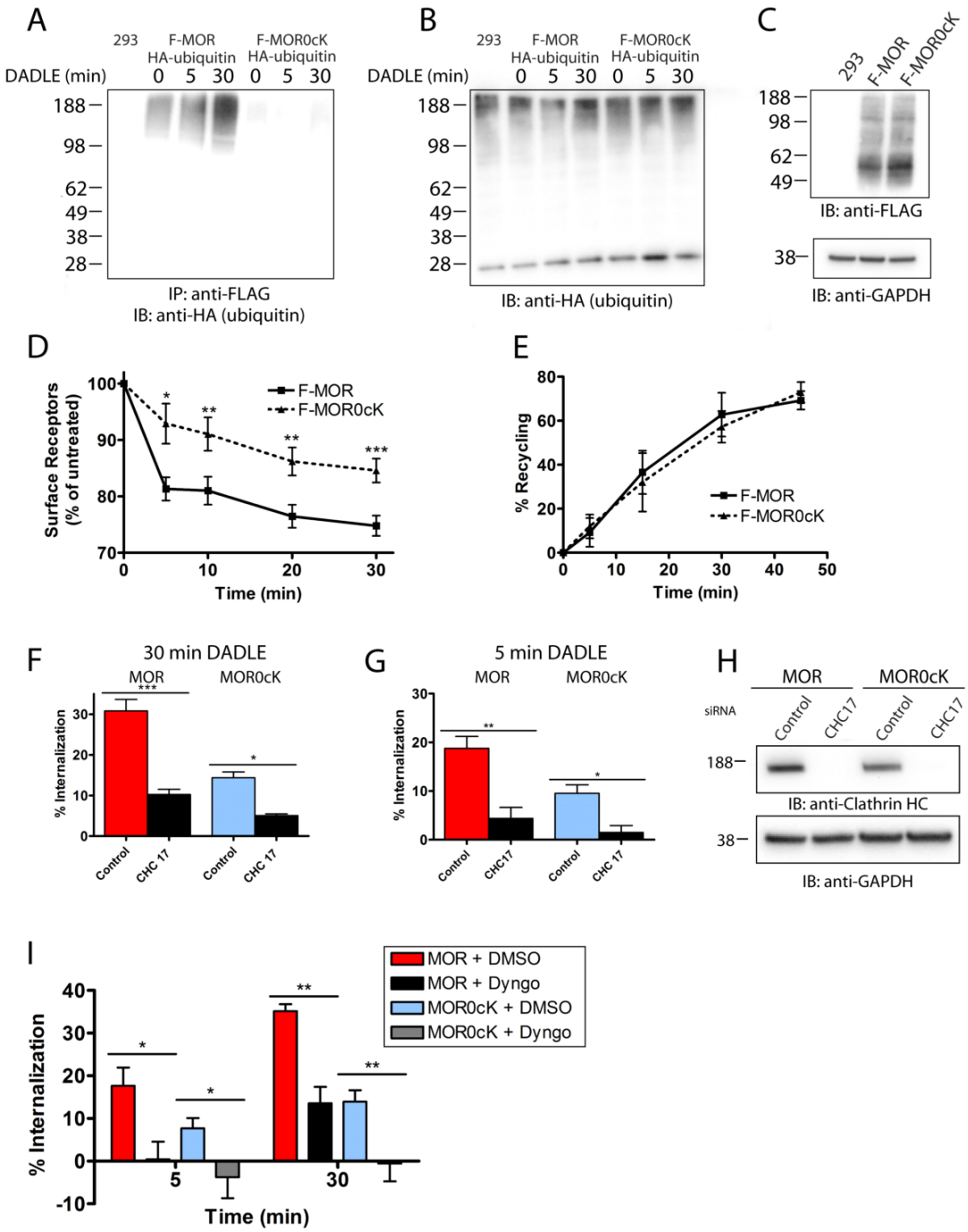


**Figure 1. Receptor ubiquitination is required for efficient endocytosis of MOR.** (A) The ubiquitination status of wildtype or lysyl-mutant MORs (F-MOR or F-MOR0cK, respectively) was examined after treatment with 10μM DADLE before extraction and immunoprecipitation with FLAG antibody. Shown is a

representative anti-HA blot of untransfected cells (293), F-MOR- (left), and F-MOR0cK –expressing cells (right). (B and C) Lysates from cells in (A) probed with HA antibody (B) or FLAG and GAPDH antibody (C) to control for equal loading and expression. (D) Time course of endocytosis for F-MOR and F-MOR0cK receptors after DADLE treatment for the indicated time points. The amount of surface receptors was measured using flow cytometry; n=4. (E) Time course of receptor recycling after 30 min DADLE treatment, agonist washout, and treatment with 10μM of opioid antagonist naloxone for the indicated times. Shown is the recycling efficiency; n=3. (F and G) Flow cytometric analysis of receptor internalization after clathrin knockdown and 30 min (F) or 5 min (G) DADLE application; n=3 and n≥4, respectively. (H) To verify clathrin knockdown, immunoblots detecting endogenous clathrin heavy chain were performed, and equal loading was confirmed by immunoblotting for GAPDH. (I) Flow cytometric analysis of receptor internalization after treatment with vehicle or the dynamin inhibitor, DYNGO, for 15 min followed by treatment with DADLE for 5 or 30 minutes; n=3. Error bars indicate standard error of the mean (SEM). P-values: one- or two-way ANOVA, Bonferroni multiple comparison test; *, $p<0.05$; **, $p<0.01$; ***, $p<0.001$.

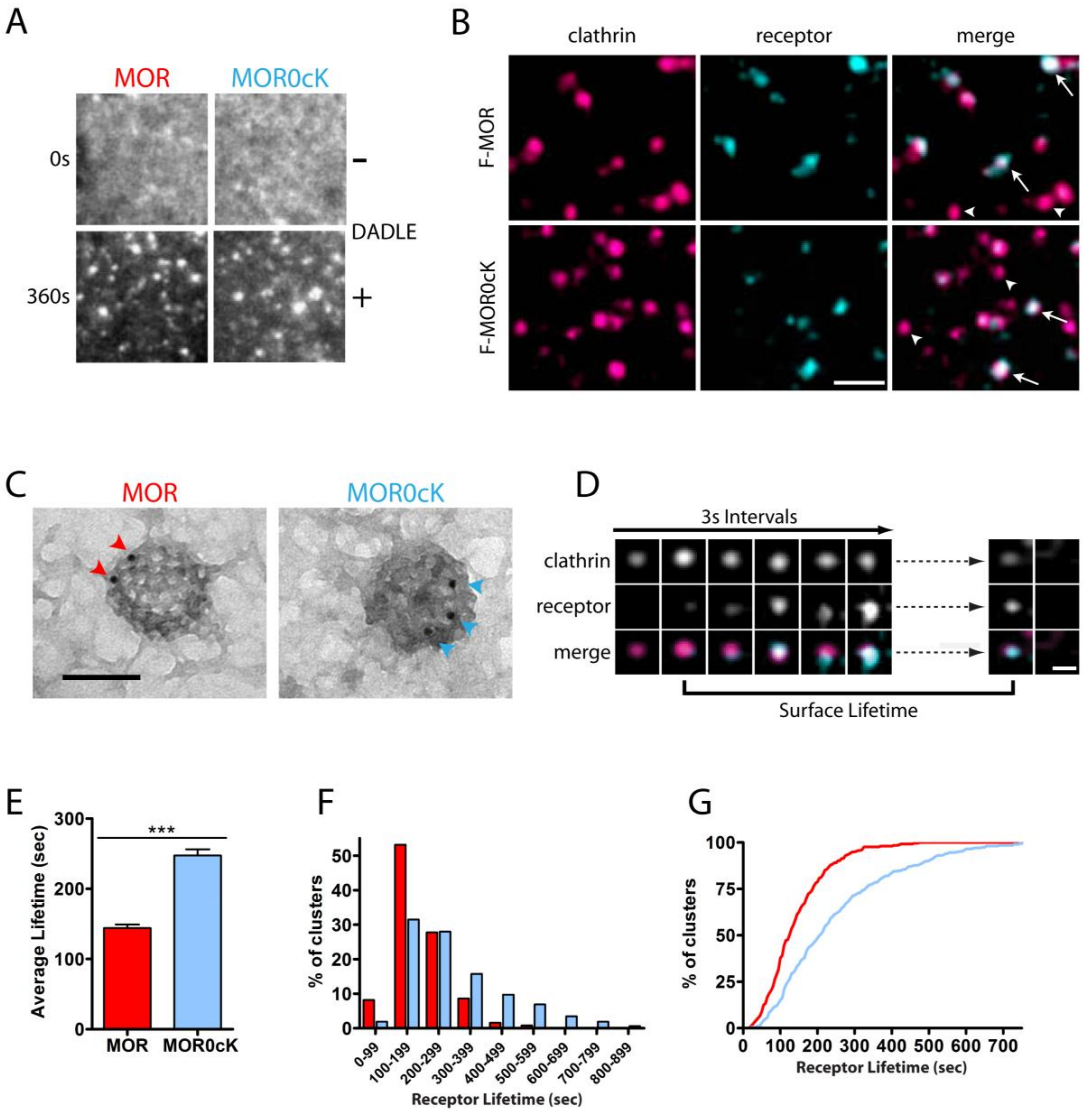


**Figure 2. MOR ubiquitination is not required for receptor entry into CCPs and selectively controls surface lifetime of receptors after clustering.** (A) TIRF live-cell imaging of cells expressing F-MOR or F-MOR0cK before and after 10 min treatment with 10µM DADLE. (B) Cells expressing DsRed-tagged clathrin light chain (shown in fushia) and either F-MOR or F-MOR0cK (shown in teal) were imaged live. Shown is a representative image ten minutes after DADLE application. Arrowheads indicate CCPs that lack receptor while arrows indicate CCPs that contain receptor; scale bar =1 µm. (C) Example immunoelectron micrographs of CCPs containing F-MORs (left) or F-MOR0cKs (right) labeled with FLAG antibody and protein A conjugated to 10 nm gold particles treated with agonist for 2min. Samples were prepared as described in *Experimental Procedures*; scale bar =100 nm. (D) Representative time lapse series showing MORs cluster into pre-existing CCPs. Cells were treated with agonist while imaging using

TIRF-M. Frames are three seconds apart; scale bar = 500nm. (E) The average lifetimes that F-MOR and F-MOR0cK clusters remain on the cell surface before undergoing endocytic scission; F-MOR n=256 clusters, 10 cells; F-MOR0cK n=318 clusters, 12 cells. (F and G) Frequency distribution (F) and cumulative probability (G) analysis of MOR (red) and MOR0cK (light blue) cluster lifetimes. Error bars indicate standard error of the mean (SEM). P-values: student's t-test; ***, $p<0.001$.

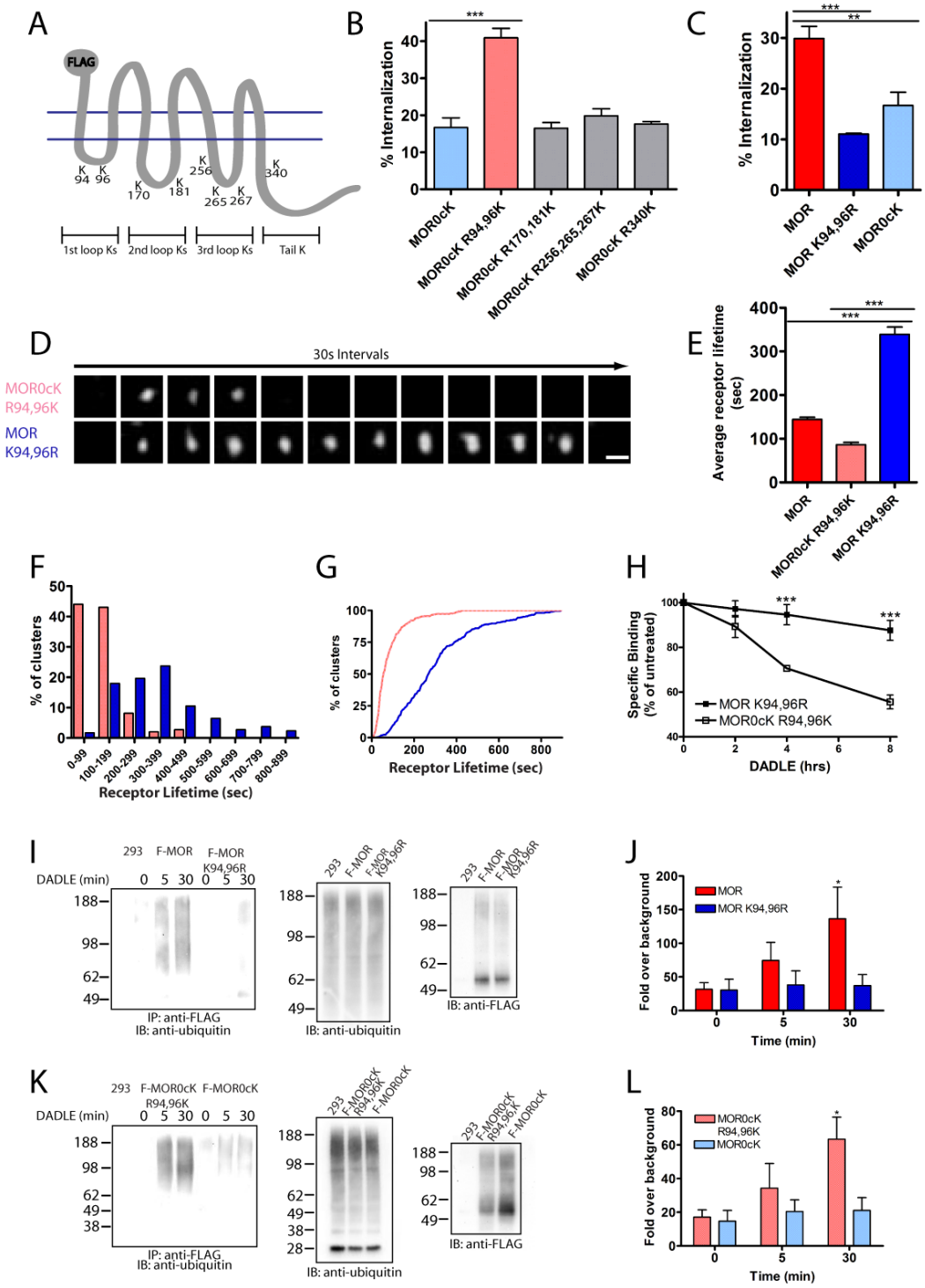


**Figure 3. Lysine 94 and 96 in the first intracellular loop of MOR control the surface lifetime of receptors and are the major sites of agonist-induced MOR ubiquitination.** (A) Schematic of MOR indicating the positions of the eight cytoplasmic lysine residues. (B) Flow cytometric analysis of the internalization of mutant receptors with no cytoplasmic lysine residues (MOR0cK) and with the selective

return of lysine residues in the different intracellular domains of the receptor corresponding to the sites shown in A. Cells were treated with 10μM DADLE for 30 min; n=3. (C) The percentage of receptor internalization was measured as in B in cells expressing wildtype MOR, MOR K94,96R, and MOR0cK; n=3. (D) Representative image sequence of clusters of mutant receptors with only the first intracellular loop lysines present (MOR0cK R94,96K) or only missing these sites (MOR K94,96R). Cells were treated with agonist while imaging using TIRF-M. Frames are 30s apart; scale bar = 500nm. (E) The average surface lifetimes of MOR, MOR0cK R94,96K, and MOR K94,96R clusters after agonist treatment; MOR n=256 clusters, 10 cells; MOR0cK R94,96K n=296 clusters, 11 cells; and MOR K94,96R n=274 clusters, 10 cells. (F and G) Frequency distribution (F) and cumulative probability analysis (G) of MOR0cK R94,96K (pink) and MOR K94,96R (blue) cluster lifetimes. (H) Cells expressing F- MOR K94,96R or F-MOR0cK R94,96K were incubated for the indicated times with agonist before undergoing freeze-thaw and radioligand binding with [$^3$H] diprenorphine. The specific binding values, expressed as a percentage of binding in untreated cells, are shown. (I) The ubiquitination status of F-MORs or F-MOR K94,96Rs was assessed after treated with 10μM DADLE for the indicated times before extraction and immunoprecipitation with FLAG antibody. A representative immunoblot detecting endogenous ubiquitin in untransfected cells (293) and in cells expressing F-MOR and F-MOR K94,96R (left) is shown. Blots were probed with antibody against endogenous ubiquitin (middle) or FLAG (right) to control for equal loading and receptor expression. (J) Immunoblots from multiple experiments were scanned to estimate the amount of ubiquitin at each time point after treatment with DADLE and expressed as a fold increase over signal in untransfected 293 cells. The results were pooled and averaged across multiple experiments; n=4. (K and L) The ubiquitination status of MOR0cK R94,96Ks or MOR0cKs was measured as in I and J; n=3. Error bars correspond to SEM and P-values: one- or two-way ANOVA, Bonferroni multiple comparison test; *, $p<0.05$; **, $p<0.01$; ***, $p<0.001$.

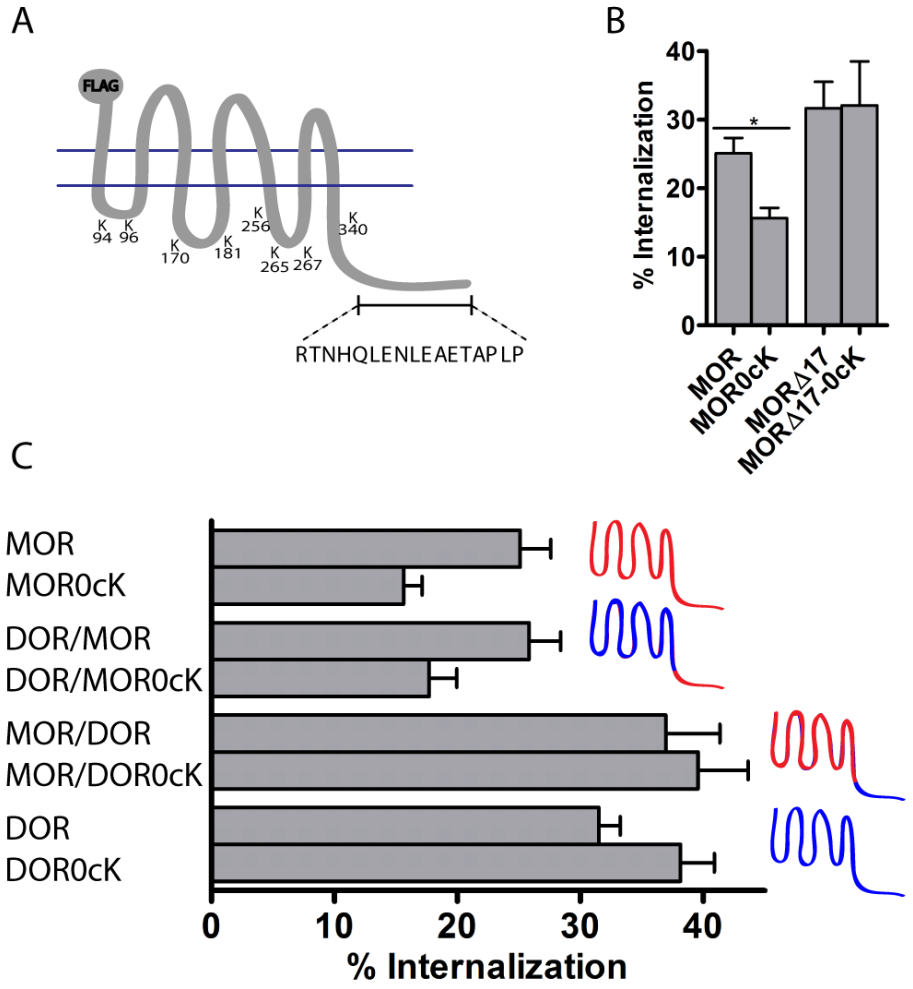


**Figure 4. The last 17 amino acids of MOR confer ubiquitin-dependent regulation of receptor endocytosis.** (A) Schematic of MOR indicating the site of the eight cytoplasmic lysine residues and of the truncation to generate MORΔ17. (B) Flow cytometric analysis of the internalization of wildtype MOR, MOR0cK, and a truncated mutant MOR that lacks its last 17 amino acids, with or without its cytoplasmic lysine residues (MORΔ17 or MORΔ17-0cK, respectively). Cells were treated with 10μM DADLE for 30 min; n≥3. (C) Cells were treated as in B, and the percentage of internalization of mutant receptors whose cytoplasmic tails have been swapped between opioid receptors was measured; n≥5. P-values: one-way ANOVA, Bonferroni multiple comparison test; *, $p<0.05$.

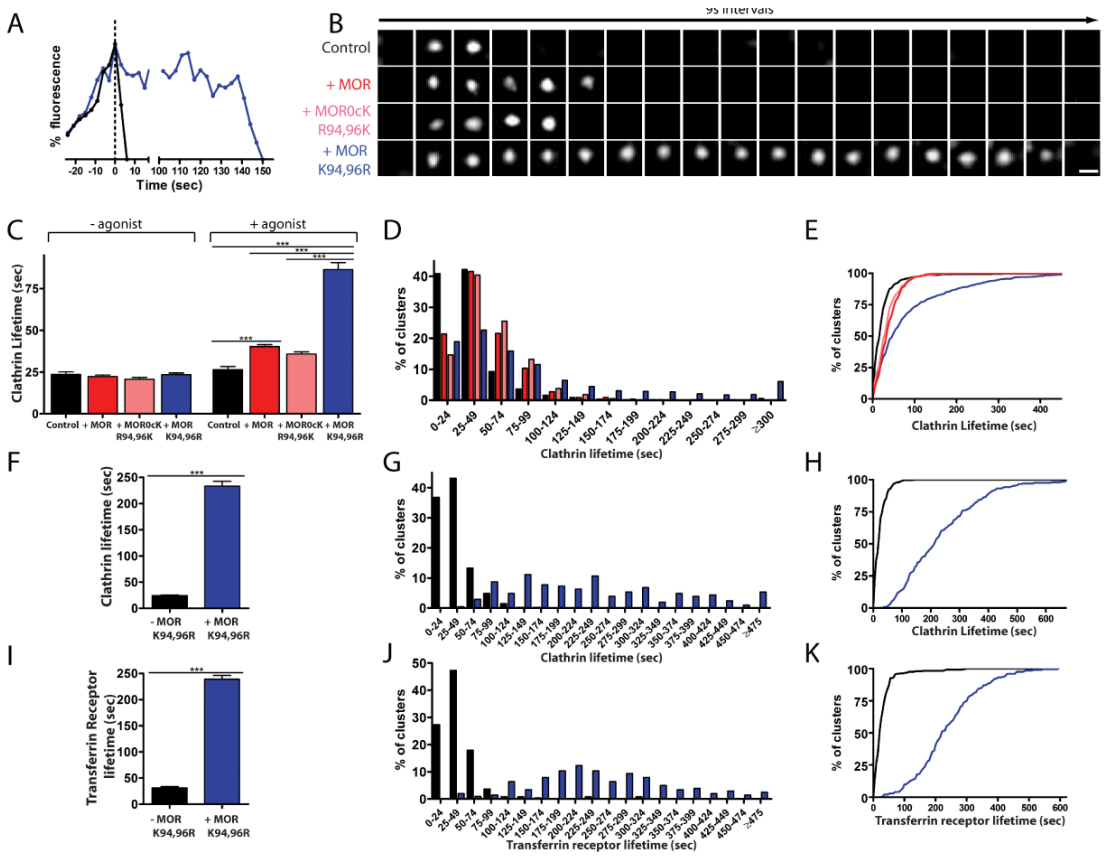


**Figure 5. MOR ubiquitination decreases the surface lifetime of clathrin and affects other cargo in MOR-containing CCPs.** (A) Clathrin fluorescence traces of representative short (black) and long-lived (blue) CCPs in a MOR K94,96R-expressing cell imaged in the presence of agonist. Traces were aligned (t=0 denotes the end of the ascending phase). (B) Representative image sequences of CCPs from Control, + MOR, +MOR0cK R94,96K, or + MOR K94,96R cells treated with agonist while imaging using TIRF-M. Frames are nine secs apart; scale bar = 500nm. (C) The average clathrin lifetimes before and after agonist treatment in cells expressing DsRed-tagged clathrin light chain and pCDNA 3.0 (Control), MOR, MOR0cK R94,96K, or MOR K94,96R. Before agonist treatment: Control (black) n=207 clusters, 5 cells; +MOR (red) n=308 clusters, 5 cells; +MOR0cK R94,96K (pink) n=135 clusters, 5 cells, +MOR K94,96R (blue) n=302 clusters, 5 cells. After agonist treatment: Control n=550 clusters, 5 cells; +MOR n=607 clusters, 5 cells; +MOR0cK R94,96K n=542 clusters, 5 cells, +MOR K94,96R n=592 clusters, 5 cells. (D-E) Frequency distribution (D) and cumulative probability (E) analysis of clathrin surface lifetimes. (F) The average clathrin lifetimes in MOR K94,96R-expressing cells treated with agonist, separated into populations based on whether they lack (-MOR K94,96R) or contain (+MOR K94,96R) receptors measured

within the same 5 cells. -MOR K94,96R n=413 clusters; +MOR K94,96R n=206 clusters. (G-H) Frequency distribution (G) and cumulative probability (H) analysis of clathrin cluster lifetimes that either lack (-MOR K94,96R, black) or contain (+MOR K94,96R, blue) MOR K94,96R receptors. (I) The average SpH-Transferrin receptor cluster lifetimes in MOR K94,96R-expressing cells treated with DADLE, separated by whether they lack (-MOR K94,96R) or contain (+MOR K94,96R) mutant receptors. -MOR K94,96R n=245 clusters, 5 cells; +MOR K94,96R n=203 clusters, 5 cells. (J-K) Frequency distribution (J) and cumulative probability (K) analysis of the lifetimes of Transferrin receptor clusters that either lack (-MOR K94,96R, black) or contain (+MOR K94,96R, blue) MOR K94,96R receptors. Error bars indicate standard error of the mean (SEM). P-values: one-way ANOVA, Bonferroni multiple comparison test; ***, p<0.001.

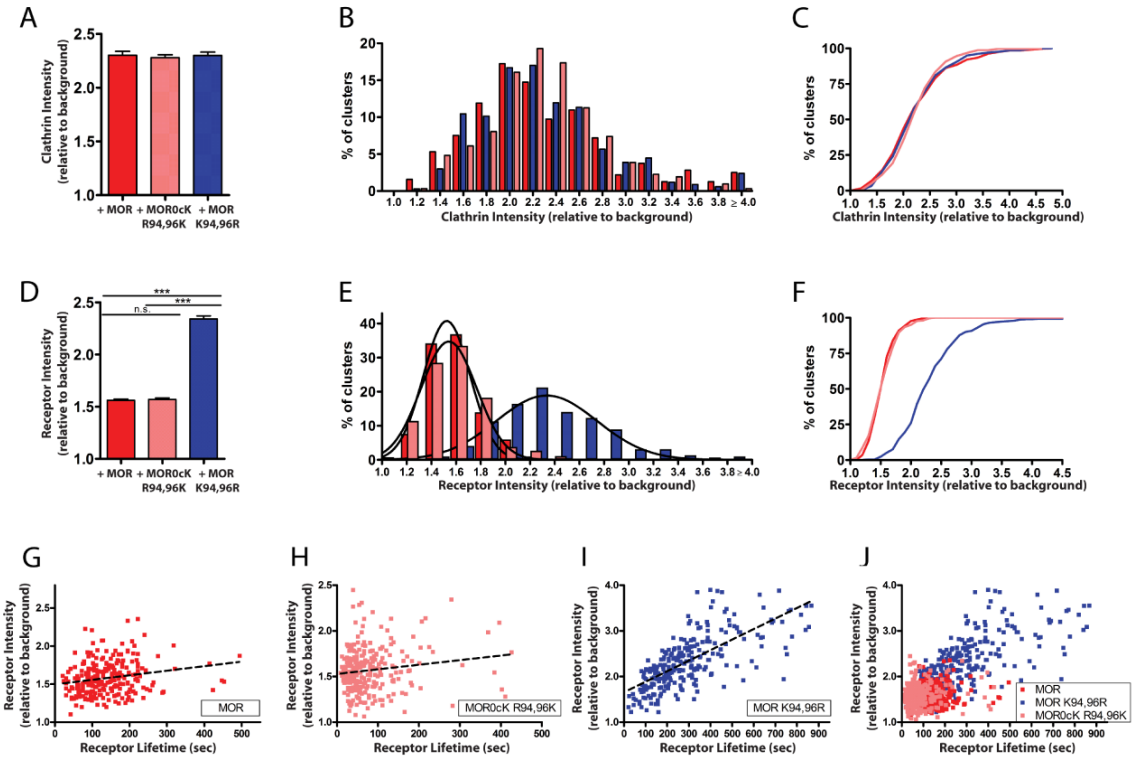


**Figure 6. MOR ubiquitination controls the amount of receptor loaded into individual CCPs.** (A) The average, normalized clathrin fluorescence intensities in cells expressing clathrin light chain and MOR, MOR0cK R94,96K, or MOR K94,96R were measured, shown as a fold increase in fluorescence over background. MOR n=319 clusters, 7 cells; MOR0cK R94,96K n=311 clusters, 5 cells; and MOR K94,96R n= 335 clusters, 7 cells. (B-C) Frequency distribution (B) and cumulative probability curves (C) of clathrin intensities in MOR (red), MOR0cK R94,96K (pink), and MOR K94,96R (blue) -expressing cells. (D) The average, normalized receptor cluster intensities in cells expressing MOR, MOR0cK R94,96K, or MOR

K94,96R treated with agonist. MOR n=301 clusters, 7 cells; MOR0cK R94,96K n=263 clusters, 8 cells; and MOR K94,96R n= 292 clusters, 7 cells. (E) Frequency distribution of receptor clusters with the specified intensities (bars) was fitted to a Gaussian curve (lines). For MOR, $R^2$ = .9890, d.f. = 16, Sy.x = 1.257, and coefficient of variation (CV) = 0.131; for MOR0cK R94,96K $R^2$ = .9958, d.f. = 16, Sy.x = 0.7041, and CV = 0.155, for MOR K94,96R, $R^2$ = .9535, d.f. = 16, Sy.x = 1.501 and CV = 0.215. (F) Cumulative probability curves for intensity measurements of wild type or mutant receptors. (G-I) Receptor intensities were plotted against lifetimes for individual clusters to assess any correlation between intensity and receptor lifetime for MOR (G), MOR0cK R94,96K (H), and MOR K94,96R (I). MOR correlation coefficient=0.2051 and $R^2$ = .04207; MOR0cK R94,96K correlation coefficient=0.1486 and $R^2$ = .02209; MOR K94,96R correlation coefficient= 0.6885 and $R^2$ = .4740. (J) The compiled results are shown at the same scale. Error bars correspond to SEM and P-values: one-way ANOVA, Bonferroni multiple comparison test; ***, p<0.001.

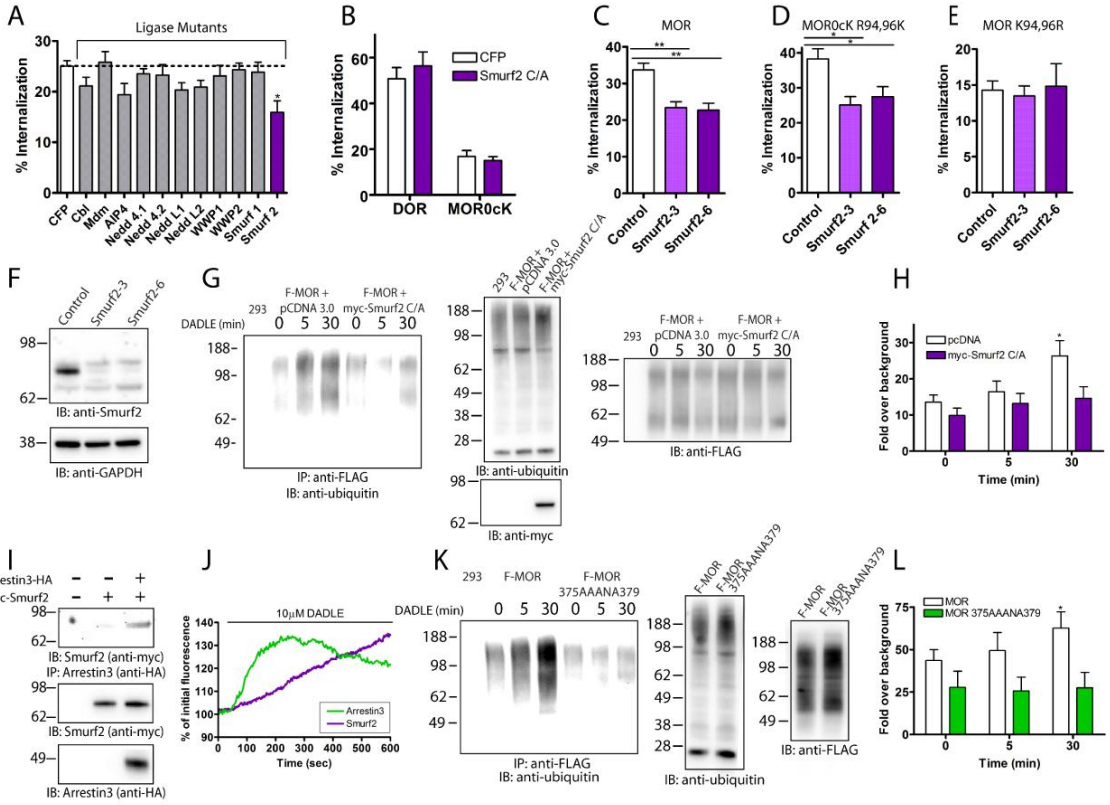


**Figure 7. Mechanism of MOR ubiquitination.** (A) Flow cytometric analysis of MOR internalization in cells expressing the specified catalytically-inactive E3 ligases after 30 min DADLE treatment; n ≥ 3. (B) Flow cytometric analysis of DOR or MOR0cK internalization after 30 min DADLE treatment in cells

transfected with CFP or an inactive mutant Smurf2; n=3. (C- E) The percentage of MOR (C, n=4), MOR0cK R94,96K (D, n=6), or MOR K94,96R (E, n=4) internalization after 30 min DADLE addition in cells transfected with control siRNA or two siRNA duplexes against Smurf2. (F) Representative immunoblot analysis of siRNA-mediated knockdown of Smurf2 with GAPDH loading control; n=3. (G) The ubiquitination status of MORs was measured in cells transfected with pCDNA 3.0 or myc-Smurf2 C/A after incubation with DADLE for 5 or 30 min. Shown is a representative blot detecting endogenous ubiquitin in untransfected cells (293) and in F-MOR cells expressing pCDNA 3.0 or myc-Smurf2 C/A (left). Loading and expression was assessed by probing for endogenous ubiquitin (top right), FLAG (middle right), and myc (bottom right). (H) Densitometry of immunoblots from multiple experiments was performed and results were averaged across multiple experiments; n=5. (I) Co-IP of Smurf2 and Arrestin3. Untransfected cells and cells expressing myc-Smurf2 with pCDNA 3.0 or HA-Arrestin3 were extracted and immunoprecipitated with HA antibody before immunoblotting for myc. Blots were probed with antibodies against myc and HA to confirm expression and equal loading. (J) The increase in intensity of Arrestin3 or Smurf2 was measured after agonist addition in F-MOR expressing cells by TIRF-M and is expressed as the % of initial fluorescence; n=12 cells. (K-L) The ubiquitination status of MOR or F-MOR 375AAANA379 receptors was measured as in G and H. A representative blot is shown detecting ubiquitin in untransfected cells and in F-MOR or F-MOR 375AAANA379 cells (left). Equal loading and expression were confirmed by probing lysates for endogenous ubiquitin (middle), and FLAG antibody (right). Densitometry of immunoblots was performed and averaged across multiple experiments; n=4. P-values: two-way ANOVA, Bonferroni multiple comparison test; *, $p<0.05$; **, $p<0.01$.

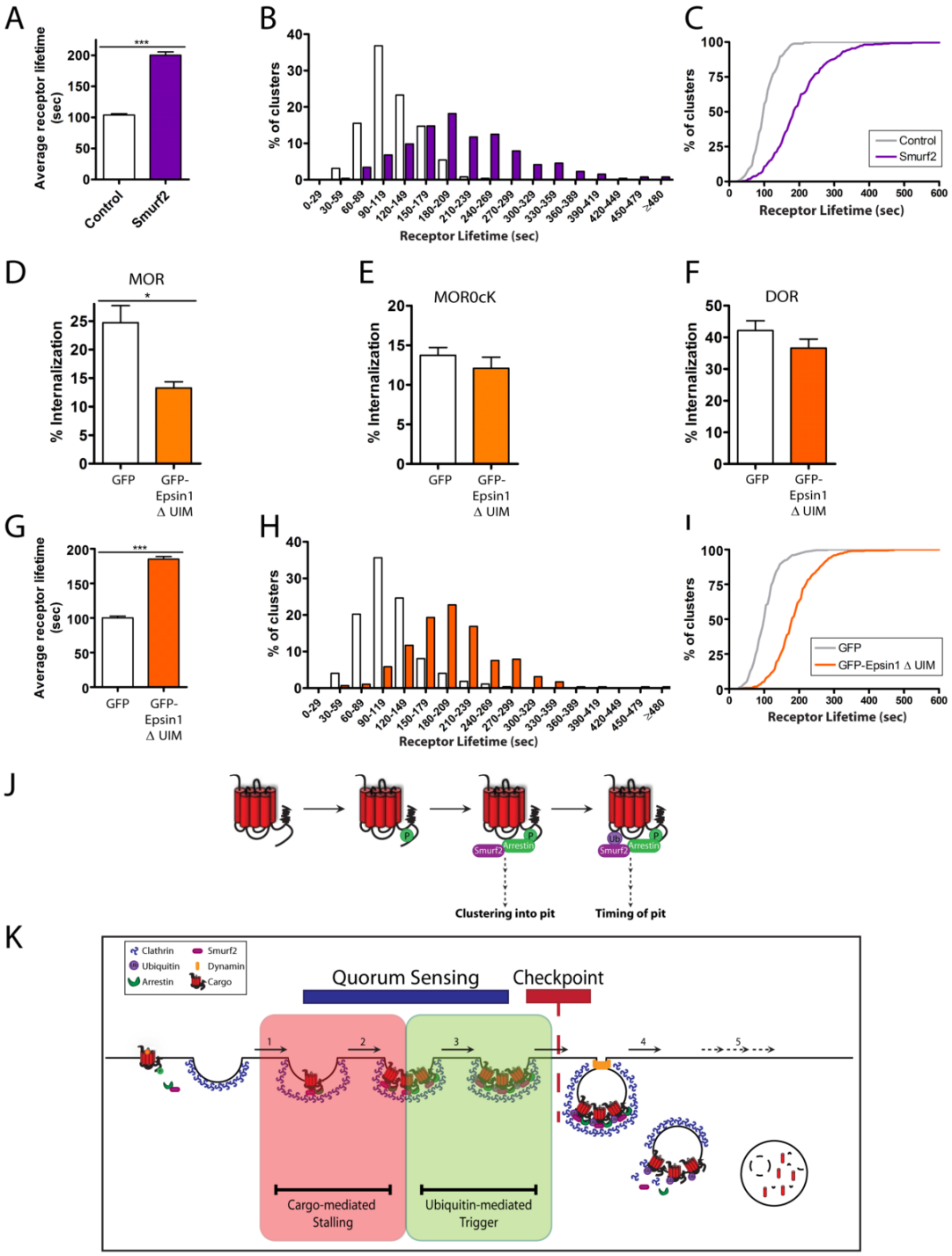


**Figure 8. Smurf-2 mediated ubiquitination of MOR controls receptor surface lifetime.** (A) The average lifetimes of MOR clusters were measured in control or Smurf2 siRNA-expressing cells after agonist treatment; Control n=258 clusters, 9 cells; Smurf2 n=264 clusters, 11 cells. (B-C) Frequency distribution (B) and cumulativie probability (C) analysis of MOR cluster lifetimes in control (white) or Smurf2 (purple) siRNA transfected cells. (D-F) MOR (D, n=5), MOR0cK (E, n=4), or DOR (F, n=4)

internalization after 30 min DADLE was measured in cells expressing receptors and GFP or GFP-Epsin1ΔUIM. (G) The average lifetime measurements of MOR clusters in GFP or GFP-Epsin1ΔUIM-expressing cells after agonist treatment; GFP n=272 clusters, 9 cells; GFP-Epsin1ΔUIM n=290 clusters, 9 cells. (H-I) Frequency distribution (H) and cumulative probability (I) analysis of MOR surface lifetimes in GFP (white) or GFP-Epsin1ΔUIM (orange) -expressing cells. Error bars correspond to SEM and P-values: student's t-test or one-way ANOVA, Bonferroni multiple comparison test; *, $p<0.05$; ***, $p<0.001$. (J) Model for the role of post-translational modifications in MOR endocytosis. After agonist addition, receptors undergo phosphorylation which recruits Arrestin3 and Smurf2 to activated receptors and promotes entry of receptors into CCPs. Smurf2 ubiquitinates MORs, modulating the lifetime of receptor-containing CCPs. (K) Model for the role of receptor-mediated control of CCPs. Receptors are recruited to CCPs via interactions with Arrestin3 (1), where they effectively stall the CCP (2) until receptors undergo Smurf2-mediated ubiquitination (3). This prompts endocytic scission (4) and functions as both a quorum sensor for cargo load and as a checkpoint for later receptor destruction (5).

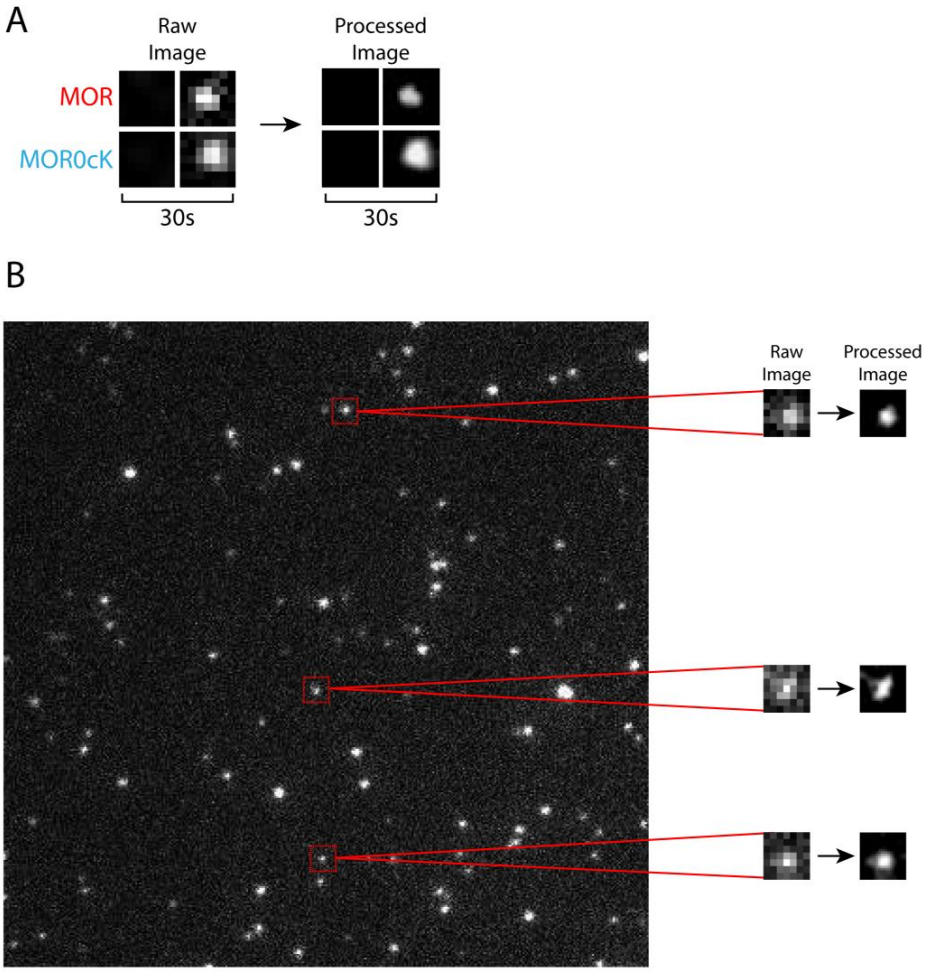


**Supplemental Figure 1. Receptor clusters imaged using TIRF-M are diffraction-limited.**

(A) Raw and processed image series of F-MOR or F-MOR0cK clusters in cells treated with agonist and imaged using TIRF-M. Frames are 30s apart. (B) Raw and processed images of 100nm fluorescent beads imaged using TIRF-M. Images were processed and pixels inserted by the interpolation algorithm of the rendering software to aid in visualization.

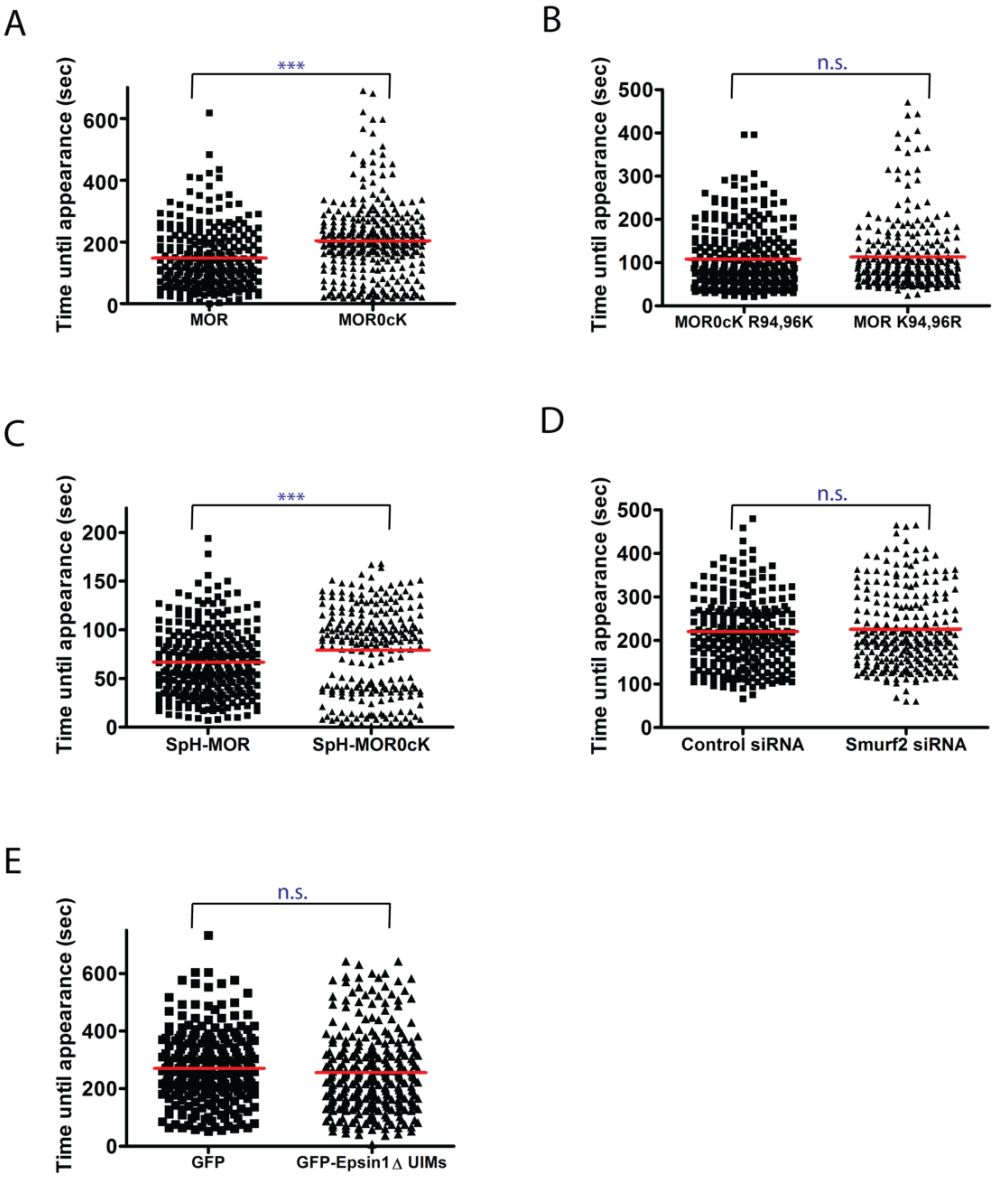


**Supplemental Figure 2. Compiled analysis of the time until appearance of receptor-containing CCPs under different conditions that affect receptor ubiquitination.** The time until cluster appearance after agonist addition is measured for F-MOR and F-MOR0cK (A), F-MOR0cK R94,96K and F-MOR K94,96R (B), SpH-MOR and SpH-MOR0cK (C), control or Smurf2 siRNA-transfected F-MOR (D), and GFP- or GFP-Epsin1 Δ UIMs-transfected (E) receptor clusters. The mean time until cluster appearance is depicted by a line for each condition analyzed. P-values: student's t-test; n.s., not significant; ***, $p<0.001$.

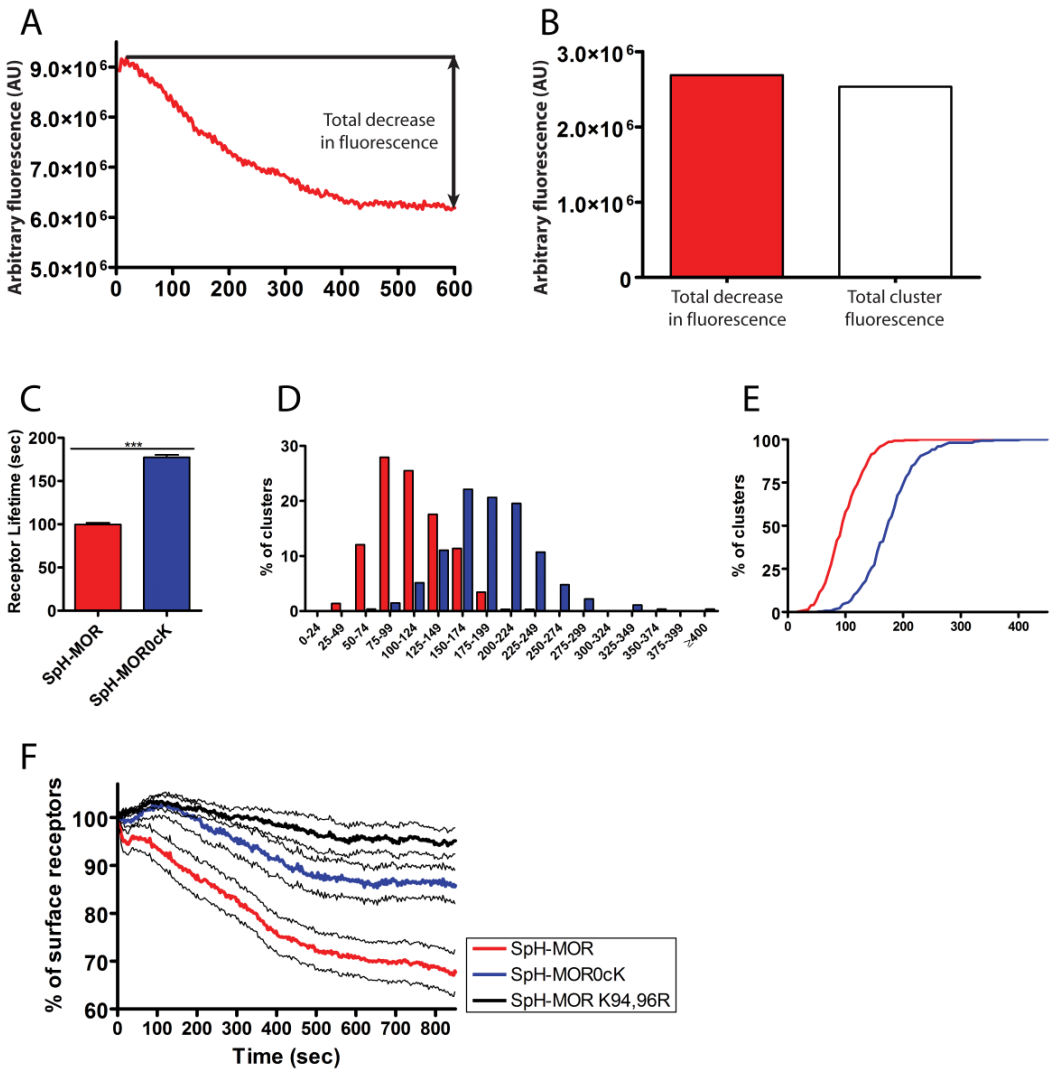


**Supplemental Figure 3. The role of receptor ubiquitination on MOR endocytosis measured using SpH-tagged receptors imaged in TIRF-M.** (A and B) The total decrease in receptor integrated fluorescence over time approximates the total fluorescence contained within receptor clusters. The total decrease in receptor fluorescence is shown for a representative F-MOR expressing cell treated with agonist at t=0 (A). The total fluorescence of all receptor clusters is measured for the same cell as in E, and is of a similar magnitude to the loss in receptor fluorescence over time (B). (C) The average surface lifetimes of SpH-MOR and SpH-MOR0cK receptor clusters after agonist treatment; MOR n=290 clusters, 8 cells; MOR0cK n=271 clusters, 8 cells. (D) Frequency distribution analysis of SpH-MOR (red) and SpH-MOR0cK (blue) receptor clusters with the specified lifetimes on the cell surface. (E) Cumulative probability analysis of receptor cluster lifetimes. (F) The normalized integrated surface fluorescence of

SpH-MOR (red), SpH-MOR0cK(blue), and SpH-MOR K94,96R (black) expressing cells measured every 3 s after agonist addition at time=0 (n=13 cells). The integrated fluorescence value at t=0 is defined as 100%. Error bars indicate standard error of the mean (SEM). P-values: student's t-test; ***, p<0.001.

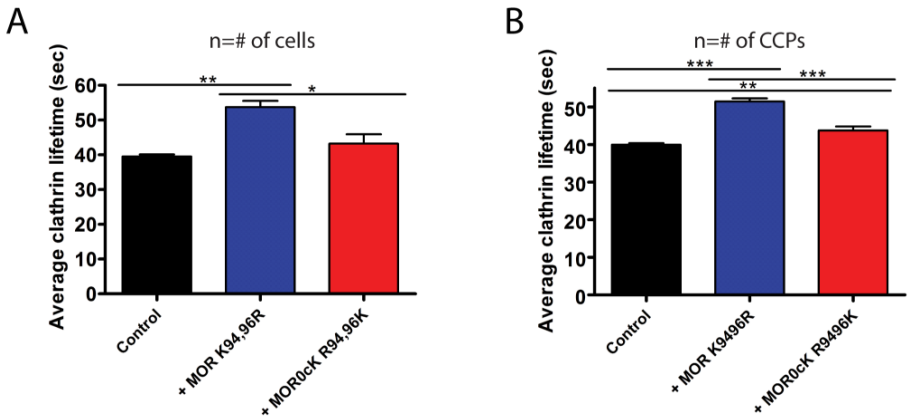


**Supplemental Figure 4. Automated analysis of overall clathrin lifetimes in receptor-expressing cells.** (A) The average clathrin lifetimes prior to agonist treatment in cells transiently expressing DsRed-tagged clathrin light chain and pCDNA 3.0 (Control), n=8 cells; F-MOR K94,96R (+ MOR K94,96), n=7cells; or F-MOR0cK R94,96K (+ MOR0cK R94,96K), n= 7cells. (B) The same average clathrin lifetimes from A, where n corresponds to the number of total clusters analyzed. Control n=14013; + MOR K94,96R n=7073; + F-MOR0cK R94,96K n=3629. Error bars indicate standard error of the mean (SEM). P-values: two-way ANOVA, Bonferroni multiple comparison test; *, p<0.05; **, p<0.01; ***, p<0.001.

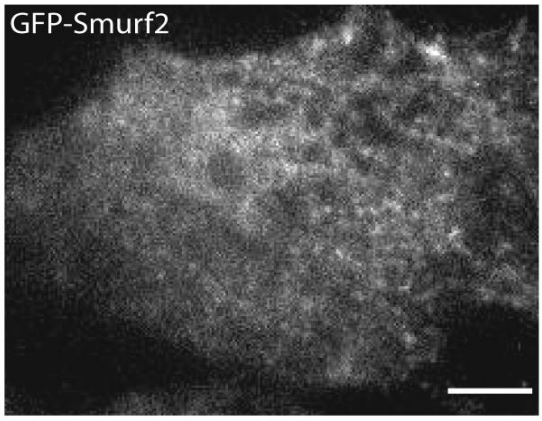


**Supplemental Figure 5. Smurf2 localizes both diffusely and in CCPs after agonist-induced recruitment.** Cells expressing GFP-tagged Smurf2 and F-MOR were imaged live using TIR-FM. Shown is a representative example showing the localization of GFP-Smurf2 in cells treated with agonist for five minutes. Scale bar = 5 μm.

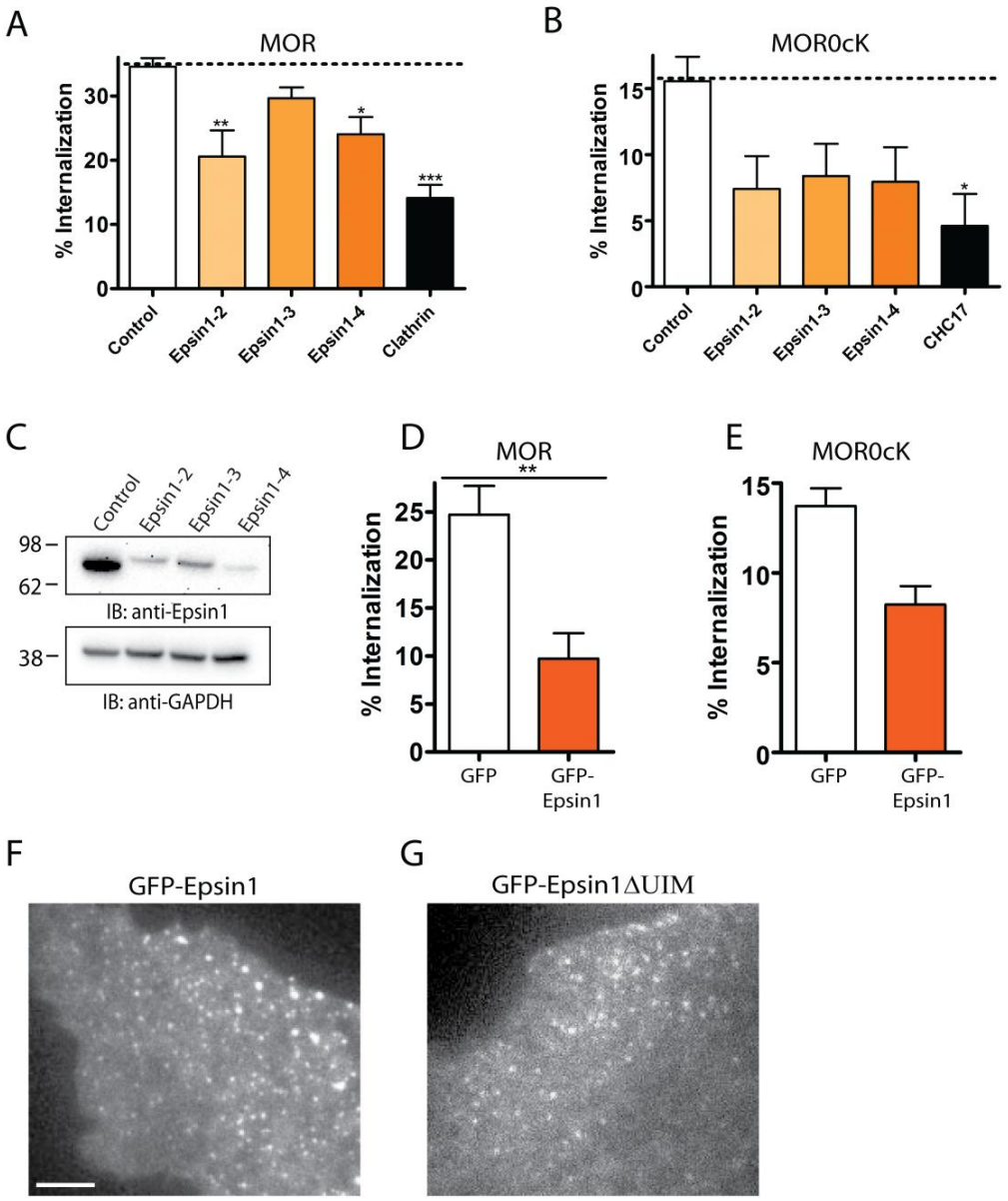


**Supplemental Figure 6. Overexpression or knockdown of Epsin1 inhibits MOR endocytosis irrespective of lysyl-mutation.** (A and B) Cells stably-expressing F-MOR (A) or F-MOR0cK (B) were transiently transfected with siRNA duplexes against Epsin1 or CHC17 (as a control) and the percentage of MOR (n≥9) or MOR0cK (n≥4) internalization after 30 minutes agonist treatment was measured using flow cytometric analysis. (C) Verification of Epsin1 knockdown by immunoblotting with an antibody against endogenous Epsin1. Shown is a representative image of three experiments, and equal loading was confirmed by immunoblot detecting GAPDH. (D and E) Cells stably-expressing F-MOR (D) or F-MOR0cK (E) were transiently transfected with either GFP alone or GFP-tagged Epsin1 and the percentage

of MOR (n=5) or MOR0cK (n=4) internalization after 30 minutes agonist treatment was measured using flow cytometry. Results were averaged across multiple experiments (shown are mean and SEM). P-values: one-way ANOVA, Bonferroni multiple comparison test; *, $p<0.05$; **, $p<0.01$, ***, $p<0.001$. (F and G) Cells expressing GFP-tagged Epsin1 and Epsin1ΔUIM and F-MOR were imaged live using TIR-FM. Shown are representative examples showing the localization of GFP-Epsin1 (F) and GFP–Epsin1 ΔUIM (G). Scale bar = 5 μm.

# Chapter 5: “Ubiquitination in the first cytoplasmic loop of μ-opioid receptors reveals a hierarchical mechanism of lysosomal down-regulation”

Anastasia Henry generated constructs and contributed data to Figure 1C, Figure 3B, and Supplemental Table1B and to the experimental design. The majority of the experiments were conceived and executed by James Hislop in the von Zastrow lab. The manuscript was written by James Hislop, Anastasia Henry, and Mark von Zastrow.

## 5.1 Abstract

μ-Type opioid receptors (MORs) are members of the large seven-transmembrane receptor family which transduce the effects of both endogenous neuropeptides and clinically important opioid drugs. Prolonged activation of MORs promotes their proteolytic degradation by endocytic trafficking to lysosomes. This down-regulation process is known to contribute to homeostatic regulation of cellular opioid responsiveness, but mechanisms that mediate and control MOR down-regulation have not been defined. We show here that lysosomal down-regulation of MORs is ESCRT (endosomal sorting complex required for transport)-dependent and involves ubiquitin-promoted transfer of internalized MORs from the limiting endosome membrane to lumen. We also show that MOR down-regulation measured by conventional radioligand binding assay is determined specifically by ubiquitination in the first cytoplasmic loop. Surprisingly, we were unable to find any role of ubiquitination in determining whether internalized receptors recycle or are delivered to lysosomes. Instead, this decision is dictated specifically by the MOR C-tail and occurs irrespectively of the presence or absence of receptor ubiquitination. Our results support a hierarchical organization of discrete ubiquitin-independent and -dependent sorting operations, which function non-redundantly in the conserved down-regulation pathway to mediate precise endocytic control. Furthermore, they show that this hierarchical mechanism discriminates the endocytic regulation of naturally occurring MOR isoforms. Moreover, they are the first to reveal, we believe, for any seven-transmembrane receptor, a functional role of ubiquitination in the first cytoplasmic loop.

## 5.3 Introduction

μ-Opioid receptors (MOP-Rs or MORs) are members of the large family of seven-transmembrane signaling receptors (7TMRs) and mediate the physiological actions of endogenous opioid neuropeptides as well as clinically important opiate drugs (1, 2). MORs are extensively regulated after ligand-induced activation, producing long term changes in cellular opioid responsiveness that influence tolerance and dependence at the level of tissues and whole animals (3–5). The number and functional activity of surface-accessible MORs are regulated by ligand-induced endocytosis via clathrin-coated pits (6), but the functional consequences of MOR endocytosis depend critically on the molecular sorting of receptors after endocytosis. Receptor sorting into the recycling pathway restores the surface-accessible receptor pool and contributes to rapid recovery of cellular opioid responsiveness. Sorting of internalized receptors to lysosomes promotes proteolytic destruction of receptors, a process that is traditionally measured pharmacologically by a time-dependent down-regulation of the total number of ligand binding sites measured in cell or tissue extracts. This down-regulation process is associated with a prolonged attenuation, rather than recovery, of signaling. MOR trafficking in the recycling pathway has been studied in some detail (7), but essentially nothing is known about sorting operations mediating down-regulation of this 7TMR. The endocytic trafficking itinerary of many signaling receptors is determined by ubiquitin-dependent sorting from the endosome-limiting membrane to the lumenal membrane compartment of late endosomes/multivesicular bodies (8–10). Ubiquitin-directed sorting to the intralumenal compartment is mediated by the endosomal sorting complex required for transport (ESCRT), and ubiquitination is thought to primarily

determine whether many signaling receptors recycle or degrade after endocytosis (11–13). It is not known if ubiquitination plays any role in the endocytic sorting or down-regulation of MORs. Furthermore, ubiquitination plays a minor and dispensable role in down-regulating a close MOR paralogue, the δ-opioid receptor (DOR), even though these receptors traverse the canonical multivesicular body pathway (14–17). MORs have the particularly interesting feature that their endocytic trafficking between recycling and lysosomal pathways is regulated by a modular MOR regulatory sequence (MRS) (18, 19), which is present in the receptor distal C-terminal tail and differs across MOR isoforms due to alternate RNA splicing (20–22). The MRS present in the MOR1 variant specifically confers rapid recycling on internalized receptors and effectively inhibits receptor trafficking to lysosomes. It is not known if ubiquitination or the ESCRT machinery plays any role in determining the down-regulation of MORs, nor is it known what functional relationship might exist between these mechanisms and sorting controlled by the MRS.

The presently described study addressed these questions. We show that down-regulation of MORs indeed occurs by the canonical ESCRT-dependent pathway, and that MORs undergo agonist-stimulated ubiquitination which promotes sorting of receptors from the endosome limiting membrane to the lumenal compartment. We also establish the MOR as the first example of a 7TMR whose topological sorting by this mechanism is controlled specifically by ubiquitination in the first cytoplasmic loop. Interestingly, in contrast to the prevailing view, the ubiquitin-directed sorting step does not control the essential trafficking fate of internalized MORs. Instead, the ubiquitin-dependent step

functions independently and effectively downstream of a primary "recycling *versus* degradation" decision that does not require receptor ubiquitination and is determined by the C-terminal MRS. Furthermore, although the ubiquitin-dependent step is not required to direct internalized receptors to lysosomes or initiate their proteolysis, it plays a specific role in promoting subsequent destruction of the receptor opioid binding site. Accordingly, MORs have the remarkable ability to undergo endocytic delivery to lysosomes and incur substantial proteolytic fragmentation without losing the ability to specifically bind an opioid radioligand. This separation of sorting steps is biologically relevant because only the first step distinguishes the down-regulation properties of naturally occurring MOR isoforms. It may also impact the interpretation of studies of MOR regulation *in vivo* because the second step is rate-limiting for loss of radioligand binding sites as estimated by a traditional pharmacological assay of down-regulation.

## 5.3 Results

*MOR Down-regulates by Lysosomal Proteolysis Requiring the ESCRT*

We generated stably transfected cell lines expressing a FLAG epitope-tagged receptor construct (F-MOR, Fig. 1*A*) at moderate levels (supplemental Table 1). Agonist-induced down-regulation was assessed by radioligand binding assay using [$^3$H]DPN, which binds to MORs with high affinity and does not detect any endogenous receptors in untransfected HEK293 cells, by the standard method of determining specific binding at saturating concentration to estimate $B_{max}$. There was little change in net cellular F-MOR binding for ~2 h after the addition to the culture medium of 10 μm DADLE, an opioid peptide agonist that robustly promotes MOR endocytosis. However, a significant reduction of net binding sites was observed after longer agonist exposure (Fig. 1*B, filled squares*). Truncation of the distal 17 residues from the MOR cytoplasmic tail (F-MORΔ17), which removes the previously defined MRS promoting receptor recycling after short term agonist exposure (18), markedly accelerated agonist-induced down-regulation observed in the prolonged presence of DADLE (Fig. 1*B, open squares*). Thus, although MORs predominantly recycle after brief agonist-induced activation and endocytosis, they undergo significant down-regulation after prolonged stimulation, and the degree to which they do so is controlled by the previously described C-terminal MRS.

Agonist-induced down-regulation of F-MOR was inhibited by chloroquine, verifying that MORs indeed down-regulate by lysosomal proteolysis. Down-regulation was also inhibited by HRS overexpression, which disrupts ESCRT0 function, as well as by siRNA-mediated knockdown of the essential ESCRT1 component TSG101/hVPS23 (Fig.

1*C* and *inset*). Down-regulation of F-MORΔ17, assessed using the same manipulations (except at 5 rather than 8 h after agonist addition due to its substantially faster kinetics), exhibited the same dependence (Fig. 1*D*). Thus, pharmacological down-regulation of MORs requires the ESCRT machinery, and the C-terminal MRS controls the extent to which internalized MORs traverse the ESCRT-dependent down-regulation pathway after prolonged activation.

*Down-regulation Assessed Pharmacologically by Agonist-induced Loss of Radioligand Binding Requires MOR Ubiquitination*

To focus on whether down-regulation of MORs also involves receptor ubiquitination, we examined the effect of mutating all eight intracellular lysine residues in the background of mutant receptor lacking the C-terminal motif (F-MORΔ17–0cK, Fig. 2*A*). The F-MORΔ17 receptor construct was clearly ubiquitinated, and ubiquitin incorporation increased in an agonist-stimulated manner (Fig. 2*B*). Lysyl mutation prevented this ubiquitination, as verified by comparison of anti-ubiquitin and anti-receptor blots prepared from the corresponding anti-FLAG immunoprecipitates (Fig. 2, *C* and *D*, respectively). Interestingly, the most highly ubiquitinated MOR species were not detectable in the corresponding anti-FLAG (receptor) blot when exposed appropriately to resolve the major species of epitope-tagged receptor protein (indicated by the *bracket* in Fig. 2, *C* and *D*). Nevertheless, specific detection of these ubiquitinated species was verified by the lack of signal in the control (HEK293) lysate (*left lane* in each *panel*). This suggests that a small fraction of the total cellular receptor pool is highly ubiquitinated at any one time in intact cells. A similar observation has been made for other 7TMRS, including the DOR and β2 adrenergic receptor (16, 26, 27). In these

experiments relatively harsh extraction and washing conditions were used to assure dissociation of residual non-receptor ubiquitinated proteins (see "Experimental Procedures"). This caused immunopurified receptors to resolve by SDS-PAGE as higher order (dimeric and multimeric) species rather than as the primarily monomeric species detected in cell extracts prepared under more gentle conditions (compare Figs. 2*D* and 3*A*). Interestingly, radioligand binding assay indicated that preventing ubiquitination in this manner effectively blocked agonist-induced down-regulation measured by diprenorphine binding for both the MRS-truncated and full-length receptor constructs (*F-MORΔ17–0cK* and *F-MOR-0cK*, Figs. 2, *E* and *F*, respectively).

*Down-regulation Assessed Biochemically by Destruction of the Receptor Ectodomain Does Not Require MOR Ubiquitination*

Although loss of diprenorphine binding sites represents the traditional method for assaying MOR down-regulation, we sought to verify mutational effects on proteolytic destruction of receptors biochemically. To do so we assessed receptor proteolysis by loss of receptor protein detected in anti-FLAG immunoblots. F-MORs present in freshly prepared cell extracts resolved by SDS-PAGE with an apparent molecular mass ranging from ~50 to 60 kDa (Fig. 3*A*), consistent with the complex-glycosylated, monomeric receptor form shown previously to predominate in cell extracts freshly prepared in isoionic buffer and in the absence of ionic detergents (18). Only a small decrease of wild type receptor immunoreactivity was detected over a 5-h time course of DADLE exposure (*F-MOR*, Fig. 3*A*, *left panel*), consistent with the slow rate of down-regulation measured by radioligand binding (Fig. 1*B*). Truncating the C-terminal MRS markedly accelerated receptor proteolysis assessed biochemically (*F-MORΔ17*, Fig. 3*A*, *middle panel*), also as

expected from previous work (18) and consistent with the radioligand binding data (Fig. 1*B*). Surprisingly, a marked disconnect between pharmacological and biochemical measures was revealed when the effects of preventing receptor ubiquitination were examined. Whereas lysyl mutation strongly inhibited pharmacological down-regulation of the lysosome-targeted truncated mutant receptor, as assessed by radioligand binding (*F-MORΔ17–0cK*, Fig. 2*E*), it did not prevent proteolysis of receptors measured biochemically in parallel studies of the same receptor construct and the same stably transfected cell clones (Fig. 3*A*, the *right panel* shows a representative example). Quantification of multiple immunoblots further verified this observation (Fig. 3*D*, compare with Fig. 2*E*).

For some 7TMRS, preventing ubiquitination may increase recycling after agonist-induced endocytosis (26, 28, 29). To investigate if this is true for MORs, FLAG-tagged receptors were endocytosed by exposing cells to 10 μm DADLE for 30 min followed by recovery in the absence of agonist and subsequent measurement of surface receptor immunoreactivity. As shown previously, truncation of the MRS markedly inhibited recycling relative to the wild type MOR (compare MORΔ17 to MOR, *blue* and *black lines* in Fig. 3*B*, respectively). Interestingly, mutating all cytoplasmic lysine residues failed to cause any detectable increase of recycling from this inhibited level (MORΔ17–0cK, *red line*). These observations are fully consistent with the proteolysis data and support the hypothesis that MOR ubiquitination, although specifically important for efficient pharmacological down-regulation of receptors, does not play a major role in

determining the overall endocytic itinerary of MORs between recycling or lysosomal fates.

To verify and further investigate this unanticipated observation, we took advantage of the fact that the critical transition of internalized MORs from the early to late endocytic pathway can be monitored immunochemically by colocalization relative to EEA1 (early endosome) and LAMP1 (late endosome/lysosome) (18). We did so by focusing on the F-MORΔ17 construct (lacking the MRS) because this receptor is efficiently sorted for lysosomal down-regulation and restricted analysis to 90 min after DADLE application, before the occurrence of significant cleavage of the epitope tag (90 min, Fig. 3*A* and Ref. 18). As expected, both the ubiquitinated F-MORΔ17 and ubiquitination-defective F-MORΔ17–0cK constructs imaged by confocal fluorescence microscopy localized to EEA1-marked early endosomes 30 min after DADLE application as determined (supplemental Fig. 1,*A* and *B*). Importantly, both constructs clearly localized to LAMP1-positive late endosomes/lysosomes within 90 min (Fig. 3*C*, *iii* and *vi*; colocalized structures appear white in the merged image, and *arrows* indicate examples of colocalized structures). As another independent verification, we repeated this colocalization experiment using an antibody recognizing the receptor endodomain and obtained the same results (supplemental Figs. 1, *C* and *D*). Thus, despite the fact that ubiquitination is required for efficient receptor down-regulation as assessed by loss of radioligand binding, the ubiquitin-independent MRS appears to control the dominant sorting operation determining delivery of internalized receptors to the proteolytic compartment.

*Ubiquitination Controls Receptor Distribution between the Limiting Endosome Membrane and Lumen but Is Not Essential for Receptor Delivery to the Proteolytic Compartment*

Because MOR ubiquitination plays a specific and relatively late function in the down-regulation pathway, we next asked whether MORs undergo ubiquitin-dependent transfer to intralumenal membranes of endosomes. GFP-tagged versions of F-MORΔ17 and F-MORΔ17–0cK (F-MORΔ17-GFP and F-MORΔ17–0cK-GFP, respectively, Fig. 4, *A* and *B*) were co-expressed with constitutively active Rab5 (CFP-Rab5-Q79L) to enlarge endosomes and facilitate optical resolution of lumen from limiting membrane in living cells (17, 30), and cells were imaged live by spinning disc confocal microscopy after agonist treatment for 90 min. F-MORΔ17-GFP was resolved both in the limiting membrane and endosome lumen, and intralumenal localization of F-MORΔ17-GFP was quite uniform across individual endosomes (Fig. 4, *C* and *E*, supplemental Fig. 2*A*). F-MORΔ17–0cK-GFP localized prominently in the limiting endosome membrane, with most endosomes showing little intralumenal fluorescence (Fig. 4, *D* and *F*, supplemental Fig. 2*B*). GFP-tagged receptor distribution across numerous endosomes and experiments, quantified by line scan analysis (Figs. 4, *E–H*, *arrows* indicate positions of the limiting membrane), verified inhibited intralumenal localization of lysyl-mutant receptors (Fig. 4, *G* and *H*). Thus, despite the fact that MOR ubiquitination has no detectable effect on the primary recycling *versus* degradation sorting decision, it strongly affects the "limiting membrane *versus* lumen" localization of receptors. Thus, recycling *versus* degradation and limiting membrane *versus* lumen evidently represent discrete sorting operations,

which are hierarchically organized and controlled by distinct biochemical determinants (the MRS or ubiquitination, respectively).

*The Downstream Endocytic Sorting Operation Is Controlled Specifically by Ubiquitination in the First Cytoplasmic Loop*

Wild type MORs contain lysine residues in every intracellular domain, and the lysyl-mutant constructs tested so far were devoid of all cytoplasmic lysine residues. Thus, we asked if there is a particular cytoplasmic domain that is the critical site for ubiquitin-dependent control of MOR down-regulation and assessed the ubiquitin-dependent sorting operation quantitatively by monitoring down-regulation by radioligand binding. We first asked if ubiquitination of a particular cytoplasmic domain is sufficient to drive pharmacological down-regulation by systematically reverting arginine to lysine residues in each intracellular domain separately in the F-MORΔ17–0cK background (Fig. 5*A*). Restoring lysine residues in the first cytoplasmic loop was fully sufficient to produce agonist-induced down-regulation as measured by radioligand binding, whereas restoring lysine residues in any of the other cytoplasmic domains was not (Fig. 5*C*). To test if ubiquitination of the first cytoplasmic loop is necessary for pharmacological down-regulation, we conversely mutated (to arginine) only this loop in the F-MORΔ17 background (Fig. 5*B*). This mutation strongly inhibited pharmacological down-regulation of receptors (Fig. 5*D*) and did so to a degree indistinguishable from that of mutating all cytoplasmic lysine residues (compare the *second bar* in Fig. 5*D* to the *left bar* in Fig. 5*B*). Thus, the critical location for ubiquitin-dependent control of MOR down-regulation, defined by the location that is both necessary and sufficient for receptor down-regulation measured by radioligand binding, is the first cytoplasmic loop. Further arguing that this

represents a *bona fide* discrete sorting determinant, we also determined by live imaging that the first cytoplasmic loop is necessary and sufficient to promote receptor localization to the intralumenal compartment of endosomes (supplemental Fig. 3).

No previous study has mapped a functionally relevant site of ubiquitination to the first cytoplasmic loop of opioid receptors or, we believe, of any 7TMR. Thus, we asked whether this loop is actually ubiquitinated in intact cells and further investigated the specificity of this location by asking if MOR ubiquitination can occur also in other cytoplasmic domain(s). To do so we replaced lysine residues either in the first or second cytoplasmic loops in the F-MORΔ17–0cK background, making the respective loops the only potential ubiquitination sites in the receptor, and investigated ubiquitination of mutant receptors biochemically using immunoblotting. Introducing lysine residues only in the first loop of the F-MORΔ17–0cK background restored both basal receptor ubiquitination and the agonist-dependent increase that is characteristic of the wild type receptor. Introducing lysine residues only in the second cytoplasmic loop restored significant basal receptor ubiquitination but did not restore its agonist-dependent stimulation (Fig. 5, *E* and *H*, show examples of anti-ubiquitin and anti-FLAG loading control blots, respectively, and Fig. 5, *F* and *G*, show the quantification across multiple experiments). These results, combined with the observation that lysine residues in the first but not second loop are sufficient to confer ubiquitin-dependent control on the downstream sorting event required for pharmacological down-regulation (Fig. 5*C*), indicate that MOR ubiquitination is not restricted to the first loop but that ubiquitination in this domain is specifically agonist-regulated and critical for controlling receptor sorting in the down-regulation pathway.

*Relevance to Naturally Occurring MOR Isoforms*

To begin to investigate the physiological significance of MOR ubiquitination in the first loop, we asked whether this post-translational modification controls the down-regulation of naturally occurring receptors. The μ-opioid receptor gene (Oprm1) transcript is subject to alternative splicing that generates structurally distinct MOR variants. The predominant MOR expressed in the rodent brain is MOR1 (corresponding to the MOR construct examined so far in the present study). MOR1B is another variant that is functional and natively expressed (21–23). Interestingly, MOR1B has an identical first cytoplasmic loop as MOR1 but a different C-terminal sequence and, accordingly, lacks the particular MRS present in MOR1. This structural difference was shown previously to selectively drive endocytic delivery of MOR1B to lysosomes (23), and we verified this effect in the present study using the immunoblot assay. Because MOR1B is a naturally expressed receptor for which differential sorting to the lysosome pathway is already known to produce significant functional consequences, we asked if ubiquitination of the first cytoplasmic loop is also relevant to its down-regulation. Indeed, lysyl mutation of only the first cytoplasmic loop in MOR1B clearly inhibited pharmacological down-regulation of receptors measured by radioligand binding assay (Fig. 6*A*). Interestingly, despite clear biochemical and functional evidence for significant differences in the endocytic sorting of MOR1 relative to MOR1B between recycling and lysosomal fates (as shown previously (23) and verified here), the down-regulation of these isoforms as estimated by radioligand binding was remarkably similar (Fig. 6*B*). This indicates that ubiquitination of the first cytoplasmic loop is required for (and apparently rate-limiting in) pharmacological down-regulation of both MOR isoforms, as defined by the traditional

pharmacological criterion of loss of opiate radioligand binding. Importantly, and as revealed initially by truncation of the MOR1 C-tail, this ubiquitin-dependent sorting operation functions effectively downstream of the (ubiquitin-independent) MRS. Thus, ubiquitination of the first loop plays a shared and highly specific role in pharmacological down-regulation but is not the primary means by which the biochemically and functionally divergent endocytic trafficking itineraries of these naturally occurring receptor isoforms are determined.

## 5.3 Discussion

Prolonged activation is well known to attenuate cellular opioid responsiveness by inducing proteolytic destruction of opioid receptors through endocytic trafficking to lysosomes. However, mechanisms that mediate and control this fundamental process of homeostatic regulation remain poorly understood. The present results provide several pieces of mechanistic insight. First, the present data establish an essential role of the ubiquitin-ESCRT system in mediating MOR down-regulation and show that this system promotes the efficient transfer of receptors from the limiting to intralumenal membranes of late endosomes. Second, the results show that MOR ubiquitination is specifically required for agonist-induced down-regulation of receptors as determined by loss of radioligand binding. In particular, we show that disrupting MOR ubiquitination has no effect on proteolysis of the N-terminal receptor ectodomain, on delivery of receptors to the late endocytic pathway, or on the specificity of receptor trafficking via the recycling pathway. Together with previous evidence suggesting that the binding site for alkaloid radioligands is located predominantly within the transmembrane helices (31), these observations suggest that MOR ubiquitination, by driving topological sorting to intralumenal membranes, specifically promotes destruction of the transmembrane helical bundle without dictating the overall endocytic fate of receptors. Third, the present results establish a precedent for 7TMR regulation through modification of the first cytoplasmic loop. Studies of other 7TMRs suggest that the location of receptor ubiquitination is not critical for regulation (32) or place the site of ubiquitination within the C-tail (33–35) or third cytoplasmic loop (36, 37). We show that ubiquitination specifically of the first cytoplasmic loop is both necessary and sufficient for pharmacological down-regulation of

MORs and for receptor transfer to the endosome lumen even though ubiquitination of receptors is not restricted to this cytoplasmic domain. To our knowledge the present results are the first to establish a specific regulatory function of ubiquitination in the first cytoplasmic loop of a 7TMR.

According to the prevailing view of ESCRT-dependent down-regulation, ubiquitination of signaling receptors mediates the primary sorting operation determining whether they recycle or traffic to lysosomes after endocytosis (8–10). Here we show that MOR down-regulation indeed requires the conserved ESCRT machinery, and that MOR ubiquitination controls topological sorting in endosomes. Interestingly, however, our results clearly show that ubiquitination of MORs is not essential for, and does not determine, the primary sorting decision controlling the delivery of internalized receptors to the proteolytic compartment. Instead, the primary endocytic itinerary of MORs after prolonged agonist exposure is determined by an ubiquitin-independent C-tail sequence (the MRS), which was shown previously to drive MOR recycling after endocytosis induced by short term agonist activation (18, 19). Thus, the mechanism of MOR down-regulation can be understood in terms of hierarchical organization of discrete ubiquitin-dependent and -independent steps, which function in sequence in the same pathway, and which are both required for complete receptor destruction (Fig. 6*C*). The ubiquitin-independent step is determined by the previously defined C-tail motif, functions effectively upstream, and determines the ultimate trafficking fate of the receptor, either recycling or delivery to the lysosome. The ubiquitin-dependent step operates effectively downstream in the same pathway and determines how efficiently the receptor is

transferred to intralumenal membranes of endosomes; this topological sorting operation promotes destruction of the receptor hydrophobic core and, hence, loss of radioligand binding activity.

We note that there is growing evidence that, at least in mammalian cells, topological transfer to intralumenal vesicles is not an absolute requirement either for sorting of signaling receptors to lysosomes or for subsequent proteolytic down-regulation (38, 39). We also note that a similar separation of steps was proposed previously for the related DOR (17). However, for this 7TMR, a structural determinant(s) has not yet been clearly identified for either sorting operation. Furthermore, whereas complete down-regulation of DORs (including destruction of the ligand binding site) can occur with nearly wild type efficiency when DOR ubiquitination is prevented by lysyl mutation (16), proteolysis of MORs is effectively stalled at an intermediate state when receptor ubiquitination is similarly prevented. Accordingly, MORs provide the first example of how receptor sorting between recycling and degradative itineraries and the process of lysosomal destruction itself are separately controlled by discrete yet sequential ubiquitin-independent and -dependent sorting operations.

Together our results support the conclusion that the mechanism directing ESCRT-dependent lysosomal down-regulation of opioid receptors is hierarchical and involves the function of at least two discrete and non-redundant molecular sorting operations. They also emphasize the importance of future work to better define the biochemical machinery mediating the upstream (ubiquitin-independent) sorting operation and to investigate the

physiological significance of hierarchical organization as revealed in the present study. In principle, each of the sorting operations in this hierarchy represents a discrete control point, and the present data clearly resolve distinct biochemical determinants mediating each. Thus, we anticipate that selective control of each may occur *in vivo*, and there may exist different functional consequences of driving one operation relative to the other. Although much of the work leading to the present understanding of hierarchical MOR sorting emerged from the study of truncated mutant receptors lacking the C-tail MRS, the present results also provide evidence that our findings are relevant to the regulation of naturally expressed receptors. This was demonstrated by comparison of two naturally occurring MOR isoforms, MOR1 and MOR1B, which result from alternative splicing of the same receptor transcript. Both of these natural receptor isoforms possess the same first loop sequence but differ in the region of the C-tail controlling the upstream sorting operation. These isoforms are known to differ markedly in their endocytic itinerary, trafficking preferentially through the recycling pathway (MOR1) or to lysosomes (MOR1B), as established previously both by biochemical analysis of receptor proteolysis and by functional assay of cellular opioid responsiveness (23). Nevertheless, when down-regulation was assessed pharmacologically using the conventional radioligand binding assay, distinct regulation of these MOR isoforms was difficult if not impossible to discern (Fig. 6*B*). This is fully consistent with the hierarchical sorting model and with the ubiquitin-dependent step occurring downstream (and shared by both receptor isoforms) being rate-limiting for destruction of the ligand binding site. Thus, the present results, in addition to providing new insight to the mechanistic basis of MOR down-regulation and identifying the first example of functionally significant regulation mediated by

ubiquitination of the first cytoplasmic loop, have potentially important implications for interpreting *in vivo* studies. In particular, they suggest that the traditional radioligand assay of receptor down-regulation, as widely used in studies of opioid effects *in vivo* and in various *ex vivo* preparations, may underestimate the occurrence of lysosomal trafficking as a cellular mechanism of opioid regulation. Moreover, they reveal a previously unappreciated layer of control in MOR endocytic trafficking, whose elucidation may reveal new targets for therapeutic manipulation of the endogenous opioid system.

## 5.5 Acknowledgements

We gratefully acknowledge Kurt Thorn and the Nikon Imaging Center at University of California, San Francisco, for advice and access to equipment used for live imaging experiments. We thank Graeme Cottrell for advice on the ubiquitination blots, Ben Lauffer for sharing opioid receptor antibody, Michael Tanowitz for valuable discussions, and Adriano Marchese, Harald Stenmark, and Marino Zerial for essential constructs.

## 5.6 Materials and Methods

*Cell Culture, cDNA Constructs, and Transfection*

GFP-tagged Rab5 cDNA was a gift from Marino Zerial (Max Planck Institute of Molecular Cell Biology and Genetics), and the Q79L mutation was generated by site-directed mutagenesis (Stratagene), with the respective coding sequences cloned into pECFP-N1. The MycHRS expression plasmid was a gift from Harold Stenmark (Norwegian Radium Hospital). The N-terminal FLAG-tagged murine MOR1 μ-opioid receptor construct (F-MOR), recycling impaired C-terminal truncation (F-MORΔ17), and MOR1B splice variant (F-MOR1B) have been previously described (18, 23). Lysine-mutant versions (F-MOR-0cK and the F-MORΔ17–0cK) and subsequent single loop mutants as indicated were generated using QuikChange site-directed mutagenesis (Stratagene). Mutated cDNAs were cloned into pcDNA3 (Invitrogen), and sequences were verified by dideoxynucleotide sequencing (ElimBio). F-MORΔ17-GFP, F-MORΔ17–0cK-GFP, F-MORΔ17-K94R,K96R-GFP, and F-MORΔ17–1st loop K-GFP fusion proteins were constructed by amplifying the respective coding sequence by polymerase chain reaction (PCR), with an AgeI restriction site incorporated into the reverse primer. PCR products were then ligated in-frame in pEGFP-N1 (Clontech). All cDNA constructs were verified by sequencing (ElimBio). Stably transfected cells expressing epitope tagged receptors were generated by selection by neomycin resistance using 500 μg/ml G418 (Geneticin, Invitrogen). Resistant colonies were clonally isolated and selected for further study based on comparable levels of receptor expression as assessed by fluorescence microscopy and saturation binding analysis (supplemental Table 1). HEK293 cells (ATCC) were maintained in Dulbecco's modified Eagle's medium

(DMEM) supplemented with 10% fetal bovine serum (University of California, San Francisco, Cell Culture Facility). For transient expression, cells were transfected using Lipofectamine 2000 (Invitrogen) according to the manufacturer instructions. Cells expressing FLAG-tagged receptors were harvested by washing with EDTA and plated in 60-mm dishes at 80% confluency before transfection with plasmid DNA. Cells were reseeded into poly-lysine-coated 6- or 12-well plates and cultured for a further 24 h before experimentation. Transfection of cells with RNAi duplexes to Tsg101 (15) was achieved using Lipofectamine RNAiMax (Invitrogen) according to the manufacturer's instructions. Cells were transfected at 50% confluency, and experiments were performed 72 h post-transfection.

*Biochemical Detection of Receptor Proteolysis and Protein Levels by Immunoblotting*

Immunoblotting to assess total cellular receptor levels was carried out as previously described. Briefly, cell monolayers were washed 3 times in ice-cold phosphate-buffered saline (PBS) and lysed in extraction buffer (0.5% Triton X-100, 150 mm NaCl, 25 mm KCl, 25 mm Tris, pH 7.4, 1 mm EDTA) supplemented with a standard protease inhibitor mixture (Roche Applied Science). Extracts were clarified by centrifugation (12,000 × *g* for 10 min) and then mixed with SDS sample buffer for denaturation. Proteins present in the extracts were resolved by SDS-PAGE using 4–12% Bis-Tris gels (NuPAGE, Invitrogen), transferred to nitrocellulose membranes, and probed for protein by immunoblotting using anti-FLAG-M1 (Sigma) and horseradish peroxidase-conjugated sheep anti-mouse IgG (GE Healthcare Life Sciences) and SuperSignal detection reagent (Pierce). Apparent molecular mass was estimated using commercial protein standards

(SeeBlue Plus2, Invitrogen). Band intensities of unsaturated immunoblots were analyzed and quantified by densitometry using FluorChem 2.0 software (AlphaInnotech Corp.).

*Biochemical Detection of Receptor Ubiquitination*

Cells were plated in 10-cm dishes and then treated before being lysed on ice in 100 μl of 10 mm Tris, pH 7.4, 1% SDS, 10 mm iodoacetamide, and protease inhibitor mixture (Roche Applied Science). The lysate was then diluted with 400 μl of extraction buffer (see above), and samples were sonicated for 5 s at a 30% duty cycle. The extract was then clarified by centrifugation (12,000 × *g* for 10 min), and the supernatant was passed through a Qia-shredder column (Qiagen) at 3000 rpm for 60 s. Another 500 μl of extraction buffer was then added to give a final volume of 1 ml and then incubated overnight at 4 °C with 2 μg of M2 anti-FLAG antibody (Sigma). 30 μl of protein A/G-agarose (Pierce) was added for 2 h at 4 °C. Immunoprecipitates were collected by centrifugation (3000 rpm, 1 min, 4 °C) and washed 3 times with 500 μl of extraction buffer before the addition of 20 μl of SDS sample buffer (Invitrogen) supplemented with β-mercaptoethanol and analysis by Western blotting using anti-ubiquitin (P4D1, Santa Cruz). Blots were then stripped (Restore Western Blot Stripping Buffer, Pierce) and reprobed with anti-FLAG M2-HRP (Sigma) to verify equal receptor levels.

*Analysis of Receptor Levels by Radioligand Binding*

Receptor down-regulation was determined by radioligand binding as previously described (16). After transfection, HEK293 cells stably expressing FLAG-tagged receptors were re-plated into 12-well plates. 24 h later 10 μm d-Ala-d-Leu-enkephalin (DADLE) was added to the cells for the indicated time period, cells were washed twice with ice-cold PBS, and 300 μl of PBS was added to the cells, and the plates were frozen.

Plates were thawed, and cells were resuspended. Binding assays were performed in triplicate in 96-well plates using 10 nm of the radiolabeled opioid receptor antagonist [$^3$H]diprenorphine (DPN) (Amersham Biosciences, 88 Ci/mmol), a saturating concentration that is sufficient to access both surface and internal receptors under these conditions, and incubated for 1 h at room temperature. Incubations were terminated by vacuum filtration through glass fiber filters (Whatman), and unbound radioligand was removed by repeated washes with TBS. Bound radioactivity was determined by liquid scintillation counting of washed filters. Nonspecific binding, determined by carrying out parallel determinations in the presence of excess unlabeled competitive antagonist (10 μm naloxone), was <10% of specific. In all assays we verified that bound diprenorphine was <10% of the total added to the assay. Data presented represent the specific binding (total minus nonspecific binding) at each time point, expressed as a percentage of specific binding in similarly transfected, but agonist naive cells.

*Fluorescence Microscopy*

Colocalization of receptors with early endosomes or lysosomes was visualized using HEK293 cells stably expressing the indicated FLAG-tagged receptor constructs plated on poly-lysine-coated glass coverslips (Corning). Cells were incubated in the presence of 10 μm DADLE for 30 or 90 min before fixing with 4% formaldehyde and permeabilizing with 0.1% Triton X-100 in PBS. Cells were labeled using rabbit anti-FLAG (Sigma) and mouse antibodies recognizing either EEA1 (BD Biosciences) or LAMP-1 and -2 (Santa Cruz Biotechnology). Localization was confirmed using a MOR antibody (generated in rabbits against a previously described GST fusion of the MOR C-terminal tail (24)), with injections and bleeds carried out according to approved procedures (Josmine

Laboratories, Napa, CA). Immunolabeling was detected using Alexa488-conjugated anti-mouse and Alexa594 anti-rabbit secondary antibodies (Invitrogen). Specimens were imaged by laser-scanning confocal fluorescence microscopy using a Zeiss LSM 510 microscope fitted with a Zeiss 63 × NA1.4 objective, with standard excitation laser lines and emission filter sets verified for lack of detectable cross-channel bleed-through and confocality achieved using a 1 Airy disc pinhole in the emission light path. Acquired optical sections were analyzed with LSM Image Examiner (Zeiss) and rendered with Adobe Photoshop software.

*Spinning-disk Confocal Microscopy and Live Image Analysis*

The extent of receptor involution was visualized using HEK293 cells transiently transfected with the indicated N-terminal FLAG-tagged, C-terminal GFP-tagged receptor constructs plated onto poly-lysine-coated glass coverslips (Corning Glass). Cells were incubated in the presence of 10 μm DADLE for 90 min before imaging. Cells were imaged in DMEM without Phenol Red supplemented with 1% fetal bovine serum (University of California, San Francisco Cell Culture Facility) and including 30 mm Hepes adjusted to pH 7.4. Live cell imaging was performed using a Yokogawa CSU22 Spinning Disk Confocal (Solamere Technology Group) interfaced to a Nikon TE2000U inverted microscope using a 100 × 1.49 NA TIRF objective and fiber-coupled 488-nm argon laser (Coherent) for excitation. Time-lapse sequences were acquired at a continuous rate of 5 frames/s, and the acquired images were analyzed with Image J software (Wayne Rasband, National Institutes of Health, Bethesda, MD). To quantify the extent of receptor involution, measurements were conducted on raw data of individual endosomes as previously described (17). To minimize the influence of out-of-plane

fluorescence from the limiting membrane (in the *z* axis), only mid-focal plane images of endosomes with a diameter of >3 μm were analyzed. For each optical section, straight-line selections were drawn across the diameter, and pixel intensities across the line were measured. Endosomal diameter was normalized to account for endosomes varying in size. The pixel numbers with the first and second maximum pixel intensities, corresponding to pixels on the limiting membrane of the endosome, were normalized to 0 and 100, respectively. The location across the line of pixel 0 was then subtracted from each pixel situated on the line, and this value was divided by the total diameter (in pixels) of the endosome. This generated normalized pixel distances corresponding to distance across the line occupied by each pixel, expressed as a percentage. Average background fluorescence was subtracted from raw pixel intensity values. The pixel intensities for the pixel numbers normalized to 0 and 100 were also normalized to 0 and 100, respectively, generating normalized fluorescence values. The background-corrected pixel intensity values corresponding to pixels that lay 40–60% across the endosomal diameter were averaged, generating a middle fluorescence value for each endosome. Middle fluorescence values were compiled across multiple cells, and the mean values quantified for each condition are shown. Representative live images shown were rendered using Adobe Photoshop software.

*Flow Cytometric Analysis of Internal and Recycled Receptors*

Fluorescence flow cytometry was used to quantify internalization and recycling of receptors by measuring cell surface fluorescence, as previously described (25). Briefly, stably transfected cells were treated for 30 min with 10 μm DADLE (internalization) before placing on ice or washing and returning to 37 °C for 45 min in the presence of

Naloxone (recycling). Cells were then washed and lifted with ice-cold PBS and incubated with Alexa647-conjugated M1 anti-FLAG antibody (Molecular Probes). Fluorescence intensity was measured using a FACSCalibur (BD Biosciences), counting 10,000 cells/sample in duplicate. Recycling was determined from surface fluorescence (F) as follows $(F_{\text{naloxone}} - F_{\text{DADLE}})/(F_{\text{untreated}} - F_{\text{DADLE}}) \times 100$.

*Statistical Analysis*

Quantitative data were averaged across multiple independent experiments, with the number of experiments specified in the corresponding figure legend. Unless indicated otherwise, *error bars* represent the S.E. determined after compiling mean determinations across experiments. The statistical significance of the indicated differences was analyzed using the appropriate variations of one or two-way ANOVA and post-test or Student's *t* test as specified in the figure legends, calculated using Prism 4.0 software (GraphPad Software, Inc.). The relative significance of each of the reported differences is specified by calculated *p* values that are also listed in the figure legends and annotated graphically in the figures.

## 5.7 References

1. Walwyn, W. M., Miotto, K. A., and Evans, C. J. (2010) *Drug Alcohol Depend.* 108, 156–165

2. Kieffer, B. L., and Evans, C. J. (2009) *Neuropharmacology* 56, 205–212

3. Koch, T., and Höllt, V. (2008) *Pharmacol. Ther.* 117, 199–206

4. Martini, L., and Whistler, J. L. (2007) *Curr. Opin Neurobiol.* 17, 556–564

5. Williams, J. T., Christie, M. J., and Manzoni, O. (2001) *Physiol. Rev.* 81, 299–343

6. von Zastrow, M., Svingos, A., Haberstock-Debic, H., and Evans, C. (2003) *Curr. Opin. Neurobiol.* 13, 348–353

7. Hislop, J. N., and von Zastrow, M. (2011) *Traffic* 12, 137–148

8. Roxrud, I., Stenmark, H., and Malerød, L. (2010) *Biol. Cell* 102, 293–318

9. Raiborg, C., and Stenmark, H. (2009) *Nature* 458, 445–452

10. Hurley, J. H., and Hanson, P. I. (2010) *Nat. Rev. Mol. Cell Biol.* 11, 556–566

11. Saksena, S., Sun, J., Chu, T., and Emr, S. D. (2007) *Trends Biochem. Sci.* 32, 561–573

12. Katzmann, D. J., Odorizzi, G., and Emr, S. D. (2002) *Nat. Rev. Mol. Cell Biol.* 3, 893–905

13. Marchese, A., Paing, M. M., Temple, B. R., and Trejo, J. (2008) *Annu. Rev. Pharmacol. Toxicol.* 48, 601–629

14. Tanowitz, M., and Von Zastrow, M. (2002) *J. Biol. Chem.* 277, 50219–50222

15. Hislop, J. N., Marley, A., and Von Zastrow, M. (2004) *J. Biol. Chem.* 279,

22522–22531

16. Hislop, J. N., Henry, A. G., Marchese, A., and von Zastrow, M. (2009)

(2011) *Traffic* 12, 170–184

18. Tanowitz, M., and von Zastrow, M. (2003) *J. Biol. Chem.* 278,

45978–45986

19. Thompson, D., Pusch, M., and Whistler, J. L. (2007) *J. Biol. Chem.* 282,

29178–29185

20. Pasternak, G. W. (2004) *Neuropharmacology* 47, 312–323

21. Koch, T., Schulz, S., Pfeiffer, M., Klutzny, M., Schröder, H., Kahl, E., and

Höllt, V. (2001) *J. Biol. Chem.* 276, 31408–31414

22. Koch, T., Schulz, S., Schröder, H., Wolf, R., Raulf, E., and Höllt, V. (1998)

*J. Biol. Chem.* 273, 13652–13657

23. Tanowitz, M., Hislop, J. N., and von Zastrow, M. (2008) *J. Biol. Chem.* 283,

35614–35621

24. Whistler, J. L., Enquist, J., Marley, A., Fong, J., Gladher, F., Tsuruda, P.,

Murray, S. R., and Von Zastrow, M. (2002) *Science* 297, 615–620

25. Hanyaloglu, A. C., McCullagh, E., and von Zastrow, M. (2005)*EMBOJ.* 24,

2265–2283

26. Jacob, C., Cottrell, G. S., Gehringer, D., Schmidlin, F., Grady, E. F., and

Bunnett, N. W. (2005) *J. Biol. Chem.* 280, 16076–16087

27. Shenoy, S. K., McDonald, P. H., Kohout, T. A., and Lefkowitz, R. J. (2001)

*Science* 294, 1307–1313

28. Chen, L., and Davis, N. G. (2002) *Traffic* 3, 110–123

29. Berthouze, M., Venkataramanan, V., Li, Y., and Shenoy, S. K. (2009) *EMBO J.* 28, 1684–1696

30. Wegner, C. S., Wegener, C. S., Malerød, L., Pedersen, N. M., Progida, C., Prodiga, C., Bakke, O., Stenmark, H., and Brech, A. (2010) *Histochem. Cell Biol.* 133, 41–55

31. Mansour, A., Taylor, L. P., Fine, J. L., Thompson, R. C., Hoversten, M. T., Mosberg, H. I., Watson, S. J., and Akil, H. (1997) *J. Neurochem.* 68, 344–353

32. Cottrell, G. S., Padilla, B., Pikios, S., Roosterman, D., Steinhoff, M., Gehringer, D., Grady, E. F., and Bunnett, N. W. (2006) *J. Biol. Chem.* 281, 27773–27783

33. Marchese, A., and Benovic, J. L. (2001) *J. Biol. Chem.* 276, 45509–45512

34. Liang, W., Hoang, Q., Clark, R. B., and Fishman, P. H. (2008) *Biochemistry* 47, 11750–11762

35. Hicke, L., and Riezman, H. (1996) *Cell* 84, 277–287

36. Martin, N. P., Lefkowitz, R. J., and Shenoy, S. K. (2003) *J. Biol. Chem.* 278, 45954–45959

37. Xiao, K., and Shenoy, S. K. (2011) *J. Biol. Chem.* 286, 12785–12795

38. Pons, V., Luyet, P. P., Morel, E., Abrami, L., van der Goot, F. G., Parton, R. G., and Gruenberg, J. (2008) *PLoS Biol.* 6, e214

39. Futter, C. E., Collinson, L. M., Backer, J. M., and Hopkins, C. R. (2001) *J. Cell Biol.* 155, 1251–1264

# 5.8 Figures

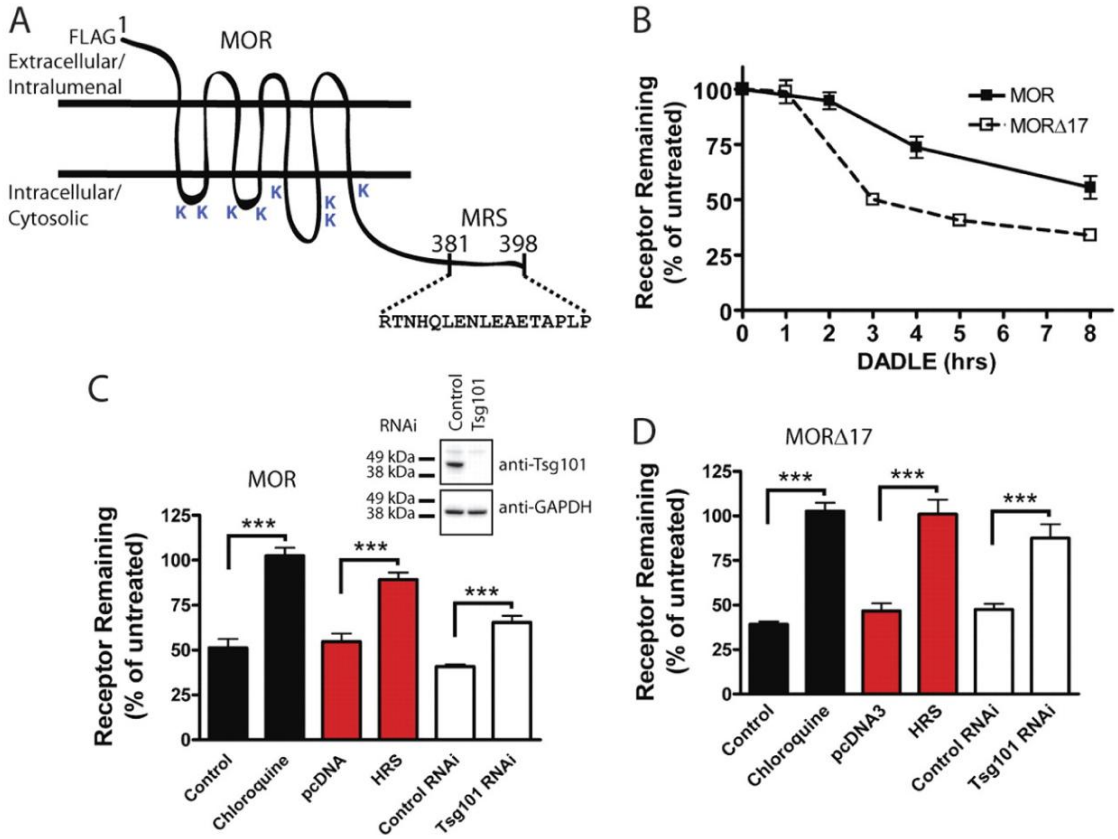


**Figure 1. Both MOR and MORΔ17 undergo ESCRT-dependent down-regulation by lysosomes.** A) Shown is a diagrammatic representation of the F-MOR and F-MORΔ17 constructs, indicating the location of cytoplasmic lysine residues and the previously identified MRS. B) Shown is the time course of the down-regulation of F-MOR and F-MORΔ17. HEK293 cells stably expressing either receptor were incubated at 37 °C with 10μM DADLE for the indicated time period, and then radioligand binding assay was carried out using the high affinity radiolabeled opioid antagonist [3H]DPN at 10 nM to estimate Bmax, as described under "Experimental Procedures." Data points represent specific binding of [3H]DPN measured at each time point, expressed as a percentage of the specific binding in cells not exposed to agonist. Points represent mean determinations from independent experiments, with each time point analyzed in triplicate tubes in each experiment. *Error bars* represent the S.E. calculated across the experiments (*n* _ 3–5). C and D) Shown is the effect of the indicated experimental manipulations on DADLE-induced down-regulation of F-MOR (*panel C*) and F-MORΔ17 (*panel D*) in stably transfected

HEK293 cells. Cells were transfected with “empty” pcDNA3 or pcDNA3-HRS (*red bars*) or transfected with control (scrambled) siRNA or siRNA targeting TSG101 (*white bars*). A final set of cells was pretreated with 200 μM chloroquine for 20 min before the start of the experiment (*black bars*). Cells were then left untreated or exposed to 10 μM DADLE for 5 h (F-MORΔ17, *panel D*) or 8 h (F-MOR, *panel C*), chosen according to the different down-regulation kinetics of these constructs, before carrying out the radioligand binding assay using 10 nM [3H]DPN. *Bars* represent the specific binding detected after agonist treatment, expressed as a percentage of that detected to identically manipulated cells except not exposed to agonist. In each experiment binding was determined in triplicate tubes. *Bars* represent average determinations, and *error bars* S.E., across multiple experiments ($n$=3–6; ***, $p$=0.001, two way ANOVA). The *inset* shows correlative immunoblot data verifying Tsg101 depletion by the siRNA.

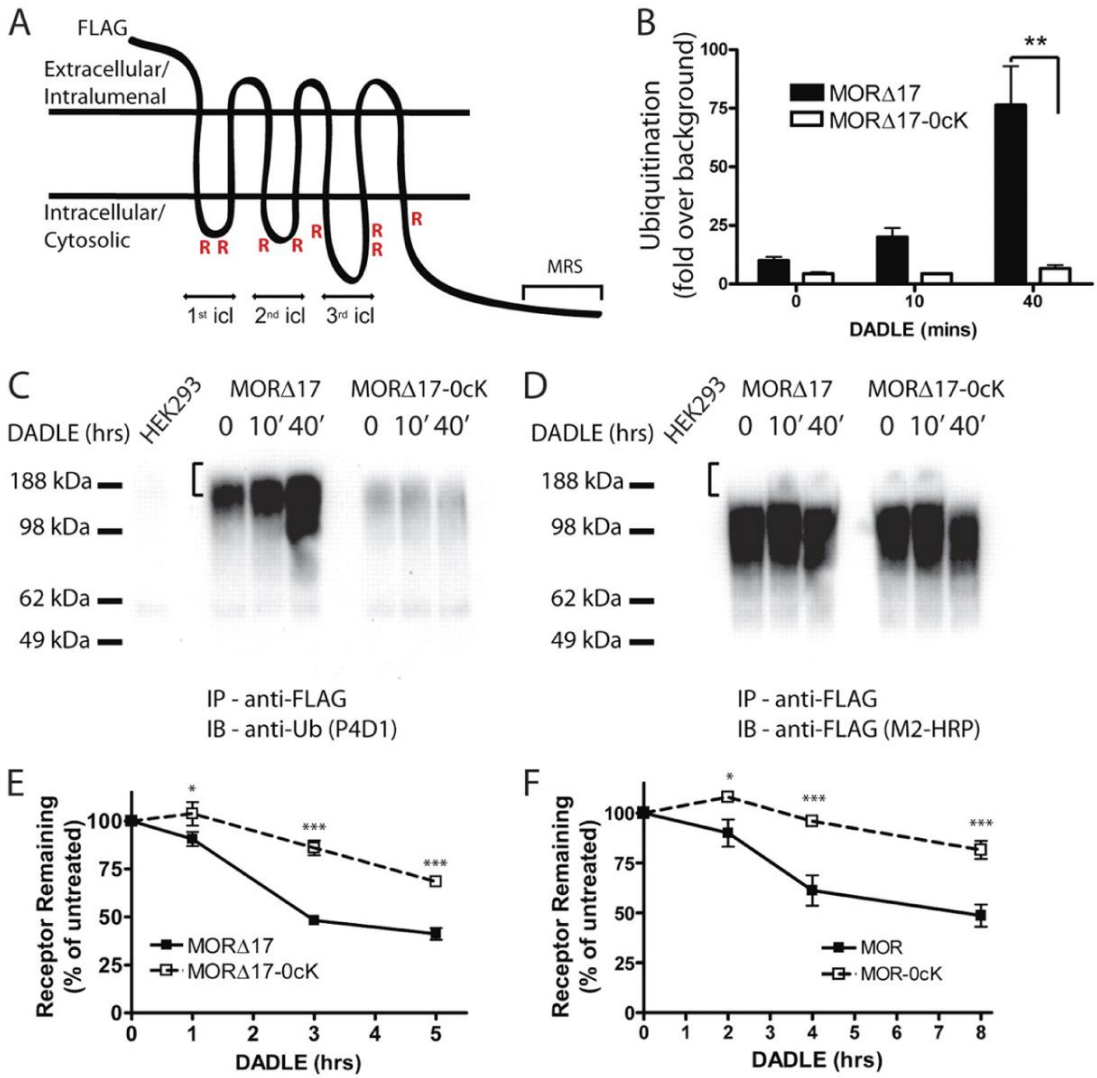


**Figure 2. MOR down-regulation measured radioligand binding requires receptor ubiquitination.** A) Shown is a diagram of the F-MOR-0cK construct indicating cytoplasmic domains containing the Lys → Arg mutation (*R*) as well as the MRS that is devoid of lysine residues. *icl*, cytoplasmic loop. B) Shown is a densitometric analysis of ubiquitin incorporation into the F-MORΔ17 and the lysyl-mutant F-MORΔ17–0cK, assessed after immunopurification of receptors in the presence of SDS. Data shown represent the mean and S.E. of densitometry from anti-ubiquitin immunoblot analysis carried out in $n = 3$ independent experiments. Scanning densitometry was carried out in the linear range and is expressed as -fold over background (defined by nonspecific signal detected in parental HEK293 cells not expressing the indicated FLAG-tagged receptor). C) A representative anti-ubiquitin immunoblot (*IB*) from the analysis summarized in *panel B*; *IP*, immunoprecipitate. D) Shown is the same blot as in *panel C*, except it was stripped and

reprobed with anti-FLAG to verify comparable loading and transfer of immunopurified receptors. E and F) Shown is the effect of the indicated lysyl mutations on DADLE-induced down-regulation. HEK293 cells stably expressing F-MORΔ17 or F-MORΔ17–0cK (*panel E*) or F-MOR or F-MOR-0cK (*panel F*) were exposed to 10 μm DADLE for the indicated time period before estimating $B_{max}$ by radioligand binding to [$^3$H]DPN. Points represent specific binding at each time point, expressed as a percentage of the specific binding in cells not exposed to agonist. In each experiment triplicate tubes were analyzed; points represent averages and *error bars* S.E. across experiments ($n$ = 4; *, $p < 0.05$; ***, $p < 0.001$, two way ANOVA).

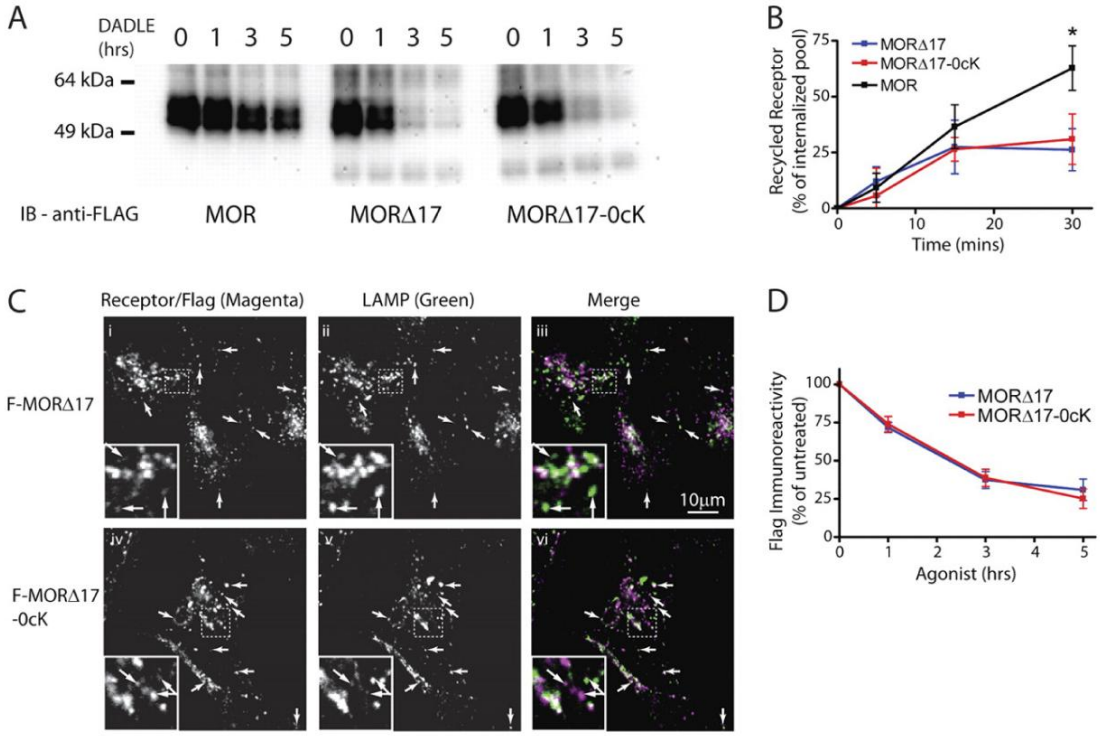


**Figure 3. MOR trafficking to lysosomes, assessed biochemically or immunochemically, does not require receptor ubiquitination and is dictated by the C-tail.** A) Representative anti-FLAG immunoblots (from three-six independent experiments) show the effects of exposing cells to 10 μm DADLE for the indicated time period on FLAG-tagged receptor signal detected in cell extracts. Stably transfected HEK293 cells initially expressing similar levels of F-MOR (*left*), F-MORΔ17 (*middle*), or F-MORΔ17–0cK (*right*) were analyzed. *Numbers above each lane* indicate the time period of DADLE incubation in hours. B) Shown is a comparison of recycling between F-MOR (*black*) F-MORΔ17 (*blue*) and F-MORΔ17–0cK (*red*). Stably transfected cells expressing the indicated receptor construct were incubated for 30 min in the presence of 10 μm DADLE to drive endocytosis and then washed and incubated

at 37 °C in the presence of 10 μm naloxone for the indicated times before surface labeling of Alexa647-conjugated M1 anti-FLAG and quantifying surface receptor immunoreactivity by flow cytometry. Displayed are the proportion of internalized receptors that recovered to the plasma membrane at the indicated time point after agonist washout, calculated as described under "Experimental Procedures" (mean ± S.E., $n$ = 3–4; *, $p < 0.05$, two-way ANOVA, Bonferroni post-test). C) Shown are representative confocal micrographs showing the localization of F-MORΔ17 (*i*–*iii*) or F-MORΔ17–0cK (*iv*–*vi*) relative to LAMP1/2 immunoreactivity in stably transfected HEK293 cells fixed after exposure to 10 μm DADLE for 90 min. Merged images (*iii* and *vii*) display receptor and LAMP channels pseudocolored in *green* and *magenta*, respectively, with areas of colocalization appearing *white. Insets* show a magnified region of the image as illustrated by the *dotted box. Arrows* indicate puncta that appear to be only single colors due to differences in relative intensity of one or the other label but are in colocalized when examined at the level of individual images. D) Quantification of agonist-induced proteolysis of F-MORΔ17 and F-MORΔ17–0cK, derived from multiple experiments corresponding to the example shown in *panel A*, were determined by exposure of anti-FLAG immunoblots in the linear detection range and scanning densitometry. Points indicate mean and *error bars* S.E. ($n$ = 6 experiments).

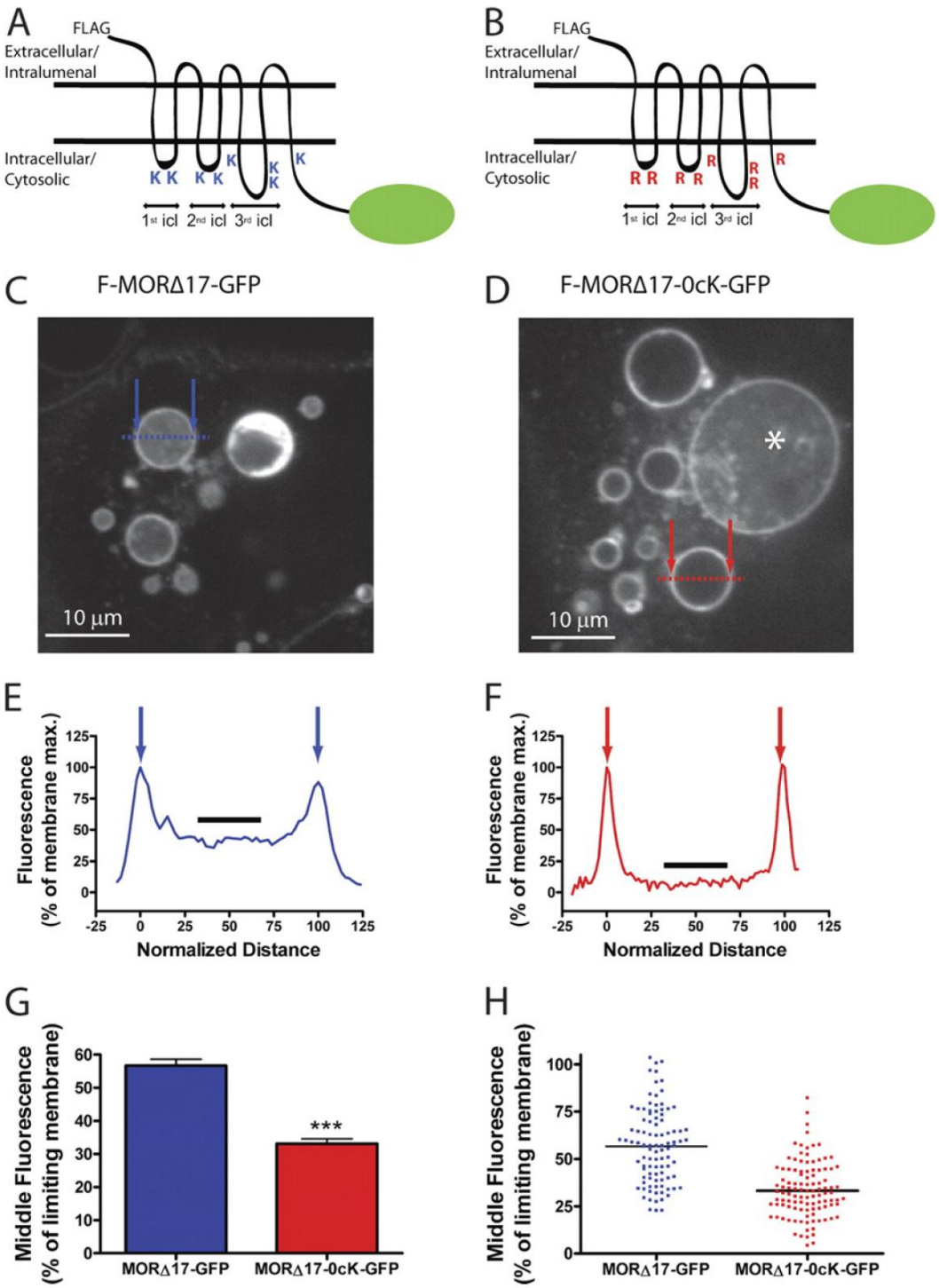


**Figure 4. Ubiquitination promotes receptor redistribution from the limiting to intralumenal endosome membranes.** A and B) Shown are schematic representations of the F-MORΔ17-GFP (*panel A*) and F-MORΔ17–0cK-GFP (*panel B*) constructs used for live imaging, with the fused GFP indicated as a *green oval. icl*, cytoplasmic loop. C and D) A representative optical section shows endosomes in HEK293

cells co-transfected with CFP-Rab5Q79L and either F-MORΔ17-GFP (*panel C*) or F-MORΔ17–0cK-GFP (*panel D*) after incubation for 90 min at 37 °C with 10 μm DADLE followed by imaging at 37 °C by spinning disc confocal microscopy in the continuous presence of agonist. Essentially all of the enlarged endosomes contained visible F-MOR-GFP fluorescence, whereas intralumenal F-MORΔ17–0cK-GFP was rarely observed. The *asterisk* in *panel D* shows an example of such a rare endosome in which detectable intralumenal F-MORΔ17–0cK-GFP fluorescence was detected. *Blue* and *red symbols* overlaid on each image indicate the position of line scans used for quantification. *Scale bars* represent 10 μm. E and F) Shown is a representative line scan analysis to quantify intralumenal fluorescence. Normalized distance represents the diameter of the endosome shown, where 0 and 100 correspond to the pixel distances between the first and second maximum pixel intensities measured across the *dashed line*, respectively (indicated by *arrows* in the diagrams overlaid on *panels C* and *D*). Normalized fluorescence represents the normalized pixel intensity measured across the *dashed line*, where the maximum pixel intensity across the line is normalized to 100. The graphs shown in *panels E* and *F* show line scans of the representative endosomes highlighted in *panels A* and *B*, respectively. The *black line* highlights the normalized fluorescence values of pixels from 40 to 60% of the normalized diameter, used for determining the mean value of intralumenal fluorescence for each endosome, as described under "Experimental Procedures," G and H) Shown are compiled results from the line scan analysis diagrammed in *panels E* and *F*. *Panel G* shows compiled data as the mean and S.E. *Panel H* shows the distribution of internal fluorescence values from individual analyzed endosomes ($n$ = 98 and 109 endosomes, respectively, each imaged from 12 independent dishes and cells; ***, $p < 0.001$, Student's $t$ test).

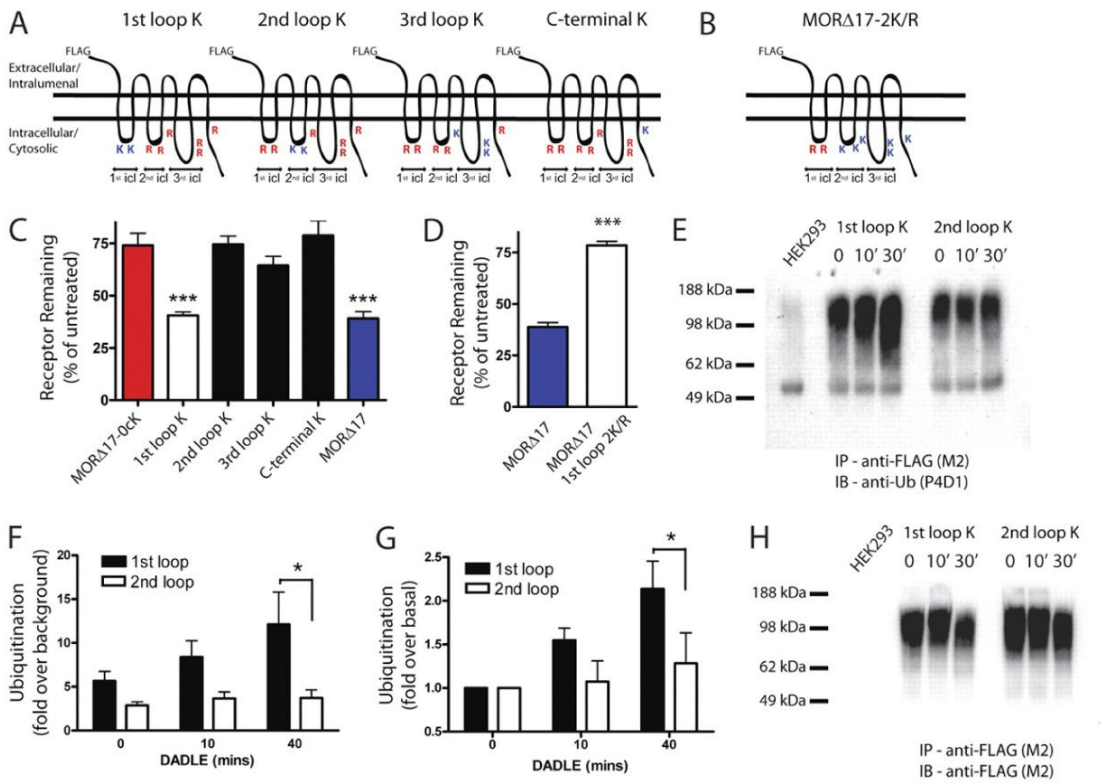


**Figure 5. Ubiquitination specifically of the first cytoplasmic loop is necessary and sufficient for agonist-induced down-regulation measured by radioligand binding.** A) Shown is a diagram of the series of receptor mutants used to test sufficiency, based on reverting arginine residues to lysine residues within individual cytoplasmic domains of the F-MORΔ17–0cK backbone separately. The positions of lysine (*K*) or arginine (*R*) residues in each construct are indicated. B) Shown is a diagram of the receptor mutant used to test necessity, based on mutating only the lysine residues present in the first cytoplasmic loop (*1st icl*) of F-MORΔ17 to arginine, as indicated. C) Shown is down-regulation of the receptor constructs diagrammed in *panel A*, assayed by [$^3$H]DPN binding after incubation of stably transfected cells expressing the indicated receptor construct with 10 μm DADLE for 5 h. In each experiment down-regulation was assessed in triplicate determinations. *Bars* represent the mean, and *error bars* are from $n = 7$ independent experiments (**, $p < 0.01$; ***, $p < 0.001$, one way ANOVA, Bonferroni post test). D) Shown is down-regulation of the receptor construct diagrammed in *panel B.* E) Shown is a representative anti-ubiquitin immunoblot (*IB*) used for the densitometry analysis summarized in *panels F* and *G*. *IP*, immunoprecipitate. F and G) Shown is quantification of relative ubiquitin incorporation from densitometry of anti-ubiquitin blots expressed as -fold over basal measured in unstimulated cells (*panel G*) or -fold over

background measured in cells not expressing FLAG-tagged receptor (*panel F*). *Bars* represent mean and S.E.; *error bars*, $n = 4$; * denotes $p < 0.05$ as determined by two-way ANOVA with the Bonferroni post-test). H) The same blot is shown in *panel E* except it was stripped and reprobed with anti-FLAG, to verify comparable receptor loading between lanes.

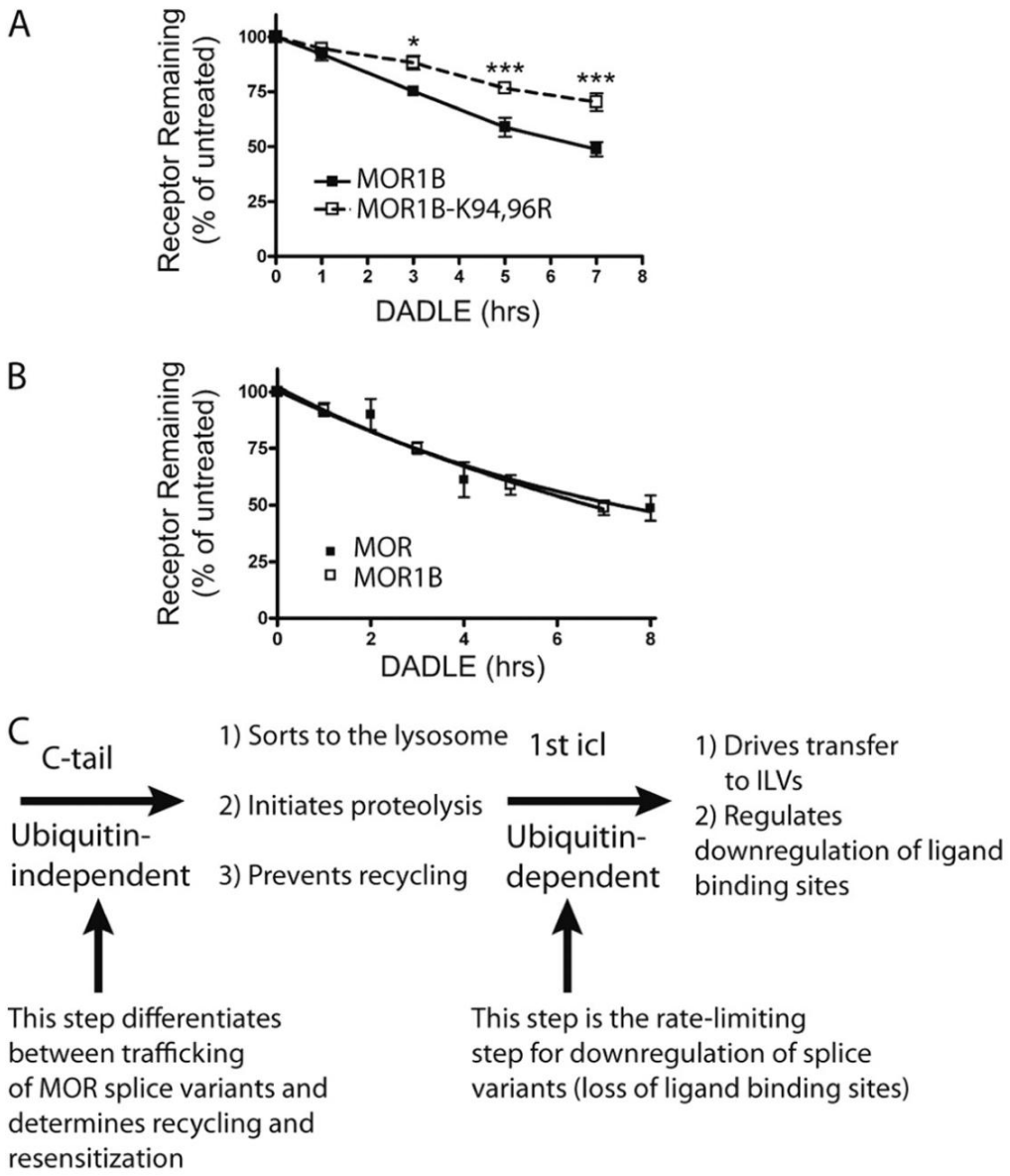


**Figure 6. Ubiquitination in the first cytoplasmic loop is also required for pharmacological down-regulation of the MOR1B isoform.** A) HEK293 cells stably expressing FLAG-tagged MOR1B (*F-MOR1B*) or FLAG-tagged MOR1B in which only the lysine residues present in the first cytoplasmic loop were mutated to arginine (*F-MOR1B-K94R,K96R*) and treated with 10 μm DADLE for the indicated time period before assessing receptor down-regulation by radioligand binding using [$^3$H]DPN. Points represent

mean determinations from independent experiments, with each time point analyzed in triplicate tubes in each experiment. *Error bars* represent the S.E. calculated across the experiments ($n$ = 4). B) Shown is a down-regulation assay comparing the MOR1 and the MOR1B splice variants. Data are replotted from Figs. 1*B* and 6*A* to reveal that, in the present experiments, there was no detectable difference in pharmacological down-regulation of the wild type versions of MOR1 (*F-MOR*) compared with MOR1B (*F-MOR1B*) isoforms. C) Shown is a diagram describing the proposed sequential sorting operations in the hierarchical sorting model. The C-tail (containing the previously described MRS) determines the overall trafficking itinerary of internalized MORs between recycling and lysosomal routes and does not require MOR ubiquitination. Ubiquitination of the first cytoplasmic loop (*1st icl*) specifically promotes redistribution of receptors from the limiting membrane to lumen of late endosomes/multivesicular bodies. This intra-multivesicular body "topological" sorting operation does not dictate the overall trafficking itinerary of internalized receptors but is required for efficient destruction of the transmembrane helical bundle containing the diprenorphine binding site. This step is effectively rate-limiting for pharmacological down-regulation of both the MOR1 and MOR1B isoforms. Therefore, traditional down-regulation assays based on loss of radioligand binding sites may not be sensitive to functionally significant differences in the regulated endocytic trafficking itinerary of naturally occurring MOR isoforms.

| Receptor Expressed | Bmax (fmol/ g) | SEM | | Kd (nM) | SEM |
|---|---|---|---|---|---|
| | | | | | |
| F-MOR | 1.071 | 0.16 | | 0.32 | 0.22 |
| F-MOR-0cK | 1.065 | 0.07 | | 0.28 | 0.09 |
| F-MOR 17 | 2.076 | 0.16 | | 0.31 | 0.11 |
| F-MOR 17-0cK | 2.081 | 0.14 | | 0.35 | 0.11 |

**Supplemental Table 1. Receptor expression levels of HEK293 stable cell lines.** Receptor levels were measured by saturation binding to [3H]-diprenorpnine, and curves fitted using nonlinear regression (GraphPad Prism).

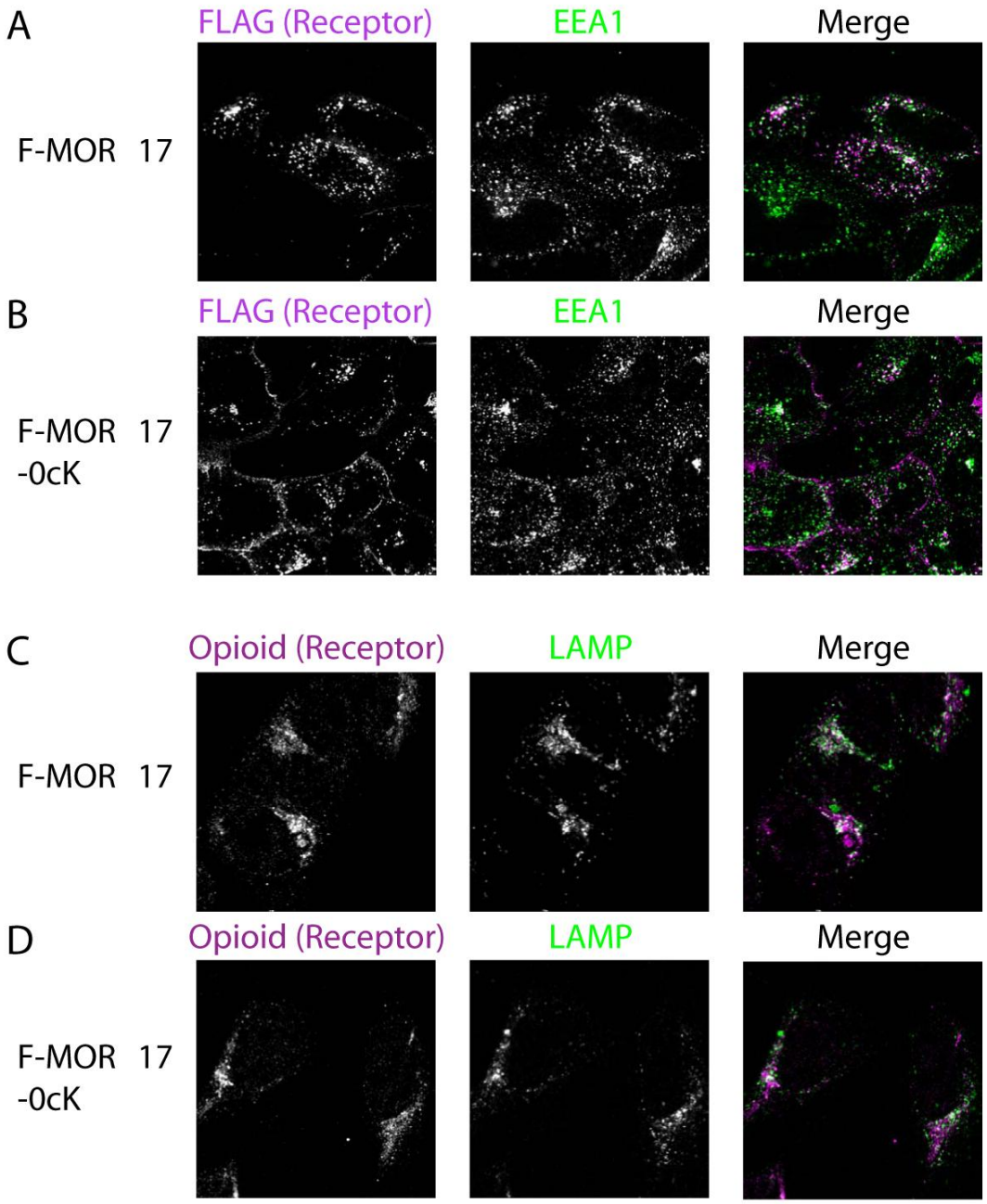


**Supplemental Figure 1. Colocalization of receptors with early and then late endosomes.** HEK293 cells expressing F-MORΔ17 (A and C) or F-MORΔ17-0cK (B and D) were treated with 10μM DADLE for 30 (A and B) or 90 minutes (C and D) before being fixed and stained. A and B) Cells were stained with anti-FLAG (magenta, left panel) to label receptor and anti-EEA1 (green, middle panel). C and D) Cells were stained with anti-opioid receptor (magenta, left panels) and anti-LAMP1 (green, middle panels).

A

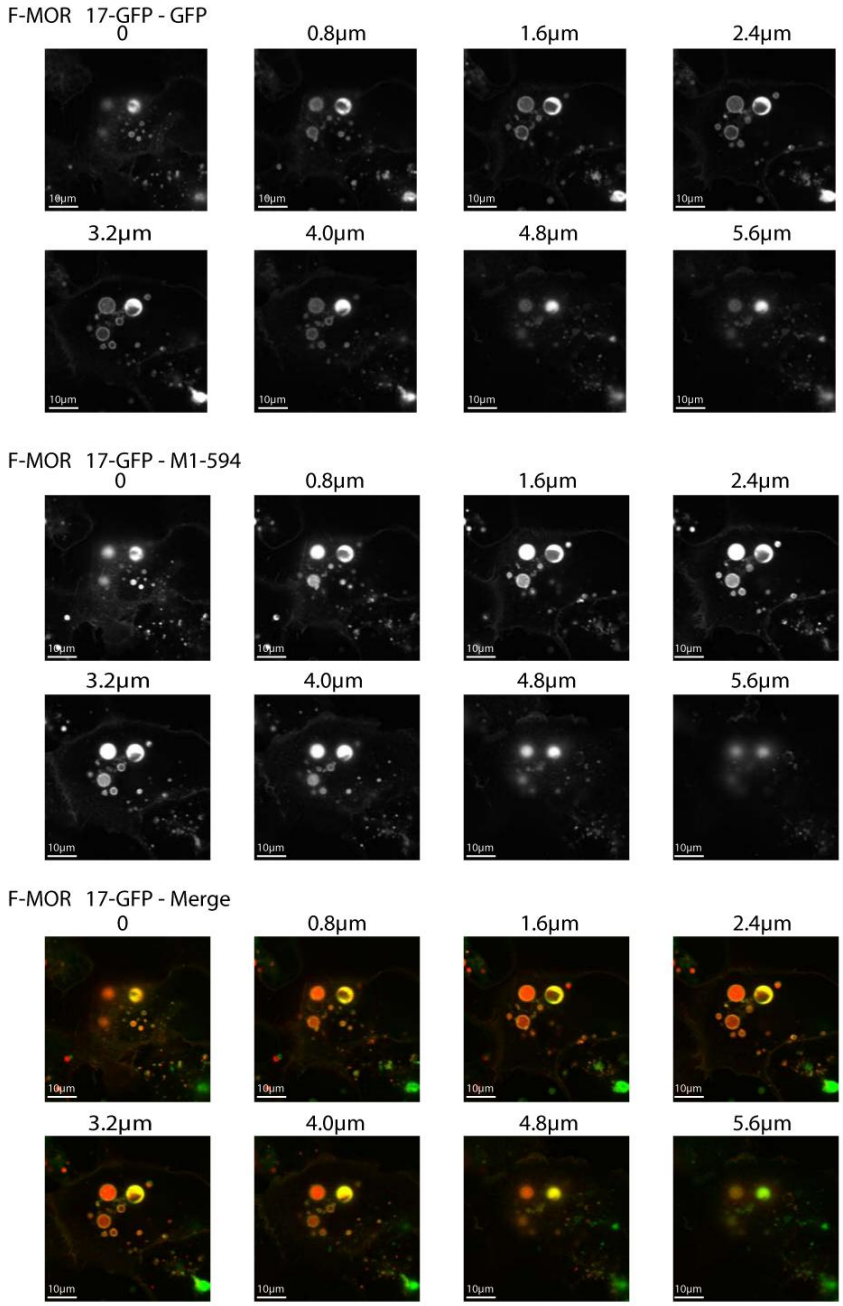
F-MOR 17-GFP - GFP
0
0.8µm
1.6µm
2.4µm
3.2µm
4.0µm
4.8µm
5.6µm
F-MOR 17-GFP - M1-594
0
0.8µm
1.6µm
2.4µm
3.2µm
4.0µm
4.8µm
5.6µm
F-MOR 17-GFP - Merge
0
0.8µm
1.6µm
2.4µm
3.2µm
4.0µm
4.8µm
5.6µm
10µm

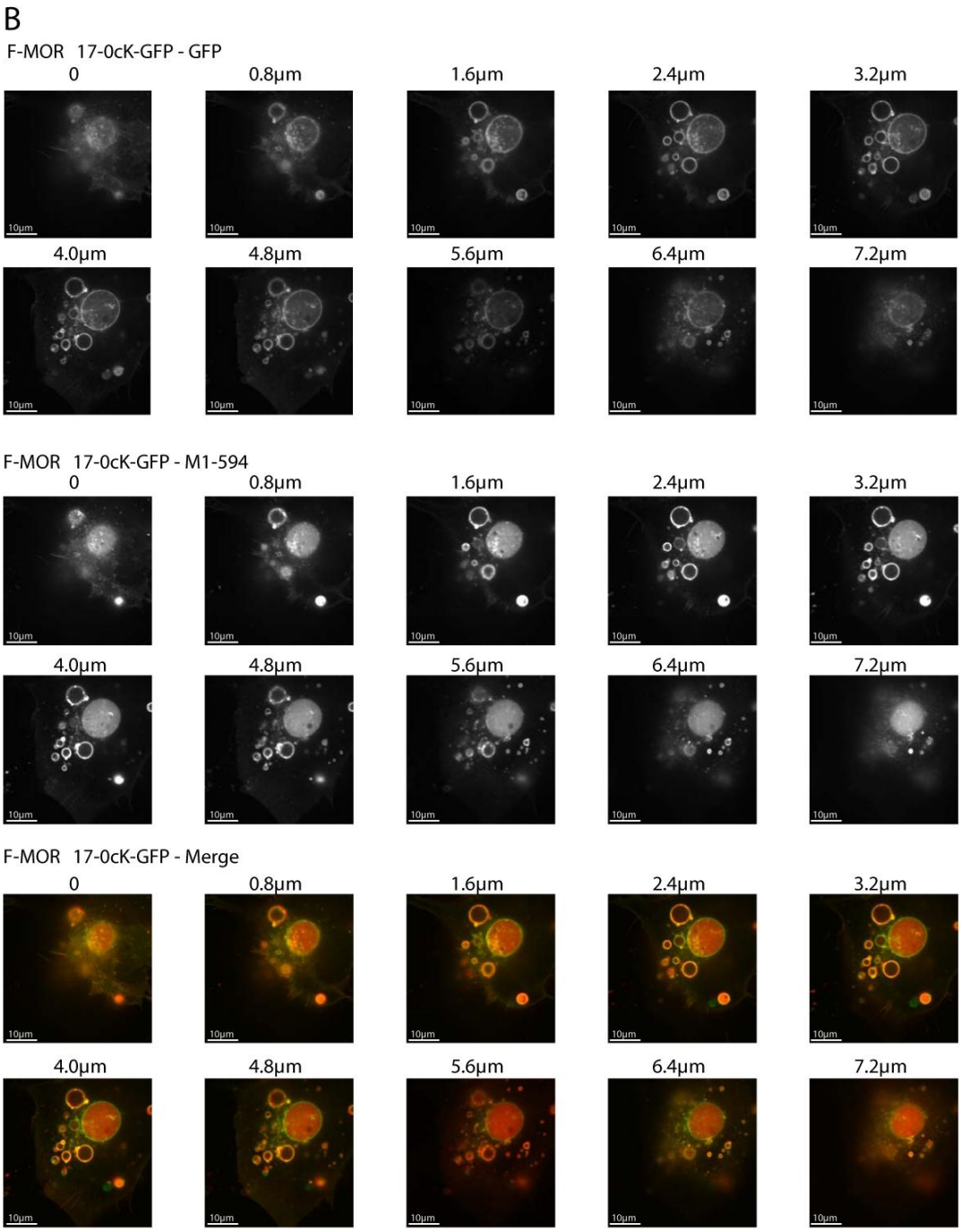


**Supplemental Figure 2. Image stack of enlarged Rab5-Q79L endosomes.**

HEK293 cells were transiently transfected with CFP-Rab5Q79L and either F-MORΔ17-GFP (A) or F-MORΔ17-0cK-GFP (B), and replated onto to coverslips before treatment for 90 minutes with 10µM DADLE. Cells were then imaged by spinning disc confocal microscopy as described in the methods section. Shown are representative image stacks of either GFP (top) or FLAG (middle) fluorescence to

localize the N or C termini respectively. Cross sections of the endosome were taken every 0.8µm, scale bars represent 10µm.

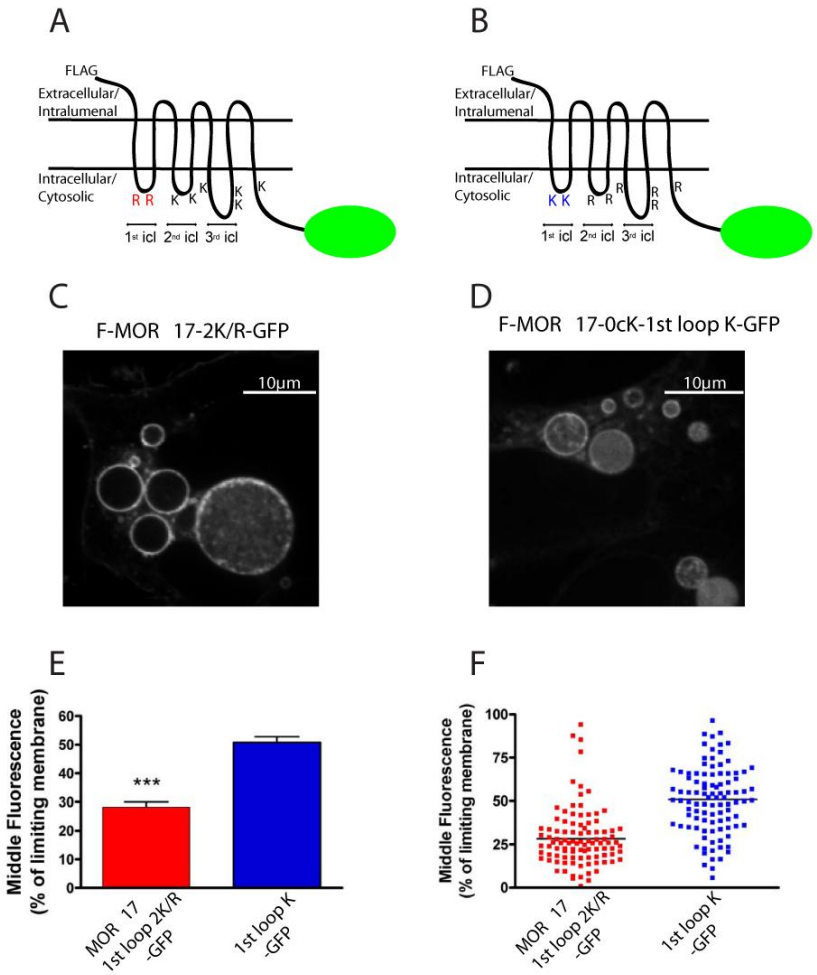


**Supplemental Figure 3. Specific lysine residues within the first intracellular loop mediate transfer to ILVs.** A and B) Cartoon depicting the F-MORΔ17-1st loop 2K/R-GFP (A) or F-MORΔ17-0cK-1st loop K-GFP (B) to show position of the lysine (**K**) and arginine (**R**) residues and the GFP. C and D) HEK293 cells were transiently transfected with CFP-Rab5Q79L and either F-MORΔ17-1st loop 2K/R-GFP (C) or F-MORΔ17-0cK-1st loop K-GFP (D), and replated onto to coverslips before treatment for 90 minutes with 10µM DADLE. Cells were then imaged by spinning disc confocal microscopy as described in the methods section. Shown are representative still images of the representative acquired image series, scale bars are 10µm. C and D) Line scan analysis to quantify involution was performed as described (see Methods and Fig.5 legend), and data of line scan analysis compiled. E) shows mean and SEM, F) shows the distribution

of internal fluorescence values *** $p<0.001$, Student's t-test, n=100 endosomes for each receptor, ≥ 12 cells).

# Chapter 6:

# Discussion

## 6.1 Ubiquitin as a regulator of endocytosis

It is well-established that ubiquitin can regulate the endocytosis of various membrane cargoes. Ubiquitination is thought to promote specifically the initial entry of different receptors into CCPs through interactions with ubiquitin-binding endocytic adaptors (Kazazic et al., 2009; Toshima et al., 2009). Supporting this, EM analysis of EGFR endocytosis demonstrated that knockdown of Epsin1, an endocytic adaptor with tandem UIMs, decreased the recruitment of receptors and stranded activated receptors at the rim of CCPs (Kazazic et al., 2009). Live-cell imaging studies in yeast also showed that preventing 7TMR ubiquitination prevented the entry of receptors into CCPs, through the function of the yeast homologues for Epsin1,2, and Eps15 (Toshima et al., 2009). Our results provide the first evidence for any function of receptor ubiquitination in the endocytosis of a 7TMR and identify a distinct function of ubiquitin in endocytosis, acting as a biochemical signal to actively control receptor endocytosis after clathrin assembly is complete and after initial cargo accumulation in CCPs has occurred. We demonstrate ubiquitination of the first intracellular loop of MOR does not affect the initial entry into CCPs but instead regulates how receptor-containing CCPs persist at the cell surface. Beyond simply linking the cargo to CCPs, the results reveal an unanticipated role of ubiquitination that conveys information about the cargo to the clathrin machinery, shaping how long receptor-containing CCPs persist at the surface.

The results included in this thesis add to accumulating evidence that ubiquitin can affect later stages of CCP maturation, after the cargo recruitment step (Jiang and Sorkin, 2003; Reider and Wendland, 2011). For example, the E3 ligase Cbl promotes EGFR

endocytosis and appears to function at a later step in the endocytic process, as expression of a mutant form of Cbl caused an accumulation of activated EGFRs in CCPs (Jiang and Sorkin, 2003). The present results support this idea and significantly extend it, by establishing a role of cargo ubiquitination in actively controlling CCP maturation. Ubiquitin has also been recently implicated in the cargo-dependent control of secretion through the biosynthetic pathway, with a study demonstrating that ubiquitination of one of the COPII proteins leads to changes in the size and structure of secretory vesicles to accommodate large cargo (Jin et al., 2012). Together, the work included in this thesis adds to an emerging role for ubiquitin in the cargo-specific regulation of coat protein dynamics.

The specific functions of ubiquitin-interacting adaptors in receptor-mediated endocytosis remain poorly understood. The present work identifies a precise role for the UIMs of Epsin1 in promoting receptor endocytosis that depends on the ubiquitination status of the receptor and the engagement of the ubiquitin-sensing mechanism, as UIM-deletion mutants of Epsin1 did not affect the internalization of MOR0cK or the related DOR, a 7TMR that does not require direct ubiquitination to internalize efficiently. This work provides the first direct evidence for a function of the UIMs of Epsin1 in the ubiquitin-dependent internalization of a 7TMR. Recent work from the Trejo lab has shown that the endocytosis of another mammalian 7TMR, PAR1, requires the UIMs of Epsin but does not require ubiquitination of the receptor itself (Chen et al., 2011). This suggests that the ubiquitin-binding domains of Epsin1 may have additional functions in receptor endocytosis, separate from its proposed function in recognizing ubiquitinated cargoes.

Some evidence suggests that the ubiquitin-binding domains within the yeast homologues of Epsin and Eps15 actually function primarily in mediating protein-protein interactions between components of the CCP, rather than in recognizing ubiquitinated cargo, as ubiquitinated receptors could still internalize in the absence of epsin and Eps15 UIMs (Dores et al., 2010). Mechanistic insight into how ubiquitinated cargo are recognized and targeted to CCPs and the function of the UIMs of epsins and Eps15 in mammalian endocytosis is still lacking. This adaptor plays a more general role in clathrin-mediated endocytosis, as its knockdown or overexpression affect endocytosis on a global level, as reported previously and corroborated here (Mettlen et al., 2009). While the present work identifies a clear role of the UIMs of Epsin1 in controlling the surface lifetime of MORs, it remains to be determined whether this is through direct interaction with Epsin1 and how Epsin1 modulates CCP dynamics. Elegant study of the dynamics of various CCP components suggest that epsins are recruited at a similar time as clathrin and increase in abundance until CCP scission has occurred (Taylor et al., 2011). Ultrastructural analysis of the related UIM-containing adaptor Eps15 reveal its localization specifically to the rim of CCPs, which, together with the previously discussed EM analysis localizing EGFRs to the rim of CCPs upon Epsin1 knockdown (Kazazic et al., 2009; Tebar et al., 1996), support the idea that these adaptors function specifically at the edge of CCPs and could aid in the transfer of cargo from the rim of CCPs to their interior for inclusion into nascent CCVs. This appealing model is supported by the present results and by unpublished work examining the consequences of coexpression of wildtype and lysyl-mutant MORs. We initially hypothesized that the ubiquitin-dependent delay of CCPs caused by preventing receptor ubiquitination would also affect the internalization of

wildtype MORs when expressed in the same cells. Intriguingly, this was not the case (Figure 1A). The simplest explanation for this trafficking behavior is that wildtype and lysyl-mutant MORs do not use the same subsets of CCPs, but live-cell TIRF-M analysis revealed that receptors do, in fact, colocalize to the same CCP population (Figure 1B). These seemingly paradoxical pieces of data could make sense if, as seen with the EM analysis of the location of action for the ubiquitin adaptors, blocking ubiquitination trapped non-ubiquitinated receptors at the rim of CCPs but still allowed other regulated cargo, including ubiquitinated wildtype MORs, to enter CCPs and internalize normally. As we established that lysyl-mutation of MORs does affect the trafficking of the TfR, this suggests that cargoes can only be trapped at the rim of CCPs if they can also engage the "brake" mechanism as appears to be the case for wildtype MORs. Obviously, additional study is required to understand how receptor ubiquitination and engagement of the adaptor Epsin1 control the dynamics of CCPs and whether these principles apply to other cargoes traversing the endocytic pathway.

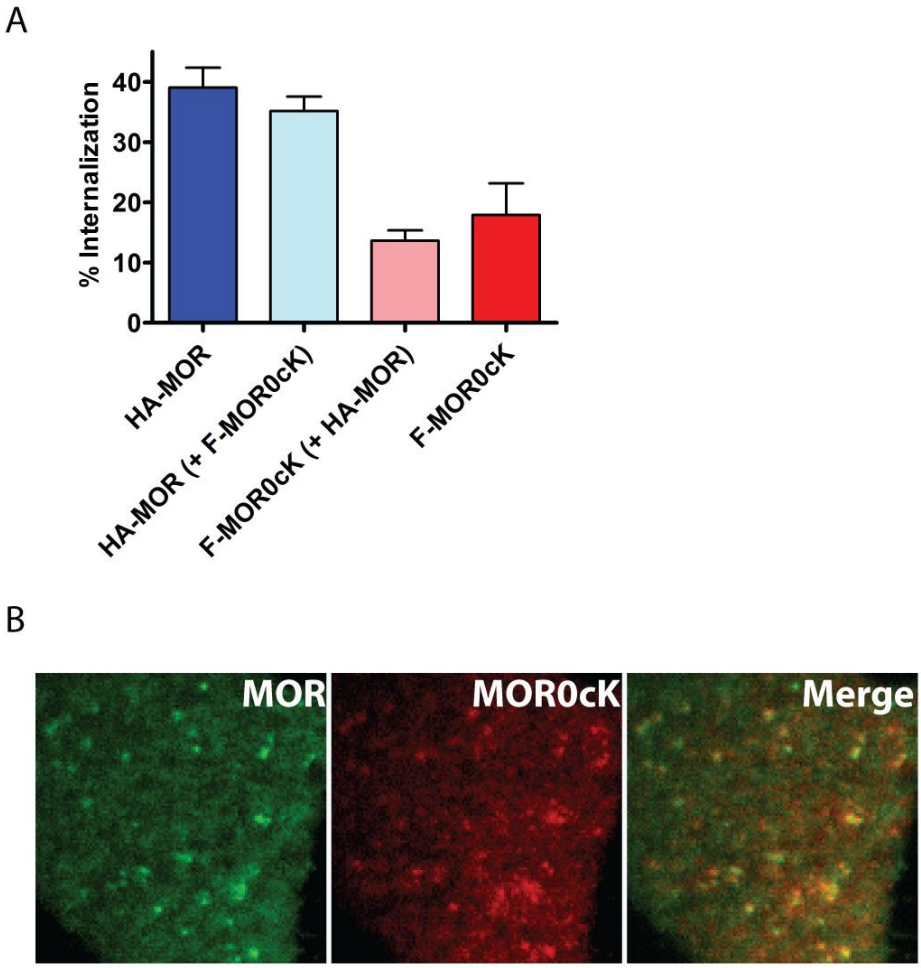


**Figure 1. Coexpression and activation of wildtype and lysyl-mutant MORs does not alter their trafficking. (A)** HEK293 cells were transiently transfected with HA-MOR and pCDNA 3.0, HA-MOR and F-MOR0cK; or F-MOR0cK alone and treated with agonist for 30 minutes before flow cytometric analysis; n=3. (B) Cells were transiently transfected with GFP-MOR and F-MOR0cK, prelabeled with Alexa-647 conjugated to M1 anti-FLAG, and imagined using TIRF-M. Shown is a representative micrograph 5 minutes after agonist addition.

## 6.2 Remaining questions in the regulation of receptor endocytosis

While many of the basic mechanisms mediating 7TMR endocytosis have been elucidated, many large questions remain as to how this process is regulated and how diverse the regulatory methods are among different 7TMRs. It is well-established that receptor phosphorylation is required for 7TMR endocytosis, leading to the recruitment of arrestins that act as adaptors between receptors and components of the CCP. Work from the Drubin lab has suggested that phosphorylation of the yeast 7TMR Ste2p is required for later receptor ubiquitination, and ubiquitination of Ste2p is the primary requirement for efficient entry of receptors into CCPs (Toshima et al., 2009). My thesis work has established that agonist-induced phosphorylation of MOR is also required for its efficient ubiquitination, through recruitment of the E3 ligase Smurf2 by arrestin, but unlike that seen in the budding yeast, phosphorylation and ubiquitination appear to regulate to different stages in the endocytic process. While phosphorylation-dependent recruitment of arrestins is required for mammalian 7TMR entry into CCPs, ubiquitination of MOR appears to regulate a later stage in the pathway, specifically controlling how long receptors persist in CCPs prior to undergoing endocytic scission. It remains to be determined why phosphorylation of yeast 7TMRs is necessary for receptor ubiquitination, as they lack classical arrestin homologues, but recently identified arrestin-related proteins could play a similar role in mediating endocytosis. While receptor ubiquitination does not appear to be a general requirement for mammalian 7TMR endocytosis, it will be interesting to see whether other 7TMRs undergo sequential

phosphorylation and ubiquitination. Arrestin-dependent recruitment of ubiquitin ligases has been shown to occur for several mammalian 7TMRs, but this function has been attributed to ensuring appropriate ubiquitination specifically for later lysosomal destruction(Bhandari et al., 2007; Shenoy et al., 2001; Shenoy et al., 2008). Whether arrestin-dependent recruitment of different E3 ligases is a general occurrence for all 7TMRs remains to be determined.

A particularly intriguing question raised by the present work is why receptor ubiquitination regulates the endocytosis of the MOR and not for the handful of other 7TMRs examined to date. My work has determined that the C-terminal tail of MOR is necessary for ubiquitin-dependent endocytosis, as its truncation allows MOR to internalize efficiently in an ubiquitin-independent manner. The C-terminus appears to possess a specific sequence that engages the ubiquitin-dependent mechanism, as its transplantation onto DOR, which normally does not require receptor ubiquitination to internalize, transforms this chimeric DOR into an ubiquitin-dependent internalizer. Interestingly, mutation of a cluster of serine and threonine residues shown to be a major site of agonist-induced phosphorylation to alanines also rescues the defect seen with lysyl-mutation of MORs, restoring internalization of a lysyl- and phospho-deficient mutant to wild type levels (Figure 1). As receptor phosphorylation is a known requirement for arrestin recruitment, it is tantalizing to propose that the interaction and recruitment of arrestin plays a role in determining whether receptors need ubiquitin to endocytose efficiently. MOR is not thought to interact with arrestin as well as the related DOR, and slow entrapment into CCPs could provide a simple kinetic explanation for why

some receptors require ubiquitin. One could imagine that 7TMRs that do not internalize rapidly may have more time to interact with whatever downstream proteins contribute to form the “brake” that appears to be released through receptor ubiquitination. Supporting this hypothesis, B2AR and DOR appear to rapidly recruit arrestin and internalize when imaged live using TIRF-M, with faster kinetics than MOR, and both receptors do not undergo ubiquitin-dependent endocytosis (Puthenveedu et al, 2006 and unpublished data). To test whether we could artificially slow receptors down, through engagement of actin, we generated mutant forms of DOR that contained the actin-binding domain (ABD) of Ezrin fused to its C-terminus or the tail of the B2AR itself, previously shown to slow down 7TMRs at the CCP (Puthenveedu and von Zastrow, 2006). These manipulations did not lead to a requirement for ubiquitination in mutant DOR endocytosis (Figure 2). Further, adding the ABD of Ezrin onto a MOR-DOR chimera, shown to no longer require receptor ubiquitination, does not inhibit receptor internalization. This suggests that simple stalling at the pit is not enough to confer ubiquitin-dependent internalization to other 7TMRs and highlights the importance of identifying interacting partners that form the “brake” that stalls receptors at the CCP.

Additional questions also remain about the nature of MOR ubiquitination and the specifics of how the ubiquitination of MORs and engagement of ubiquitin-dependent machinery is regulated. For example, it is unclear whether MORs undergo mono- or poly-ubiquitination after they become activated. Simple Western blot analysis reveals a “smear” of receptor ubiquitination, a problem commonly seen when working with membrane proteins, which prevents one from counting shifts in molecular weight to

determine the protein's ubiquitination status. Monoubiqutination has been proposed to function preferentially in the endocytosis of membrane proteins, based on work in yeast, and polyubiquitin chains, linked at K63, have been suggested to be important for the lysosomal destruction of receptors. As MOR ubiquitination is required for both its endocytosis and later MVB-mediated destruction, it will be informative to learn about the specific ubiquitination status of MORs, which may change over time after agonist addition. It is also unclear whether both lysine residues in the first intracellular loop are ubiquitinated, and our analysis revealed that either lysine residue could rescue receptor internalization to wild type levels but not to the levels seen when both lysine residues were replaced (Figure 3A). As there is only a methione residue between the two lysine residues, simultaneous ubiquitination of both sites may be impossible due to steric constraints. Mass spectrometric analysis could provide a useful tool to answer this question and to analyze changes in receptor ubiquitination over varying times of agonist treatment and between different ligands. It is intriguing that there is specificity between the two lysine residues in the first intracellular loop for downregulation of receptors (James Hislop, personal communication). Together, these data support a model whereby sequential ubiquitination, deubiquitination, and additional ubiquitination regulate the endocytic trafficking of MORs. Supporting this, two separate E3 ligases appear to regulate MOR trafficking, with Smurf2 specifically involved in MOR ubiquitination and endocytosis and AIP4 involved in the lysosomal destruction of MORs (James Hislop, unpublished data). Additionally, two DUBs reported to play a role in receptor sorting and degradation, AMSH and UBPY, do not appear to be required for efficient receptor

internalization but are necessary for downregulation of MORs (Figure 3B and James Hislop, personal communication).

While this work established a role for the UIMs of Epsin1 in MOR endocytosis, many other candidates were explored on the hunt for the "downstream protein," looking for proteins that can bind ubiquitin, specifically control the endocytosis of receptors that can be ubiquitinated (i.e. do not affect the lysyl-mutant MOR), and function in endocytic trafficking. One intriguing candidate was a Rab5 GEF, Rabex5, which possesses two non-canonical ubiquitin-binding domains (Raiborg et al., 2006). Rabex5 was shown previously to bind to activated EGFRs, an interaction that depends on the either of the UBDs, suggesting this protein could be recruited to ubiquitinated membrane cargoes (Penengo et al., 2006). Further, manipulations of Rab5 activity have been reported to inhibit clathrin-mediated endocytosis of various cargoes, but the mechanism of inhibition is unknown(Stenmark et al., 1994). With these previous findings, Rabex5 emerged as a potential candidate that could be recruited to membranes containing ubiquitinated receptors and control the cargo-dependent activation of Rab5. Knockdown of Rab5 and Rabex5 appeared to inhibit MOR endocytosis, but knockdown of these proteins also affected MOR0cK internalization (Figure 4 A and B). As an alternative approach, we assessed receptor endocytosis with the co-expression of a dominant negative mutant of Rab5 (Rab5 S34N), which preferentially binds GDP (Stenmark et al., 1994). Interestingly, overexpression of the S34N mutant appeared to inhibit the endocytosis of MORs but not MOR0cK (perhaps even accelerating its internalization) (Figure 4 C and D). While Rabex5 knockdown affected the endocytosis of both wildtype and lysyl-mutant

MORs, this specific effect piqued our interest and lead us to consider alternative Rab5 GEFs. While Rabex5 is reported to localize predominantly to early endosomes, the Rab5 GEF GAPVD1 localizes to the plasma membrane. Knockdown of GAPVD1 appeared to also inhibit the internalization of opioid receptors regardless of their ability to be ubiquitinated or undergo ubiquitin-dependent internalization in preliminary experiments, so this candidate was not pursued further (Figure 4 E-G). The precise function of Rab5 and its various GEFs in endocytosis remains mysterious, and there have been hints in previous work Rab5 may play a cargo-specific or activity-specific role in the endocytic pathway. For example, studies of Frizzled receptors, putative Gi/Go coupled 7TMRs, in *Drosophila Melanogaster* reported that $G\alpha_o$ recruits Rab5 to the plasma membrane in an activity-dependent manner (Purvanov et al., 2010). Clearly, additional study of the role of Rab5 in regulating this process is certainly warranted.

Other intriguing potential candidates for the "downstream protein" were components of the ESCRT-0 complex, HRS and Stam, which both contain UIMs and N-terminal VHS domains (which weakly interact with ubiquitin, with an affinity of ~100-500 μM) (Shields and Piper, 2011). Analysis of the role of HRS in receptor recycling and degradation also revealed that its overexpression inhibited receptor internalization as well. As knockdown and overexpression of HRS yields the same defect in MOR recycling, we hypothesized that knockdown may also inhibit MOR internalization (Hanyaloglu et al., 2005). Surprisingly, knockdown of HRS, Stam1, or Stam2 all increased receptor internalization after treatment with agonist for 5 or 30 minutes (Figure 5 A and B). This suggests that these proteins may play a role in regulating MOR

internalization, perhaps in the “brake” function engaged by the receptor. Supporting this, TIRF-M imaging revealed that both proteins exhibit a diffuse staining pattern with some punctae found at the cell surface (Figure 5 C and D). These punctae coloclalize with a subpopulation of receptors after agonist addition (Figure 5E). Together, these results suggest that HRS and the Stams may function in receptor endocytosis, but additional study is required to elucidate what this exact function is.

Many questions remain as to the particular players involved in regulating each stage of receptor endocytosis, and the multifunctional role many endocytic adaptors play in the process make elucidating their precise functions challenging. Future analysis that takes a more directed approach, through manipulations of particular protein domains or activity, may help to define their roles and reveal how receptor endocytosis is precisely controlled in response to agonist addition.

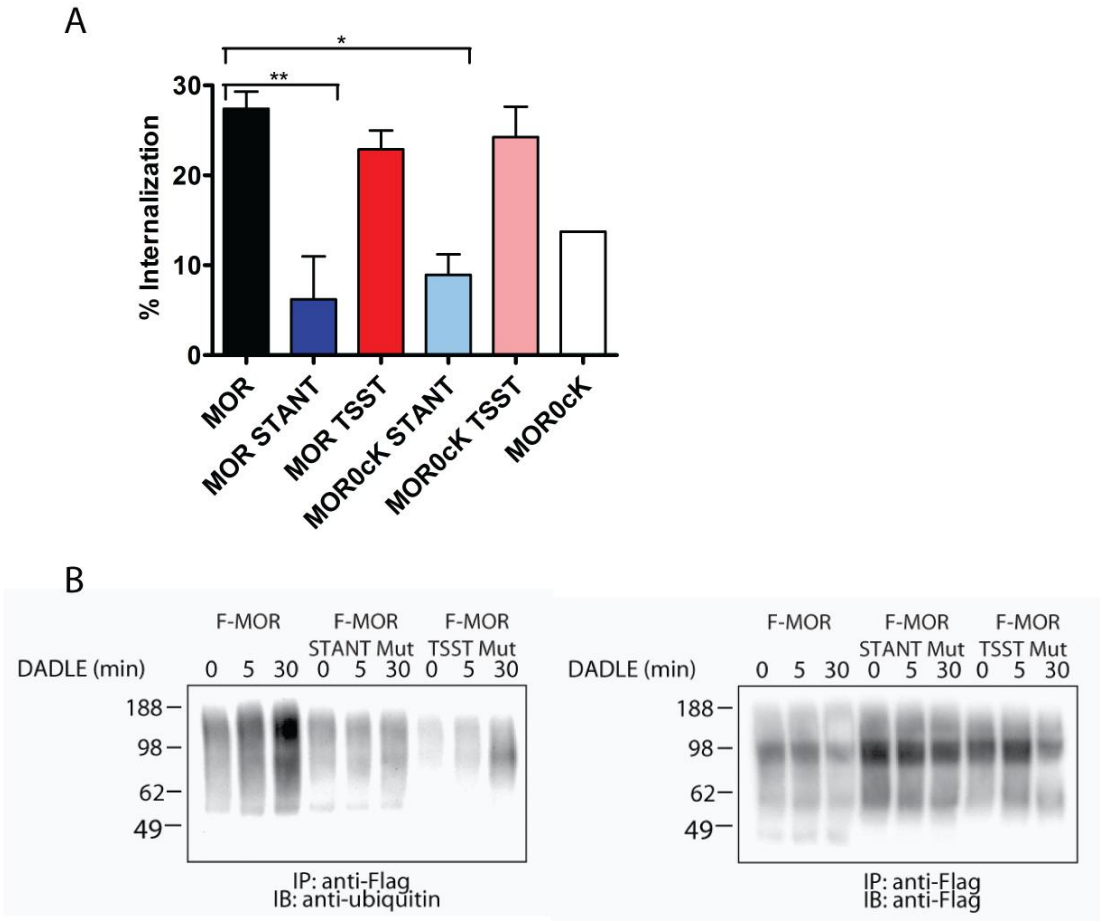


**Figure 1. Coordination and consequences of phosporylation on ubiquitination and ubiquitin-dependent trafficking of MORs.** (A) HEK293 cells were transiently transfected with FLAG-tagged MOR, MOR0cK, and serine and threonine -> alanine mutants in the STANT or TSST region: MOR STANT, MOR TSST, MOR0cK STANT, MOR0cK TSST and treated with agonist for 30 minutes before flow cytometric analysis; n=3. (B) Ubiquitin blots for the different serine and threonine-> alanine mutant MORs after agonist treatment.

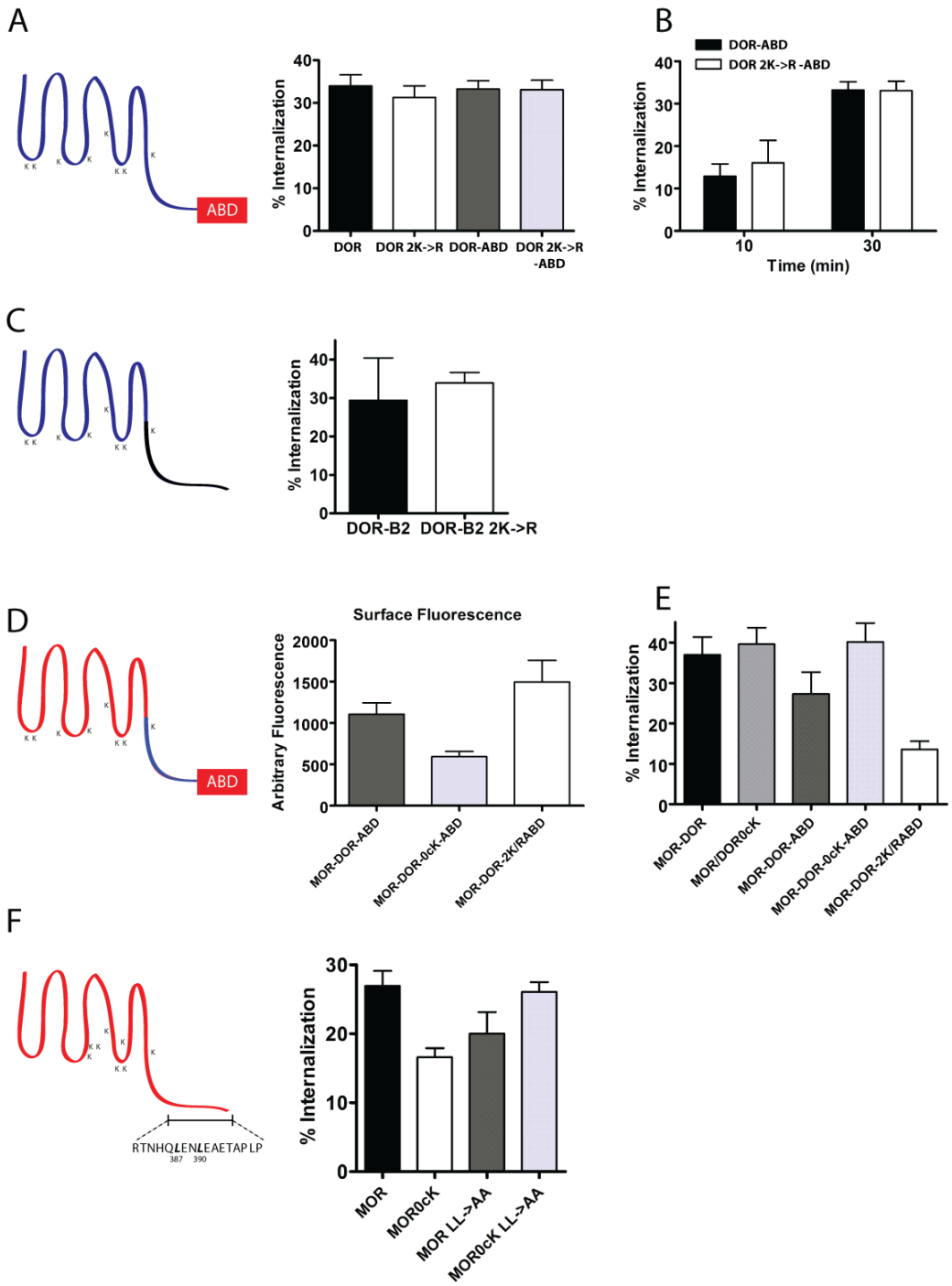


**Figure 2. Assessment of the importance of the C-terminus of receptors to ubiquitin-dependent regulation.** (A) HEK293 cells were transiently transfected with FLAG-tagged DOR, DOR 2K->R , and versions of the two with the actin-binding domain of Ezrin attached to the C-terminus and treated with agonist for 30 minutes before flow cytometric analysis; n=3. (B) Time course of internalization of DOR-ABD and DOR 2K->R ABD; n=3. (C) Cells were transiently transfected with mutant DORs with the tail

swapped with the tail of the B2AR, with or without the lysine residues in the first intracellular loop present; n=2. (D-E) Mutant MORs were generated that had their C-terminus swapped with DOR and the ABD of Ezrin attached to the C-terminus, with or without any lysine residues or just those missing in the first loop, and flow cytometric analysis was performed showing the basal surface receptor expression levels (D) and after DADLE treatment for 30 minutes (E); n≥3. (F) Mutant MORs were generated with a previously used mutation of two leucines to alanine in the MOR C-terminus with and without cytoplasmic lysine residues, and cells were treated as above; n=3.

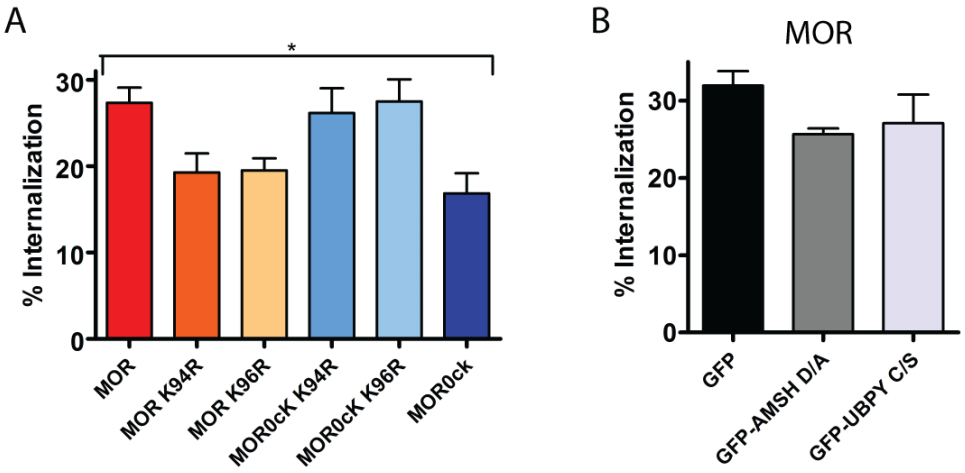


**Figure 3. Role of single lysine residues and DUBs in MOR internalization.** (A) HEK293 cells were transiently transfected with MOR, MOR0ck, or different mutant versions of the two with single lysine residues missing or restored, and receptor internalization was measured after 30 min DADLE treatment using flow cytometry; n≥3. (B) HEK293 cells stably-expressing FLAG-tagged MOR were transiently transfected with GFP alone, GFP-tagged catalytically inactive versions of AMSH (AMSH D/A) and UBPY (UBPY C/S) and treated as in A; n=3.

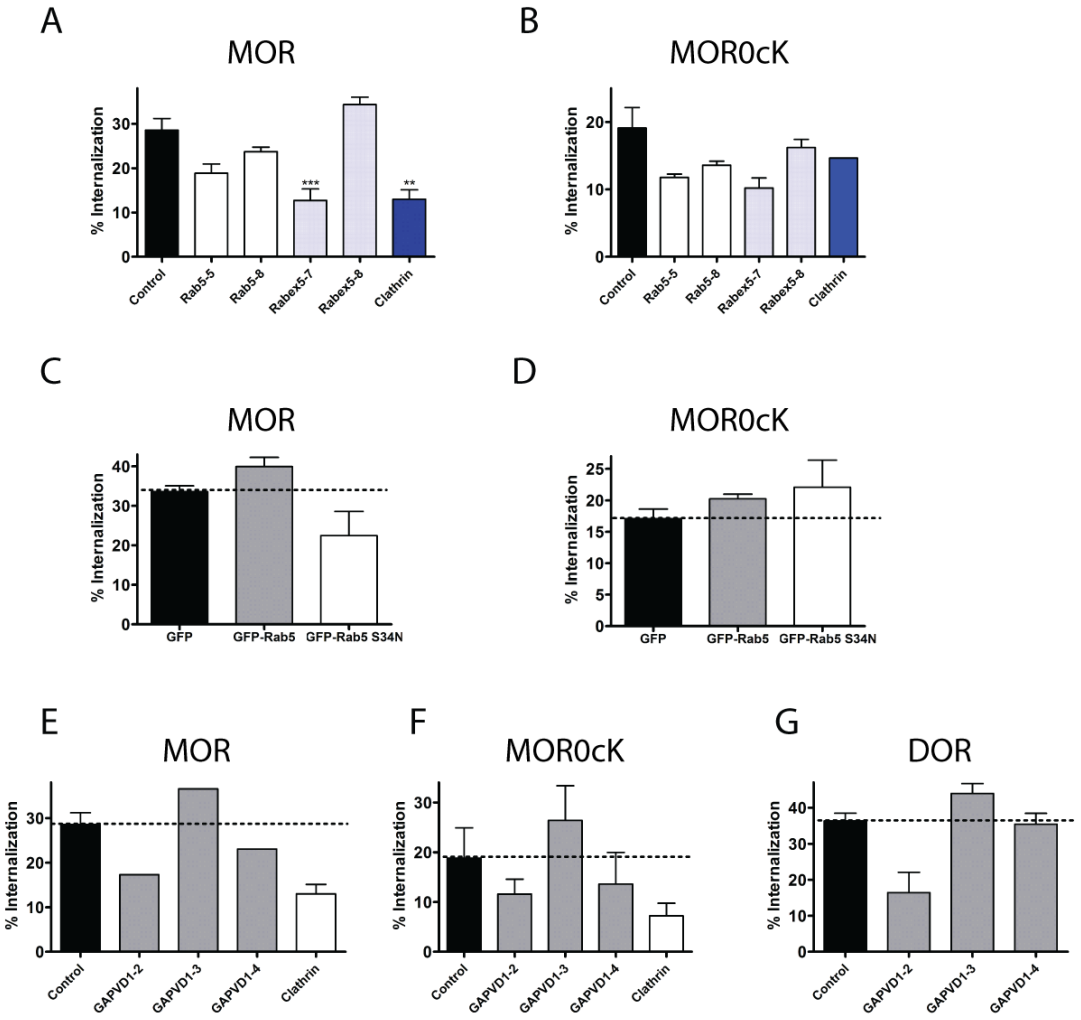


**Figure 4. Role of Rab5 and its GEFs in opioid receptor endocytosis. (**A-B) HEK293 cells stably-expressing MOR (A) or MOR0cK (B) were transfected with a scrambled siRNA sequence or with siRNA against Rab5, Rabex5 (a Rab5 GEF), or clathrin, and receptor internalization was assessed 30 minutes after DADLE treatment with flow cytometry; A: n=4, B:n=2. (C –D) HEK293 cells stably-expressing MOR (C) or MOR0cK (D) were transfected with GFP, GFP-tagged wildtype Rab5 or Rab5-S34N mutant and treated as above; n=3. (E-G) Cells stably-expressing MOR (E), MOR0cK (F), or DOR (G) were transiently transfected with a scrabled siRNA sequence or siRNA against GAPVD1 (a plasma membrane specific Rab5 GEF) and treated as above; E: n=1, F: n=3, G: n=3.

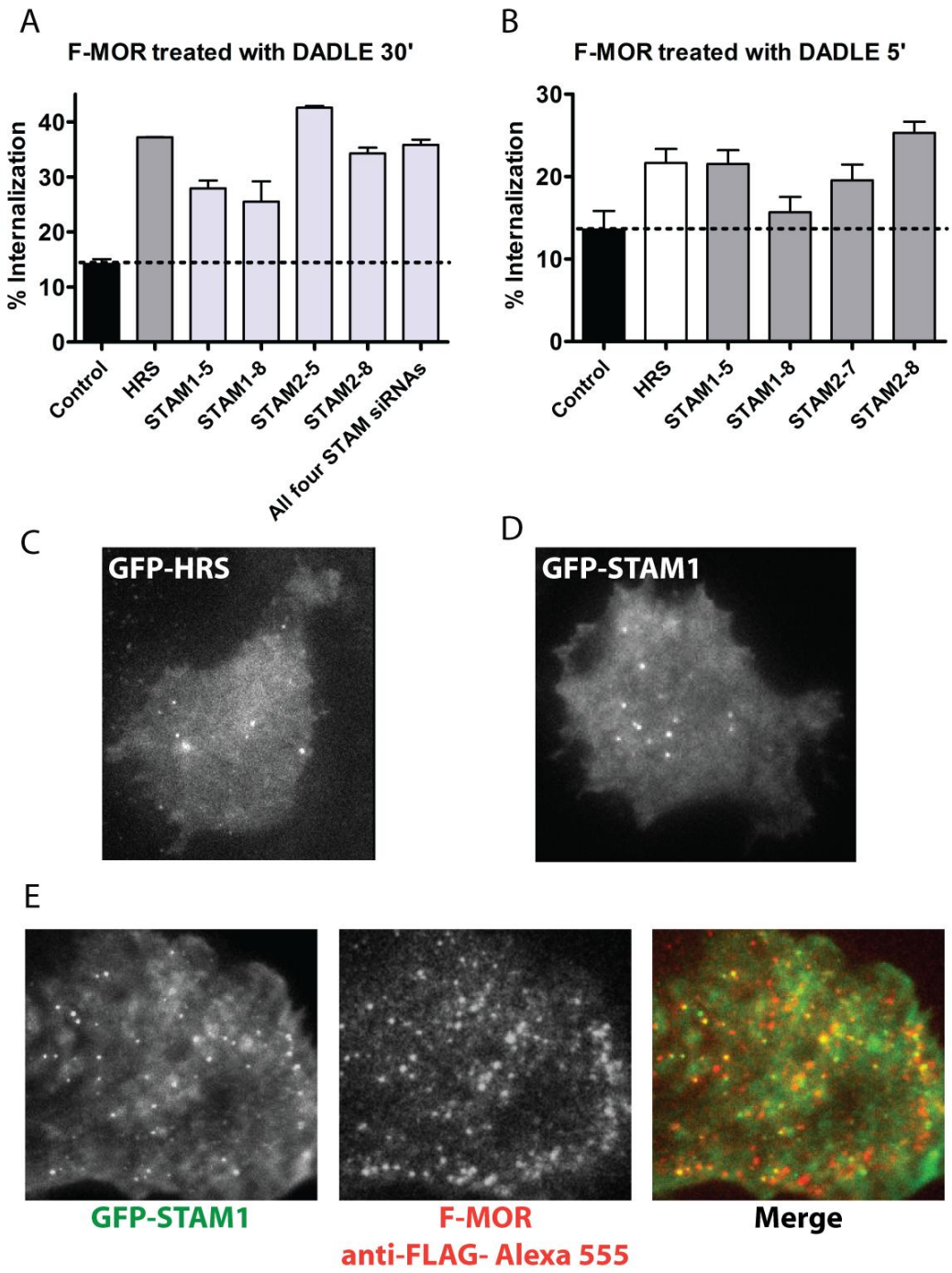


**Figure 5. Role of HRS and STAM in MOR endocytosis. (**A-B) HEK293 cells stably-expressing FLAG-tagged MOR were transiently transfected with a scrambled siRNA sequence or with siRNA against HRS, STAM1, or STAM2, and receptor internalization was assessed 30 minutes (A) or 5 minutes (B) after DADLE treatment with flow cytometry; A: n=2, B:n≥2. (C –D) HEK293 cells were transiently transfected with F-MOR and GFP-HRS and myc-Stam1 (C) or GFP-Stam1 and myc-HRS (D) and imaged using TIRF-

M. (E) Cells transiently expressing F- MOR labeled with M1-Alexa 555, GFP-Stam1, and myc-HRS were treated with agonist and imaged using TIRF-M. Image is ~5 min after agonist application.

## 6.3 Sorting at the plasma membrane

While some 7TMRs clearly segregate from one another and traffic to diverse locales within the cell, whether sorting decisions can occur prior to receptor endocytosis remains an intriguing question. In principle, receptors could be sorted to different locations from the plasma membrane by differential rates of entering the endocytic pathway (a kinetic mechanism for sorting) or by the physical separation of receptors into different CCPs (a spatial mechanism for sorting). In support of the kinetic mechanism, studies from our lab of chimeric forms of the B2AR demonstrated that the same PDZ ligand that delays CCP lifetime also promotes receptor recycling after endocytosis (Puthenveedu and von Zastrow, 2006). My thesis work also shows that the C-terminus of MOR, the same sequence that determines whether receptors recycle predominantly or are targeted to the lysosome for degradation, also specifies whether receptors use ubiquitin to control how long receptors remain at the surface before undergoing endocytosis. Arguing against a simple kinetic model, however, we find that the actual modulator of CCP lifetime and the endocytic rate of receptors, MOR ubiquitination, does *not* affect the postendocytic sorting of receptors. As there does appear to be some correlation between the "sorting sequences" and regulation of receptor endocytosis, future studies more directly test whether kinetic delays at the surface directly influence postendocytic sorting will likely be informative. The alternative mechanism for sorting receptors, through their physical separation into different subsets of CCPs, appears to effectively separate some 7TMRs destined for different postendocytic trafficking fates, such as is the case for the purinergic receptors (Mundell et al., 2006). While this has not been reported for additional 7TMRs and preliminary studies did not observe this with the DOR and MOR, careful analysis of

clustering behavior for receptors that traffic differently are warranted to further test this hypothesis. The coexpression of multiple types of 7TMRs in the same cell occurs physiologically and understanding how receptors are regulated in a more heterogeneous receptor expression system could improve our understanding of how this regulation operates in the context of tissues and the whole animal.

While it remains to be determined whether segregation of 7TMRs from one another at the cell surface operates as a sorting mechanism for downstream trafficking, it has been suggested that many 7TMRs segregate from other membrane cargoes and traffic to a subset of the total population of CCPs (~ 40% of all CCPs in HEK 293 cells) (Cao et al., 1998; Mundell et al., 2006; Puthenveedu and von Zastrow, 2006). How 7TMRs are targeted to specific subpopulations of CCPs and whether sorting into these subsets has any functional consequence is unclear, and I believe this is one exciting (but difficult) question worth pursuing in the field of 7TMR trafficking. A possible mechanism to achieve selective incorporation of 7TMRs into a portion of CCPs could be through interactions with 7TMR-specific endocytic adaptors present in limiting amounts. Prime candidates for such proteins are the arrestins, and studies from our lab demonstrated that overexpression of arrestin increased the percentage of CCPs that contained receptors (Puthenveedu and von Zastrow, 2006). These studies beg the question, if arrestin controls which CCPs 7TMRs enter, what recruits arrestin to select portions of the overall CCP population? Is such segregation achieved through the stochastic interaction and capture of limiting amounts of arrestin by other core components of the clathrin machinery?

Alternatively, is there an as yet unknown earlier identifier that is recognized by arrestin to target 7TMRs to subsets of CCPs?

This large question of how subsets of 7TMR-containg CCPs are generated also highlights other holes in our understanding of the selective mechanisms controlling 7TMR endocytosis. For example, detailed analysis of when arrestin interacts with receptors and how they are brought to CCPs is lacking. Preliminary TIRF-M studies hinted at the possibility that arrestin is recruited to CCPs *before* receptors are, supporting a controversial "cart before the horse" model whereby arrestin arrives at the CCP first and leads to the later recruitment of activated 7TMRs. Obviously, this idea requires further examination and experimentation. Additionally, it remains unclear when, precisely, arrestin disassociates from CCPs for Class A 7TMRs. My preliminary findings from TIRF-M imaging of receptors and GFP-tagged Arrestin3 suggested that B2AR and arrestin disappear from the TIRF illumination field concomitantly, but MORs were removed prior to complete arrestin disassociation (Figure 1). Additional studies are required with using the ecliptic pHluorin to ensure that receptors that A possible explanation for this behavior is that arrestins enter CCPs with some receptors (perhaps those that specifically do not require ubiquitin to endocytose) and are restricted to the rim of CCPs for others (like MORs). The Marsh lab has shown that arrestin appeared to be restricted to the edge of CCPs that contain CCR5, providing further support for this idea (Mark Marsh, personal communication). Clearly, many questions remain about the role of arrestin in receptor entry into CCPs, its specific kinetics for association and

disassociation from activated 7TMRs, and whether specific sorting mechanisms operate at the CCP to segregate 7TMRs from other membrane cargo or even, from each other.

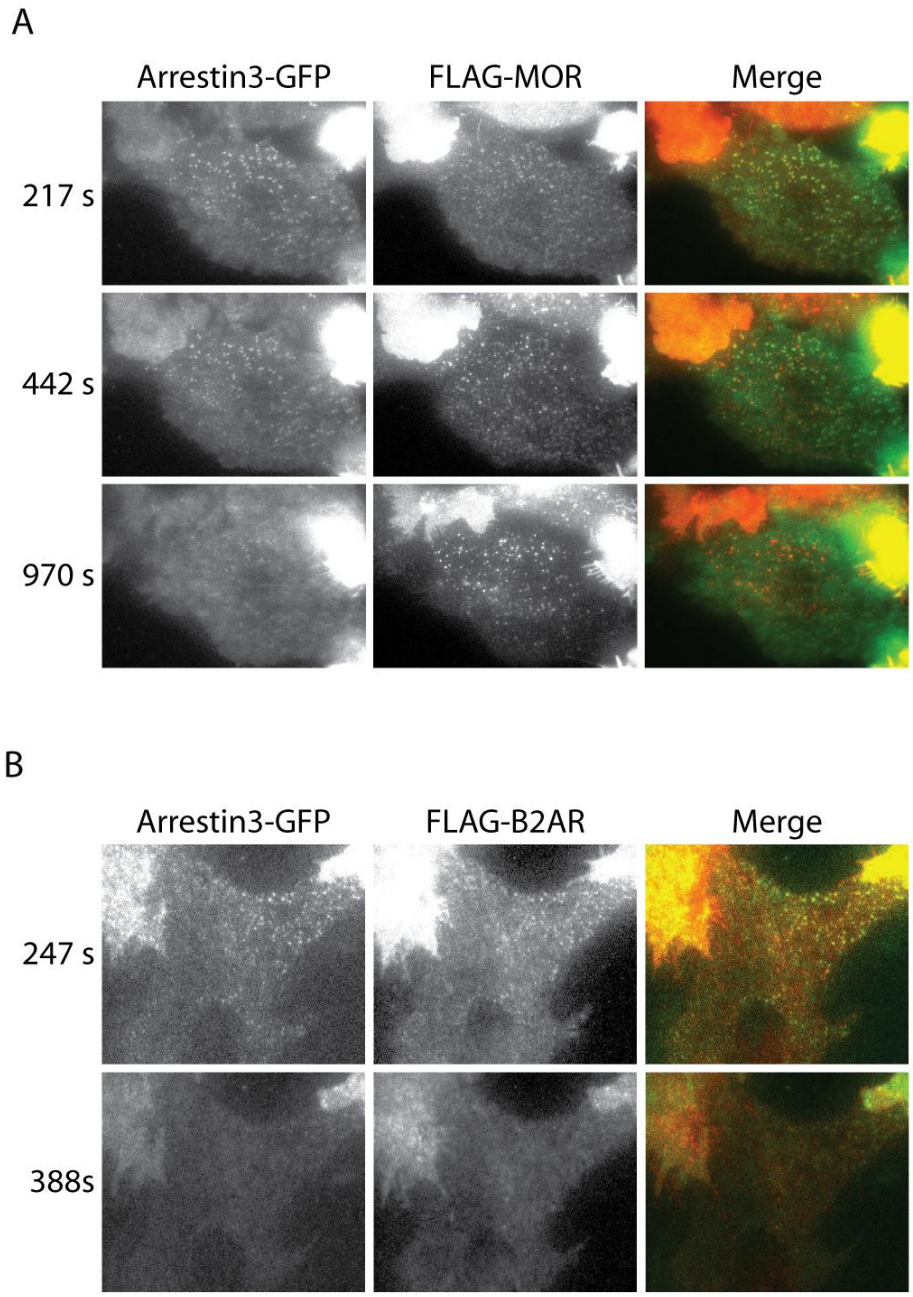


**Figure 1. Dual color imaging of arrestin and 7TMRs. (**A-B) HEK293 cells were transiently transfected with FLAG-tagged MOR (A) or B2AR (B) and Arrestin3-GFP and imaged using TIRF-M after agonist addition. Shown are representative micrographs which show receptor colocalization with arrestin (first time point shown) and Arrestin3 remaining after MOR undergoes endocytosis (middle time point) until

both receptor and arrestin have been removed from the TIRF field (last time point for both). MOR-containing endocytic vesicles can be seen in the third time point, illustrating the importance of repeating these experiments using the ecliptic phluorin.

## 6.4 Two step model for protein sorting in the endocytic pathway

Our work on the role of ubiquitin in the post-endocytic trafficking of receptors supports a new model for how sorting decisions are made that involves two separate steps, rather than one simple decision of whether to recycle or degrade. While receptor ubiquitination does appear sufficient to regulate this decision for some 7TMRs and other membrane cargo, we found that ubiquitination of opioid receptors has no effect on their ability to return to the cell surface or traffic to the lysosome. In trying to find any function for ubiquitin in receptor destruction, a second sorting was revealed that specifically controls the transfer of receptors from the limiting endosomal membrane to ILVs, a process required for the full destruction of receptors. Contrary to previous models whereby receptor involution was seen as a mechanism for physically removing receptors from possible retrieval to the recycling pathway, our work on ubiquitin functionally isolates these two process of 1) deciding whether receptors recycle or are targeted to lysosomes and 2) controlling the efficient involution of receptors into the endosomal lumen. This model is also supported by work on the yeast 7TMR Ste3p. Ste3p recycles and undergoes turnover in an essentially ubiquitin-independent manner, and its ubiquitination, instead, specifically modulates the amount of receptor found on ILVs (Chen and Davis, 2002). Further, our unpublished work on the B2AR also supports this model and reveals a new twist in how receptors maneuver these two pathways. B2ARs are actively recycled through a retromer/SNX27/actin dependent mechanism, and preventing its association with the PDZ machinery (through the addition of an HA epitope tag) targets receptors for

destruction via lysosomes (Cao et al., 1999; Lauffer et al., 2010; Puthenveedu et al., 2010; Temkin et al., 2011). Surprisingly, although B2AR-HAs are effectively targeted to late endosomes/lysosomes after 2 hours agonist treatment, neither B2ARs nor B2AR-HAs downregulate substantially even after 24 hours agonist treatment (Figure 1). Using the imaging-based involution assay developed in Chapter 2 of this thesis, we found that unlike the DOR, the B2AR-HA receptor does not appear to transfer effectively to ILVs and remains at the limiting membrane (Figure 2 A-C). This apparent lack of involution was validated using immuno-electron microscopy (Figure 2D), and suggests that the B2AR does not effectively undergo the second sorting step in this process and provides further support for our model that sorting and involution do not occur through the same step in the pathway.

Our findings also introduce many unanswered matters for future study. A question of fundamental importance that remains unclear is how proteins are retained away from the default recycling pathway and targeted for lysosomal degradation. In principle, any interactions that slow flux through the sorting compartment could be considered degradative sorting determinants. For example, many different factors could limit mobility of 7TMRs including biophysical properties of seven-membrane spanning receptors or of the membrane itself (such as the existence of lipid rafts or other membrane microdomains), receptor oligomerization, or alternative endosomal scaffolding molecules. Our lab has identified GASP and Dysbindin as interacting proteins that may target opioid receptors for lysosomal destruction, although detailed analysis of how these proteins accomplish this sorting is lacking (Marley and von Zastrow, 2010;

Whistler et al., 2002). While targeting of many 7TMRs back to the cell surface appears to be an active process, one must consider the possibility that once receptors escape the default recycling mechanism, receptors destined for the lysosome may not be sorted through an "active" process and instead may be simply retained on endosomes as they mature to late endosomes/lysosomes and eventually are fully destroyed. Further, while much has been learned recently about how B2ARs recycle back to the cell surface, the mechanisms governing MOR recycling are poorly understood. Apart from a specific sequence required to return receptors back to the cell surface, no downstream interacting proteins or additional mechanisms have been identified that mediate MOR recycling. Mass spectrometry analysis of interacting proteins or studies examining the biophysical properties of MORs in endosomal membranes may be informative to elucidate the mechanism mediating this process. Finally, it remains to be determined how widespread the "two step sorting model" is for all 7TMRs or for other membrane cargoes more generally, and careful analysis of how sorting and involution of membrane proteins are regulated will demonstrate whether this is a general property of 7TMRs or instead one method used by some receptors to increase the diversity and number of points of regulation of 7TMRs in the endocytic pathway.

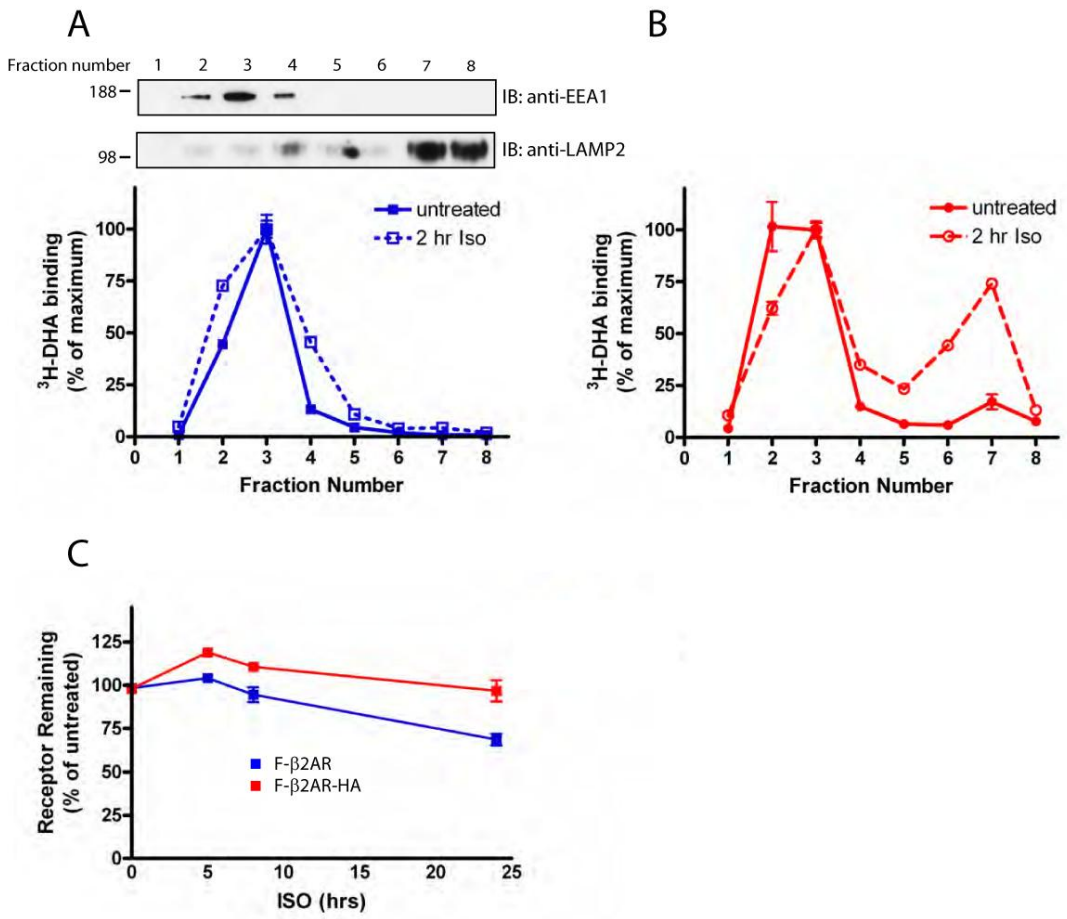


**Figure 1. B2ARs retain radioligand binding capacity long after delivery to lysosomes.** (A and B) Cells stably-expressing F-B2AR (A) or F-B2AR-HA were either left untreated or treated with 10μM isoproterenol before subcellular fractionation on a Percoll gradient to separate early endosomes from late endosomes. Western blots in (A) show where early endosomes (labeled by EEA1) and late endosomes/lysosomes (labeled by LAMP2) localize in the different fractions isolated. The amount of receptors in each fraction was quantified using radioligand binding. The lowest and highest specific binding values were normalized to 0 and 100%, respectively, and data shown are the relative % of maximum binding for each fraction. (C) Cells expressing either F-B2AR or F-B2AR-HA, were treated for the indicated time with 10μM isoproterenol before freezing and undergoing radioligand binding. Shown is the total specific binding detected at each time point expressed as a percentage of the total specific binding in naïve cells. Data shown is the total specific binding expressed as a percentage of that seen in untreated cells.

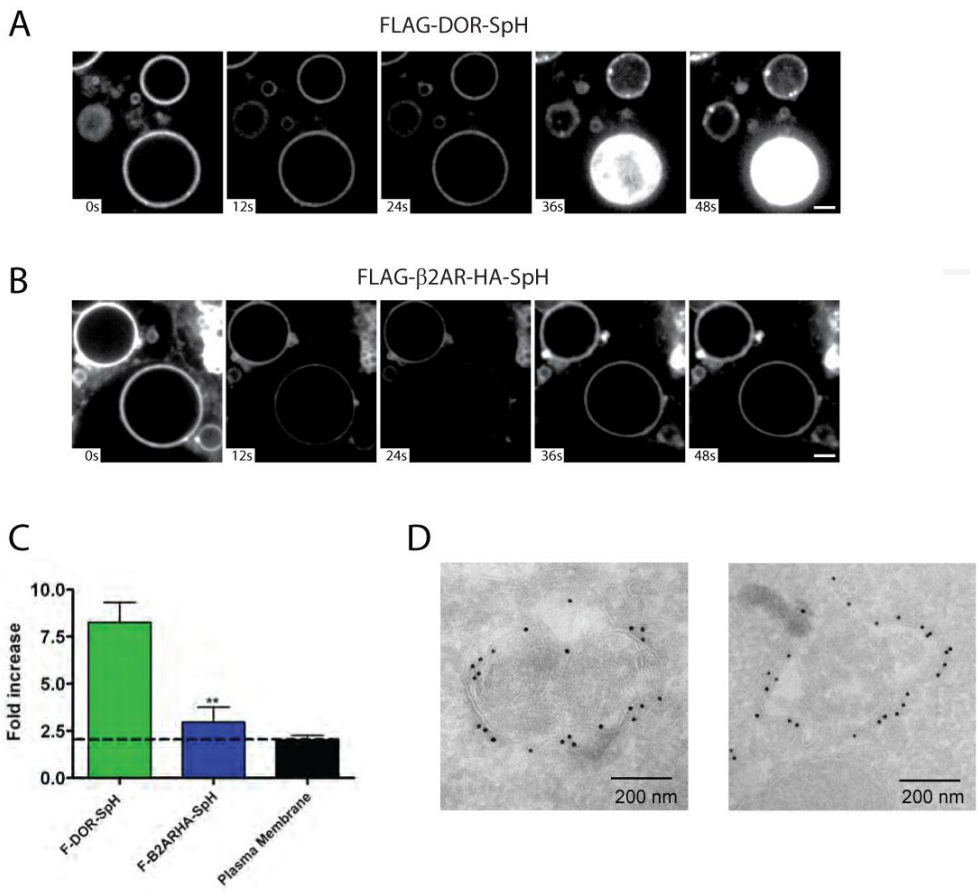


**Figure 2. B2ARs do not undergo transfer from the limiting membrane of endosomes to ILVs.**

(A and B) Representative image sequence of cells expressing CFP-Rab5-Q79L and either F-DOR-SpH (A) or F-B2AR-HA-SpH (B) and treated for 90 min with 10µm agonist. Cells were imaged at a rate of 5 frames per second by spinning disc confocal microscopy and treated with 1 mM chloroquine after 50 frames. (C) Quantification of the chloroquine-induced increase in fluorescence intensity. Mean and SEM are shown for F-DOR-SpH- (endosomal DOR-SpH, $n$ = 8 cells, 24 endosomes) and F-B2AR-HA-SpH-containing endosomes (endosomal F-B2AR-HA-SpH, unpaired $t$-test; $^{**}p < 0.01$, $n$ = 7 cells, 22 endosomes), and F-DOR-SpH expressed on the plasma membrane (plasma membrane, $n$ = 11 cells). Scale bar = 2 µm. (D) The lack of intralumenal localization of the C-terminal epitope was confirmed by electron microscopy, representative images are shown, scale bar = 200nm.

## 6.5 Implications for signaling and physiology

While it is clear that a variety of mechanisms regulate the endocytic trafficking of opioid receptors, the role of these trafficking decisions on downstream signaling pathways and their function in a physiological context remain poorly understood. The work presented in this thesis identified two previously unanticipated functions of ubiquitin in controlling the trafficking of opioid receptors, both of which may be relevant in terms of controlling the strength and duration of receptor-mediated signaling and have potential implications at the physiological level. First, we found that ubiquitination of MORs specifically controls how long receptors remain in clathrin-coated pits prior to their endocytic scission, leading to a reduction in the net endocytic uptake of MORs after agonist activation. From a simple perspective, MOR ubiquitination could serve as a mechanism to ensure efficient internalization after activation, either by sequestering receptors away from signaling components present at the cell surface (and contributing to signal attenuation), by promoting the later dephosphorylation and recycling of receptors back to the cell surface (promoting signal recovery), or through a combination of the two. When assessing the ability of receptor activation of either wildtype MORs or MOR0cKs to lead to the inhibition of cAMP production, we noticed a slight rightward shift in the dose-response curve for the lysyl-mutant receptors, suggesting they may possess a minor defect in G protein coupling (Figure 1). Whether the endocytic defect caused by preventing receptor ubiquitination affects receptor desensization or later resensitization has not been examined and will be an interesting question for future study. While MOR phosphorylation and arrestin recruitment is believed to contribute to receptor desensitization, we have found that MOR ubiquitination appears to occur after, and is

promoted by, phosphorylation-dependent recruitment of arrestin, suggesting a role for MOR ubiquitination in acute receptor desensitization seems unlikely. Future studies should be conducted to address whether receptor ubiquitination, and the kinetic control it exerts on CCPs, have any consequences on the recovery of MOR-regulated signaling.

We also identified a more downstream function of ubiquitin in modulating the transfer of receptors from the limiting membrane of late endosomes to ILVs. A largely unanswered question concerns *when* opioid receptors lose their ability to bind ligand and their ability to engage signaling machinery. While the early stages of receptor destruction do not require ubiquitination and are determined by additional regulatory mechanisms, we found ubiquitination is required for their complete destruction, leading to a loss of the ligand binding site detected using radioligand binding assays. The existence of two separate sorting steps could allow precise modulation of how long receptors remain in particular locations, and in turn, how long they can engage specific signaling effectors. Emerging evidence supports that some 7TMRs can continue to signal from endosomes (Calebiro et al., 2009; Kotowski et al., 2011), and controlling how long receptors persist at the endosomal membrane could affect compartmentalized signaling responses. Compartmentalization of signaling could be extremely important in the context of the neuron, which contains structurally diverse compartments like the axon and somatodendritic compartment and specialized membrane microdomains such as the dendritic spine, axonal terminal, or primary cilia.

As opioid receptors are best known for their role in modulating the sensation of pain, and agonists that activate MOR are some of the most effective analgesics on the market, it is enticing to suggest that receptor ubiquitination could play some role in modulating the response to opiates in the intact animal. However, the role of endocytosis and later endocytic trafficking in the physiological functions of opioid receptors remains poorly understood. Some studies have suggested that MOR endocytosis (or lack thereof, rather) plays a key physiological role in the development of tolerance and physical dependence to drugs of abuse. Morphine exerts its physiological actions through MORs, but unlike peptide ligands, morphine triggers little to no endocytosis. Intriguingly, as recently reported and corroborated here, morphine treatment does not increase receptor ubiquitination, providing additional evidence for biases in the receptor's responses to different agonists (Groer et al., 2011 and data not shown). A simple model was proposed, termed the "RAVE" hypothesis (for relative activation versus endocytosis), to understand the connection between signaling and trafficking effects of different opioid agonists and their propensity to cause tolerance, which suggests that agonists that do not trigger efficient internalization may be more likely to produce tolerance and dependence to opiates (Martini and Whistler, 2007; Whistler and von Zastrow, 1998). In support of this model, it has been demonstrated that increasing the ability of MORs to endocytose in response to morphine leads to enhanced antinociception, reduced tolerance, and reduced with withdrawal in a mouse model (Kim et al., 2008). Additionally, a correlation between decreased recovery from desensitization and recycling of receptors was recently shown using a FLAG-tagged MOR transgenic animal after chronic morphine treatment, further supporting that endocytic trafficking contributes to regulation of opioid receptor-mediated signaling (Quillinan et al., 2011). However, there also exists evidence that questions the dogmatic view that receptors require endocytosis for resensitization, reporting that endocytosis of MORs is not required for recovery from desensitization or the dephosphorylation of MORs (Doll et al., 2011). Further adding to the

confusion, previous work using beta-arrestin2 KO mouse showed that loss of beta-arrestin2 also decreased tolerance, a result that appears somewhat contradictory to other works suggesting that promoting endocytosis and recycling decrease tolerance to morphine (Bohn et al., 2000).

Some of the confusion may arise from the multiple functions downstream proteins and regulatory processes play in the process. For example, beta-arrestins also contribute to desensitization, and the inability to uncouple their functions in desensization and endocytosis make it difficult to make strong conclusions about the roles of particular stages of receptor regulation. The lysine mutant receptors generated in this study could be a very useful tool to tease apart these questions, as receptor ubiquitination likely plays no role in the initial desensitization process but significantly affects receptor endocytosis. The generation of a knock-in mouse, possessing the lysyl-mutant MOR, could be very informative to assess any potential defects of specifically affecting receptor trafficking on resensitization, tolerance, and dependence to opiates. It is likely that a diverse array of regulatory mechanisms contribute to these complex processes and that many adaptations occur in response to chronic receptor activation, making it rather difficult to pinpoint critical points of regulation but also opening up many exciting avenues that merit future study. The considerable body of work examining the function and behavior of opioid receptors clearly highlights the vast toolbox available to introduce diverse modes of regulation and to precisely control many stages in the life cycle of this important class of signaling receptors.

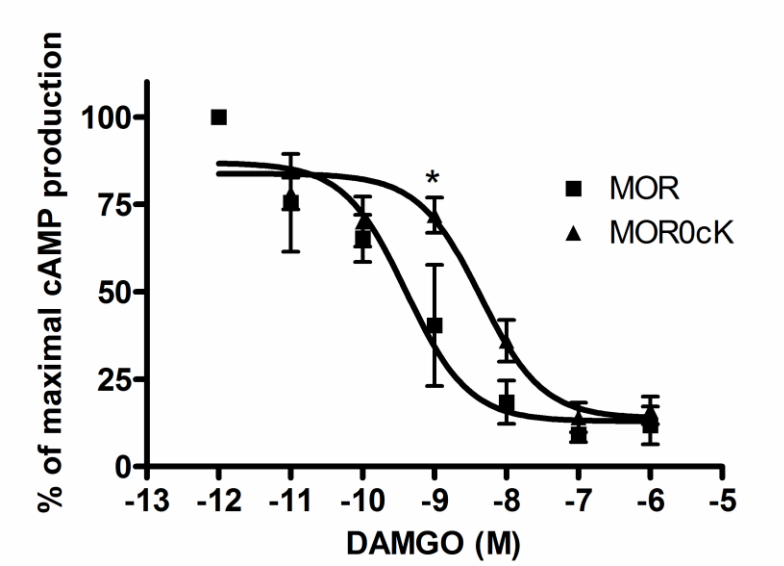


**Figure 1. Dose response curves for cAMP generation for MOR and MOR0cK.** Cells stably-expressing either MOR or MOR0cK at comparable levels were stimulated with a range of DAMGO concentrations for 10 minutes in the presence of 1mM IBMX. Normalized % maximal Camp values were determined by defining the amount of cAMP generated at the highest concentration of agonist for each receptor as 100%; n = 3. logEC50 values were determined: MOR= -9.390; MOR0Ck: -8.360. Data were fit to a sigmoidal dose-response curve and EC50 values calculated using GraphPad Prism software. Two-way anova, *$p<0.05$**.**

## 6.6 References

Bhandari, D., Trejo, J., Benovic, J. L., and Marchese, A. (2007). Arrestin-2 interacts with the ubiquitin-protein isopeptide ligase atrophin-interacting protein 4 and mediates endosomal sorting of the chemokine receptor CXCR4. J Biol Chem *282*, 36971-36979.

Bohn, L. M., Gainetdinov, R. R., Lin, F. T., Lefkowitz, R. J., and Caron, M. G. (2000). Mu-opioid receptor desensitization by beta-arrestin-2 determines morphine tolerance but not dependence. Nature *408*, 720-723.

Calebiro, D., Nikolaev, V. O., Gagliani, M. C., de Filippis, T., Dees, C., Tacchetti, C., Persani, L., and Lohse, M. J. (2009). Persistent cAMP-signals triggered by internalized G-protein-coupled receptors. PLoS Biol *7*, e1000172.

Cao, T. T., Deacon, H. W., Reczek, D., Bretscher, A., and von Zastrow, M. (1999). A kinase-regulated PDZ-domain interaction controls endocytic sorting of the beta2-adrenergic receptor. Nature *401*, 286-290.

Cao, T. T., Mays, R. W., and von Zastrow, M. (1998). Regulated endocytosis of G-protein-coupled receptors by a biochemically and functionally distinct subpopulation of clathrin-coated pits. J Biol Chem *273*, 24592-24602.

Chen, B., Dores, M. R., Grimsey, N., Canto, I., Barker, B. L., and Trejo, J. (2011). Adaptor protein complex-2 (AP-2) and epsin-1 mediate protease-activated receptor-1 internalization via phosphorylation- and ubiquitination-dependent sorting signals. J Biol Chem *286*, 40760-40770.

Chen, L., and Davis, N. G. (2002). Ubiquitin-independent entry into the yeast recycling pathway. Traffic *3*, 110-123.

Doll, C., Konietzko, J., Poll, F., Koch, T., Hollt, V., and Schulz, S. (2011). Agonist-selective patterns of micro-opioid receptor phosphorylation revealed by phosphosite-specific antibodies. Br J Pharmacol *164*, 298-307.

Dores, M. R., Schnell, J. D., Maldonado-Baez, L., Wendland, B., and Hicke, L. (2010). The function of yeast epsin and Ede1 ubiquitin-binding domains during receptor internalization. Traffic *11*, 151-160.

Groer, C. E., Schmid, C. L., Jaeger, A. M., and Bohn, L. M. (2011). Agonist-directed interactions with specific beta-arrestins determine mu-opioid receptor trafficking, ubiquitination, and dephosphorylation. J Biol Chem *286*, 31731-31741.

Hanyaloglu, A. C., McCullagh, E., and von Zastrow, M. (2005). Essential role of Hrs in a recycling mechanism mediating functional resensitization of cell signaling. Embo J *24*, 2265-2283.

Jiang, X., and Sorkin, A. (2003). Epidermal growth factor receptor internalization through clathrin-coated pits requires Cbl RING finger and proline-rich domains but not receptor polyubiquitylation. Traffic *4*, 529-543.

Jin, L., Pahuja, K. B., Wickliffe, K. E., Gorur, A., Baumgartel, C., Schekman, R., and Rape, M. (2012). Ubiquitin-dependent regulation of COPII coat size and function. Nature *482*, 495-500.

Kazazic, M., Bertelsen, V., Pedersen, K. W., Vuong, T. T., Grandal, M. V., Rodland, M. S., Traub, L. M., Stang, E., and Madshus, I. H. (2009). Epsin 1 is involved in recruitment of ubiquitinated EGF receptors into clathrin-coated pits. Traffic *10*, 235-245.

Kim, J. A., Bartlett, S., He, L., Nielsen, C. K., Chang, A. M., Kharazia, V., Waldhoer, M., Ou, C. J., Taylor, S., Ferwerda, M., *et al.* (2008). Morphine-induced receptor

endocytosis in a novel knockin mouse reduces tolerance and dependence. Curr Biol *18*, 129-135.

Kotowski, S. J., Hopf, F. W., Seif, T., Bonci, A., and von Zastrow, M. (2011). Endocytosis promotes rapid dopaminergic signaling. Neuron *71*, 278-290.

Lauffer, B. E., Melero, C., Temkin, P., Lei, C., Hong, W., Kortemme, T., and von Zastrow, M. (2010). SNX27 mediates PDZ-directed sorting from endosomes to the plasma membrane. J Cell Biol *190*, 565-574.

Marley, A., and von Zastrow, M. (2010). Dysbindin promotes the post-endocytic sorting of G protein-coupled receptors to lysosomes. PLoS One *5*, e9325.

Martini, L., and Whistler, J. L. (2007). The role of mu opioid receptor desensitization and endocytosis in morphine tolerance and dependence. Curr Opin Neurobiol *17*, 556-564.

Mettlen, M., Stoeber, M., Loerke, D., Antonescu, C. N., Danuser, G., and Schmid, S. L. (2009). Endocytic accessory proteins are functionally distinguished by their differential effects on the maturation of clathrin-coated pits. Mol Biol Cell *20*, 3251-3260.

Mundell, S. J., Luo, J., Benovic, J. L., Conley, P. B., and Poole, A. W. (2006). Distinct clathrin-coated pits sort different G protein-coupled receptor cargo. Traffic *7*, 1420-1431.

Penengo, L., Mapelli, M., Murachelli, A. G., Confalonieri, S., Magri, L., Musacchio, A., Di Fiore, P. P., Polo, S., and Schneider, T. R. (2006). Crystal structure of the ubiquitin binding domains of rabex-5 reveals two modes of interaction with ubiquitin. Cell *124*, 1183-1195.

Purvanov, V., Koval, A., and Katanaev, V. L. (2010). A direct and functional interaction between Go and Rab5 during G protein-coupled receptor signaling. Sci Signal *3*, ra65.

Puthenveedu, M. A., Lauffer, B., Temkin, P., Vistein, R., Carlton, P., Thorn, K., Taunton, J., Weiner, O. D., Parton, R. G., and von Zastrow, M. (2010). Sequence-dependent sorting of recycling proteins by actin-stabilized endosomal microdomains. Cell *143*, 761-773.

Puthenveedu, M. A., and von Zastrow, M. (2006). Cargo regulates clathrin-coated pit dynamics. Cell *127*, 113-124.

Quillinan, N., Lau, E. K., Virk, M., von Zastrow, M., and Williams, J. T. (2011). Recovery from mu-opioid receptor desensitization after chronic treatment with morphine and methadone. J Neurosci *31*, 4434-4443.

Raiborg, C., Slagsvold, T., and Stenmark, H. (2006). A new side to ubiquitin. Trends Biochem Sci *31*, 541-544.

Reider, A., and Wendland, B. (2011). Endocytic adaptors--social networking at the plasma membrane. J Cell Sci *124*, 1613-1622.

Shenoy, S. K., McDonald, P. H., Kohout, T. A., and Lefkowitz, R. J. (2001). Regulation of receptor fate by ubiquitination of activated beta 2-adrenergic receptor and beta-arrestin. Science *294*, 1307-1313.

Shenoy, S. K., Xiao, K., Venkataramanan, V., Snyder, P. M., Freedman, N. J., and Weissman, A. M. (2008). Nedd4 mediates agonist-dependent ubiquitination, lysosomal targeting, and degradation of the beta2-adrenergic receptor. J Biol Chem *283*, 22166-22176.

Shields, S. B., and Piper, R. C. (2011). How ubiquitin functions with ESCRTs. Traffic *12*, 1306-1317.

Stenmark, H., Parton, R. G., Steele-Mortimer, O., Lutcke, A., Gruenberg, J., and Zerial, M. (1994). Inhibition of rab5 GTPase activity stimulates membrane fusion in endocytosis. Embo J *13*, 1287-1296.

Taylor, M. J., Perrais, D., and Merrifield, C. J. (2011). A high precision survey of the molecular dynamics of mammalian clathrin-mediated endocytosis. PLoS Biol *9*, e1000604.

Tebar, F., Sorkina, T., Sorkin, A., Ericsson, M., and Kirchhausen, T. (1996). Eps15 is a component of clathrin-coated pits and vesicles and is located at the rim of coated pits. J Biol Chem *271*, 28727-28730.

Temkin, P., Lauffer, B., Jager, S., Cimermancic, P., Krogan, N. J., and von Zastrow, M. (2011). SNX27 mediates retromer tubule entry and endosome-to-plasma membrane trafficking of signalling receptors. Nat Cell Biol *13*, 715-721.

Toshima, J. Y., Nakanishi, J. I., Mizuno, K., Toshima, J., and Drubin, D. G. (2009). Requirements for Recruitment of a G Protein-coupled Receptor to Clathrin-coated Pits in Budding Yeast. Mol Biol Cell.

Whistler, J. L., Enquist, J., Marley, A., Fong, J., Gladher, F., Tsuruda, P., Murray, S. R., and Von Zastrow, M. (2002). Modulation of postendocytic sorting of G protein-coupled receptors. Science *297*, 615-620.

Whistler, J. L., and von Zastrow, M. (1998). Morphine-activated opioid receptors elude desensitization by beta-arrestin. Proc Natl Acad Sci U S A *95*, 9914-9919.

# Appendices

**Appendix 1: Protocol for subcellular fractionation to separate early and late endosomes**

Modified from (Schaub et al., 2005), optimized for use with 293 cells.

1. Plate cells in 10-cm tissue culture dishes (one dish of cells per sample to be analyzed) and grow to 100% confluence before fractionation (younger passages are preferred).
2. Perform agonist treatments.
3. Wash cells twice with 10 ml ice-cold PBS, and scrape into 2 ml cold 1× homogenization buffer (HB; 2.5 M sucrose, 10 mM EDTA, Complete Protease Inhibitor tablets (Roche)). Rinse the dish with an additional 2 ml of 1× HB and pool the contents with the material.
4. Centrifuge the harvested cell suspension 5 min at ~260 × g, 4°C.
5. Aspirate the supernatant and add 850 µl of 1× HB to the pellet (so at least 10X as much HB buffer as volume of cell pellet).
6. Resuspend by trituration, and homogenize the suspension using six strokes through a 25-G needle. Add 850 µl of 1× HB to the homogenized suspension, and centrifuge 10 min at ~370 × g, 4°C.Collect the supernatant.
7. Prepare a Percoll gradient by adding 1.2 ml of 10× HB to a 16 × 76–mm Beckman Polyallomer Centrifuge tube (the sucrose cushion). Using a pipet, carefully layer 8.5 ml of 1× HB/17.5% Percoll (Sigma-Aldrich) on top of the sucrose cushion.
8. Carefully layer the PNS on top of the Percoll gradient. When PNS layering is complete, weigh each tube to ensure they are of equivalent weights (Adding 1× HB as necessary).
9. Spin in a 70.1 Ti Rotor cooled to 4˚ C at 36000g (~19800 rpm) for 65 min.
10. Carefully remove tubes. There should be faint membraneous bands near the top and bottoms of the tubes (indicative of a good separation of light and heavy membrane fractions).
11. Using a pipette, collect fractions from the top of the gradient and deposit them into eppendorf tubes. Standardize each fraction size by marking pipette (~ 1.25mL/fraction for 8 fractions total)
12. Analyze fractions probing for receptor and organelle markers via WB and ligand binding.

a) Receptor at the plasma membrane/early endosomes is found in Fractions 2-4.

b) Early endosomes (marked by EEA1) are found in Fractions 2-4.

c) Late endosomes/lysosomes are found in Fractions 4-8, with strongest concentration in Fractions 7 and 8.

**Reference**

Schaub, B. E., Nair, P., and Rohrer, J. (2005). Analysis of protein transport to lysosomes. Curr Protoc Cell Biol *Chapter 15*, Unit 15 18.

**Appendix 2: Protocol for FLAG opioid receptor purification.**

Modified from Paul Temkin (personal communication).

1) Plate 8-15 cm dishes of cells stably expressing FLAG-tagged DOR.

2) Perform agonist treatments (20 min 10μM DADLE).

3) Wash cells twice with cold PBS, and scrape into 1 ml cold homogenization buffer (HB2; 10mM HEPES, 100mM KCl, 1mM EDTA, 250 mM sucrose, Complete Protease Inhibitor tablets).

4) Spin at 1000 rpm for 5 min (4˚C) and discard supernatant. Add 10X pellet volume of HB2, triturate, and homogenize the suspension using five strokes through a 25-G needle.

5) Spin at 1350 rpm for 10 min (4˚C) and collect post-nuclear supernatant. Increase volume to 10mL with HB2.

6) Add 0.1% n-Dodecyl β-D-maltoside (DDM, Sigma-Aldrich) and mix for 1 hour (4˚C).

7) Clear M2 agarose beads (Sigma-Aldrich, A2220) by spinning at 3000 rpm for 3min in HB2. Add beads to cell preparation and rotate for 3 hours (4˚C).

8) Equilibrate column by washing 3X with IP buffer and spin at 1000 rpm for 3 min each wash.

9) Incubate sample with 20μL 3XFLAG peptide (150ng/μL in IP buffer; Sigma-Aldrich, F4799) on ice for 30 min.

10) Elute by adding sample to column and spinning at 1000 rpm for 1 min. Repeat step 9 and combine eluates.

11) Assess yield by Western blotting.

**Appendix 3: Protocol for assessing receptor ubiquitination via Western blot analysis**

1) Plate 10 cm dish for each time point so cells are about 90% confluent day of experiment. You should also have one 10 cm dish with just 293 cells without any of your protein to be examined.

2) Treat cells with agonist as desired.

3) Wash cells 2-3 X with ice cold PBS. After final wash, tilt each dish and completely aspirate so no media remains.

4) Lyse each dish in 100µL 1% SDS, 10 mM Tris, protease inhibitor tablets, and iodoacetamide made fresh (10mM iodoacetamide final concentration). **The iodoacetamide is very important to include.**

5) Scrape cells, put on ice, and add 400µL standard IP buffer plus protease inhibitor tablets.

6) Sonicate cells on setting 3, at 30-40% duty cycle, for 5- 10 seconds.

7) Spin at 14000 rpm for 10'.

8) Run the supernatant for each sample through a tube from Qiashredder kit (Qiagen). These are are not absolutely necessary if you have sonicately your cells efficiently.

9) Spin at 5000 rpm. Here, take out 2 aliquots of 10µL from each sample, and add 5µL sample buffer to each. Save these to blot for your total lysate later.

10) Add another 500µL IP buffer (with protease inhibitor tablets) to each sample. The final volume should now be 1mL with a final concentration of 0.1% SDS.

11) Add 1.5µL primary antibody to each sample and shake overnight.

Day two of experiment:

12) Add 30µL protein AG beads and shake for 2 hours.

13) Spin down at 3000 rpm for 30 sec. Wash pellet with IP buffer, spin at 3000 rpm for 30 sec. Repeat 2x.

14) Aspirate, elute in 20µL sample buffer.

15) Run gel and transfer.

16) Blot for ubiquitin using an antibody against a tag that is attached to ubiquitin that you have transfected in OR using endogenous ubiquitin (Santa Cruz, sc-8017).

**Publishing Agreement**

*It is the policy of the University to encourage the distribution of all theses, dissertations, and manuscripts. Copies of all UCSF theses, dissertations, and manuscripts will be routed to the library via the Graduate Division. The library will make all theses, dissertations, and manuscripts accessible to the public and will preserve these to the best of their abilities, in perpetuity.*

***Please sign the following statement:***

*I hereby grant permission to the Graduate Division of the University of California, San Francisco to release copies of my thesis, dissertation, or manuscript to the Campus Library to provide access and preservation, in whole or in part, in perpetuity.*

Author Signature

8-31-12

Date